Le récepteur 3 de la neurotensine/Sortiline dans la régulation de l'état dépressif

Sébastien Moreno

▶ **To cite this version:**

Sébastien Moreno. Le récepteur 3 de la neurotensine/Sortiline dans la régulation de l'état dépressif. Biologie cellulaire. Université Côte d'Azur, 2017. Français. NNT : 2017AZUR4136 . tel-01740184

HAL Id: tel-01740184
https://theses.hal.science/tel-01740184

Submitted on 21 Mar 2018

HAL is a multi-disciplinary open access archive for the deposit and dissemination of scientific research documents, whether they are published or not. The documents may come from teaching and research institutions in France or abroad, or from public or private research centers.

L'archive ouverte pluridisciplinaire **HAL**, est destinée au dépôt et à la diffusion de documents scientifiques de niveau recherche, publiés ou non, émanant des établissements d'enseignement et de recherche français ou étrangers, des laboratoires publics ou privés.

Université Côte d'Azur – UFR Sciences
École Doctorale des Sciences de la Vie et de la Santé

T H E S E de D O C T O R A T

Présentée pour obtenir le titre de

DOCTEUR en SCIENCES de la VIE
De l'Université Côte d'Azur
Mention : « *Interactions moléculaires et cellulaires* »

Soutenue le 21 décembre 2017 par :

Sebastien MORENO

UMR 7275 CNRS / UNS - IPMC - Sophia Antipolis

Le récepteur 3 de la neurotensine/Sortiline dans la régulation de l'état dépressif.

Jury composé de :

Prof. Robert MARSAULT	Président du jury
Prof. Marie-Odile JAUBERTEAU	Rapporteur
Prof. Jean-Marc MULLER	Rapporteur
Dr. Jean MAZELLA	Directeur de thèse

UNIVERSITÉ CÔTE D'AZUR

ipmc

REMERCIEMENTS

Dans un premier temps, je tiens à remercier les membres du jury qui ont permis l'évaluation de ce travail de thèse. Merci au Prof. Robert Marsault d'avoir accepté de présider le jury, et merci aux rapporteurs, Prof. Marie-Odile Jauberteau et Prof. Jean-Marc Muller.

L'occasion m'est donnée, par la présente partie, d'exprimer mes sincères remerciements à toutes les personnes qui ont assuré, de près comme de loin, au bon déroulement de cette thèse de 3 ans.

Au départ, je suis arrivé dans l'équipe du Dr. Jean Mazella en tant qu'ingénieur d'étude avec la ferme intention de ne pas m'engager dans ce schéma complexe que représentent le doctorat et son avenir. Force est de constater que si j'écris ces quelques lignes aujourd'hui, c'est que Jean a su trouver la faille pour me convaincre de rejoindre cette « fantastique » aventure. Je te remercie donc Jean, mon directeur de thèse, pour ta confiance et pour m'avoir donné tant de liberté et d'autonomie dans mon travail. Et non, je ne suis toujours pas apte à rendre une analyse de Western Blot en l'espace d'une journée, manips comprises !

Je remercie les membres de l'équipe ex-302/B28. La grande Sophie, adepte des cascades à cheval et que j'ai souvent embêté, me valant le droit à de savants noms d'oiseaux en retour. Thierry, que j'ai d'abord croisé en tant que professeur et tortionnaire d'étudiants à l'université, et avec qui j'ai passé de nombreuses heures à discuter. Je te remercie de tous les conseils prodigués tant sur le plan scientifique que personnel. Christelle et Morgane, un dynamisme sans faille et un déterminisme à toutes épreuves, merci d'avoir animé aussi bien le labo. Et Céline H., voisine de thèse et de galère, dont je félicite la réussite !

Je remercie également les personnes qui m'ont beaucoup appris, tant sur les techniques que sur le plan scientifique. L'équipe du Dr Heurteaux, Thomas Lorivel, la plateforme de protéomique et mon comité des Doctorants/Post doctorants.

Durant ces années à l'IPMC, j'ai eu l'occasion de rencontrer de nombreuses personnes et certaines sont devenues de véritables amis. Céline M., même si tu me considère d'une génération plus jeune et que tu me fustiges de doux noms d'animaux (Chaton), ta bonne humeur permanente a été agréable et motivante au quotidien. Malika, je pu vraiment compter sur toi pour débattre sur tous domaines confondus (et comploter pour tourmenter Céline), ce qui m'a permis d'avoir une activité saine et intellectuelle au labo. Audrey, la petite du groupe, avec qui j'ai partagé des bières, tu as parfaitement complété ce groupe et tu as su trouver la motivation pour nous accompagner dans notre périple sportif du midi. Je me dois de finir ces lignes avec un ami de plus longue date, Thom, un véritable partenaire, aussi farfelu que sérieux, toujours disponible et prêt à aider. Je vous remercie tous sincèrement !

Et enfin, les personnes qui comptent le plus pour moi, ma Famille. D'abord mes parents, qui m'ont toujours accompagné afin que je puisse choisir et tracer ma voie sans difficulté, et ce, sans jugement et en soutenant mes choix. Merci pour tout, je n'oublie pas d'où je viens et c'est cela qui me fait avancer aujourd'hui. Mon petit frère Pierre, petit par l'âge mais grand par la taille et le cœur. Tu fais ma fierté et je serai toujours là pour toi. Enfin, ma belle famille, une seconde famille pour moi, vous avez été très présents, toujours là pour me soutenir et je vous en remercie beaucoup. Et bien sûr Leslie, ma femme, mon cœur, celle qui me soutient au quotidien et qui comble ma vie de bonheur. Tu représentes ma réussite d'aujourd'hui et celle de demain. Tu m'as donné le plus beau cadeau, celle qui est m'est indissociable, ma fille Maëlle. Ma petite fille, je te remercie pour ces nombreuses nuits de sommeil, pour tes multiples interrogations sur la vie et pour l'incroyable capacité que tu as à faire passer le temps beaucoup plus vite que je ne le pense.

ABREVIATIONS

5-HIAA	5-hydroxyindole acétique
5-HT	5-hydroxytryptamine - sérotonine
AA	Acide arachidonique
ACTH	Adrenocorticotropin hormone
AKAP150	Protéine d'ancrage A-Kinase
ALA	Acide alphalinoléique
APOE	Apolipoprotéine e
ATC	Antidépresseurs tricycliques
BDNF	Brain-derivated neurotrophic factor
BTT	Behavior trial trigger
CA3	Champ ammonien 3
CCA	Cortex cingulaire antérieur
CCAd	Cortex cingulaire antérieur dorsal
CCAv	Cortex cingulaire antérieur ventral
CPE	Carboxypeptidase E
CPF	Cortex préfrontal
CREB	C-AMP Response Element-binding protein
CRH	Corticotropin-releasing hormone
DBS	Deep brain stimulation
DRG	Ganglions de la racine dorsale
DSM-V	Diagnostic and Statistical Manual of Mental Disorders V
ECT	Electroconvulsivothérapie
EDC	Episodes dépressifs caractérisés
EGF	Epidermal growth factor
EGFR	Epidermal growth factor receptor
FST	Force swim test
GGAs	Golgi-localized
GWAS	Genome wide association studies
HPA	Axe hypothalamo-hypophyso-surrénalien
IMAO	Inhibiteurs de la monoamine oxydase
IP3	Inositol trisphosphate
ISRS	Inhibiteurs spécifiques de la recapture de la sérotonine
LDL	Low density lipoprotein
LH	Learn helpness
M6P	Manose-6-phosphate
M6PR	Récepteur du manose-6-phosphate
MADRS	Montgomery-Åsberg depression rating scale
MAO	Monoamine oxydase

MAPK	Mitogen-activated protein kinases
MDD	Major depressive disorder
Mtap 2	Microtubule-associated protein
NGF	Nerve growth factor
NSF	Novelty suppressed feeding
NT	Neurotrophine
NTS	Neurotensine
NTSR	Neurotensin receptor
OMS	Organisation mondiale de la santé
PCPA	Para-chlorophenylalanine
PE	Propeptide
PKA	Protéines kinases A
PKC	Protéines kinases C
PSD-95	Postsynaptic density protein 95
PUFA	Polyunsaturated Fatty Acids
RAP	Receptor-associated protein
RCPG	Récepteur couplé aux protéines G
RE	Réticulum endoplasmique
SAP-97	Synapse-associated protein 90
SEM	Standard Error of the Mean
siRNA	Small interfering RNA
SNC	Système nerveux central
Spadine	Sortilin Peptide antidepressant (IN)
tPA	Tissue plasminogen activator
TREK-1	TWIK-Related K+ channel 1
Trk	Récepteurs kinases liés à la tropomyosine
TRPV1	Transient receptor potential vanilloid 1
TST	Tail suspension test
VLDL	Very low density lipoprotein
VPS10p	Vacuolar protein sorting 10 protein

LISTE DES FIGURES

Figure 1 : Régions des anomalies cérébrales impliquées dans la dépression majeure. 9
Figure 2 : Synthèse et dégradation de la sérotonine 11
Figure 3 : Régulation de l'axe hypothalamo-hypophyso-surrénalien dans le stress. 13
Figure 4 : Mécanismes d'action des antidépresseurs. 16
Figure 5 : Les classes des canaux potassiques. 18
Figure 6 : Arbre phylogénique des K2P chez l'humain 20
Figure 7 : Schéma du contrôle multiple de TREK-1. 25
Figure 8 : Schéma des récepteurs à domaine Vps10p. 31
Figure 9 : La structure du NTSR3/Sortiline. 32
Figure 10 : Représentation schématique du NTSR3/Sortiline humain. 33
Figure 11 : Transport des hydrolases lysosomales nouvellement synthétisées vers les lysosomes. ... 35
Figure 12 : Modèle schématique de la formation du complexe récepteur-p75NTR. 37
Figure 13 : La synthèse et le tri du BDNF. 39
Figure 14 : Séquence de la Spadine conçue à partir de la séquence propeptide. 42
Figure 20 : Comportement relatif à la dépression chez les souris KO-NTSR3. 49
Figure 22 : Expression membranaire de TREK-1 et potentiel de membrane chez les souris KO-NTSR3. 52
Figure 23 : Effet de la délétion du gène NTSR3/Sortiline sur la régulation du BDNF. 53
Figure 24: Interface de Behavior Trial Trigger v1.0. 87
Figure 25 : Système de connexion en série dans le test de la boite clair-obscur 88
Figure 17 : Représentation de la moyenne ± SEM des sites de liaison totales et des sites de liaison sensibles et insensibles à la lévocabastine 103
Figure 18 : Concentrations de NTS dans les sérums et dans le cerveau de souris WT et KO-NTSR3 . 104
Figure 19 : Réponses analgésiques des souris WT et KO-NTSR3. 105
Figure 15 : Peptides synthétisés et affinités. 116
Figure 16 : Concentrations de propeptide dans les sérums de patients sains (Controls) et patients atteints d'un trouble dépressif majeur (MDD) non traités (T0) et traités (T1) pendant 12 semaines. 117
Figure 26 : Comportement des souris KO-NTSR3 dans la résignation acquise et la mémoire spatiale. 128

SOMMAIRE

REMERCIEMENTS .....
ABREVIATIONS .....
LISTE DES FIGURES .....
SOMMAIRE .....
INTRODUCTION 1
1 HISTOIRE DE LA DEPRESSION 1
2 LE TROUBLE DEPRESSIF AUJOURD'HUI 3
2.1. L'épisode dépressif caractérisé (EDC) 3
2.1.1. Diagnostic 3
2.1.2. Formes cliniques 4
2.2. Les types de troubles dépressifs 4
2.2.1. Trouble dépressif caractérisé 4
2.2.2. Trouble disruptif avec dysrégulation émotionnelle 4
2.2.3. Trouble dépressif persistant 5
2.2.4. Trouble dysphorique prémenstruel 5
3 EPIDEMIOLOGIE 5
4 LA BIOLOGIE DE LA DEPRESSION 5
4.1. Anomalies cérébrales 6
4.1.1. Anomalies corticales 6
4.1.1.1. Le cortex préfrontal 6
4.1.1.2. Le cortex cingulaire antérieur 7
4.1.1.3. Le cortex insulaire 7
4.1.2. Anomalies des régions limbiques 8
4.2. L'hypothèse monoaminergique : la sérotonine 9
4.3. Neurogénèse et BDNF 11
4.4. Stress et dépression 12
5 STRATEGIES THERAPEUTIQUES 14
5.1. Les stratégies pharmacologiques 14
5.1.1. Inhiber les monoamines oxydase 15
5.1.2. Inhiber la recapture des monoamines 15
5.2. Les stratégies non-pharmacologiques 16
Conclusion 17

6 LE CANAL TREK-1, ACTEUR EMERGENT DANS LA DEPRESSION 17
6.1. Généralités sur les canaux potassiques 17
6.2. La classe des K_{2P} 18
6.3. Expression et localisation de TREK-1 20
6.4. Propriété électrophysiologique de TREK-1 20
6.5. La régulation de TREK-1 21
6.5.1. Sensibilité mécanique 21
6.5.2. Sensibilité thermique 22
6.5.3. Régulation par le pH 22
6.5.4. Régulation par les lipides 22
6.5.5. Régulation par les RCPGs 23
6.6. Rôle de TREK-1 dans la dépression 23
6.7. Les partenaires de TREK-1 25
7 LE NTSR3 / SORTILINE, UNE PROTEINE ASSOCIEE A DE MULTIPLES FONCTIONS 26
7.1. La neurotensine et ses récepteurs 26
7.1.1. Généralités 26
7.1.2. Le NTSR1 27
7.1.3. Le NTSR2 28
7.2. Le NTSR3 / Sortiline 29
7.2.1. Purification et clonage du NTSR3 / Sortiline 29
7.2.2. Structure 30
7.2.3. Maturation 33
7.2.4. Distribution 34
7.3. Fonctions du NTSR3/Sortiline 34
7.3.1. Régulation du trafic intracellulaire 34
7.3.2. Viabilité neuronale 36
7.3.2.1. Co-recepteur du p75NTR 36
7.3.2.2. Régulation du BDNF 37
7.3.3. Physiopathologie 39
8 NTSR3/SORTILINE, PROPEPTIDE (PE), TREK-1 ET DEPRESSION 41
OBJECTIFS 45
Etude de la délétion du NTSR3/Sortiline dans la régulation de l'état dépressif 47
Article 1: Altered TREK-1 function in sortilin deficient mice results in an antidepressant phenotype. 48

1. Contexte de l'étude....48
2. Résultats et discussion....49
Développement d'outils pour l'analyse du comportement chez le rongeur....85
Article 2: *Behavior Trial Trigger*: Free standalone software using keyboard keys with possibility to connect serial device (Arduino ®) for timing and analysis rodents during behavioral tests. 86
Etude de la délétion du NTSR3/Sortiline dans le système neurotensinergique....101
Article 3: Increased Brain Neurotensin and NTSR2 Lead to Weak Nociception in NTSR3/Sortilin Knockout Mice. 102
1. Contexte de l'étude....102
2. Résultats et discussion....103
Etude du niveau circulant de propeptide dans l'affect dépressif....114
Article 4: Serum sortilin-derived propeptides concentrations are decreased in major depressive disorder patients....115
1. Contexte de l'étude....115
2. Résultats et discussion....116
DISCUSSION GENERALE et CONCLUSION....124
PERSPECTIVES....129
ANNEXES....131
REFERENCES....176
RESUME....193

INTRODUCTION

1 HISTOIRE DE LA DEPRESSION

Dépression, un terme qui représente un des maux le plus répandus de la fin du XXe siècle, mais il est intéressant de savoir qu'historiquement cette désignation s'est accommodée de divers emprunts à travers les âges, renvoyant souvent au même syndrome, et que, de cette complexité de lui soustraire une identité distincte, en résultait l'idée d'un concept difficilement définissable sur le plan de la pathologie mentale. De l'Antiquité jusqu'à fin des années 1970, la dépression était une affectation qui pouvait se manifester chez tout individu et dans toutes pathologies sans pour autant en être considérée comme une.

L'émergence des symptômes de l'état dépressif prend ses origines très tôt dans notre histoire. On peut citer le papyrus d'Ebers, découvert en 1862 à Louxor par Edwin Smith, ancien traité médical datant du XVIe siècle avant notre ère, qui y référence, sous le chapitre « livre des cœurs », des descriptions des états pathologiques de la démence ou encore de la dépression.

Au Ve siècle avant J-C, Hippocrate avancera le terme de *melancholia,* correspondant étymologiquement à la « bile noire » nommé aussi atrabile, qui aura pour siège la rate (*spleen*), et sera une des quatre humeurs de la *théorie des humeurs*, popularisée par le *Corpus Hippocraticum* qui posera les bases de la médecine antique. Cette mélancolie définira un état de tristesse et de peur.

Le philosophe Sénèque exprimera au Ier siècle avant J-C, le concept de *Taedium vitae* ou fatigue de vivre, qui touchera d'ailleurs le poète philosophe Lucrèce, disciple d'Epicure, et qui exclamera que « l'homme est un malade qui ignore la cause de son mal » (*De rerum natura*).

C'est vers le IVe siècle qu'apparaitra dans la vie monastique le terme d'acédie, néologisme grecque ancien, signifiant la privation de soi, la négligence (*acedia*) et décrite comme un manque de soin à l'égard de sa propre vie spirituelle (dépression spirituelle). L'acédie se distingue par une approche théologique de l'affect dépressif, alors que la mélancolie était liée à une notion physiologique chez les Grecs. Par ailleurs, elle sera considérée comme un péché contre Dieu par Saint François d'Assise. Cette acédie tendra à s'amenuiser, et deviendra *paresse* à partir du XIIIe siècle, décontextualisant ce péché théologique pour en faire un péché sociétal. A cette époque apparaitra également le lien entre amour contrarié et mélancolie, lien qu'expose le médecin Jacques Ferrand en 1610 dans *Traicté de l'essence et guérison de l'amour ou de la mélancholie érotique*,

précisant que *« l'Amour ou passion Érotique est une espèce de rêverie, procedante d'un désir déréglé de jouir de la chose aimable, accompagnée de peur, et de tristesse »*.

Le XVIIIe siècle, début du siècle des Lumières, période de la critique sociale, de l'esprit, des sciences, où la connaissance est promue face à l'obscurantisme, verra l'émergence des disciplines psychologiques et permettra l'évolution de la pensée à l'égard des maladies mentales. Le médecin Johann Christian Reil avancera le terme de *psychiatrie* en 1808 et considéra l'idée que les traitements des maladies psychiques répondent des méthodes médicales. La mélancolie empruntera à ce moment-là deux destins, celui de subsister comme trait des hommes de génies, prenant part au Romantisme (fin du XVIIIe siècle), incarnant chez l'artiste l'allégorie du tragique et du malheur dont le sublime est à la hauteur de l'esprit et renvoyant au questionnement d'Aristote; *« Pourquoi tous les hommes qui furent exceptionnels en philosophie, en politique, en poésie ou dans les arts étaient-ils manifestement bilieux […] »*, et de l'autre, une maladie au sens médicale du terme pour l'homme commun. Maladie qui devient *« nerveuse »* quand les nerfs et le cerveau sont considérés comme le siège du comportement intellectuel et physique de l'individu, et qui sera *« interprétée comme la conséquence d'un choc psychique ou d'une tension excessive due aux circonstances extérieures »* (Jean Starobinski, *Histoire du traitement de la mélancolie des origines à 1900*).

Il faudra attendre le XIXe siècle pour que le terme dépression prenne un sens métaphorique. Provenant du latin *depressio*, qui signifie « enfoncement », il représentera de façon plus générale un état mental de lassitude, intégrante de la mélancolie, mais moins important. Esquirol, en 1819, reprendra le terme de mélancolie pour le classer en un délire partiel, qui nommera lypémanie, une monomanie où prédomine *« une passion triste et dépressive »*. La mélancolie deviendra par la suite un trouble distinct intégré à la manie (folie), que ce soit Jean Pierre Ferlet avec *la folie circulaire* (1854) ou encore Emil Kraepelin et ses travaux sur la psychose périodique *maniaco-depressive*, ils expliqueront qu'il existe une oscillation entre phase de manie et de dépression (deviendra le trouble bipolaire d'aujourd'hui). A noter qu'à cette époque, les étiologies des maladies mentales écartaient les altérations psychologiques et se centraient principalement sur les lésions neurologiques, exemple avec le psychiatre Valentin Magnan qui décrit la manie et la mélancolie comme syndromes pouvant relever d'étiologies telles que la paralysie, l'alcoolisme, l'épilepsie, la dégénérescence (théorie).

Vers la fin du XIXe siècle, apparaitra la neurasthénie, inventée par l'américain George Miller Beard (1860), qui va s'imposer comme la maladie de la vie moderne, amenant la notion de trouble fonctionnel et clivant le modèle de liaison syndrome – lésion des maladies. Elle est caractérisée par un épuisement nerveux prenant son étiologie dans le facteur social (vie moderne) (A Practical

Treatise on Nervous Exhaustion, 1869) et composera les bases de la notion d'exogène (conséquence d'un évènement externe induisant une réaction interne). Sigmund Freud, ainsi que Pierre Janet, s'intéresseront à l'étude de la neurasthénie et montreront, cette fois-ci, une notion d'endogène, résultante d'une origine psychique. La neurasthénie sera, par la suite, intégrée dans le spectre de la névrose.

Jusqu'à la fin de la Seconde guerre mondiale, la mélancolie de la psychose maniaco-dépressive restera l'entité majeur des formes de la dépression, gravitant autour des formes plus atténuées, dépression réactionnelle, et des formes névrotiques, dépression névrotique. L'avènement de la sismothérapie (appelée aujourd'hui l'électro-convulsivothérapie (ECT)) en 1940, va grandement améliorer les troubles de l'humeur et son utilisation va dépasser le seul cadre de la mélancolie. Par la suite, et avec l'arrivée des traitements chimiques, la notion de dépression va prendre son essor et va devenir un trouble de l'humeur à part entière où sera finalement réorganisée la mélancolie.

On ne peut que constater, de par cette brève rétrospective, l'hétérogénéité sémantique et la difficulté sémiologique que la dépression a parcouru durant des siècles, et on se rend bien compte que l'étiologie de ce mal, qui est au carrefour de multiples disciplines, reste encore de nature indistincte et grandement discutée aujourd'hui.

A ce jour, la dépression est à mettre dans les troubles dépressifs, et le terme en lui-même se réfère surtout à la dépression majeure ou trouble dépressif caractérisé persistant.

2 LE TROUBLE DEPRESSIF AUJOURD'HUI

Le trouble dépressif fait partie des troubles de l'humeur dit unipolaire, c'est-à-dire qui ne s'exprime qu'en une seule humeur sans alternance périodique avec une autre. Un trouble dépressif est déterminé à la suite d'**épisodes dépressifs caractérisés** (EDC) et peut-être d'intensité légère, modérée ou sévère.

2.1. L'épisode dépressif caractérisé (EDC)

2.1.1. Diagnostic

Selon la 5ème édition du *Diagnostic and Statistical Manual of Mental Disorders* (DSM-V), le diagnostic établit d'un épisode dépressif caractérisé doit faire état des critères suivants : présenter au moins 5 des symptômes listés ci-dessous, en incluant une humeur dépressive ou une anhédonie, et ce sur une période d'au moins 2 semaines.

Liste des symptômes relatifs à un trouble dépressif, établie par la DSM-V :

- Humeur dépressive (sentiment de tristesse ou vide).
- Anhédonie.
- Perte ou gain de poids significatif ou d'appétit.
- Insomnie ou hypersomnie.
- Agitation ou ralentissement psychomoteur.
- Fatigue ou perte d'énergie.
- Sentiment de dévalorisation ou de culpabilité excessive ou inappropriée.
- Diminution de l'aptitude à penser ou à se concentrer ou indécision.
- Pensées de mort ou idées suicidaires récurrentes.

2.1.2. Formes cliniques

Il existe plusieurs formes cliniques distinctes pouvant préciser le caractère de l'EDC. On retrouvera la caractéristique mélancolique, forme très sévère présentant une forte probabilité suicidaire et associée à une intense humeur dépressive, le caractère atypique, se distinguant par une humeur réactive et positive s'opposant à l'humeur dépressive habituelle (anhédonie paradoxale), le caractère psychotique, relevant de la même symptomatologie que l'épisode mélancolique avec association d'idées psychotiques (délires ou hallucinations), et enfin, la détresse anxieuse et le caractère post partum.

2.2. Les types de troubles dépressifs

En fonction du contexte de manifestation et également de la progression du ou des épisodes, il est défini, selon la DSM-V, différents types de troubles dépressifs.

2.2.1. Trouble dépressif caractérisé

Le trouble dépressif caractérisé correspond à la présence d'épisodes dépressifs caractérisés, c'est-à-dire, à une humeur dépressive latente occupant une importante part de la journée, et ce, sur plusieurs jours consécutifs, sans inclure spécifiquement les symptômes de variations de poids et de pensées suicidaires.

2.2.2. Trouble disruptif avec dysrégulation émotionnelle

Ce trouble désigne l'expression d'une dérégulation émotionnelle centrée sur un état d'irritabilité sévère et persévérant. Il y a manifestation régulière de crises de colère et une importante humeur d'irritabilité qui persistent depuis au moins 1 an.

2.2.3. Trouble dépressif persistant

L'humeur dépressive est récurrente et se manifeste depuis plus de deux ans tous les jours. Il peut faire suite à des épisodes dépressifs caractérisés ou une dépression caractérisée. Ce trouble réunit la dépression majeure et la dysthymie explicitée dans l'ancienne version du DSM (DSM-IV).

2.2.4. Trouble dysphorique prémenstruel

Le trouble dysphorique prémenstruel se rapporte à une symptomatologie dépressive durant le cycle menstruel et peut résulter d'une instabilité émotionnelle, d'une forte anxiété ou de manifestations physiques (douleurs musculaires, articulaires, tensions mammaires).

Enfin, il existe également des troubles dépressifs induit par une substance ou encore dû à une autre affection médicale.

3 EPIDEMIOLOGIE

Selon l'Organisation Mondial pour la Santé, les troubles dépressifs représentent le 1er facteur de morbidité et d'incapacité sur le plan mondial et deviendront la seconde cause d'invalidité d'ici 2020. On estime à plus de 300 millions le nombre de personnes souffrant de troubles dépressifs, avec une prévalence de l'EDC en France aux alentours de 7,5 % au cours des douze derniers mois (Baromètre santé de l'Inpes, 2010). La dépression majeure (trouble dépressif persistant) atteint près de 24 % de la population française, avec deux fois plus de risques chez les femmes que les hommes (Lépine and Briley, 2011). Pour un coût annuel total estimé à 118 milliards d'euros en Europe, ce qui représente près de 1% de l'économie européenne totale (PIB), la dépression correspond au plus onéreux des troubles mentaux (Sobocki et al., 2006). L'incidence de cette maladie sur la qualité de vie des patients est préoccupante et la dépression pose un problème de santé majeur à travers le monde. Malgré les avancées des recherches dans ce domaine, il reste encore de nombreuses zones d'incompréhension sur la physiopathologie de ce mal du siècle.

4 LA BIOLOGIE DE LA DEPRESSION

Avant de s'attarder sur les causes et conséquences biologiques de la dépression, il est important de rappeler que cette pathologie repose aussi sur un aspect psychologique et social. Brièvement, il semblerait qu'il existe une relation prédictive entre l'état et les traits émotionnels, et la dépression. En effet, une tendance permanente à l'expérience des émotions négatives ou une attitude négative serait précurseur du développement et de la persistance du trouble dépressif majeur (Morris et al., 2009), ce qui concorde avec l'idée fonctionnaliste qui lie l'émotion à l'adaptation. Il existe également des travaux mettant en lumière la conséquence de l'environnement social dans l'étiologie de la maladie, par exemple des événements indésirables de la vie et le faible soutien social sont des

facteurs de risque connus de dépression (Paykel et al., 1969), ou encore, un traumatisme durant l'enfance, supplémenté d'une réponse à un stress, accroit le risque d'une dépression à l'âge adulte (Heim et al., 2008). Par ailleurs, selon le degré de l'épisode dépressif de départ, il existe une vulnérabilité plus ou moins importante de l'influence sociale sur l'issue d'une dépression majeure (Leskelä et al., 2006).

Sur le plan biologique, c'est le cerveau, médiateur du comportement animal, qui fait l'objet d'une attention particulière dans l'étude des causes et conséquences du trouble dépressif. Les recherches basées sur le système nerveux central apportent des éléments de réponses dans la compréhension et la biologie de la pathologie, en s'appuyant notamment sur des dysfonctionnements et dérégulations aux niveaux anatomiques et biochimiques.

4.1. Anomalies cérébrales

L'imagerie cérébrale connait une croissance notable dans l'étude de la dépression depuis plusieurs années et les techniques utilisées ont permis de mettre en lumière des anomalies cérébrales au niveau de la morphologie, de l'activité et également des circuits neuronaux (Pandya et al., 2012).

4.1.1. Anomalies corticales

Les régions corticales associées à la dépression sont le cortex préfrontal dorsolatéral et ventromédian, le cortex orbitofrontal, le cortex cingulaire antérieur dorsal et ventral et l'insula (**Figure 1**).

4.1.1.1. Le cortex préfrontal

Situé dans la partie antérieure du lobe frontal, excluant la région postérieure motrice, le cortex préfrontal (CPF) a un rôle central dans le traitement et le contrôle de l'information émotionnelle. Le CPF fait partie d'un réseau neuronal étendu qui projette et intègre de nombreuses connexions avec d'autres régions, qui sont notamment responsables du contrôle de la dopamine, de la noradrénaline et de la sérotonine, trois neurotransmetteurs importants dans la régulation de l'humeur.

La partie dorsolatérale du CPF, qui joue un rôle dans la planification et les fonctions exécutives, présente une baisse d'activité chez les patients dépressifs, traduite par une diminution du flux sanguin et du métabolisme glucidique (Kimbrell et al., 2002) et, de façon intéressante, il est possible de reverser cette activité par un traitement antidépresseur (Mayberg et al., 1999). En outre, une lésion de cette même région peut entrainer une vulnérabilité au développement d'une dépression (Koenigs et al., 2008).

Le CPF ventromédian est impliqué dans l'évaluation du potentiel de récompense des stimuli. Il projette des afférences directement sur l'amygdale, et joue donc un rôle dans l'inhibition de réactions émotionnelles, et dans le processus décisionnel. A l'inverse du CPF dorsolatéral, il existe une hyperactivité cérébrale chez les patients dépressifs (Drevets et al., 1992) et une lésion bi-latérale de la région entraine un faible risque de dépression (Koenigs et al., 2008).

4.1.1.2. Le cortex cingulaire antérieur

Le cortex cingulaire antérieur (CCA) a également un rôle prépondérant dans la physiopathologie de la dépression. Chez les patients dépressifs, il apparait une diminution du métabolisme glucidique dans le cortex cingulaire antérieur **ventral** (Drevets et al., 1997) mais également des anomalies dans la partie **dorsale** et **ventrale** du CCA (Mayberg et al., 1999). Il existe une division fonctionnelle du CCA entre sa partie dorsale et ventrale, en effet, **le CCA dorsal** est impliqué dans l'aspect cognitif des émotions, y compris la résolution des conflits de stimuli émotionnels avec valence négative (Etkin et al., 2006; Vogt et al., 1992), tandis que **le CCA ventral** ou subgenual, joue un rôle dans l'aspect affectif de l'émotion. Ce dernier est connecté aux régions limbiques tels que l'amygdale, le thalamus dorsomédian et l'hippocampe mais également au cortex orbitofrontal et CPF ventromédian, ce qui l'implique dans la régulation de la réponse émotionnelle (Critchley, 2004; Vogt et al., 1992). Le CCA ventral a également des connexions vers l'hypothalamus, impliqué dans la réponse au stress.

4.1.1.3. Le cortex insulaire

L'insula est une structure du cortex cérébral située dans la profondeur de la scissure de Sylvius, le sillon latéral, et est subdivisée en deux parties : une large insula antérieure et une petite insula postérieure. Les parties antérieure et postérieure de l'insula reçoivent des afférences du noyau ventral du thalamus, et la partie antérieure projette et reçoit des afférences directement de l'amygdale. Son implication prend part dans l'autosuggestion, le dégout, l'évaluation des états viscéraux internes, et la réponse aux stimuli du goût et de l'odorat. Chez les patients déprimés, il existe une augmentation de la sensibilité de l'insula face à des stimuli négatifs (Surguladze et al., 2010) mais également, il apparait une réduction du volume cérébral dans cette région (Sprengelmeyer et al., 2011).

4.1.2. Anomalies des régions limbiques

L'hippocampe, l'amygdale et l'hypothalamus sont les principales régions affectées par la dépression (**Figure 1**). Elles font partie du système limbique, système qui représente le régulateur central du comportement et plus particulièrement des émotions comme la peur, le plaisir et l'agressivité, et joue également un rôle crucial dans les mécanismes mnésiques.

L'hippocampe, structure localisée dans le lobe temporal médian, est impliqué dans la mémoire, la navigation spatiale et également dans l'inhibition du comportement. On suggère son implication dans le comportement émotionnel par l'existence de connexions avec des structures associées comme le septum, l'hypothalamus et le complexe nucléaire antérieure du thalamus, d'où son inclusion dans le système limbique. Chez les personnes souffrant d'une dépression, le volume hippocampique est significativement réduit (Lorenzetti et al., 2009), et de façon intéressante, les patients en rémission, après traitement, présentaient un volume hippocampique de départ plus important que ceux qui ne répondaient pas aux traitements, suggérant une sensibilité de réponse induite par l'hippocampe (MacQueen et al., 2008). Concernant **l'amygdale**, c'est une structure qui se situe dans le lobe temporal en avant de l'hippocampe et qui est impliquée dans la reconnaissance et l'évaluation de la valence émotionnelle des stimuli sensoriels, dans l'apprentissage associatif et dans les réponses comportementales et végétatives associées en particulier dans la peur et l'anxiété. Il existe, comme dans l'hippocampe, une atrophie de l'amygdale lors d'une dépression majeure (Hamilton et al., 2008), mais également une hyperactivation cérébrale (Drevets et al., 2002) qui engendrerait une importante stimulation de l'axe hypothalamique pituitaire surrénalien (HPA) et par conséquent une sécrétion de l'hormone du stress, le cortisol.

Il demeure également d'autres structures cérébrales étudiées lors d'une dépression majeure, comme le striatum ou encore le thalamus, mais il apparait des divergences dans les résultats obtenus et ils ne permettent pas de statuer sur les conséquences exactes de l'affect dépressif sur leurs morphologies ou l'activité cérébrale.

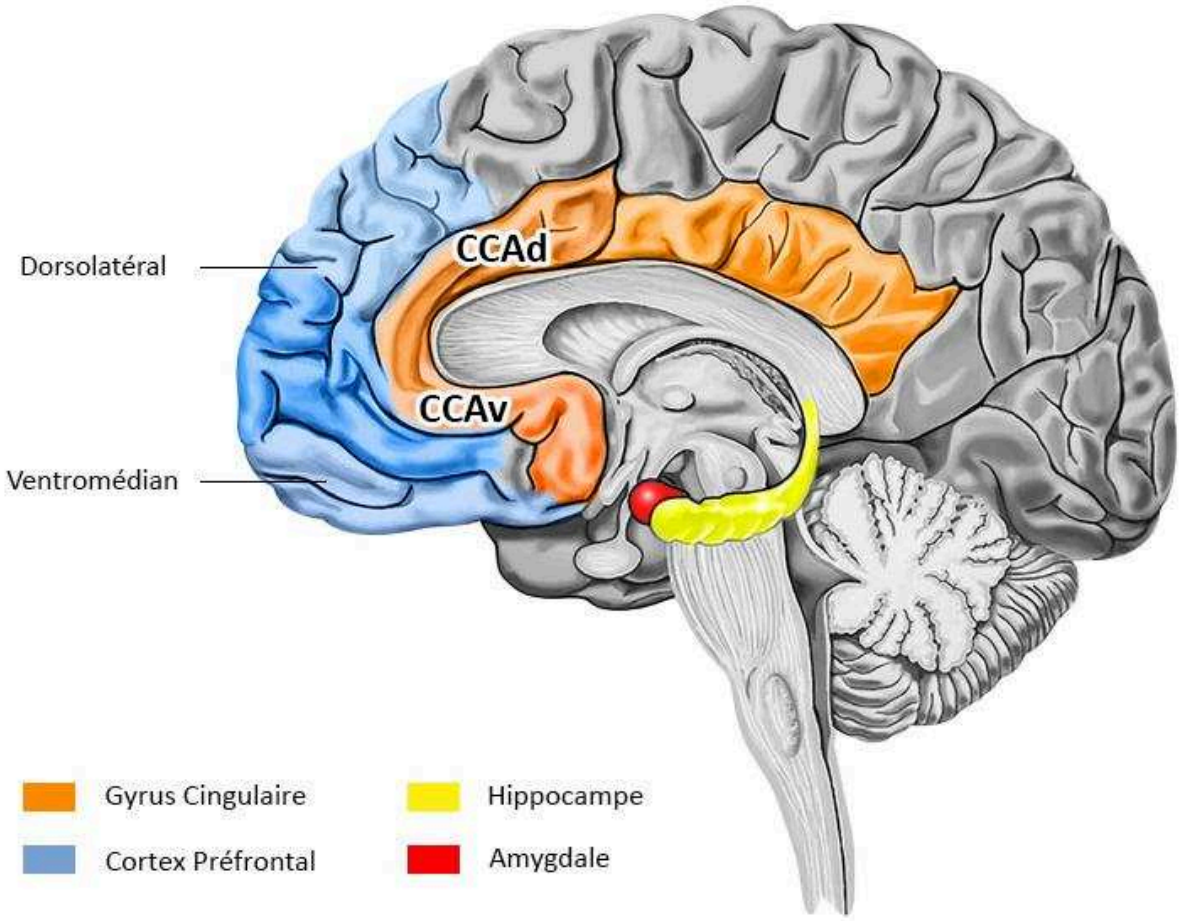

*Figure 1 : Régions des anomalies cérébrales impliquées dans la dépression majeure. - **CCAd :** Cortex Cingulaire Antérieur dorsal **; CCAv :** Cortex Cingulaire Antérieur ventral*

4.2. L'hypothèse monoaminergique : la sérotonine

C'est sur une découverte fortuite que l'hypothèse d'un déficit en monoamines est apparue. En effet, deux familles de molécules, mises au point pour des affections non psychiatriques, à savoir l'iproniazide et l'imipramine, ont eu de puissants effets antidépresseurs chez l'homme et se sont révélées par la suite capables d'accroître la transmission de la sérotonine (5-hydroxytryptamine (**5-HT**)) ou de la noradrénaline, ce qui a suggéré l'existence d'un déficit dans ces neurotransmetteurs. Cette hypothèse est largement admise, cependant, seulement quelques études ont tenté de réellement mettre en évidence cette insuffisance chez les patients dépressifs. Une première approche a été d'abaisser le taux de sérotonine et d'en évaluer les conséquences. La méthode consiste à réduire la concentration plasmatique et cérébrale du tryptophane, précurseur de la sérotonine, en administrant un régime avec un mélange d'acides aminés exempt de ce dernier. Comme la conversion du tryptophane en 5-hydroxytryptophane par le tryptophane hydroxylase

(**Figure 2**) est l'étape limitante de synthèse de la sérotonine, il a été possible de produire une baisse transitoire de l'activité 5-HT cérébrale. Les résultats suggèrent qu'il n'y a pas de changement significativement de l'humeur chez des patients sains, cependant les patients dépressifs en rémission, après un traitement, présentent un retour temporaire des symptômes dépressifs (Smith et al., 1997). En outre, l'existence d'un taux anormalement faible d'acide 5-hydroxyindole acétique (5-HIAA) (**Figure 2**), le principal métabolite de la sérotonine, a été retrouvé dans le liquide céphalorachidien de personnes dépressives ayant fait au moins une tentative de suicide (Asberg, 1997), ce qui soutient l'hypothèse du déficit de sérotonine. Dernièrement, ce sont les récepteurs de la sérotonine qui ont fait l'objet d'une investigation afin d'évaluer leurs implications dans la maladie. Parmi les 30 protéines réceptrices différentes identifiées (Raymond et al., 2001), ce sont surtout les autorécepteurs 5-HT_{1A} qui semblent responsables ; leurs densités s'avèrent réduites dans le noyau du raphé dorsal, principale localisation des neurones sérotoninergiques, chez les patients déprimés et suicidaires (Arango et al., 2001), et une délétion génique chez la souris, induit une perte de sensibilité à l'effet antidépresseur de la fluoxétine (Mayorga et al., 2001). Il semble réellement exister une corrélation entre la sérotonine et ces récepteurs dans l'étiologie de la dépression, et à l'heure actuelle, les traitements les plus efficaces restent encore les modulateurs de la neurotransmission sérotoninergique.

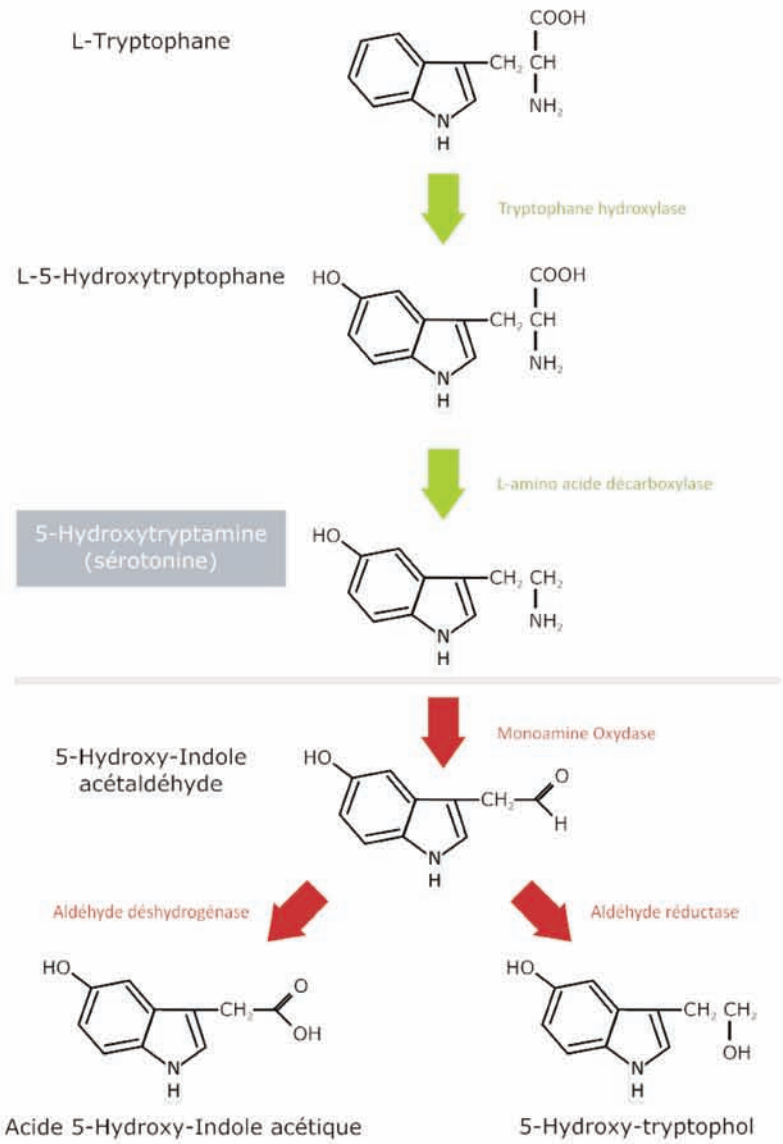

Figure 2 : Synthèse et dégradation de la sérotonine

4.3. Neurogénèse et BDNF

S'il existe bien une diminution volumétrique des aires cérébrales dans la dépression, il demeure néanmoins des questions sur ces origines. L'hypothèse la plus communément admise s'appuie sur la diminution des facteurs neurotrophiques responsables de la neurogenèse. Ces facteurs de croissance, exprimés dans le développement neuronal, régulent la plasticité cérébrale chez l'adulte (Monteggia et al., 2004). Le facteur neurotrophique qui porte le plus d'intérêt aujourd'hui est le facteur neurotrophique dérivé du cerveau ou BDNF (Brain-derivated neurotrophic factor), exprimé notamment dans l'hippocampe, il est crucial dans la croissance et la viabilité neuronale, et la plasticité synaptique. Une délétion de son gène entraine des conséquences cérébrales graves et peut être léthale chez la souris. La mutation génétique humaine, qui substitue une valine en méthionine (Val66Met) dans son prodomaine, empêche sa libération et provoque une

diminution du volume hippocampique et des troubles de mémoire et d'apprentissage (Bath and Lee, 2006). Dans la dépression, il subsiste un affaiblissement du taux plasmatique et sérique du BDNF (Cunha et al., 2006; Palomino et al., 2006), mais également un déficit au niveau hippocampique, de pair avec une baisse de l'expression des ARNm, de son récepteur TrkB et de la protéine CREB (C-AMP Response Element-binding protein), observés post-mortem sur des patients ayant commis un suicide (Dwivedi et al., 2003; Karege et al., 2005). Autre point intéressant, les antidépresseurs permettent une augmentation de l'expression du BDNF, notamment dans l'hippocampe (Chen et al., 2001), et une injection bilatérale de BDNF dans le gyrus denté révèle des effets antidépressifs (Shirayama et al., 2002). Le BDNF a une contribution non négligeable dans l'affect dépressif et se pose comme une cible potentielle dans la régulation de ce trouble.

4.4. Stress et dépression

Les facteurs de stress environnants, en particulier le stress interpersonnel et le rejet social, sont connus pour favoriser le risque d'apparition d'une dépression majeure. Dans ce schéma dépressogène, l'acteur prééminent est l'axe hypothalamo-hypophyso-surrénalien (HPA), qui joue un rôle dans l'adaptation au stress. Lors d'un stress, les régions associatives corticales et limbiques (hippocampe et amygdale) sont stimulées et envoient un message nerveux vers l'hypothalamus qui va ensuite synthétiser le CRH (corticotropin-releasing hormone), neurohormone qui va être libérée dans le sang vers l'hypophyse, où elle va induire la maturation et la libération d'ACTH (adrenocorticotropin hormone) en activant les récepteurs spécifiques des cellules endocrines. Par la suite, l'ACTH va stimuler la glande surrénale qui va pouvoir synthétiser les glucocorticoïdes, notamment le cortisol qui engendre une libération d'adrénaline et noradrénaline, permettant, entre autres, de mobiliser les muscles en augmentant le métabolisme glucidique (glycolyse) et de produire une réponse adéquate à la situation. Cette réponse se termine par à un rétrocontrôle négatif des glucocorticoïdes sur leurs récepteurs (récepteurs glucocorticoïde, GR) hypophysaires et hypothalamiques, empêchant la libération d'ACTH, et réduisant la cortisolémie (**Figure 3**).

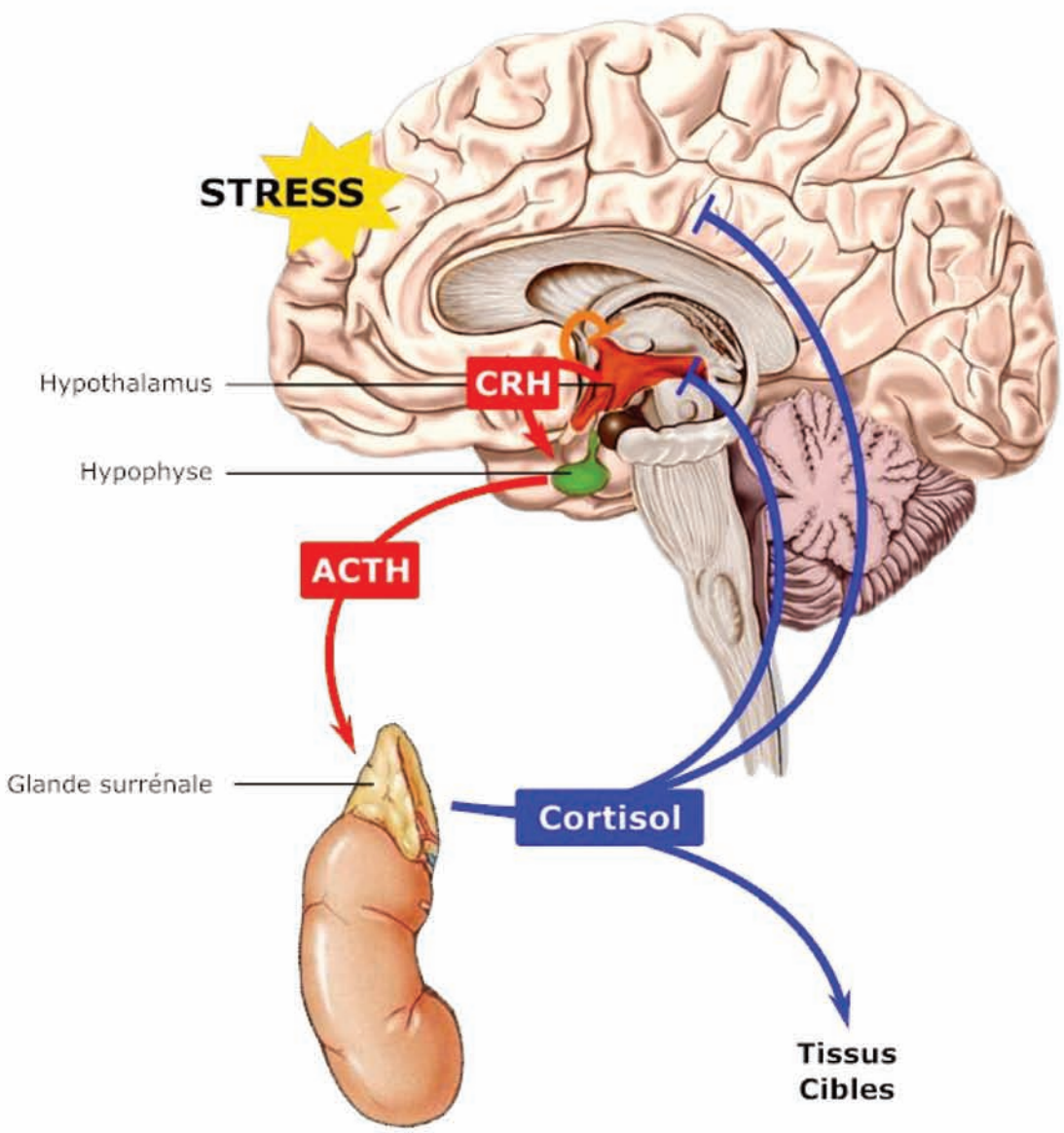

Figure 3 : Régulation de l'axe hypothalamo-hypophyso-surrénalien dans le stress. ***– CRH :*** *Corticotropin-Releasing Hormone ;* ***ACTH :*** *Adrenocorticotropin Hormone*

Au cours d'une dépression majeure, les patients présentent un taux élevé de cortisol plasmatique, une augmentation de CRH dans le liquide céphalo-rachidien, mais également une augmentation de l'expression d'ARN messager et protéique de CRH dans les régions limbiques et corticales (Burke et al., 2005; Merali et al., 2004). En outre, chez la majorité des patients dépressifs, il y a une absence de réponse au Dexaméthasone, glucocorticoïde de synthèse qui se fixe sur les GR de l'hypophyse et de l'hypothalamus et qui permet d'activer le rétrocontrôle négatif, indiquant un déficit dans l'autorégulation des glucocorticoïdes (Carroll et al., 2007). Enfin, au niveau anatomique, il y a une hyperplasie de la glande surrénale et une augmentation du volume de l'hypophyse.

L'hypothèse qui rend compte de ces anomalies suggère que l'hypercortisolémie, induite par l'augmentation de CRH, est responsable de l'hyperplasie des surrénales qui va, à posteriori, maintenir le cortisol circulant. Par la suite, l'exposition prolongée au cortisol va conduire à la désensibilisation des récepteurs glucocorticoïde à l'ACTH (Gold et al., 1986), mais également à la perte des neurones contenant les GR dans l'hippocampe (Sapolsky et al., 1984), d'où le déficit de la boucle de rétroaction négative des glucocorticoïdes. D'ailleurs, la délétion ciblée des GR dans le cerveau de souris adultes induit une augmentation de l'activité de l'axe HPA et conduit à une augmentation de l'immobilité dans les tests de résilience (Force Swim Test), et peut être reversées par les antidépresseurs (Boyle et al., 2005). Enfin, l'hypertrophie de l'hypophyse résulterait de l'augmentation de sécrétion de CRH dans le cerveau. Cette augmentation de CRH constante pourrait s'expliquer par la répétition prolongée des situations de stress avec une forte sensibilité à ces événements, qui va instaurer progressivement une stimulation autonome de l'axe HPA.

Le stress altère également la neurogénèse et le BDNF, mais aussi la réponse sérotoninergique. La contention de souris par l'intermédiaire d'une enceinte restreinte, accroit le stress et produit un remodelage réversible des dendrites apicales des neurones pyramidaux CA3 et la suppression de la neurogenèse, avec une diminution d'expression de BDNF, dans le gyrus denté, changements morphologiques associés aux déficits de mémoire dépendante de l'hippocampe (Angelucci et al., 2005; Reagan et al., 2004). Les neurones sérotoninergiques du noyau dorsal du raphé augmentent leurs fréquences de décharges en réponse à un stress aigu. Quand le stress devient chronique, il y a une altération de la décharge, probablement induite par une désensibilisation des récepteurs 5-HT, notamment 5-HT_{A1}, pouvant être responsable du déficit monoaminergique (Mahar et al., 2014).

5 STRATEGIES THERAPEUTIQUES

5.1. Les stratégies pharmacologiques

Les traitements les plus représentés dans la sphère thérapeutique de la dépression, sont les molécules ciblant le déficit monoaminergique. Le mode d'action de ces antidépresseurs se focalise principalement sur des mécanismes permettant de réguler le niveau des neurotransmetteurs et notamment la sérotonine. Deux schémas de mécanismes sont utilisés : l'inhibition du système de dégradation des monoamines et celui de la recapture des monoamines. On retrouve donc la classe des antidépresseurs inhibiteurs de la monoamine oxydase (**IMAO**) (système de dégradation) et les inhibiteurs de la recapture ; les antidépresseurs Tricycliques (**ATC**) et les inhibiteurs spécifiques de la recapture de la sérotonine (**ISRS**).

5.1.1. Inhiber les monoamines oxydase

La monoamine oxydase (MAO) est une enzyme présente dans la membrane mitochondriale externe des cellules neuronales et non neuronales. Elle est responsable de la désamination oxydative des monoamines endogènes avec fonctions de neurotransmission : noradrénaline, adrénaline, dopamine, sérotonine et, indirectement, tyramine (Baker et al., 1985). Les MAOs sont des flavoprotéines présentent sous 2 isoformes, la monoamine oxydase-A (MAO-A), qui désamine préférentiellement la sérotonine, noradrénaline et adrénaline, et la monoamine-oxydase B (MAO-B), qui cible la dopamine (Strolin Benedetti and Dostert, 1987). De façon prédominante, ce sont les inhibiteurs de la MAO-A qui sont utilisés, de par leur action sur les neurotransmetteurs considérés comme essentiels dans la dépression, à savoir la noradrénaline et la sérotonine (**Figure 4**).

5.1.2. Inhiber la recapture des monoamines

La seconde cible des antidépresseurs est le système de recapture des monoamines au niveau présynaptique. Le mode d'action vise directement les transporteurs qui permettent de recouvrer une partie des neurotransmetteurs libérés dans la fente synaptique. D'une part, il y a les ATC, qui inhibent la recapture de manière compétitive en se fixant sur le site de liaison des transporteurs de la transmission sérotoninergique et noradrénergique (Delgado and Moreno, 1999). D'autre part, on retrouve les ISRS, les antidépresseurs les plus largement utilisés pour réduire les symptômes de la dépression, incluant le plus connu, la fluoxétine (Prozac ®). A la différence des autres classes d'antidépresseurs, les ISRS inhibent de façon sélective le transport de la sérotonine, SERT, au niveau présynaptique, et permet ainsi d'augmenter le niveau de 5-HT (**Figure 4**). L'avantage d'une telle sélectivité est la suppression en grande partie des effets secondaires incommodant retrouvés dans les classes précédentes, sans pour autant perdre l'efficacité antidépresseur (Hyttel, 1994).

En considérant le déficit monoaminergique comme un pivot dans la dépression, il y une évidence dans l'utilisation des IMAO, ATC et ISRS pour pallier à cette insuffisance. Cependant, il subsiste des contraintes à l'utilisation de ce type de molécule pharmacologique. D'une part, les effets secondaires sont nombreux ; les ATC provoquent des effets anticholinergiques périphériques et centraux (sécheresse buccale, constipation, rétention urinaire, mydriase, vision trouble et tachycardie, confusion mentale, tremblements des extrémités, risques épileptogènes) ou encore une sédation, de même que les IMAO et ISRS peuvent provoquer des nausées, constipation ou diarrhées, insomnies et migraines. D'autre part, les effets bénéfiques ne sont pas immédiats et nécessitent un temps d'adaptation de 21 jours en moyenne (Manji et al., 2001). Enfin, le diagnostic de la pathologie nécessite d'être précis, car, en vue des différentes formes du trouble dépressif, la réponse au traitement antidépresseur peut varier et même être négative. Le développement de nouvelles

molécules gravite toujours autour de la défaillance monoaminergique mais cherche à réduire les effets secondaires. A noter qu'il existe des traitements pharmacologiques avec action différente mais qui prouvent une efficacité certaine, comme les thymorégulateurs (le lithium, l'acide valproïque, la lamotrigine), l'agomélatine (analogue de la mélatonine), le bupropion et le pramipexole (dopaminergiques) ou encore les hormones thyroïdiennes.

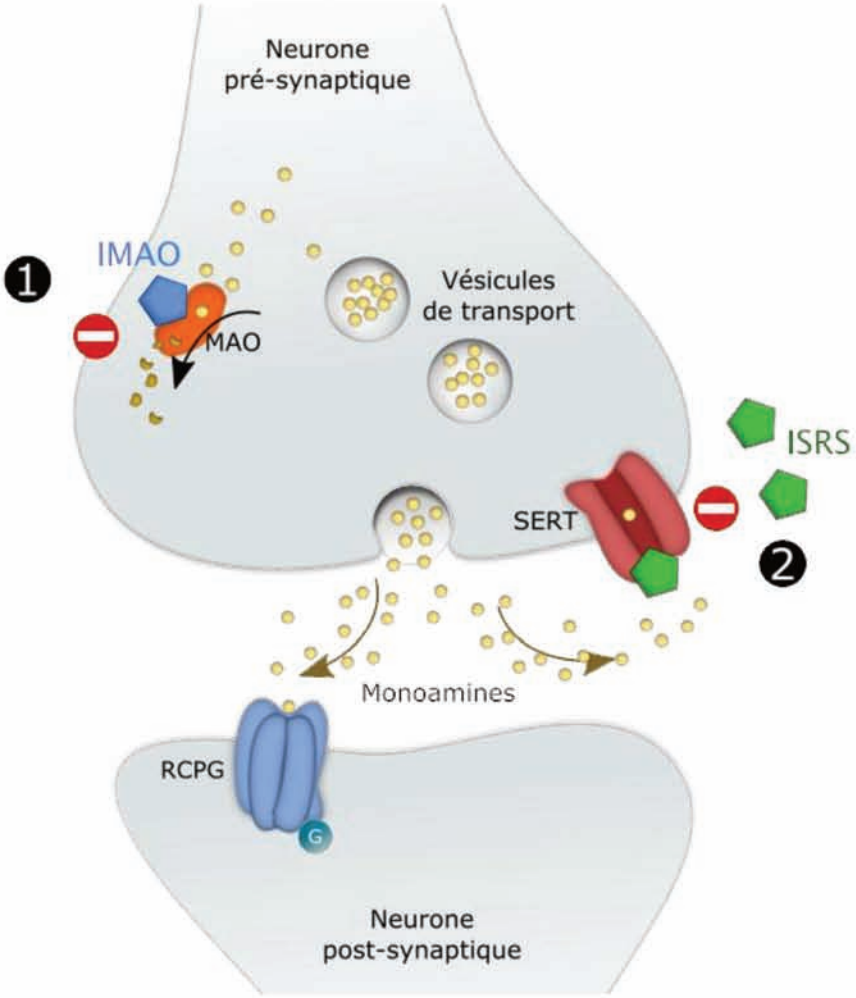

Figure 4 : Mécanismes d'action des antidépresseurs. 1) Inhibition de la dégradation par les inhibiteurs de monoamine oxydase, 2) Inhibition de la recapture par les ISRS en bloquant SERT. D'après (Elhwuegi, 2004).

5.2. Les stratégies non-pharmacologiques

En dehors d'une thérapeutique pharmacologique, il existe aussi des méthodes psychologiques et, plus invasives, des méthodes de stimulation cérébrale, qui sont généralement employées en complément d'antidépresseurs ou lorsque ces derniers sont inefficaces. La psychothérapie ou encore la thérapie cognitivo-comportementale, permet de faire un travail psychologique avec le patient afin d'identifier les causes et d'améliorer le comportement et la pensée. Les stimulations cérébrales consistent à appliquer une stimulation électrique soit générale

sur le crâne du patient (électroconvulsivothérapie, **ECT**), soit de manière plus invasive mais ciblée (stimulation cérébrale profonde, *Deep Brain Stimulation*, **DBS**), en insérant une électrode directement sur des zones spécifiques du cerveau par stéréotaxie. L'ECT et le DBS sont des méthodes particulièrement efficaces pour traiter les troubles de la dépression (Perrin et al., 2012), et sont surtout utilisées pour les cas les plus sévères. Malgré l'efficacité du traitement, les mécanismes induit ne sont pas encore connus et il existe néanmoins des effets secondaires, comme une perte de mémoire transitoire, un gain de poids ou encore un changement de personnalité (Sackeim et al., 2007).

Conclusion

La compréhension du trouble dépressif représente un investissement important face au nombre grandissant de personnes touchées chaque année. Maladie d'atteinte psychologique et biologique, incriminant un des organes les plus complexe et élaboré qu'est le cerveau, les causes et conséquences de cette pathologie s'appuient sur de nombreux axes disciplinaires, complexifiant l'émergence d'approches thérapeutiques efficaces pour une réelle guérison. Les traitements actuels tentent principalement d'améliorer l'humeur des patients, en modulant l'hypothétique déficit monoaminergique ou, dans les cas les plus critiques, en stimulant électriquement le cerveau. Techniques d'usage acceptées, efficientes, mais parfois utilisées sans compréhension intégrale du modèle mécanistique, les effets ne sont pas immédiats, la période de traitement est généralement longue, les effets secondaires marqués et parfois, on note l'apparition d'un syndrome de sevrage à l'arrêt du traitement. Le besoin réel de trouver de nouveaux traitements semble univoque, tant pour la compréhension de cet affect psychologique, que pour soulager les patients.

6 LE CANAL TREK-1, ACTEUR EMERGENT DANS LA DEPRESSION

Récemment, des études précliniques basées sur des modèles expérimentaux de souris, ont apporté des preuves convaincantes impliquant le canal potassique TREK-1 (TWIK-Related K+ channel 1) dans la physiopathologie de la dépression (Heurteaux et al., 2006).

6.1. Généralités sur les canaux potassiques

Les canaux potassiques sont des canaux ioniques largement répandus chez les organismes vivants et ont pour fonctions la régulation de nombreux processus cellulaires. Ce sont des protéines membranaires permettant le passage sélectif du potassium à travers la membrane. On les retrouve dans l'excitabilité neuronale, où ils sont responsables des potentiels d'action et définissent le potentiel de repos membranaire, la nociception et le volume cellulaire. Les canaux potassiques sont regroupés en trois grandes classes basées sur leur organisation structurale (Lesage et al., 1997) ; **1)** les canaux à 6 segments transmembranaires et un domaine pore (**6TM-1P**), contenant les canaux

voltage dépendants (K_v) et activés par le calcium (BK et SK), **2)** les canaux à 2 segments transmembranaires et un domaine pore (**2TM-1P**), qui sont des canaux à rectification entrante activés par les protéines G ou ATP sensible (K_{IR} et K_{ATP}) et, enfin, **3)** les canaux à 4 segments transmembranaires et 2 domaines pore, les K_{2P} (**4TM-2P**), des canaux de fond contribuant au potentiel de repos incluant TREK-1 (**Figure 5**).

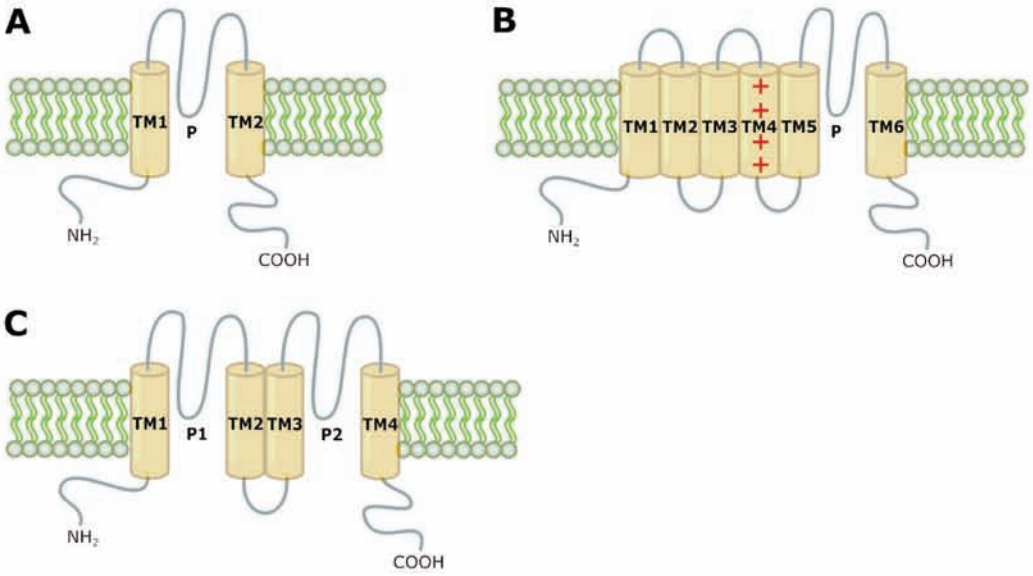

Figure 5 : Les classes des canaux potassiques. ***A)*** *Canaux à 2 segments transmembranaires et un domaine pore.* ***B)*** *Canaux à 6 segments transmembranaires et un domaine pore.* ***C)*** *Canaux à 4 segments transmembranaires et 2 domaines pore.*

6.2. La classe des K_{2P}

Cette classe ne représente pas moins de 15 types de canaux, qui sont regroupés en six sous-familles (TWIK, TASK, TALK, THIK, TRESK et TREK) sur la base de similitudes dans leur séquence d'acides aminés et leurs propriétés fonctionnelles (**Figure 6)**.

Les canaux TWIK (Tandem of pore domains in a Weak Inward rectifying K+ channe), TWIK-1, TWIK2 et KCNK7, sont des canaux à faible rectification entrante de courant potassique, dont l'expression a été détectée dans plusieurs tissus, notamment les reins, le cerveau et les poumons (Arrighi et al., 1998; Chavez et al., 1999; Lesage et al., 1996; Patel et al., 2000).

Les canaux TASK (TWIK-related Acid-Sensitive K+ channel), clonés à partir de rein humain, sont des canaux sensibles aux variations du pH extracellulaire physiologique (Duprat et al., 1997). Ils sont inhibés par une acidification extracellulaire tandis qu'un changement de pH intracellulaire n'affecte pas leur activité (Duprat et al., 1997). On les retrouve dans la modulation de fonctions comme la chemoreception (Buckler et al., 2000), la détection de l'hypoxie (Hartness et al., 2001), la vasoconstriction pulmonaire (Gardener et al., 2004), l'excitation des motoneurones (Talley et al.,

2000), la régulation de la décharge de potentiels d'actions (Brickley et al., 2007), l'épilepsie ou encore l'apoptose (Lauritzen et al., 2003).

Les canaux TALK (TWIK-related Alkaline pH- activated K+ channel), qui regroupent TASK-2, TALK-1 et TALK-2 (Reyes et al., 1998), sont également des canaux sensibles à la variation de pH comme les TASK, à la différence que cette sensibilité se situe dans des pH alcalins. TASK-2 est impliqué dans la réabsorption du bicarbonate dans le rein. L'augmentation du transport du bicarbonate dans les cellules tubulaires proximales alcalinise le compartiment basolatéral et active une conductance potassique (Warth et al., 2004). On le retrouve également impliqué dans le potentiel de repos des cellules musculaires lisses de l'artère pulmonaire chez le rat (Gönczi et al., 2006). En ce qui concerne TALK-1 et TALK-2, ils sont activés par l'oxyde nitrique (NO) et les espèces réactives d'oxygène (Duprat et al., 2005) et sont proposés comme cibles auxiliaires lors de la stimulation physiologique vagale.

Les canaux THIK (Tandem pore domain Halothane-Inhibited K+ channel), THIK-1 et THIK-2, produisent une fuite de courant potassique et ne sont pas influencés par l'acidification ou par le changement de température, mais peuvent être inhibé par l'halothane (Rajan et al., 2001).

La famille TRESK (Twik-Related Spinal Cord K^+ channel), qui ne contient qu'un seul canal (KCNK18), a été cloné à partir de moelle épinière humaine (Sano et al., 2003) et peut être régulé par le calcium ou par interaction protéique. Une augmentation expérimentale de calcium cytosolique est suffisant pour activer le canal (Czirják et al., 2004) et une coexpression de TRESK avec le récepteur M_3 muscarinique l'active de 40 à 80 % dans des cellule COS-7 (Kang and Kim, 2006).

Et enfin, la famille des canaux TREK (TWIK-Related K+ channel) qui comporte TREK-1, TREK-2 et TRAAK (TWIK-related arachidonic acid activated K+ channel). TREK-1 a été le premier membre de cette classe à être identifié et à être caractérisé comme un canal potassique à rectification sortante (Fink et al., 1996). Ces canaux réagissent aux acides gras, à l'étirement mécanique, à la température, au pH et aux neurotransmetteurs par l'intermédiaire de récepteurs couplés aux protéines G (RCPG)(Feliciangeli et al., 2015).

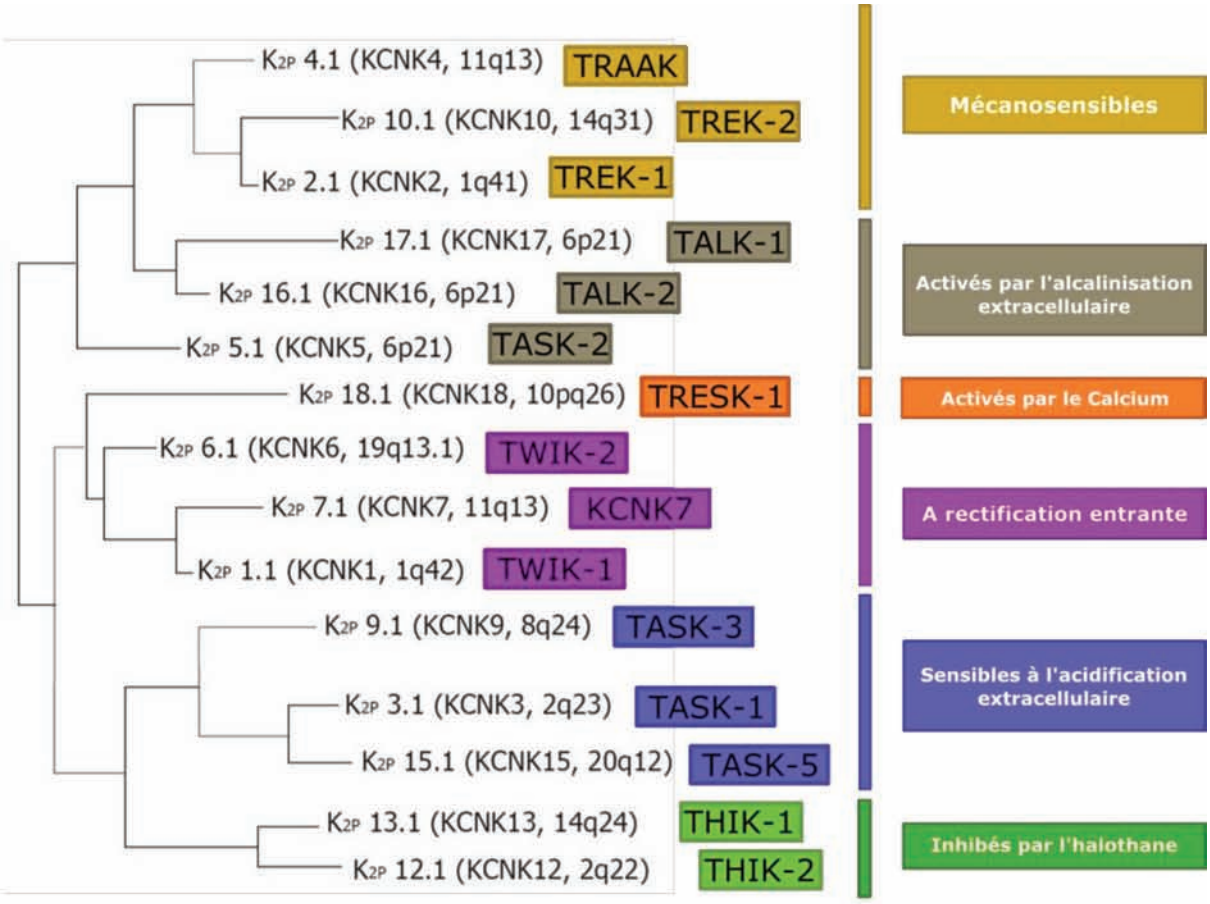

Figure 6 : Arbre phylogénique des K2P chez l'humain. D'après (Zhou et al., 2012)

6.3. Expression et localisation de TREK-1

TREK-1 chez l'homme est principalement exprimé dans le système nerveux central ; il est abondant dans le cerveau, la moelle épinière, le cœur, le rein, les ovaires et l'intestin grêle. Mais plus précisément, TREK-1 est fortement exprimé dans l'amygdale, les ganglions de la base, le cortex, les ganglions de la racine dorsal (DRG) et l'hippocampe. Il est retrouvé dans une moindre mesure dans la peau, les muscles, les testicules et la prostate (Chapman et al., 2000; Hervieu et al., 2001) et au niveau périphérique, dans le tractus gastro-intestinal et les neurones mécanosensibles qui innervent la vessie et le côlon, où il est impliqué dans la détection et la transduction des déformations de la peau et des organes.

6.4. Propriété électrophysiologique de TREK-1

Les canaux TREK-1 sont à l'origine de courants de fond qui permettent le maintien du potentiel de repos des cellules et leur excitabilité. TREK-1 a été caractérisé initialement comme un canal potassique à rectification sortante (Fink et al., 1996). Lorsque ces canaux sont ouverts, les ions potassium passent du milieu intracellulaire au milieu extracellulaire, ce qui provoque une perte de charge positive et hyperpolarise la cellule. A l'inverse, la fermeture du canal entraine une

accumulation de potassium et donc de charges positives, ce qui provoque la dépolarisation de la membrane. Il existe deux mécanismes indépendants qui sous-tendent la modulation de sa conductance. Dans un premier temps, en absence de cations bivalents extracellulaires, la relation courant-voltage (I-V) de TREK-1 en condition de concentration potassique symétrique, est linéaire ou légèrement rectifiant entrante (Lesage et al., 2000; Xian Tao Li et al., 2006). En revanche, en concentration physiologique de Mg^{2+} ou Ca^{2} , la conductance de TREK-1 diminue lorsque le potentiel de membrane devient négatif, jusqu'à saturer en potentiel très négatif (Kim et al., 2001; Patel et al., 1998). Dans un second temps, TREK-1 présente un caractère voltage dépendant (Patel et al., 1998). Lorsque le potentiel de membrane est très positif, la probabilité d'ouverture des canaux TREK-1 (Po) est élevée, pouvant aller jusqu'à 0.6. A l'inverse, un potentiel de membrane négatif réduit fortement Po (Maingret et al., 2002).

6.5. La régulation de TREK-1

La régulation hétérogène inhérente au canal TREK-1 résulterait de la composition en acides aminés de la queue cytoplasmique adjacente au quatrième segment transmembranaire. Ce sont les seconde et quatrième hélices α transmembranaires qui sont responsables de la formation du pore interne. La structure secondaire de cette quatrième hélice, suggère la présence d'un allongement intracellulaire pouvant jouer un rôle central dans la régulation de l'activité du canal (Morais-Cabral et al., 2001). L'activité de TREK-1 peut être sous le contrôle d'une sensibilité mécanique ou thermique, de lipides, du pH, régulé par les RCPG ou encore par des interactions avec des protéines partenaires (**Figure 7**).

6.5.1. Sensibilité mécanique

TREK-1 peut être activé par des variations de pression dépendante de la courbure membranaire, mais également être régulé par des tensions membranaires. Des forces de cisaillements activent le canal, alors que des contraintes d'étirement de la cellule induit une hyperosmolarité extracellulaire qui réduit l'amplitude des courants de TREK-1.(Maingret et al., 2000a; Patel et al., 1998). De manière générale, l'ouverture de TREK-1 est facilitée par une déformation convexe de la membrane. L'insertion asymétrique d'une molécule amphiphatique dans la bicouche lipidique, comme le trinitrophénol anionique, provoque une courbure convexe et active le canal, à l'inverse, une déformation concave produite par la formation du radical cationique de la chlorpromazine, induit une inhibition de TREK-1(Maingret et al., 2000a). Enfin, il est possible d'activer, de façon graduelle et réversible, le canal, en appliquant une pression mécanique négative sur la partie extracellulaire de la membrane(Maingret et al., 1999). Cette mécanosensibilité peut-être altérée ou réduite lorsque que la partie C-terminal adjacente au quatrième domaine

transmembranaire est partiellement tronquée, suggérant l'importance de ce motif (Patel et al., 1998).

6.5.2. Sensibilité thermique

De la même manière qu'une régulation mécanique est possible, les canaux TREK-1 peuvent être activés par des variations de température dans une gamme allant de 14 à 42°C (Maingret et al., 2000b), avec une activité plus importante à partir de 22°C, pouvant atteindre une amplitude de courant sept fois plus importante. Cependant, et de façon intéressante, cette thermosensibilité est perdue après une excision par patch-clamp, malgré des conditions de régulation mécanique, de pH ou d'acide arachidonique maintenues, ce qui suggère l'hypothèse que la régulation thermique n'est pas inhérente au propriété du canal mais à un possible co-facteur (Maingret et al., 2000b).

6.5.3. Régulation par le pH

TREK-1 est sensible à la variation de pH, principalement intracellulaire. Les protons activent le canal et le sensibilisent aux stimuli mécaniques (Maingret et al., 1999). A l'instar de la régulation mécanique, c'est également sur la partie terminale COOH intracellulaire que réside le senseur aux protons qui régule la sensibilité au pH, et qu'une coupure de cette région aboutit à une diminution progressive de sa sensibilité (Maingret et al., 1999). Il est possible d'inhiber le canal TREK-1 humain par une acidification du pH extracellulaire. Deux résidus histidines situés sur la première boucle extracellulaire (avant le premier domaine pore) témoignent d'une sensibilité au pH significative en condition de pH physiologique (35% d'inhibition à pH 6.5 par rapport à pH 7.5) (Cohen et al., 2008). Cependant, chez le modèle murin, cette sensibilité à l'acidification est plus faible, surement en raison de la présence d'une glutamine à la place du premier résidu histidine. A noter que l'acidification extracellulaire réduit Po sans influencer la conductance unitaire du canal TREK-1 humain (Cohen et al., 2008).

6.5.4. Régulation par les lipides

L'activité des canaux TREK-1 peut être régulée par les acides gras polyinsaturés (PUFA, PolyUnsaturated Fatty Acids) comme l'acide arachidonique (AA), l'acide alphalinoléique (ALA), l'acide l'linolénique ou encore le l'acide docosahexaénoïque (Fink et al., 1998). Cependant, les acides gras saturés n'ont pas d'effet sur le canal. Cette activation n'est pas dépendante de l'intégrité cellulaire, et l'effet est médié par la partie C-terminal de TREK-1 (Fink et al., 1998; Kim et al., 2001). En ce qui concerne les lysophospholipides, l'activation se fait plus rapidement que par les PUFAs mais nécessite par contre l'intégrité de la cellule (Maingret et al., 2000a).

6.5.5. Régulation par les RCPGs

Il existe une régulation par les seconds messagers résultant de l'activité des RCPGs. En effet, la stimulation des protéines kinases A (PKA) et C (PKC) aboutit à une diminution des courants potassiques induite par une phosphorylation sur des sites différents du canal TREK-1(Fink et al., 1996). Ce sont les résidus sérine S333 et S300, en bordure du quatrième segment transmembranaire et de la partie C-terminale intracellulaire, qui sont ciblés par la PKA et PKC respectivement, et sont importants dans cette régulation de TREK-1 (Murbartián et al., 2005). Par déduction de ce mécanisme de régulation, les agonistes des RCPGs tendent à inhiber les courants potassiques.

6.6. Rôle de TREK-1 dans la dépression

La distribution ubiquitaire et les régulations multiples de TREK-1 en font un canal pouvant s'impliquer dans de nombreuses fonctions physiologiques. C'est notamment dans la douleur et la régulation de l'humeur que TREK-1 a révélé des résultats particulièrement intéressants. Au niveau de la nociception, l'invalidation du gène codant pour le canal ionique chez des souris a montré une hypersensibilité aux stimuli thermique à des seuil bas, entre 46 et 50°C, une hyperalgésie qui va de pair avec une allodynie (Alloui et al., 2006). Cette hausse de sensibilité peut s'expliquer par la présence abondante de TREK-1 dans les neurones sensoriels de faible diamètre (fibres C nociceptives polymodale) et sa large co-localisation avec TRPV1 (transient receptor potential vanilloid 1), un canal cationique non sélectif thermosenseur activé par la capsaïcine. Le taux de décharges afférentes des fibres C chez les animaux invalidés dépasse celui des sauvages, et le seuil de déclenchement induit par le stimulus thermique est plus faible (-5°C de différence)(Alloui et al., 2006; Noël et al., 2009).

Sur le plan de la régulation de l'humeur, l'invalidation de TREK-1 a entraîné l'expression d'un phénotype de résistance dans des tests comportementaux relatifs à la dépression (Heurteaux et al., 2006). Les souris sont plus mobiles dans le test de nage forcée (*Force Swim Test* ; FST) et de suspension par la queue (*Tail Suspension Test* ; TST). Elles présentent également des latences d'évasion plus courtes suite à une exposition à des chocs électrique aversifs non contrôlés sur les pattes (*Learn Helpness test*, LH). Dans le test de suppression de la nourriture par la nouveauté (*Novelty Suppressed Feeding* ; NSF), les souris TREK-1 -/- mangent plus facilement les aliments dans un environnement menaçant (Heurteaux et al., 2006). Les résultats obtenus sont similaires à ceux de souris sauvages traitées avec des ISRS (fluoxetine) et il n'y a pas d'avantage d'effet lorsque les souris TREK-1 -/- sont traitées par ces antidépresseurs. Le canal TREK-1 est fortement exprimé dans les neurones sérotoninergiques du noyau dorsal du raphé. De façon intéressante, lorsque les souris invalidées pour TREK-1 sont traitées avec de la fluoxetine associée au Fenclonine (*para-*

chlorophenylalanine ; PCPA), un inhibiteur sélectif et irréversible du tryptophane hydroxylase qui appauvrit le niveau de sérotonine, les souris perdent leur phénotype antidépressif. De plus, les neurones sérotoninergiques du noyau dorsal du raphé des souris mutantes présentent une activité plus importante, au même niveau que ceux de souris sauvages traitées avec des ISRS, avec une fréquence de décharge de deux fois celle des sauvages non traitées (Heurteaux et al., 2006). Cette augmentation d'activité accroit la libération de sérotonine vers des structures comme l'hippocampe, et provoque une amélioration de l'activité tonique des récepteurs 5-HT_{1A} postsynaptique de la partie antérieure, au niveau du champ ammonien 3 (CA3), cette même amélioration qui est observée lors de traitements ISRS sur le long terme (Haddjeri et al., 1998; Heurteaux et al., 2006). Plus récemment, un peptide issu de la maturation du récepteur 3 de la neurotensine (Sortiline), le propeptide (PE) ou son analogue synthétique la Spadine, a été identifié comme bloqueur spécifique de TREK-1. Cette inhibition de TREK-1, à l'instar de la délétion, engendre également en un phénotype de résistance à la dépression chez les souris sauvages.

Des études ont également mis en évidence une augmentation de l'expression de TREK-1 dans le cortex préfrontal lors de dépression induite chez le rat, expression réversée suite à un traitement à la fluoxetine (Chen et al., 2015). En outre, six polymorphismes nucléotidiques du gène codant TREK-1, *KNCK2*, sont impliqués dans les troubles majeurs de l'humeur et l'efficacité des antidépresseurs chez l'homme (Congiu et al., 2015).

Tout ceci semble indiquer un rôle pivot de TREK-1 dans la régulation de l'humeur, lui conférant un potentiel statut de cible thérapeutique dans le trouble dépressif.

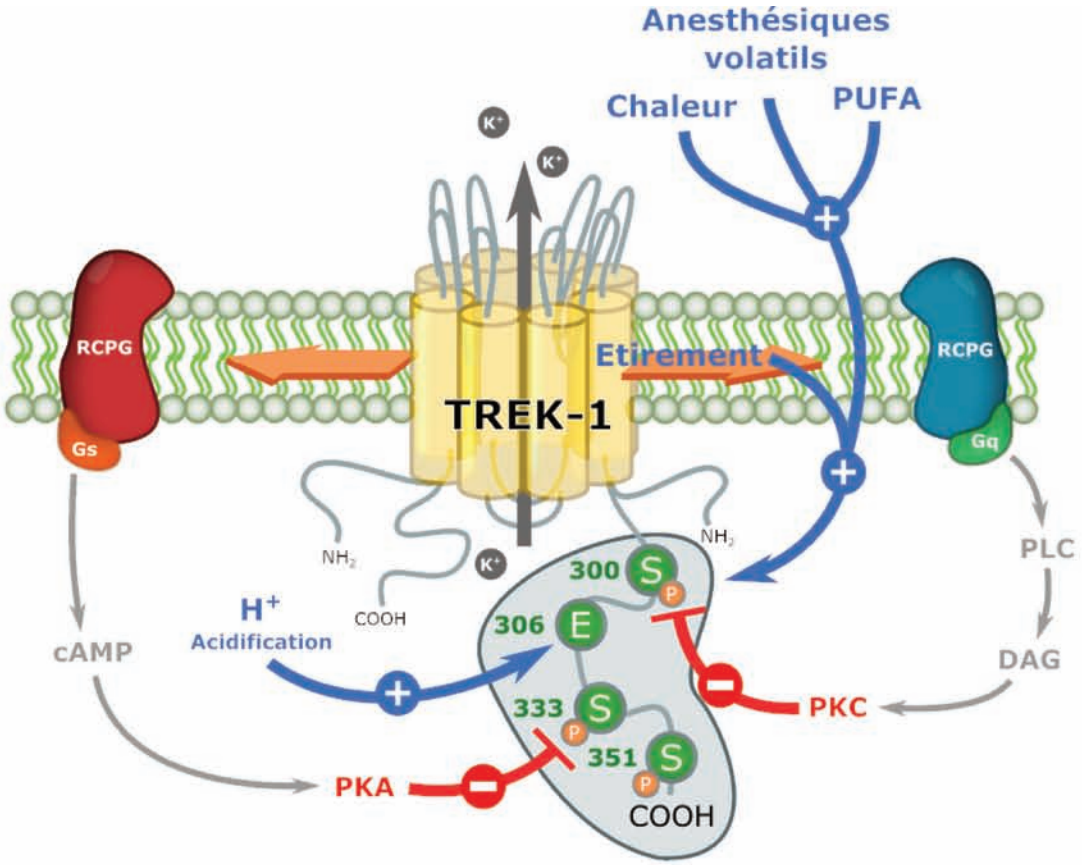

Figure 7 : Schéma du contrôle multiple de TREK-1. Les canaux TREK sont activés par des changements physico-chimiques, tels que l'étirement ou la déformation convexe de la membrane plasmique, la dépolarisation, la chaleur et l'acidose intracellulaire. Les acides gras polyinsaturés (PUFA) dont l'acide arachidonique (AA) et une grande variété d'anesthésiques volatils ouvrent également des canaux TREK. L'activation des voies de signalisation Gs/cAMP/PKA et Gq/PLC/DAG/PKC inhibe les voies de signalisation TREK en phosphorylant les résidus de sérine définis sur la queue COOH-terminale. D'après (Czirják et al., 2004).

6.7. Les partenaires de TREK-1

Un des premiers partenaires identifiés, grâce à une approche protéomique, est la protéine d'ancrage A-Kinase (AKAP150), protéine d'échafaudage qui se lie notamment à PSD95, SAP97 et des RCPG (Sandoz et al., 2006). L'interaction se fait au niveau proximal de la queue de TREK-1, entre les résidus V298 et R311, région importante dans la régulation de l'activité du canal. Cette co-expression modifie de façon importante les propriétés fonctionnelles de TREK-1 (Sandoz et al., 2006). Elle transforme la faible activité de rectification sortante en une conductance robuste de fuite insensible aux acides gras polyinsaturés, à l'étirement membranaire et à l'acidification (Sandoz et al., 2006).

Mtap 2, Microtubule-associated protein, est un autre partenaire constitutif de TREK-1. Il favorise l'augmentation du courant du canal sans pour autant affecter ses propriétés intrinsèques (Sandoz et al., 2008). Cette amélioration est imputable à l'augmentation de la densité de TREK-1 à la membrane plasmique et réside dans la liaison entre Mtap 2 et les microtubules. Les résidus associés à cette liaison se situent entre les résidus E335 et Q360, très proches de ceux d'AKAP150 (Sandoz et al., 2008). A noter que la liaison simultanée d'AKAP150 et Mtap 2 permet un effet additif sur les courants de TREK-1 (Sandoz et al., 2008).

Le récepteur 3 de la neurotensine (NTSR3), aussi appelé Sortiline, a été récemment identifié comme partenaire de TREK-1(Mazella et al., 2010). Une co-expression et co-localisation ont été mises en évidence dans des cellules COS-7 et des neurones corticaux de souris (Mazella et al., 2010). La sortiline est une protéine aux fonctions multiples et complexes. C'est un récepteur, un co-récepteur et surtout une protéine d'adressage vers le lysosome ou la membrane plasmique. L'expression de TREK-1 à la membrane plasmique, mesurée sur des préparations de membranes purifiées ou en utilisant une biotinylation de surface cellulaire, augmente d'un facteur de 3 et 6 lorsque la sortiline est co-transfectée dans des cellules COS-7, suggérant l'interaction entre les deux protéines (Mazella et al., 2010).

Le NTSR3/Sortiline étant le point central de ce manuscrit, il sera plus amplement développé dans la suite du mémoire.

7 LE NTSR3 / SORTILINE, UNE PROTEINE ASSOCIEE A DE MULTIPLES FONCTIONS

Partenaire de TREK-1, le NTSR3/Sortiline est un récepteur de haute affinité pour la neurotensine. Ce récepteur fait partie du système neurotensinergique, mais également de la famille des récepteurs à un domaine transmembranaire VPS10p (Vacuolar protein sorting 10 protein) (Petersen et al., 1997).

7.1. La neurotensine et ses récepteurs

7.1.1. Généralités

La neurotensine (NTS) est un peptide de 13 acides aminés purifié à partir d'hypothalami bovin (Carraway and Leeman, 1973). Ce neuropeptide est exprimé dans le système nerveux central ainsi que dans la périphérie. Il est présent dans des régions cérébrales telles que l'hypothalamus, la substance noire, les tubercules quadrijumeaux, le bulbe olfactif, l'hippocampe, l'amygdale, l'hypophyse et la substance gélatineuse de la moelle épinière (Cooper et al., 1981). Située dans les corps neuronaux et les terminaisons des cellules nerveuses, il est absent des cellules gliales. Dans la

périphérie, il se situe dans le tractus gastro-intestinal, synthétisé dans le jéjunum et l'ilion (Helmstaedter et al., 1977), et également dans le système cardiovasculaire (Reinecke et al., 1982) et la circulation sanguine (Polak et al., 1977).

Au niveau du SNC, la neurotensine est capable d'augmenter le taux de décharge des neurones dopaminergiques et de contrôler la libération de dopamine dépendamment des régions cérébrales (Blaha and Phillips, 1992; Mercuri et al., 1993; Okuma et al., 1983; Pinnock, 1985; Tanganelli et al., 1994), de réduire la prise alimentaire par l'intermédiaire de la leptine (Sahu et al., 2001), d'induire également une réponse antinociceptive indépendante des récepteurs μ opioïdes dans une variété de tests de douleurs, comme la plaque chaude, les crampes abdominales induites par l'acide acétique ou encore le test de retrait de la queue (Clineschmidt et al., 1979, 1982). Cet effet analgésique est rapporté comme plus puissant que la morphine à des doses équimolaires et toujours efficace même en présence de deux antagonistes opioïdes structurellement apparentés, la naloxone ou la naltrexone (Roussy et al., 2010). La neurotensine a aussi un effet hypothermiant (Popp et al., 2007) et peut prévenir des risques cérébraux induits par l'hypoxie (Choi et al., 2012). Enfin, elle peut réguler le système endocrinien et contrôler la libération d'hormones comme la CRH et la GRH par la stimulation des neurones hypothalamiques (Ceccatelli et al., 1989; Nicot et al., 1997; Niimi et al., 1991).

Au niveau de la périphérie, la neurotensine permet de faciliter l'absorption des lipides et d'augmenter la sécrétion biliaire (Gui et al., 2001). Elle augmente également la sécrétion d'insuline à faible concentration de glucose et diminue le glucose insulino-dépendant (Béraud-Dufour et al., 2010; Dolais-Kitabgi et al., 1979).

Les effets de la neurotensine passent par trois récepteurs : le NTSR1, le NTSR2 et le NTSR3 ou Sortiline. Le NTSR1 et NTSR2 sont des récepteurs à 7 domaines transmembranaires couplés aux protéines G, alors que la Sortiline est un récepteur de type 1, à un seul domaine transmembranaire.

7.1.2. Le NTSR1

Les effets de la neurotensine sont médiés principalement par son récepteur de haute affinité le NTSR1, qui possède une affinité sub nanomolaire pour la neurotensine (Kd = 0.1–0.3 nmol/L) et est insensible à la Lévocabastine, une molécule qui possède des propriétés antihistaminiques H1 et qui est un agoniste du NTSR2 (Schotte et al., 1986). Il est exprimé au niveau du cerveau, dans les neurones du septum, de la substance noire, de l'aire tegmentale ventral, du noyau suprachiasmatique et également dans le cortex préfrontal, entorhinal et cingulaire postérieur (Elde et al., 1990; Nicot et al., 1994). Des études immunohistochimiques ont mis en évidence la présence

de NTSR1 dans les terminaisons nerveuses du noyau caudé, de la strie terminale, des tubercules olfactifs mais aussi dans le septum latéral, l'amygdale et le noyau accumbens (Boudin et al., 1996; Fassio et al., 2000). Le NTSR1 est couplé à la phospholipase C et la cascade de signalisation de l'inositol phosphate via la sous-unité Gαq/11 (Vincent et al., 1999; Wang and Wu, 1996). L'activation exogène de NTSR1 entraîne la prolifération cellulaire, la survie, la mobilité et l'invasion des cellules cancéreuses d'origines diverses (Thomas et al., 2003; Wu et al., 2012) corrélé à l'activation de kinases. La PKC, activée par l'IP3, induit une activation de MAPK (Mitogen-activated protein kinases) par la stimulation de Raf-1 ou du récepteur à l'EGF (Epidermal Growth Factor), ce qui peut provoquer une croissance cellulaire incontrôlée (Guha et al., 2003; Müller et al., 2011). La neurotensine, agissant par l'intermédiaire du NTSR1, réduit la fonction physiologique du récepteur à la dopamine D2 (Jomphe et al., 2006). De plus, il existe une modification de l'expression de l'ARNm des récepteurs dopaminergique chez les souris invalidées pour le NTSR1 (Liang et al., 2010). Chez ces mêmes souris, il y a également une perte de l'effet hypothermiant et de l'effet anorexigène de la NTS lors de son injection au niveau centrale, suggérant que ces effets passent par l'intermédiaire du NTSR1 (Kim et al., 2008; Remaury et al., 2002). En revanche, l'effet analgésique ne semble pas être directement dépendant du NTSR1 (Kim et al., 2008) cependant, la délétion du récepteur provoque une diminution de la nociception dépendante de la morphine(Roussy et al., 2010).

7.1.3. Le NTSR2

Le NTSR2, quant à lui, est identifié comme le récepteur à faible affinité pour la NTS (Kd = 3-10 nmol/L) et est sensible à la Lévocabastine (Mazella et al., 1996). L'expression du récepteur est particulièrement dense dans des régions recevant des innervations neurotensinergiques, comme le noyau de la strie terminale, le bulbe olfactif, la substance noire, l'aire tegmentale ventral et la substance grise périaqueducale mais également dans le cortex cérébral, l'hippocampe et le cervelet (Lépée-Lorgeoux et al., 1999; Sarret et al., 2003a; Walker et al., 1998). Lorsque la séquence codante du clone murin du NTSR2 est exprimée dans des ovocytes de xénopes, la neurotensine ainsi que la lévocabastine sont capables de déclencher un courant entrant calcium dépendant (Mazella et al., 1996). Dans des cellules CHO transfectées avec de l'ADNc NTSR2 humain ou de rat, cette mobilisation intracellulaire de calcium est plus importante avec la lévocabastine qu'avec le NTS ,et phosphoryle Erk1/2 (Botto et al., 1997; Gendron et al., 2004; Yamada et al., 1998) . Le NTSR2 joue un rôle dans la protection des cellules bêta contre des agents externes cytotoxiques (staurosporine, IL-1β) par l'intermédiaire de la voie kinase PI3 (Béraud-Dufour et al., 2009; Coppola et al., 2008). Il est également responsable de l'effet analgésique médié par la neurotensine (Dubuc et al., 1999; Smith et al., 2012). Plus récemment, le NTSR2 a été impliqué dans la mémoire de peur. Dans le test contextuel de condition de peur, la réponse de *freezing* (position prostrée) a été significativement

réduite chez les souris déficiente NTSR2 (NTSR2-/-) comparativement aux souris de type sauvage (Yamauchi et al., 2007).

Cependant, l'action de la NTS sur le NTSR2 reste encore ambiguë. En fonction de l'espèce à partir de laquelle le NTSR2 a été isolé (Mazella et al., 1996) et le système cellulaire utilisé pour évaluer la signalisation, la neurotensine peut aussi bien agir en tant qu'agoniste, qu'antagoniste. La neurotensine et la lévocabastine exercent une activité espèce dépendante ; agoniste chez la souris (Mazella et al., 1996), antagoniste chez l'humain (Richard et al., 2001; Vita et al., 1998).

7.2. Le NTSR3 / Sortiline

Troisième récepteur de la neurotensine, le NTSR3, ou Sortiline, a été identifié par 3 approches différentes. A la différence des deux autres récepteurs, le NTSR3/Sortiline est une protéine réceptrice à un seul domaine transmembranaire, ou récepteur de type I, et possède une structure Vps10p.

7.2.1. Purification et clonage du NTSR3 / Sortiline

Une première identification a pu être réalisée grâce à l'utilisation d'un analogue radioactif et photoactivable de la NTS. Une protéine identifiée d'environ 100 kDa, solubilisable par le détergent CHAPS, a montré des propriétés pharmacologiques similaires aux deux autres récepteurs de la neurotensine et s'est avérée capable de lier la neurotensine avec une haute affinité (Kd = 0.2 nM) (Mazella et al., 1988). Elle a été ensuite purifiée à partir de cerveaux de souris et d'humain et identifiée comme le récepteur 3 de la neurotensine(Mazella et al., 1989; Zsürger et al., 1994). Le NTSR3 a par la suite été montré comme impliqué dans l'internalisation de la NTS, dans des cultures de neurones primaires, de même que le NTSR1 et NTSR2 (Chabry et al., 1993).

Lors de la caractérisation, par colonne d'affinité, de partenaires de la protéine RAP (receptor-associated protein), protéine endoplasmique de 40 kDa localisée au niveau du réticulum et de l'appareil de Golgi et impliqué dans la maturation des récepteurs des LDL (Low Density Lipoprotein), une glycoprotéine d'environ 95 kDa a été identifiée dans les vésicules intracellulaires contenant RAP (Battey et al., 1994; Gliemann et al., 1994; Willnow, 1998). Purifiée à partir de cerveau humain et clonée dans une bibliothèque d'ADNc humain, son gène, localisé sur le chromosome 1p, code pour une protéine de 833 acides aminés. Cette glycoprotéine n'est cependant pas homologue aux récepteurs LDL, mais présente une structure caractéristique des récepteurs de type I, avec des homologies avec la protéine Vps10p de levure, impliqué dans le transport intracellulaire, et les récepteurs cation-dépendants et cations-indépendants du mannose-6-phosphate (Petersen et al., 1997). C'est d'ailleurs par ce domaine Vsp10p que la protéine est capable

de se lier à la partie carboxyterminale de RAP (Tauris et al., 1998). Par ses caractéristiques, elle sera identifiée comme la Gp95/Sortilin qui s'avérera être 100 % homologue avec le récepteur 3 de la neurotensine (Mazella et al., 1998).

En parallèle, une équipe isole une protéine de 110kDa à partir de vésicules intracellulaires, contenant le transporteur du glucose Glut4, et l'identifie comme un des composés majeurs de ces vésicules. Clonée à partir d'adipocytes de rat, elle présentera une forte homologie de séquence avec le NTSR3/Sortiline humaine (93 %) et sera envisagée comme l'analogue de la sortiline du rat (Lin et al., 1997).

7.2.2. Structure

Le NTSR3/Sortiline est un récepteur de type I de la famille des récepteurs Vps10p contenant quatre autres membres : SorCS1, SorCS2, SorCS3 et SorLA. Cette famille de protéine transmembranaire possède un long domaine N-terminal homologue à la protéine Vps10p, qui représente soit le seul élément de la partie luminal/extracellulaire, soit est associé à d'autres domaines, et un court domaine cytoplasmique. Vps10 est une protéine de tri vacuolaire retrouvée chez la levure (Vacuolar protein sorting) et qui possède deux régions homologues contenant chacun un motif C-terminal riche de 10 résidus cystéine (10CC motif) espacés par un nombre constant d'acides aminés. C'est une protéine d'adressage de la carboxypeptidase Y retrouvée majoritairement dans le golgi tardif, là où les protéines vacuolaires sont triées (Marcusson et al., 1994). Après transport vers des compartiments endosomaux prévacuolaires et maturation de la carboxypeptidase Y, la protéine Vps10p est capable de revenir vers le Golgi (Marcusson et al., 1994). Ces récepteurs à domaine Vps10p présentent tous une séquence consensus de clivage de proprotéine convertase (RXXR) qui définit le propeptide N-terminal (**Figure 8**).

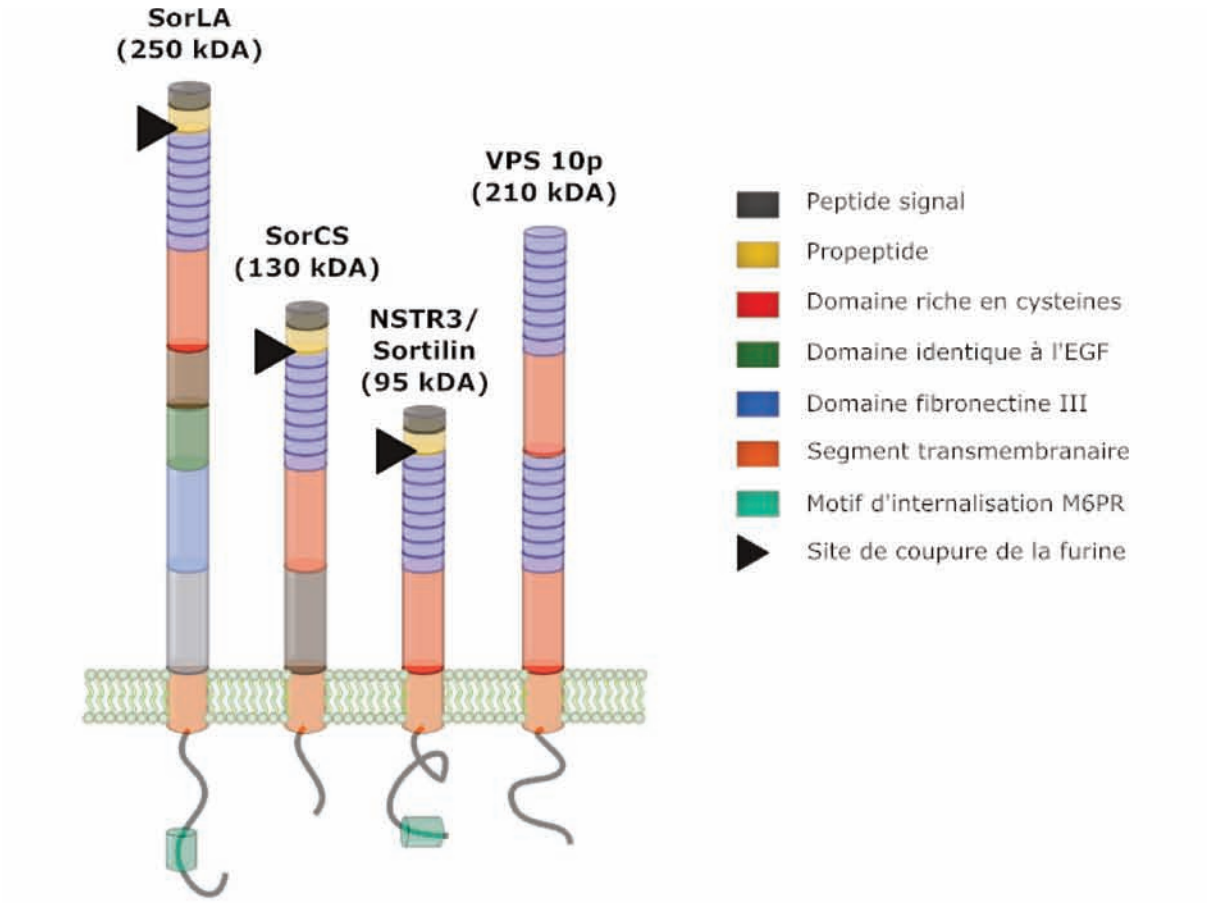

Figure 8 : Schéma des récepteurs à domaine Vps10p. Les membres de la famille des récepteurs Vps10p (SorLA, Sortilin et SorCS) partagent des motifs communs, y compris le domaine riche 10CC, un seul segment transmembranaire, un peptide signal, au moins un site de coupure de la furine et une courte queue cytoplasmique. SorLA et le NTSR3/Sortiline portent le motif d'internalisation des récepteurs M6P. D'après (Mazella, 2001).

Le NTSR3/Sortiline, protéine de 833 acides aminés, contient principalement un domaine Vps10p et un court domaine cytoplasmique. Les résidus cystéine du domaine C-terminal Vps10p forment un motif de cinq ponts disulfures identiques (Westergaard et al., 2004). De plus, la structure cristallographique du domaine Vps10p du Le NTSR3/Sortiline, complexé avec son ligand la NTS, a révélé que la partie N-terminale est en effet dotée d'une structure en hélice constituée par 10 motifs de feuillets β et est suivie de deux petits domaines, désignés 10CC-a et 10CC-b, qui constituent le motif 10CC. Tous deux ont une faible teneur en structure secondaire et interagissent directement avec cette hélice (**Figure 9**) (Quistgaard et al., 2009). Ce domaine hélice forme un large tunnel d'environ 25-37 Å légèrement conique qui se rétrécit vers le côté de la face d'interaction 10CC et contient de nombreux sites de liaisons. C'est d'ailleurs dans ce tunnel que la NTS se lie par l'intermédiaire de sa partie C-terminale (Quistgaard et al., 2009).

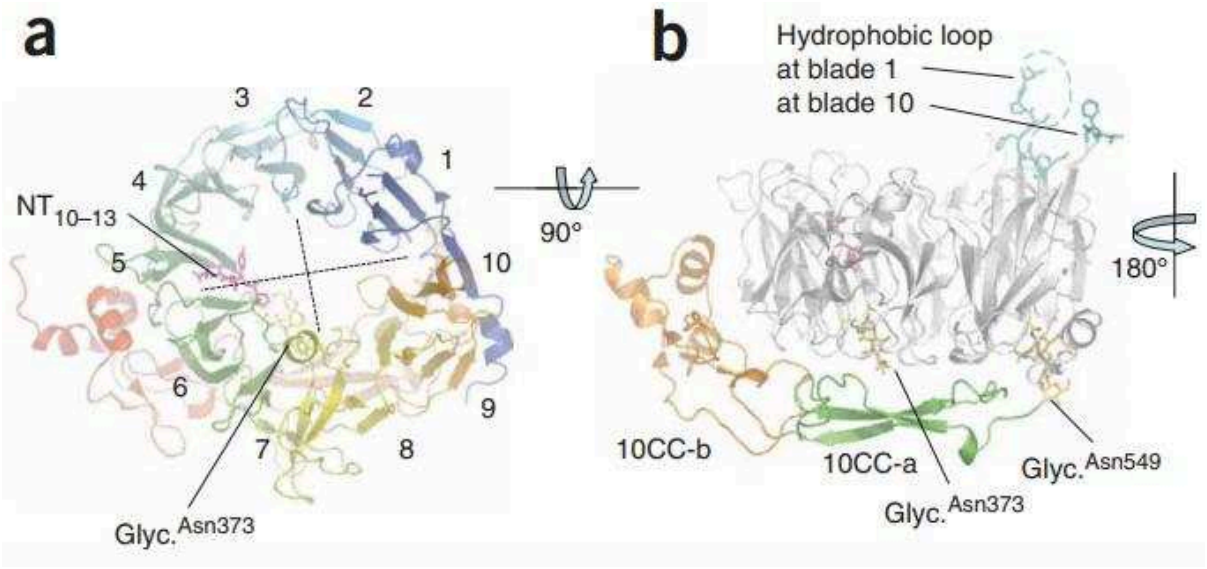

Figure 9 : La structure du NTSR3/Sortiline. ***(a)*** *Représentation cartoon du NTSR3/Sortiline vue du côté ouvert du tunnel. Les motifs de feuillets β sont numérotés et colorés du bleu au rouge, du N- au C-terminal. La neurotensine (magenta) et les fractions glucidiques (Glyc., jaune) sont représentées sous forme de bâtonnets.* ***(b)*** *Vue latérale. L'hélice est représentée en gris, 10CC-a en vert et 10CC-b en orange. La boucle hydrophobe (résidus 97-108) et la pointe hydrophobe de la boucle voisine (résidus 559-560) sont représentées sous forme de bâtonnets turquoise, à l'exception d'une partie désordonnée représentée par une ligne pointillée turquoise. D'après (Quistgaard et al., 2009)*

En ce qui concerne le court domaine carboxy-terminale, celui-ci est notamment responsable de l'internalisation du récepteur (Mazella et al., 1998), présente une homologie de séquence avec le récepteur du Manose-6-phosphate, responsable du transport d'enzymes lysosomiales (Johnson and Kornfeld, 1992), mais contient également plusieurs séquences signal conformes à des motifs consensus connus pour être impliqués dans l'endocytose, le ciblage basolatéral et le tri des endosomes golgien (Nielsen et al., 2001) (**Figure 10**).

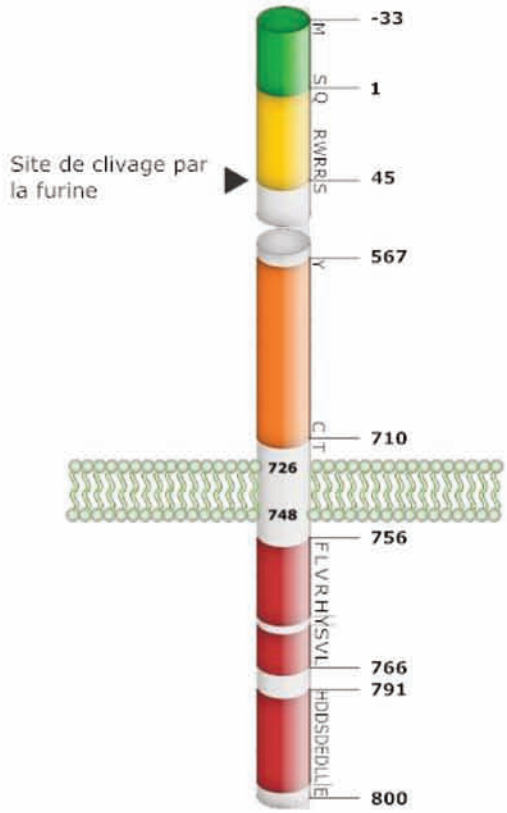

Figure 10 : Représentation schématique du NTSR3/Sortiline humain. En vert, peptide signal ; en jaune, le propeptide ; en orange, le domaine riche en cystéine homologue à la protéine VPS10p ; en rouge, le domaine homologue au récepteur mannose-6-phosphate.

7.2.3. Maturation

Il existe un site consensus de clivage protéique (RXXR) commun à tous les récepteurs de la famille Vps10p (Seidah and Chrétien, 1997) situé sur la partie N-terminal, ce qui suggère l'existence d'une maturation d'une forme précurseur pendant l'adressage cellulaire. Le NTSR3/Sortiline présente sur sa séquence post clivage les résidus $R^{41}WRR^{44}$, résidus correspondant à la séquence consensus de clivage (R-x-R/L-R) de la protéase à sérine, la furine. Le NTSR3/Sortiline est synthétisé en tant que précurseur, la pro-sortiline, puis converti dans le réseau trans-golgien en récepteur mature par le clivage de la furine et la dissociation subséquente d'un propeptide (PE) de 44 acides aminés (Mazella et al., 1998). La libération du propeptide semble importante pour exposer les régions de liaisons des ligands. En effet, le propeptide est capable de lier le NTSR3/Sortiline avec une forte affinité et d'inhiber la liaison des ligands, mais permettrait également la prévention de liaisons prématurées de ligands au récepteur avant maturation. Le propeptide est capable de rentrer en compétition avec la liaison de RAP et de la NTS, et, de manière intéressante, la liaison RAP ou NTS ne peut être établie lorsque le récepteur est sous sa forme immature, suggérant cette propriété de prévention du propeptide (Munck Petersen et al., 1999; Petersen et al., 1997; Westergaard et al.,

2004). La maturation de la sortiline représente donc une étape importante pour l'acquisition de son activité fonctionnelle.

7.2.4. Distribution

Au niveau tissulaire, le NTSR3/Sortiline est principalement exprimé dans le cerveau et plus particulièrement au niveau de l'hippocampe, du gyrus denté et du cortex cérébral (Hermans-Borgmeyer et al., 1999). Il se retrouve également exprimé fortement dans la moelle épinière, les testicules et le muscle squelettique. Dans une moindre mesure, la sortiline est présente dans le cœur, le placenta, les tissus adipeux et la prostate (Petersen et al., 1997).

Le NTSR3/Sortiline est majoritairement intracellulaire (environ 90 %). Il est localisé au niveau des compartiments golgiens et également du réticulum endoplasmique. A la surface cellulaire, au niveau de la membrane plasmique, le NTSR3/Sortiline mature ne représente que 5 à 10 % d'expression et permet de lier et d'internaliser des ligands extracellulaires (Nielsen et al., 1999).

7.3. Fonctions du NTSR3/Sortiline

Le rôle du NTSR3/sortiline s'étend sur de nombreuses fonctionnalités dues notamment à sa structure et ses similitudes avec d'autres protéines. On lui reconnait des propriétés de récepteur, de co-récepteur et une implication dans le trafic et le tri intracellulaire.

7.3.1. Régulation du trafic intracellulaire

Le NTSR3/Sortiline est majoritairement localisé dans la cellule et présente des similitudes structurelles avec des récepteurs impliqués dans le tri et le transport intracellulaire. Sa partie extracellulaire N-terminal est un domaine Vps10p impliqué dans le tri de la carboxypeptidase Y (CPY) chez la levure (Marcusson et al., 1994) et son extrémité C-terminal est étroitement apparenté au segment fonctionnelle important du récepteur du manose-6-phosphate (M6PR) (Johnson and Kornfeld, 1992). En plus d'une séquence analogue au M6PR, le NTSR3/Sortiline co-localise avec lui au niveau du réseau trans-golgien (Mari et al., 2008). Ce récepteur M6P est impliqué dans le transport des vésicules du réticulum endoplasmique vers les endosomes tardifs. Il s'associe, du côté luminal, au motif M6P des hydrolases lysosomale et à l'adaptin, côté cytosolique, associée au manteau de clathrine. De cette façon, les M6PR contribuent à envelopper les hydrolases dans des vésicules qui vont sortir du réseau trans-golgien pour apporter leur contenu à des endosomes qui finissent par se développer en lysosomes matures, où les hydrolases récemment libérées peuvent commencer à digérer la matière endocytée (**Figure 11**) (Coutinho et al., 2012). Le NTSR3/Sortiline est également internalisé dans un manteau de clathrine et les signaux d'internalisation identifiés sont connus pour faciliter la liaison au complexe AP-2 (complexe multiprotéique associé à la clathrine et qui permet

d'internaliser). Le récepteur délivre des ligands internalisés aux lysosomes et joue un rôle de transport entre le réseau trans-golgien et les endosomes, par l'intermédiaire de protéines adaptatrices du golgi comme les GGAs (Golgi-localized, γ-adaptin-ear-containing, ADP-ribosylation factor-binding proteins) (Nielsen et al., 1999, 2001). D'autres résultats montrent que le trafic du NTSR3/Sortiline est également facilité par l'AP-1 et que la récupération endosome-TGN est facilitée par le complexe rétromère (Canuel et al., 2008; Mari et al., 2008; McCormick et al., 2008; Seaman, 2007). Enfin, le NTSR3/Sortiline permet également l'adressage lysosomal des SAPs (sphingolipid activator proteins), des sphingomyelinase acides et des cathepsin D et H (Canuel et al., 2008; Lefrancois et al., 2003; Ni and Morales, 2006).

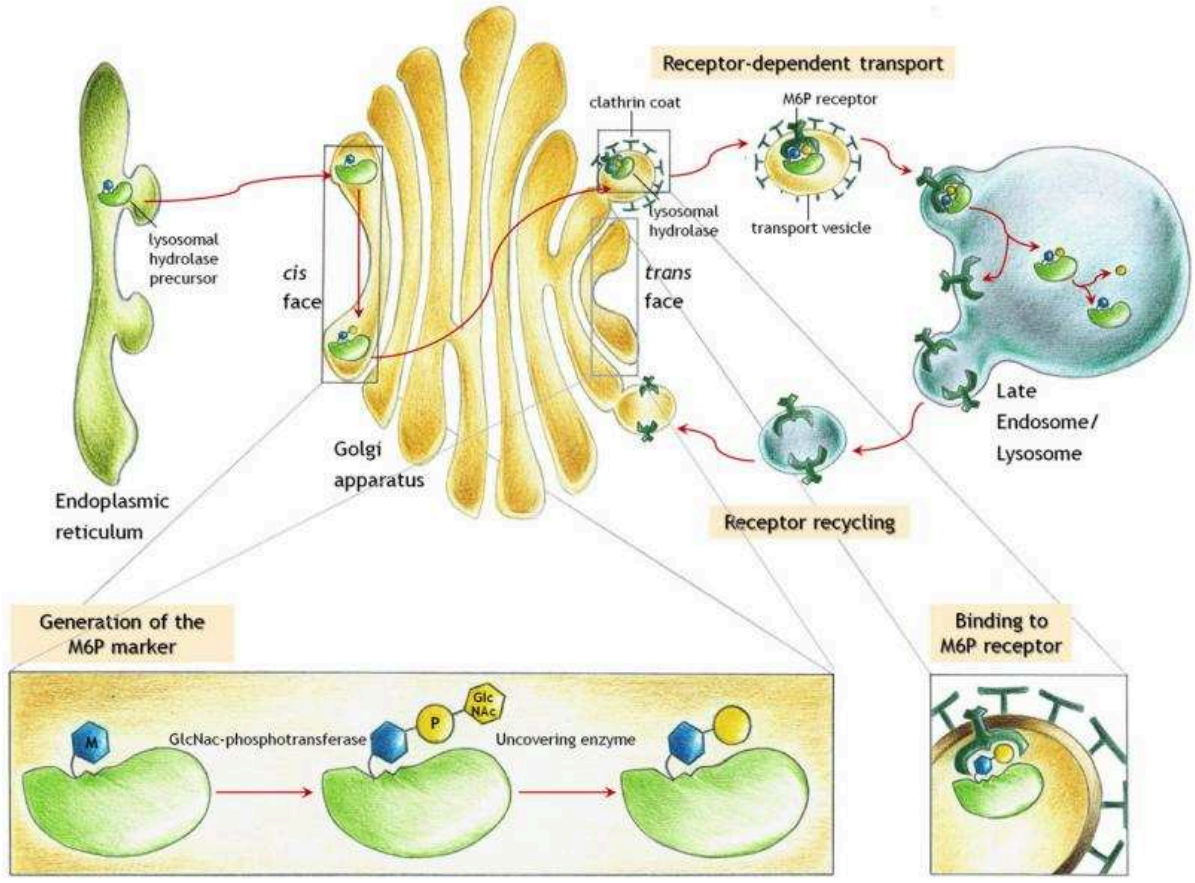

Figure 11 : Transport des hydrolases lysosomales nouvellement synthétisées vers les lysosomes. Les hydrolases lysosomales sont synthétisées dans le réticulum endoplasmique et se déplacent vers le réseau cis Golgien, où elles sont modifiées par l'ajout de groupes mannose-6-phosphate (M6P). Sur le réseau trans Golgien, le signal M6P permet la séparation des hydrolases lysosomales de tous les autres types de protéines par liaison sélective aux récepteurs M6P. Les vésicules recouvertes de clathrine produisent des bourgeons et fusionnent avec des endosomes tardifs. A bas pH de l'endosome tardif, les hydrolases se dissocient des récepteurs M6P et les récepteurs vides sont recyclés dans l'appareil Golgi pour d'autres cycles de transport. D'après (Coutinho et al., 2012).

Le NTSR3/Sortiline est fortement exprimé dans les adipocytes. Des études l'ont identifié comme un composant essentiel des vésicules de stockage du transporteur de glucose 4' (GLUT4) (Lin et al., 1997; Morris et al., 1998). Le domaine luminal N-terminal du NTSR3/Sortiline interagit avec GLUT4, tandis que la queue cytoplasmique interagit avec les protéines d'adaptation pour faciliter la formation des vésicules de stockage. Il a été démontré dans les adipocytes et les myocytes que le NTSR3/Sortiline était nécessaire pour l'absorption de glucose insulinodépendant (Huang et al., 2013; Morris et al., 1998; Shi and Kandror, 2005).

7.3.2. Viabilité neuronale

La fonction du NTSR3/Sortiline ne s'arrête pas au ciblage lysosomal. Le NTSR3/Sortiline est capable de circuler entre la surface des cellules et divers compartiments intracellulaires afin d'acheminer les protéines cibles vers différentes destinations, y compris l'exposition à la surface membranaire pour permettre la transduction d'un signal, ou encore à travers des voies régulées.

Le NTSR3/Sortiline reconnait la pro-forme du NGF (proNGF, Nerve Growth Factor) mais également d'autres neurotrophines (NT) et pro-neurotrophines, comme le BDNF. Les NT sont des facteurs de croissance essentiels au développement et au maintien du système nerveux. Cette famille regroupe le NGF, le BDNF, ainsi que la neurotrophine 3 (NT3) et la neurotrophine 4 (NT4). Toutes les NT sont synthétisées sous forme précurseurs puis converties en leurs équivalents matures par clivage protéolytique dans les voies de biosynthèses ou l'espace extracellulaire. Les activités des NTs sont médiées par deux classes de récepteurs : les récepteurs kinases liés à la tropomyosine TrkA, -B et -C qui présentent une spécificité pour des NTs particulières, et le récepteur de promiscuité neurotrophin p75 (p75NTR) qui augmente la spécificité des Trks envers leurs ligands. De façon intéressante, les formes précurseur pro-NTs possèdent une activité biologique souvent inverse de leur forme mature. Le proNGF et le proBDNF sont capables d'induire un signal pro apoptotique, alors que le NGF et le BDNF sont impliqués dans la croissance, la prolifération et la survie cellulaire. Ces effets sont en réalité dépendants de l'assemblage de leur récepteur respectif.

7.3.2.1. Co-recepteur du p75NTR

Les effets positifs du NGF et BDNF passent par l'assemblage du récepteur p75 avec les récepteurs TrkA et TrkB respectivement. Le p75NTR est un membre de la superfamille des récepteurs TNF (Tumor necrosis factor) et est surtout connu pour son rôle dans l'apoptose neuronale et la neurodégénérescence (Dechant and Barde, 2002). Il possède une région cytoplasmique juxtamembranaire, appelé « Chopper », qui induit la cascade des caspases et calpaine et la mort cellulaire (Coulson et al., 2000). La libération du domaine intracellulaire par des sécrétases favorise aussi bien l'apoptose, que la survie cellulaire (Kenchappa et al., 2006; Kommaddi et al.,

2011). Il s'avère que l'effet pro apoptotique du p75NTR nécessite une association avec le NTSR3/Sortiline. En effet, le NTSR3/Sortiline reconnait la forme précurseur proNGF et proBDNF *via* le prodomaine et le p75NTR reconnait la partie mature de ces NT. Il a été montré que le NTSR3/Sortiline augmente l'affinité du p75NTR pour les NT. Les cellules exprimant seulement le p75NTR se lie au proNGF avec une affinité de Kd = 15 nM, alors qu'une co-expression avec le NTSR3/Sortiline augmente l'affinité d'environ 100 fois, Kd =160 pM, ce qui diminue de façon importante la concentration effective des proNTs nécessaires à la signalisation apoptotique du p75NTR (**Figure 12**) (Nykjaer et al., 2004). D'autres études ont mis en évidence le même mécanisme apoptotique avec le proBDNF. Le proBDNF s'associe également avec le NTSR3/Sortilin et le p75NTR et induit la mort cellulaire à une concentration subnanomolaire (0.2nM) (Teng et al., 2005).

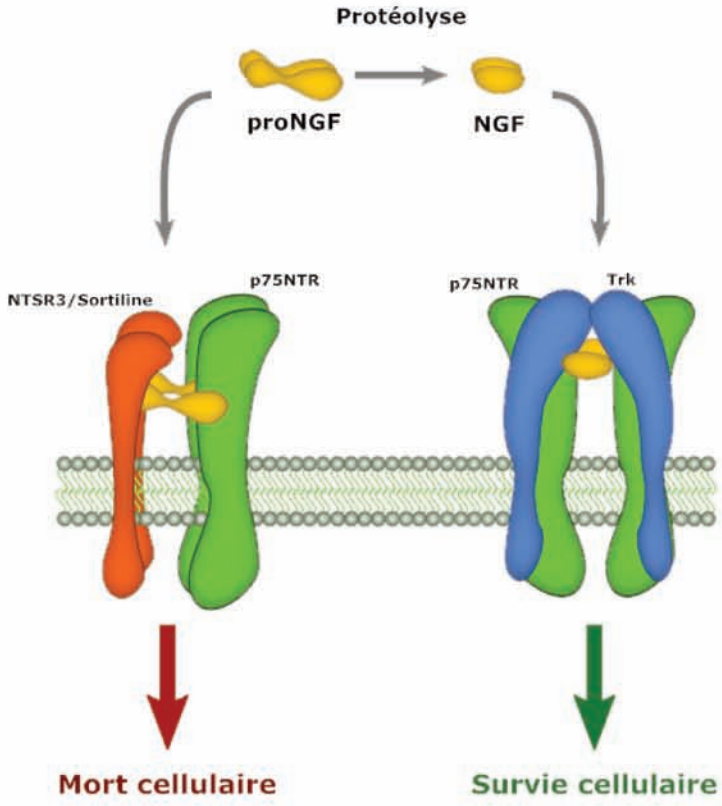

Figure 12 : Modèle schématique de la formation du complexe récepteur-p75NTR. L'interaction du p75NTR avec les Trks améliore l'affinité pour le NGF mature et permet de favoriser la survie et la croissance. En revanche, lorsqu'il est lié au NGF immature, le proNGF, un complexe p75NTR-NTSR3/Sortiline induit la mort cellulaire. D'après (Nykjaer et al., 2004).

7.3.2.2. Régulation du BDNF

La liaison du proBDNF avec le NTSR3/Sortiline ne se limite pas qu'à la régulation du signal apoptotique médié par le p75NTR. Le récepteur permet également une régulation intracellulaire de

la sécrétion et du recyclage du BDNF. L'identification du polymorphisme Val66Met du BDNF a suggéré l'existence d'un signal de trafic dans le prodomaine impliqué dans le ciblage optimal du BDNF dans la voie de sécrétion régulée (Egan et al., 2003). Dans un premier temps, une étude a mis en évidence la présence d'une région dans le prodomaine du BDNF, des résidus 44 à 102, responsable de l'interaction avec le domaine luminal du NTSR3/Sortiline à partir d'homogénats de cerveaux, et ce, localisée dans les mêmes compartiments granulaires de sécrétion de neurones. Cette région possède des similitudes avec la séquence du NGF surtout au niveau de la Box 3. Cependant, en dépit des similitudes de séquences, cette région peut avoir des fonctions différentes pour ces deux neurotrophines. La délétion de la Box 3 dans le NGF induit une diminution de l'expression protéique de NGF, suggérant une importance possible dans le repliement de la protéine (Suter et al., 1991). En revanche, cette même délétion pour le BDNF, n'altère pas son niveau d'expression protéique mais réduit de manière significative sa sécrétion régulée. A noter que, bien que le précurseur du NGF soit clivé en majorité dans l'appareil de golgi, le BDNF reste en majorité sous sa proforme dans la cellule et peut être libéré ainsi (Chen et al., 2004; Mowla et al., 1999; Pang et al., 2004). Fait intéressant, un autre motif de tri a été révélé dans le domaine mature du BDNF. Composé de quatre résidus (I144, E146, I233, D234), il interagit avec une protéine de triage, la carboxypeptidase E (CPE) et la mutation des résidus acides (E146, D234) en alanines conduit à une perte du BDNF dans la voie constitutive (Lou et al., 2005).

La substitution de la méthionine 66 en valine du BDNF entraine une diminution significative de l'interaction avec le NTSR3/Sortiline. Il a été démontré que cette substitution conduit à une diminution de la co-localisation dans les granules de sécrétion, et également une diminution de la sécrétion régulée du BDNF-Val66Met dans les neurones (Egan et al., 2003 ; Chen et al., 2004). Afin de déterminer si le NTSR3/Sortiline est nécessaire pour l'adressage du BDNF dans la voie de sécrétion régulée, une construction du NTSR3/Sortiline tronquée, dépourvue de la région transmembranaire et cytoplasmique du NTSR3/Sortiline, a été utilisée dans des cellules PC12. En présence de NTSR3/Sortiline tronqué, la distribution du BDNF est plus diffuse dans la cellule, et il y a une diminution significative du niveau de co-localisation dans les vésicules de sécrétion. De même, la stimulation par dépolarisation, pour déclencher la voie régulée, aboutit à une diminution de la quantité de BDNF extracellulaire. Ce même phénomène est observé avec le BDNF-Val66Met, que ce soit avec la forme entière du NTSR3/Sortiline ou sa forme tronquée(Chen et al., 2005). A partir de culture de neurones primaires corticaux et hippocampaux, la co-tansfection de NTSR3/Sortiline tronqué et de BDNF induit une diminution de la sécrétion de BDNF dans la voie régulée avec une augmentation concomitante de la voie constitutive (Chen et al., 2005). Ce résultat a été obtenu de façon identique avec la transfection d'un siRNA (small interfering RNA) qui réduit significativement le

niveau de NTSR3/Sortiline endogène (Chen et al., 2005). Le mécanisme de contrôle de la voie régulée du BDNF nécessite en somme l'interaction du prodomaine avec la queue C-terminale du NTSR3/Sortiline, qui va permettre un repliement adéquate, et la liaison entre le domaine mature et le CPE (**Figure 13**).

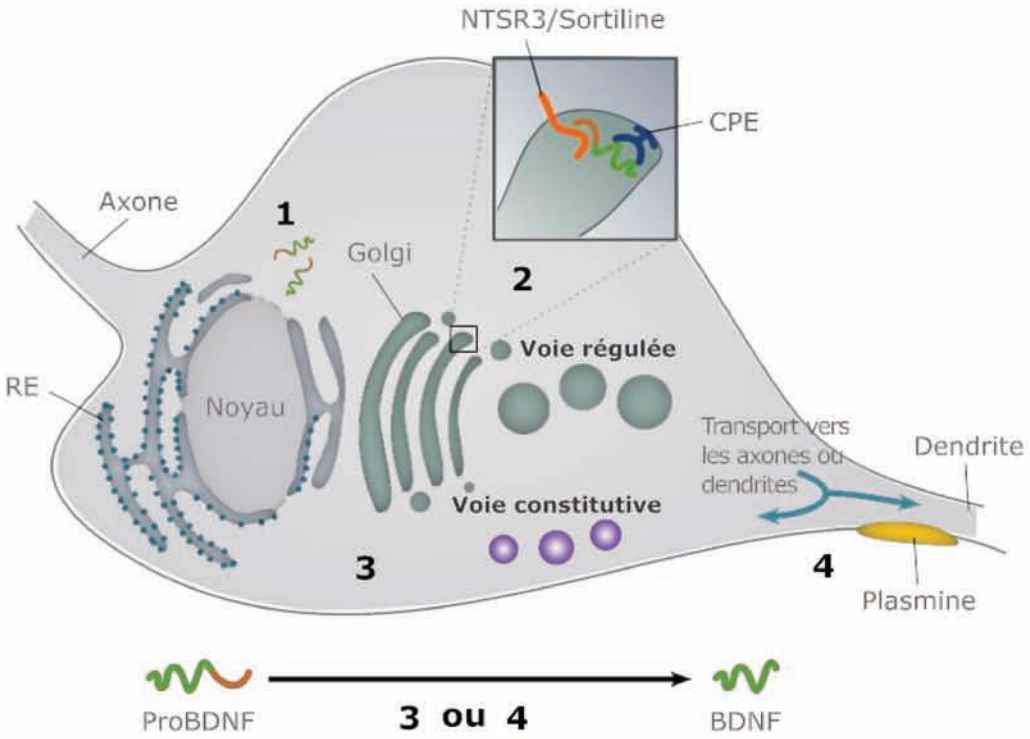

*Figure 13 : La synthèse et le tri du BDNF. D'abord synthétisé dans le réticulum endoplasmique (RE) **(1)**, le proBDNF (précurseur du BDNF) se lie au NTSR3/Sortiline intracellulaire du Golgi pour faciliter le repliement correct du domaine mature **(2)**. Un motif dans le domaine mature du BDNF se lie à la carboxypeptidase E (CPE), une interaction qui permet le tri du BDNF en grandes vésicules à noyau dense, qui sont une composante de la voie régulée. En l'absence de ce motif, le BDNF est envoyé dans la voie constitutive. Le BDNF est ensuite transporté vers les axones dendrites. Dans certains cas, le pro-domaine n'est pas clivé intracellulairement par la furine ou les protéines convertases (comme la protéine convertase 1, PC1) **(3)**, le proBDNF peut être libéré par les neurones. Les protéases extracellulaires, telles que les métalloprotéinases et la plasmine, peuvent ensuite cliver la pro-région pour produire du BDNF mature (mBDNF) **(4)**. D'après (Lu et al., 2005).*

Enfin, pour étendre la fonctionnalité de ce processus, une étude récente a révélé que le NTSR3/Sortiline soluble, induit par un processus de *shedding*, coupure de son ectodomaine, permet de rediriger le pool de BDNF, destiné à la dégradation lysosomale, vers la voie constitutive (Evans et al., 2011).

7.3.3. Physiopathologie

Etant donnée l'implication du NSTR3/Sortiline dans les mécanismes de régulation des neurotrophines, et par voie de conséquences, sur la survie et mort cellulaire, ce récepteur a suscité

un intérêt dans l'étude de son implication dans les cancers. Des études ont montré que le NTSR3/Sortiline permettait de réguler à la fois les neurotrophines mais également ces récepteurs, et pouvait jouer sur la progression des cellules cancéreuses (Akil et al., 2011). On le retrouve fortement exprimé dans des lignées cellulaires humaines cancéreuses. Le NTSR3/Sortiline est capable de se dimériser avec le NTSR1 et d'être internalisé par la stimulation de la NTS, et d'induire des voies de signalisation par modification des MAP kinases et le *turnover* du phosphoinositide (PI) facilitées par NTSR1 dans la lignée cellulaire HT29 (adénocarcinome) (Martin et al., 2002). Les lignées de cellules cancéreuses sensibles aux effets trophiques de la NTS expriment toutes le NTSR3/Sortiline. Si la séquestration du peptide à l'intérieur de sa cellule cible est une étape fondamentale dans l'activité sur la croissance cellulaire, le NTSR1 ou le NTSR3/Sortiline pourrait être en mesure d'agir comme médiateur de la réponse trophique au NTS (Dal Farra et al., 2001). Enfin, le NTSR3/Sortiline est capable de former un complexe avec le TrkB et l'EGFR (epidermal growth factor receptor) dans les exosomes libérés par les cellules cancéreuses du poumon, qui transmettent un contrôle microenvironnemental sur les cellules endothéliales (Wilson et al., 2014).

De plus en plus de preuves suggèrent que la sortiline est fonctionnellement associée aux processus du métabolisme des lipides. Les GWASs (Genome Wide Association Studies) ont montré une forte corrélation entre le gène du NTSR3/Sortiline, SORT1, et le taux de lipides plasmatiques (Guo et al., 2015; Wang et al., 2011).La surexpression hépatique du NTSR3/Sortiline augmente le taux de lipides plasmatiques et vice versa (Sparks et al., 2015). Le déficit de NTSR3/Sortiline diminue la sécrétion hépatique des lipoprotéines de très faible densité (very low density lipoprotein , VLDL), ce qui abaisse le taux de lipides plasmatiques (Kjolby et al., 2010, 2015). Le NTSR3/Sortiline favorise l'accumulation de lipides dans les macrophages et la formation de cellules spumeuses (Patel et al., 2015). Le déficit en NTSR3/Sortiline montre également une réduction spectaculaire de la zone adipocytaire dans le tissu adipeux des souris invalidées pour le gène (Rabinowich et al., 2015). Le niveau de NTSR3/Sortiline hépatique est diminué dans des conditions de résistance à l'insuline, ce qui contribue au trouble lipidique plasmatique dans le diabète de type 2 (Li et al., 2015). Dans l'ensemble, ces études corroborent l'hypothèse selon laquelle le NTSR3/Sortiline participe probablement aux troubles du métabolisme des lipides (Kjolby et al., 2015; Ogawa et al., 2016; Schmidt and Willnow, 2016)

Il a également été proposé que le NTSR3/Sortiline soit impliqué dans la pathogenèse de la maladie d'Alzheimer. La perte d'expression du récepteur entraine une accumulation d'APOE (Apolipoprotéine E) et d'Aβ dans le cerveau et une aggravation des plaques. De plus, les neurones primaires dépourvus de NTSR3/Sortiline présentent une diminution significative de l'absorption des

complexes APOE/ Aβ malgré l'expression appropriée des autres récepteurs APOE. Malgré des niveaux d'APOE cérébraux plus élevés que la normale, les animaux présentant un déficit du récepteur présentent des anomalies dans le métabolisme des lipides cérébraux (ex. accumulation de sulfatides) le même que chez les souris déficientes en APOE, ce qui indique une carence fonctionnelle dans les voies cellulaires d'absorption de l'APOE (Carlo et al., 2013).

Il existe également un lien entre le complexe proNGF-p75NTR-NTSR3/Sortiline dans la maladie de Parkinson. La voie de signalisation de mort cellulaire médiée par le complexe proNGF-p75NTR-NTSR3/Sortiline semble être responsable de la dégénérescence dans les neurones dopaminergiques au niveau ventral de la substance noire, suggérant l'implication de ce complexe dans la progression de la maladie (Chen et al., 2008).

8 NTSR3/SORTILINE, PROPEPTIDE (PE), TREK-1 ET DEPRESSION

L'implication du NTSR3/Sortiline dans la dépression prend son origine en partie dans son lien avec le canal potassique, décrit précédemment, TREK-1. Le NTSR3/Sortiline et TREK-1 sont fortement distribués dans des structures cérébrales impliquées dans la physiopathologie de la dépression, comme le cortex préfrontal et cingulaire, l'amygdale, l'hippocampe, le noyau accumbens, le raphé dorsal et l'hypothalamus (Hervieu et al., 2001; Sarret et al., 2003b). Il a été montré qu'une délétion fonctionnelle de TREK-1 aboutissait à un phénotype dit de résistance à la dépression (Heurteaux et al., 2006). Partant de l'idée que le NTSR3/Sortiline a des propriétés de trafic similaires aux partenaires de TREK-1, AKAP150 et Mtap 2, capables de réguler l'expression à la membrane, et qu'il est localisé dans des régions analogues à celles du canal, l'équipe du Dr Mazella s'est penchée sur l'implication du NTSR3/Sortiline dans la régulation de TREK-1. Dans un premier temps, il a été montré, par immunoprécipitation, que le récepteur et le canal forment un complexe et ce, à la membrane plasmique. Dans des cellules COS-7, la purification de membrane plasmique a montré une augmentation d'un facteur 3 à 6 de l'expression de TREK-1 lorsque que le NTSR3/Sortiline était co-transfecté. Dans un second temps, sachant qu'il existe une régulation du récepteur par son propre propeptide libéré suite à sa maturation (Munck Petersen et al., 1999), l'équipe s'est intéressée à l'action du PE, et d'un dérivé, sur l'activité de TREK-1. Ce PE est constitué de 44 acides aminés et est capable de s'associer au NTSR3/Sortiline avec une haute affinité (Kd d'environ 5nM). Des études structure-fonction ont révélé que la partie Gln^{1} – Arg^{28} était aussi efficace sur l'activité de liaison que le propeptide entier (Gln^{1}-Arg^{44}) alors que l'affinité du peptide Gln^{1}-Arg^{16} était très faible (Westergaard et al., 2004). A l'aide de ce constat, un peptide, nommé la Spadine (**S**ortilin **P**eptide **A**nti**D**epressant (**IN**)), plus petit que le propeptide, a été synthétisé en conservant la séquence 17 à 28 et en y ajoutant la séquence 12-16 pour maintenir le stress

conformationnel (**Figure 14**). L'affinité de ce peptide sur le NTSR3/Sortiline a été évaluée sur une lignée cellulaire de microglie, les C13NJ, n'exprimant que le NTSR3/Sortiline comme récepteur à la NTS (Martin et al., 2003). Les résultats ont confirmé que le peptide présente des propriétés de liaison et des propriétés fonctionnelles identiques à celles du propeptide entier. Afin d'évaluer la sélectivité de la Spadine, des expériences de compétitions ont été réalisées entre la Spadine marquée radioactivement à l'iode 125 et la Spadine non marquée, la NTS ou le fragment Gln^{1}-Arg^{16}, sur des homogénats de membranes de cellules COS-7 transfectées ou non avec TREK-1. Les résultats ont montré que la Spadine était capable de se lier spécifiquement à TREK-1 avec une affinité de 10nM, spécificité traduite par l'incapacité de la NTS à déplacer la liaison. Quant au fragment Gln^{1}-Arg^{16}, il montre une affinité plus faible (1µM) pour TREK-1. Par ailleurs, sur des cellules entières COS-7, la liaison de la Spadine marquée I^{125} atteint un plateau au bout de 30 minutes. L'élimination de la radioactivité liée à la surface, par lavage acide, a révélé qu'environ 80 % de la quantité totale de Spadine iodée était intracellulaire, ce qui indique que le peptide a été internalisé avec TREK-1 après interaction. Tout ceci suggère donc que le NTSR3/Sortiline joue un rôle de partenaire de trafic pour le canal TREK-1. L'hypothèse émise suggère que lorsque les 2 protéines atteignent la membrane cellulaire, le propeptide est libéré, se fixe sur le NTSR3/Sortiline ou TREK-1 et module l'activité du canal en bloquant une partie des canaux exprimés, et en favorisant leur internalisation (Mazella et al., 2010).

Figure 14 : Séquence de la Spadine conçue à partir de la séquence propeptide.

L'effet de la Spadine sur les courant TREK-1 a ensuite été évalué par électrophysiologie. Le peptide est capable d'inhiber (IC_{50} = 70.7 nM) les courants potassiques TREK-1 stimulés par l'acide arachidonique sur des cellules COS-7 transfectées avec le canal. Des résultats similaires ont été observés sur des neurones pyramidaux de tranches de cerveau hippocampique de la région CA3 (riche en TREK-1 et NSTR3/Sortiline) (Mazella et al., 2010).

Comme la délétion du gène *kcnk2* codant pour TREK-1 induit un phénotype de résistance à la dépression, la suite logique était de regarder si le blocage de TREK-1 par le peptide induisait un

phénotype similaire. De façon intéressante, les souris injectées avec la Spadine montrent un comportement identique à celui des souris délétées pour TREK-1 ou des souris sauvages traitées par un antidépresseur, et ce de manière doses dépendantes. En effet, que ce soit dans le FST et le TST, il y a une diminution de l'immobilité qui traduit une diminution de la résignation. L'immobilité est interprétée comme un " état de désespoir ", en ce sens que l'animal aura perdu sa motivation à adopter des comportements d'évasion. On retrouve également une diminution du temps de la latence pour s'échapper dans le test de résignation acquise (Learn Helpness) (Mazella et al., 2010).

Enfin, l'activité moyenne de décharges des neurones sérotoninergiques chez les animaux traités avec la Spadine est presque identique à celle observée chez les souris *kcnk2 -/-*, c'est-à-dire une augmentation du taux de décharges de ces neurones. De plus, il existe une augmentation de la neurogénèse induite par la phosphorylation de CREB dans les neurones hippocampaux, de pair avec une hausse de deux marqueurs de la synaptogénèse, le PSD95 (post-synaptic density protein of 95 kDalton) et le BDNF, tant au niveau protéique qu'au niveau des ARNms (Devader et al., 2015; Mazella et al., 2010).

Tout ceci suggère que le NTSR3/Sortiline est capable de moduler l'activité de TREK-1, que ce soit par une régulation du trafic ou par l'inhibition du canal par son produit de maturation.

Plus récemment, des études ont mis en évidence l'implication de NTSR3/Sortiline soluble dans la dépression. Le domaine extracellulaire du NTSR3/Sortiline (NTSR3/Sortiline soluble) est libéré de façon à la fois constitutive et régulée par protéolyse à la surface des neurones et d'autres types de cellules (Evans et al., 2011; Hermey et al., 2006; Navarro et al., 2002). La fonction de ce motif soluble n'est pas claire, mais il a été démontré qu'elle inhibe la conversion du proBDNF en BDNF mature par la plasmine et qu'elle protège les neurones des propriétés apoptotiques du proBDNF (Teng et al., 2005). Ce NTSR3/Sortiline soluble forme un complexe avec le récepteur BDNF/TrkB et le récepteur EGF et ce complexe ternaire est internalisé et libéré, par la suite, dans les exosomes (Wilson et al., 2014). Le NTSR3/Sortiline soluble peut être détectée dans le sérum et le plasma. Il existe une augmentation significative du taux sérique de ce récepteur soluble chez les sujets déprimés comparativement aux témoins et des corrélations significatives entre ces taux sériques et les taux sériques de BDNF et de VEGF. De façon intéressante, des taux élevés de NTSR3/Sortiline soluble étaient associés à une dépression légère et modérée, mais pas à une dépression grave (Buttenschøn et al., 2015).

Toutes ces données placent le NTSR3/Sortiline au centre de mécanismes impliqués dans la régulation du comportement. A la fois récepteur, co-recepteur et protéine d'adressage, il agit sur

des composantes importantes du système nerveux central, comme la régulation des neurotrophines, ou encore l'adressage de canaux potassiques impliqué dans le maintien des potentiels de membrane. L'objectif des travaux de ce manuscrit était donc d'étendre la compréhension de ce récepteur au sein d'une pathologie complexe. D'une part, l'évaluer comme un possible marqueur biologique dans le trouble dépressif, et d'autre part, regarder, par différentes approches biologiques, les conséquences d'une perte fonctionnelle sur un organisme entier.

OBJECTIFS

Durant ces trois années de doctorat, j'ai eu la possibilité de travailler sur différents aspects du NTSR3/Sortiline. L'objectif était de replacer, sur différents niveaux, le récepteur dans l'affect pathologique qu'est la dépression, tout en approfondissant les mécanismes sous-jacents.

Dans un premier temps, l'objectif de mes travaux a été de caractériser la délétion fonctionnelle du NTSR3/Sortiline dans un modèle murin, et plus particulièrement au sein du système nerveux central. Comme décrit précédemment, le NTSR3/Sortiline a des propriétés de tri cellulaire, notamment de neurotrophines importantes dans la viabilité et la croissance neuronale. Parmi eux le BDNF, qui se présente comme un facteur crucial dans la régulation de fonctions émotionnelles et cognitives. Le NTSR3/Sortiline influence également l'activité du canal ionique TREK-1, pouvant être impliqué dans la régulation de l'humeur. C'est par différentes approches expérimentales que je me suis donc intéressé à la fonction du récepteur sur ces facteurs intervenants dans la modulation du comportement, plus particulièrement dans les états pathologiques du trouble dépressif, et ceci à partir d'un modèle murin dépourvus de NTSR3/Sortiline fonctionnel. Les souris mutantes, notées *Sort1 -/-*, ont été générées par l'équipe du Dr Morales grâce à l'introduction d'une cassette dans le gène *Sort1* entre l'exon 2 et l'exon 3, limitant ainsi la production d'une forme protéique fonctionnelle du récepteur (Zeng et al., 2009). De manière cohérente et inhérente aux fonctions du NTSR3/Sortiline, j'ai donc évalué les conséquences de la perte fonctionnelle du récepteur sur le comportement, la biochimie et, de façon logique, l'électrophysiologie au niveau du système nerveux central. Par ailleurs, étant donné que le NTSR3/Sortiline est d'abord identifié comme une composante du système neurotensinergique, il a été évident, en utilisant ce modèle de souris, d'en déterminer également l'impact sur celui-ci.

Une autre partie de mon travail a été d'évaluer si le NTSR3/Sortiline, plus particulièrement le propeptide issu de sa maturation, pouvait présenter des variations chez des personnes dépressives comparativement à des sujets sains. Cette démarche partait du principe qu'étant donné la place que prend le NTSR3/Sortiline dans la régulation de neurotrophines et l'effet sur l'humeur de son produit de maturation, serait-il possible, à l'instar de la forme soluble, que le propeptide soit un indicateur du trouble dépressif ? En effet, s'il est possible de mesurer des variations sériques de BDNF ou de NTSR3/Sortiline soluble, et d'étayer le diagnostic dépressif, il serait alors intéressant d'évaluer le niveau d'un peptide qui fait état de propriété antidépressive.

En parallèle de mes recherches, j'ai pu développer des outils informatiques dans le but de simplifier l'acquisition et le traitement de données expérimentales. C'est dans souci d'améliorer, de faciliter, et aussi parce que je ne suis pas adepte des tâches répétitives, que j'ai mis au point un logiciel capable de mesurer des occurrences et surtout des durées lors de tests comportementaux chez la souris. Les fichiers générés en sortie permettent d'accéder à de nombreuses données en un temps réduit tout en occultant le possible coût prohibitif des outils mis à disposition dans le commerce.

Etude de la délétion du NTSR3/Sortiline dans la régulation de l'état dépressif.

Article 1: Altered TREK-1 function in sortilin deficient mice results in an antidepressant phenotype.

MORENO Sebastien, *DEVADER Christelle, PIETRI Mariel, BORSOTTO Marc, HEURTEAUX Catherine and MAZELLA Jean*

Submitted for publication in the ***British Journal of Pharmacology (Under Review)***

1. Contexte de l'étude

Dans l'étude précédente, la délétion du NTSR3/Sortiline a conduit à la modification d'expression d'un de ces partenaires du système neurotensinergique, le NTSR2, et a induit un phénotype de désensibilisation à la douleur. Récemment, un autre de ces partenaires, le canal de fond potassique TREK-1, a fait l'objet d'une attention particulière dans le phénotype de dépression et d'anxiété. En effet, la délétion du gène codant pour le canal chez la souris résulte en un phénotype de résistance dans les tests comportementaux relatifs à la dépression. Ces souris révèlent un comportement identique à des souris naïves traitées avec des antidépresseurs comme la fluoxétine. Au-delà de cet aspect phénotypique, la délétion de TREK-1 a également entrainé une augmentation de la neurogenèse hippocampique et du taux de décharges des neurones sérotoninergiques du noyau du raphé dorsal. Par ailleurs, une inhibition du canal par un dérivé peptidique du propeptide issu du NTSR3/Sortiline, la Spadine, produit des effets similaires antidépressifs. Il a été démontré l'existence d'un complexe protéique entre le canal TREK-1 et le NSTR3/Sortiline et que l'expression du canal au niveau de la membrane plasmatique des cellules COS-7 est augmentée lorsque celui-ci est co-exprimé avec le récepteur. De plus, le NTSR3/Sortiline de par ses propriétés de tri, est capable de réguler des neurotrophines, comme le BDNF, importante dans le système nerveux central.

Puisque le NTSR3/Sortiline et le TREK-1 sont associés aux niveaux cellulaire et moléculaire (Mazella et al., 2010) et que le NTSR3/Sortiline joue un rôle important dans le triage de nombreuses protéines, nous avons émis l'hypothèse que l'absence du récepteur pourrait entraîner une modification de l'expression du TREK-1, de sa localisation cellulaire et de sa fonction. D'autre part, comme TREK-1 a été décrit comme une cible puissante dans la dépression (Heurteaux et al., 2006b), le but du présent travail était aussi d'analyser le phénotype des souris KO-NTSR3 par rapport au comportement dépressif.

2. Résultats et discussion

Ce sont par des approches comportementales, biochimiques et électrophysiologiques que nous avons regardé les conséquences de la délétion du NTSR3/Sortiline sur la régulation du canal potassique TREK-1 mais également sur le système neurotrophique qui régule le BDNF.

Dans un premier temps, afin de valider la preuve d'un complexe NTSR3/Sortiline / TREK-1 et le rôle de TREK-1 dans l'état dépressif, nous avons exploré le comportement des souris KO-NTSR3 dans des tests relatifs à la dépression mais également à l'anxiété, qui est une constante intégrante de cet état. Dans le test de nage forcée, la Spadine a été utilisée sur les souris sauvages pour valider l'effet antidépresseur induit par le blocage de TREK-1 et a donc permis une diminution de l'immobilité comparées aux souris sauvages non traitées (**Figure 20A**). De façon intéressante, les souris délétées pour le NTSR3/Sortiline montrent également une diminution de l'immobilité ($n = 19$, $p<0.001$ versus WT) et la Spadine n'induit pas d'effet supplémentaire sur ces souris (86.1 ± 11.6 sec, $n = 14$, $p = 0.999$) (**Figure 20A**). Pour préciser ce résultat, nous avons réalisé deux autres tests ; le test de suspension par la queue (TST) et le test de suppression de la nourriture par la nouveauté (NSF). Dans le TST, les souris KO-NTSR3 présentent également une diminution de l'immobilité en comparaison aux souris sauvages (**Figure 20B**). Dans le NSF, les souris KO-NTSR3 ont une latence plus réduite pour accéder à la nourriture par rapport aux sauvages (**Figure 20C**), ce qui traduit une tendance plus prompte à explorer et surpasser l'environnement aversif en l'absence de prise alimentaire depuis 24h. Ces résultats suggèrent un comportement de résistance dans ces tests relatifs à la dépression, similaires à ceux retrouvés chez les souris KO-TREK-1.

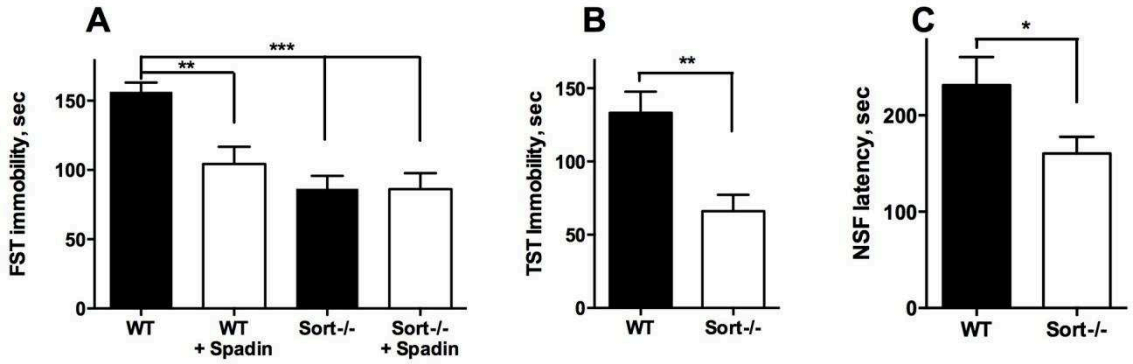

Figure 20 : Comportement relatif à la dépression chez les souris KO-NTSR3. ***A)*** *FST ; temps d'immobilité avec ou non injection de Spadine.* ***B)*** *TST ; temps d'immobilité.* ***C)*** *NSF ; latence pour atteindre la nourriture au centre de l'appareil.*

En ce qui concerne les tests d'anxiété, les souris KO-NTSR3 ont révélé une augmentation d'un état anxieux. En effet, dans le test de la boite claire obscure, les souris KO-NTSR3 passent plus de temps dans le compartiment fermé et évitent l'exploration comparées aux souris sauvages, résultats qui se retrouvent également dans le test de la croix surélevée où les KO-NTSR3 explorent moins les bras ouverts de l'appareil (**Figure 21A et 21C**). Pour compléter ces résultats, nous avons regardé la capacité des souris KO-NTSR3 à enterrer des objets (ici des billes), test pouvant traduire un phénotype lié à l'anxiété et aux troubles obsessionnels compulsifs (Deacon, 2006). De façon impressionnante, les souris KO-NTSR3 enterrent la quasi-totalité des billes par rapport aux souris sauvages, confortant l'état anxieux précédemment observé (**Figure 21D et 21E**). Cependant la concentration sérique de corticostérone dans les conditions basales demeure inchangée entre les souris KO-NTSR3 et les sauvages, ce qui indique que le comportement anxieux des souris KO-NTSR3 n'est pas la conséquence de l'augmentation hormonale (**Figure 21F**).

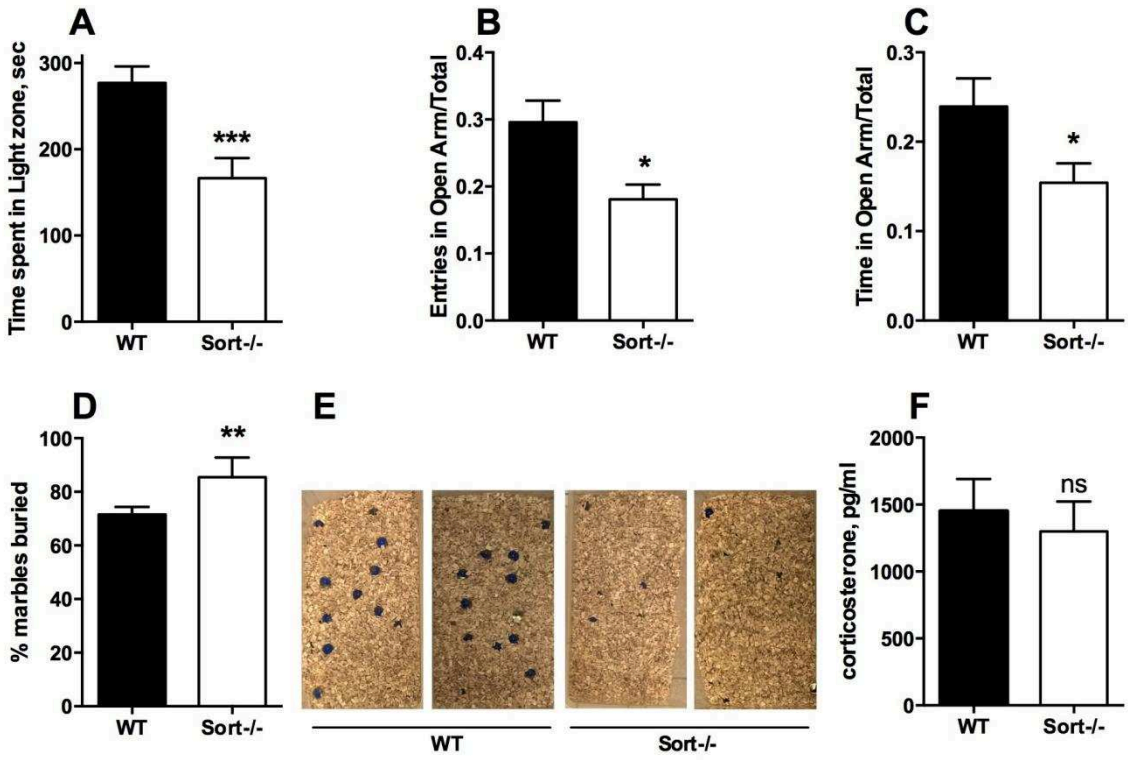

Figure 21 : ***Comportement relatifs à l'anxiété chez les souris KO-NTSR3. A)*** *Test de la boite claire-obscure ; temps passé dans zone claire.* ***B & C)*** *Test de la croix surélevée ; B) Ratio du nombre d'entrées dans les bras ouverts. C) Temps passé dans les bras ouverts.* ***D & E)*** *Test de l'enfouissement des billes ; D) Pourcentage de billes enfouies.* ***F)*** *Niveau de corticostérone.*

Ce phénotype de résistance des souris KO-NTSR3 comparable à celui souris KO-TREK-1 laisse suggérer un dysfonctionnement du canal potassique, qui pourrait se traduire par une inhibition ou suppression de son expression. Pour vérifier cette hypothèse, nous avons dans un premier temps évalué l'expression de TREK-1 à diffèrent niveaux de la cellule, et de façon intéressante, l'expression membranaire du canal potassique, dans des homogénats de cerveaux de souris KO-NTSR3, diminue fortement d'environ 36 % par rapport aux souris sauvages (**Figure 22A**). Cette perte d'expression membranaire semble compensée, mais de manière non significative, par une augmentation au niveau des vésicules de haute et basse densité. La quantité totale de TREK-1 chez les souris KO-NTSR3 n'est pas modifiée par rapport aux souris sauvages. Cette perte du canal TREK-1 à la surface de la cellule, sans modification de l'expression totale du TREK-1, est cohérente avec le rôle, déjà observé, du NTSR3/Sortiline dans le tri cellulaire du canal (Mazella et al., 2010).

TREK-1 est un canal potassique de fond qui permet de maintenir le potentiel de membrane et, par conséquent, de moduler l'activité des neurones. La modification d'expression membranaire des souris KO-NTSR3 laissait supposer des conséquences possibles sur les propriétés électrophysiologiques des cellules. En effet, en mesurant le potentiel de membrane de neurones issus de cortex cérébraux de souris KO-NTSR3, nous avons observé une augmentation du potentiel d'environ 18 mV comparé à ceux de souris sauvages (44.7 ± 1.3 mV KO-NTSR3 ; 62.9 ± 3.6 mV WT) (**Figure 22B**). Ce résultat renforce l'hypothèse d'une perte fonctionnelle de TREK-1 à la membrane. En effet, TREK-1 permet la diffusion du potassium intracellulaire vers le milieu extracellulaire, par conséquent, son blocage ou sa délétion entraine une accumulation de potassium intracellulaire et donc une dépolarisation transitoire. Par ailleurs, cette dépolarisation neuronale a été également observée avec le blocage de TREK-1 par la Spadine (Devader et al., 2015). Des études antérieures ont montré que le blocage (Mazella et al., 2010) ou la délétion (Heurteaux et al., 2006b) de TREK-1 améliore le taux de décharge des neurones 5-HT du cerveau moyen, un paramètre clé prédictif de l'efficacité des antidépresseurs. Par conséquent, nous avons effectué des enregistrements unitaires extracellulaires de neurones 5-HT dans le noyau dorsal du raphé (DRN) chez des animaux anesthésiés. L'activité de décharge basale a été enregistrée à la fois chez les souris sauvages et KO-NTSR3 par des traces successives le long du DRN. Les neurones 5-HT trouvés chez les souris sauvages déchargeaient dans une gamme de fréquences normales (1,5-2 Hz) avec une moyenne qui était plus de deux fois inférieure à celle des souris KO-NTSR3 (1,46 ± 0,09 Hz contre 3,42 ± 0,21 Hz, $p < 0,001$).

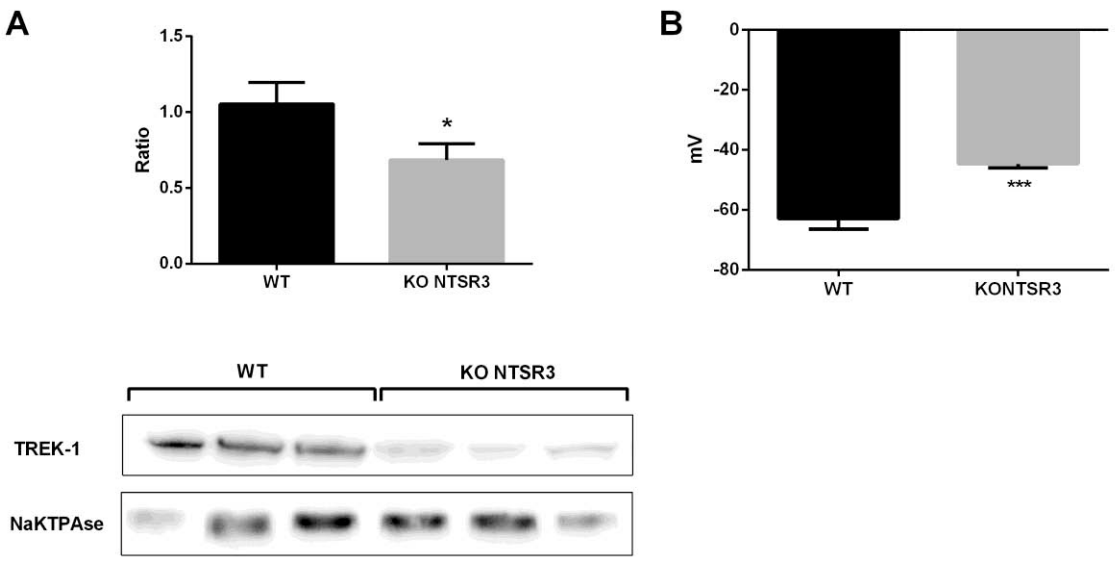

Figure 22 : Expression membranaire de TREK-1 et potentiel de membrane chez les souris KO-NTSR3. ***A)*** *Expression de TREK-1 à la membrane ; Western Blot.* ***B)*** *Valeurs moyennes du potentiel de membrane obtenues sur les neurones corticaux primaires de souris KO-NTSR3 et WT (ΔmV = 18,21 mV, n = 19, p< 0,001).*

Pour étayer un peu plus les conséquences fonctionnelles de la perte du NTSR3/Sortiline sur le système nerveux centrale, nous avons évalué l'expression d'un autre de ces partenaires essentiels pour la fonction neuronale, le BDNF. Il a été démontré que la libération du BDNF dans la voie régulée dépendait de la présence du NSTR3/Sortiline (Chen et al., 2005). Nous avons donc regardé les l'expression protéique du BDNF mais également de son précurseur, le proBDNF, qui interagit notamment avec la partie N-terminale du NTSR3/Sortiline. De façon intéressante, bien qu'il n'y ait pas de modification de l'expression du proBDNF (**Figure 23B**), le BDNF est significativement augmenté (**Figure 23A**) dans les cerveaux de souris KO-NSTR3 par rapport à ceux des souris sauvages. Nous avons alors évalué la phosphorylation du récepteur du BDNF, le TrkB, qui traduit l'activité du récepteur. L'expression cérébrale de phospho-TrkB est significativement plus élevée chez les souris KO-NTSR3 comparée aux souris sauvages. Pour déterminer quelle voie de sécrétion du BDNF a été affectée chez les souris KO-NTSR3, nous avons examiné à la fois l'expression de la furine, responsable de la maturation intracellulaire du proBDNF jusqu' à la voie de sécrétion constitutive, et l'expression du complexe plasmine-tPA, responsable de la maturation extracellulaire de la sécrétion régulée du proBDNF (Lu et al., 2005). Chez les souris KO-NTSR3, l'expression cérébrale de la furine est fortement augmentée, tandis que l'expression du tPA (tissue plasminogen

activator), l'activateur de la plasmine, a diminué significativement. La plasmine, qui permet le clivage du proBDNF extracellulaire, n'est pas modifié chez les souris KO-NTSR3.

De façon intéressante, il y a une surexpression des formes phosphorylées ERK1/2 et CREB qui peut être corrélée à l'augmentation de l'expression du BDNF et de son récepteur activé TrkB, suggérant une activité constitutive du système de signalisation du BDNF.

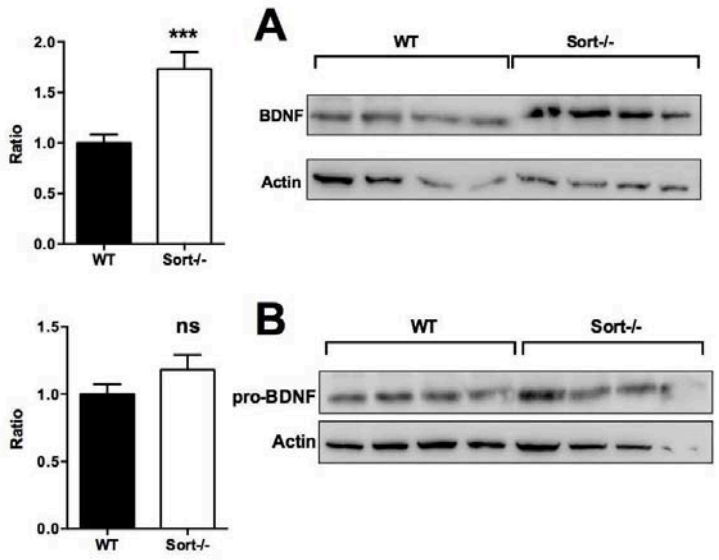

Figure 23 : Effet de la délétion du gène NTSR3/Sortiline sur la régulation du BDNF. Analyse et quantification Western Blot ***A)*** *BDNF* ***B)*** *Pro-BDNF. Les histogrammes représentent la moyenne ± SEM de la quantification des protéines à partir d'échantillons de cerveaux. Mann-Whitney, *p< 0,05; **p< 0,01, ***p< 0,001, ns; non significatif.*

Ces travaux présentent pour la première fois une altération de la localisation et de la fonction de TREK-1 chez les souris déficientes pour le NTSR3/Sortiline, qui conforte l'idée d'une interaction fonctionnelle entre les deux protéines. Cette altération aboutit à l'expression d'un phénotype de résistance à la dépression dans les tests comportementaux, comparable à celui retrouvé chez les souris dont le canal TREK-1 est absent ou encore chez des souris traitées avec des antidépresseurs. En revanche le comportement anxieux des souris KO-NTSR3 apparait comme un comportement paradoxal à la vue des résultats précédents, mais il n'est cependant pas corrélé à une perturbation du niveau sérique de corticostérone, responsable de la régulation du stress. Une étude récente a montré également une augmentation du stress chez les souris KO-NTSR3 (Ruan et al.,2016) mais aussi qu'un stress chronique induit chez des souris sauvages menait à l'augmentation de l'expression de NSTR3/Sortiline conduisant à l'expression d'un phénotype dépressif. Ces résultats

sont en accord avec l'idée que le phénotype de résistance à la dépression serait la conséquence de l'absence de NSTR3/Sortiline.

Nous avons également observé une diminution de l'expression de TREK-1 à la membrane plasmique au niveau des cerveaux des souris KO-NTSR3, suggérant un rôle crucial du récepteur dans le trafic du canal potassique. La conséquence neuronale qui en résulte réside en une augmentation du potentiel membranaire des neurones et une activité des neurones sérotoninergiques du DRN supérieure d'un facteur deux, ce qui indique une augmentation de l'efficacité de la neurotransmission sérotoninergique. De façon intéressante, ces deux observations sont très semblables à celles obtenues avec le blocage de l'activité de TREK-1 par la Spadine (Devader et al., 2015 ; Mazella et al., 2010) et par la fluoxétine (Heurteaux et al., 2006b) ou lorsque le gène KCNK2, codant pour TREK-1, a été supprimé chez la souris (Heurteaux et al., 2006b).

Enfin, la régulation du BDNF semble intimement liée au NTSR3/Sortiline, car en effet, chez les souris KO-NTSR3 il y a une augmentation de BDNF et de l'activité de son récepteur TrkB. Cette augmentation neurotrophique n'est cependant pas dépendante d'une augmentation de son précurseur le proBDNF qui reste inchangé chez les KO-NTSR3. L'explication tiendrait compte d'un déséquilibre entre la voie constitutive et régulée du BDNF. En absence de NTSR3/Sortiline dans la voie régulée, le proBDNF serait maturé principalement dans la voie constitutive intracellulaire, ce qui expliquerait l'augmentation de l'expression de la furine et la diminution de la maturation extracellulaire avec la baisse d'expression du tPA. De plus, une augmentation de l'activité du récepteur TrkB, inhérent au niveau de BDNF, induirait une augmentation de l'activité de CREB et par conséquent, la possibilité d'une transcription de gènes importants dans l'activité neuronale.

En conclusion, ces résultats mettent en lumière l'importance du NTSR3/Sortiline dans les mécanismes moléculaires et physiologiques qui régulent le comportement relatif à l'humeur et plus particulièrement dans le phénotype de résistance à la dépression observé lorsque l'expression de TREK-1 est réduite ou totalement absente.

Altered TREK-1 function in sortilin deficient mice results in an antidepressant phenotype

Running Title : Depression resistance of sortilin deficient mice

Sébastien Moreno, Christelle Devader, Mariel Pietri, Marc Borsotto, Catherine Heurteaux and Jean Mazella*

CNRS, Institut de Pharmacologie Moléculaire et Cellulaire, UMR 7275, Université Côte d'Azur, 660 route des Lucioles, 06560 Valbonne, France.

Corresponding author : Jean Mazella, phone: 33 4 93 95 77 61; fax: 33 4 93 95 77 08 email: mazella@ipmc.cnrs.fr CNRS, Institut de Pharmacologie Moléculaire et Cellulaire, UMR 7275, Université Côte d'Azur, 660 route des Lucioles, 06560 Valbonne, France

Acknowledgements

We thank Carlos Morales (McGill University, Montreal) for providing *Sort1*$^{-/-}$ mice. We thank E-Phys-Science for the 5-HT firing rate experiments. We thank the French Government for the "Investments for the Future" LABEX ICST # ANR-11 LABX 0015. This work was supported by the Centre National de la Recherche Scientifique and the Agence Nationale de la Recherche (ANR-13-SAMA-0001 and -0002 and ANR-13-RPIB-0001 and -0002).

For Peer Review

Abstract

Background and purpose. The background potassium channel TREK-1 has been shown to be a potent target for depression treatment. Indeed, deletion of the channel in mice resulted in a depression resistant phenotype. The association of TREK-1 with the sorting protein sortilin prompted us to investigate the behavior of mice deleted from the gene encoding sortilin (*Sort1*$^{-/-}$).

Experimental approach. To characterize the consequences of sortilin deletion on TREK-1 functionality, we combined behavioral, electrophysiological and biochemical approaches performed *in vivo* and *in vitro*.

Key results. Analyses of *Sort1*$^{-/-}$ mice revealed that they display 1) a corticosterone-independent anxiety-like behavior, 2) a resistance to depression as demonstrated by several behavioral tests and 3) an increased efficacy of 5-HT neurotransmission. All these properties were due to TREK-1 action defficiency consequently to a decrease of its cell surface expression and to the modification of its electrophysiological activity. An increase of BDNF expression through activation of the furin-dependent constitutive pathway as well as an increase of the BDNF receptor TrkB were in agreement with the depression-resistant phenotype of *Sort1*$^{-/-}$ mice.

Conclusions and implications. Our results demonstrate that the TREK-1 function is altered in the absence of sortilin confirming the importance of this channel in the regulation on the mood as a crucial target to treat depression.

Keywords. Depression, sortilin, TREK-1, behavior, electrophysiology

For Peer Review

Abbreviations

5-HT : Serotonin

AD : Antidepressant

BDNF : Brain derived nerve factor

BrdU : 5-bromo-2'-deoxyuridine

CREB : cAMP response element-binding protein

DCX : Doublecortin

DRN : Dorsal raphe nucleus

FST : Forced swimming test

H/LDM : High and low density microsomes

MAP kinase : Mitogen activated protein kinase

NSF: Novelty suppressed feeding

NT: neurotensin

NTSR2 : Neurotensin receptor-2

NTSR3 : Neurotensin receptor-3

PM: Plasma membrane

p75NTR : Neurotrophin receptor of 75 kDa

TGN38 : Trans-golgi network protein of 38 kDa

TrkB : Tropomyosin receptor kinase B

TST : Tail suspension test

WT : Wild type

For Peer Review

Introduction

Phenotyping mice in which a gene has been deleted may appear relatively easy in terms of preliminary observations for detecting a major health problem or a motor defect. After a series of physical exams including body weight and temperature, home cage locomotion, grooming, nesting and sleeping, neurological reflexes can be tested before starting behavioral tasks dealing with anxiety and mood disorders (Crawley, 1999). In the field of depression and anxiety-related disorders, the background potassium channel TREK-1 (KCNK2) has been one of the first target for which deletion in mice (*Kcnk2*$^{-/-}$) resulted in a depression-resistant phenotype highlighted by behavioral tests (Heurteaux et al., 2006b). The properties of these mutant mice are spectacular. *Kcnk2*$^{-/-}$ mice behave similarly to naive mice treated with antidepressants (Ads) like fluoxetine. In addition, an increase in hippocampal neurogenesis and firing rate of serotoninergic neurons from the dorsal raphe nucleus strongly correlated with the AD-like behavior of *Kcnk2*$^{-/-}$ mice (Heurteaux et al., 2006b). Taking together, results obtained from *Kcnk2*$^{-/-}$ mice led to the hypothesis that the search of selective blockers of the TREK-1 channel could lead to a new type of AD. More recently, the discovery of spadin, which is a sortilin-derived peptide acting as a potent AD and targeting TREK-1 channels, supported this hypothesis (Mazella et al., 2010). Interestingly, in addition to the AD properties of spadin, we have demonstrated the existence of a protein complex between the TREK-1 channel and sortilin. The expression of the channel at the plasma membrane of COS-7 cells is increased when TREK-1 is co-expressed with sortilin (Carlo, Nykjaer & Willnow, 2014). Consequently, because sortilin is crucial in the sorting of several factors and enzymes (Kandror & Pilch, 2011; Lefrancois, Zeng, Hassan, Canuel & Morales, 2003), we analyzed in details the depression-related phenotype of mice in which the gene encoding sortilin (*Sort1*) has been inactivated, with a focus on the expression of its partner TREK-1 and the subsequent consequences on the TREK-1 function.

To date, inactivation of *Sort1* gene demonstrated that sortilin is involved in the proNGF-induced neuronal cell death when associated with p75NTR (Nykjaer et al., 2004) as well as in the binding

For Peer Review

and internalization of the fronto-demential protein progranulin (Hu et al., 2010). More recently a controversial role of sortilin in the regulation of cholesterol metabolism has been described (Kjolby et al., 2010; Musunuru et al., 2010), and largely commented in the literature (Dube, Johansen & Hegele, 2011; Tall & Ai, 2011). Sortilin (also called neurotensin (NT) receptor-3 (NTSR3)) belongs to the neurotensinergic system (Mazella et al., 1998). A recent sudy showed that the lack of sortilin expression leads to the increase in brain of both NT and NTSR2 receptors. These *Sort1*$^{-/-}$ mice are less sensitive to thermal and chemical nociception (Devader et al., 2016).

Because sortilin and TREK-1 have been shown to be associated at the cellular and molecular levels (Mazella et al., 2010) and because sortilin plays an important role in the sorting of numerous proteins we hypothesized that the absence of sortilin could result in modification of TREK-1 expression, its cellular location and its function. On another hand, since TREK-1 was described to be a potent target in depression (Heurteaux et al., 2006b), the aim of the present work was also to analyze the phenotype of *Sort1*$^{-/-}$ mice regarding depression behavior.

For Peer Review

Materials and Methods

Primary Culture of Cortical Neurons

Primary cortical neurons were isolated from 14-day-old mouse embryo cortice (E14). Cells were mechanically dissociated and seeded in 35 mm diameter previously treated with Poly-D-Lysine and maintained in culture in a Neurobasal / B27 medium for 10-14 days.

Data ans Statistical Analysis

Animal studies were conducted in compliance with the ARRIVE guidelines (Kilkenny et al., 2011; McGrath & Lilley, 2015). Adult male (8-10 weeks old) mice were housed under controlled laboratory conditions according to the FELASA guidelines and recommendations ; 6 mice/cage with a 12 h dark-light cycle, a temperature of 21 ± 2°C, and a 40–60% humidity. They have free access to standard rodent diet and tap water. The NTSR3/sortilin homozygous KO mice (*Sort1*$^{-/-}$) were generated by the Morales's laboratory by incorporation of a GFP cassette after exon 1 (Zeng, Racicott & Morales, 2009) and controls were C57Bl/6J male mice from Janvier Labs (St Berthevin, France). The local Ethics Committee (CIEPAL) (protocol number 00893.02) approved experimental procedures and animal care are in accordance with the policies on the care and use of laboratory animals of European Community legislation 2010/63/EU.

Group sizes : the group size provided for the following experiments were variable due to the difficulties to obtain regularly the same amount of adult males (8-10 weeks old) house breeded animals (ie : *Sort1*$^{-/-}$ mice). For each kind of experiment, we adapted the number of WT mice to the number of available *Sort1*$^{-/-}$ mice.

Each animal was used once and the total of 218 male WT and *Sort1*$^{-/-}$ mice, and 5 female WT and *Sort1*$^{-/-}$ mice, were used for this sudy. Behavioral experiments were performed with naïve mice for all used tests. Mice were isolated 30 minutes in neutral room before tests. The experimenter was blind to randomized experimental groups. Randomization was performed using the TST software (Bioseb, France).

For Peer Review

Behavioral tests used in this work have been validated for mouse behavioral phenotypes related to neuropsychiatric disorders, such as depression or anxiety (for review, see (Samsom & Wong, 2015)). Group sizes for behavioral, biochemical and electrophysiological experiments were equal with the exception for firing rate recordings for which measurements were recorded from 36 5-HT neurons for WT and 26 neurons for *Sort1*$^{-/-}$ mice. These in vivo experiments were performed on 5 animals for each group and the number of recorded neurons from each animal varied pending on the position of electrodes.

For Western blot analyses, results were normalized using either an intracellular protein (actin) or a protein specific for a given intracellular compartment for sub-cellular fractionation experiments.

All data (displayed as mean ± SEM) were analysed using Prism 6-2 Software (GraphPad, San Diego, USA). For the comparison of two groups, Mann-Whitney test was used. All remaining data were compared using a one-way ANOVA with a Tukey's multiple comparison test. The level of significance was set at $P < 0.05$. The data and statistical analysis comply with the recommendations on experimental design and analysis in pharmacology (Curtis et al., 2015).

Behavioral tests

Forced swimming test (FST)

FST was performed according to the procedure initially described (Porsolt, Le Pichon & Jalfre, 1977). Each animal was placed in a cylinder (height 30 cm, diameter 15 cm) filled with 15-cm water at 22•±•1 °C with no escape possibility during 6 min. The period of immobility was measured only during the last 4 min of the trial. We considered an immobile mouse when it only remained floating with slight movements to maintain head above surface.

Novelty suppressed feeding (NSF)

Mice were deprived from food for 24h. On test day, mice were placed in a highly brightly lit box (45•×•45•×•20 cm), with floor covered with wood chip bedding, during 10 min. At the center of the box, a food pellet was placed on a white platform. The latency for the animal to eat the pellet

For Peer Review

was measured as previously described (Santarelli et al., 2003).

Tail Suspension Test (TST)

Mice were suspended by the tail by using a piece of adhesive tape. After 'agitation' or 'escape-like' behavior, mice adopted an immobile posture, suggested to mirror a state of depression. We recorded the immobility time during a 6 min test session according to (Cryan, Mombereau & Vassout, 2005).

Marble Burying

Burying object relates to a natural defense mechanism that occurs in mice under stress condition or anxiety state. Marble burying is able to detect anxiety and obsessive compulsive disorders-related phenotypes (Deacon, 2006). In response to novel bedding/environment mice exhibit digging behavior. Mice were placed during 30 min in a cage filled with approximately 5 cm deep with wood chip bedding and a regular pattern of 13 glass marbles disposed on the surface, evenly spaced, each about 4 cm apart. At the end of the time, buried marbles were counted (2/3 minimum of depth). 75% of buried marbles was a typical score for naïve C57BL/6.

Elevated Plus Maze

Elevated Plus Maze allowed to define an anxiety response in rodents (Gross et al., 2002). The apparatus consisted of central platform (5x5cm), two open arms and two closed arms across from each other and perpendicular, with the same size (45x5cm) and 15 cm wall height for the closer arms. The apparatus was placed at 45 cm height above the floor. Mice were placed in the central platform facing one open arm and were allowed to freely move during 10 minutes. During this period, number of entries and time spent in both arm were measured. To define an anxiety response, the time and number of entries in open arms were evaluated in relation to whole time spent or the total entries.

Light Dark

Mice were placed in a box divided into two compartments by a black partition with a small opening that allows mouse to move from one compartment to the other (Welch et al., 2007). One

For Peer Review

compartment, corresponding to one-third of the surface area, was made of white plastic and was brightly illuminated. The adjoining smaller compartment was black and dark. Mice were placed in the white compartment and allowed to move freely between the two chambers for 5 min. Time spent in the white chamber, and latency to the first transition were recorded. Mice tended to avoid the white compartment. The measures of exploration in this area were used as experimental indices of anxiety.

Measurement of serum corticosterone levels

Corticosterone concentration present in the serum from WT and *Sort1*$^{-/-}$ mice was determined using the ELISA kit from Enzo Life Science according to the manufacturer recommendations.

Whole Cell Patch Clamp Recordings and Membrane Potential Measurements

Electrophysiological experiments were performed on primary cortical neurons seeded at a density of 100,000 cells/35 mm dish after 10 days of culture. Membrane potential was recorded in whole cell configuration (Hamill, Marty, Neher, Sakmann & Sigworth, 1981) in current clamp mode (no current is injected, I = 0). Each membrane potential was evaluated by using a RK 400 patch clamp amplifier (Axon Instruments, USA), low-pass filtered at 3 kHz and digitized at 10 kHz using a 12-bit analogue-to-digital converter Digidata (1322 series, Axon Instruments, USA). Patch clamp pipettes were pulled using vertical puller (PC-10, Narishige) from borosilicate glass capillaries and had a resistance of 10 – 8 MΩ. The bath solution contained (in mM) 150 NaCl, 5 KCl, 3 MgCl2, 1 CaCl2, and 10 HEPES adjustedto pH 7.4 with NaOH. The pipette solution contained (in mM) 155 KCl, 3 MgCl2, 5 EGTA, and 10 HEPES adjusted to pH 7.2 with KOH. All experiments were performed at room temperature (21-22°C). Data acquisition was carried out using a microcomputer (Dell Pentium) with commercial software and hardware (pClamp 8.2). All values of membrane potentials are expressed in mV as mean±standard error of the mean (SEM).

For Peer Review

Sub-cellular fractionation

In order to quantify the amount of TREK-1 expressed at the plasma membrane and intracellularly, we performed sub-cellular fractionation from brain homogenates. Plasma membranes were prepared from brain homogenates of WT or KO-NTSR3/Sortilin mice according to the protocol previously described (Clancy & Czech, 1990). 30 µg of crude homogenates, purified plasma membranes and high and low density vesicles (H/LDM) were submitted to Western blot analysis using the rabbit polyclonal antibody against Anti-K2P2.1 (TREK-1) (1:500) (Alomone Labs (Israel)). Proteins detected with this antibody were normalized using antibodies specific for each intracellular compartment (NaKATPase for plasma membranes, TGN38 for H/LDM and beta-actin for total extracts) from SantaCruz technologies (USA).

Western Blot

Mouse brains were dissected on ice and then homogenized in a solubilization buffer containing 20 mM HEPES (pH:7.4), 1 mM EDTA, 1 mM PMSF, 250 mM sucrose, and protease inhibitor cocktail using a polytron at the lowest speed. The homogenates were centrifuged 20 min at 100,000×g at 4°C. Supernatants were resupended in 20 mM HEPES (pH: 7.4), 1mM EDTA and stored at −20°C until further use. Solubilized proteins were loaded at 50 µg in SDS buffer, separated on 10% SDS PAGE gels and then transferred to a nitrocellulose membrane.

Membranes were incubated with rabbit polyclonal Anti-BDNF (1:1000) (GeneTex (USA)), Anti-Phospho(Tyr705)TrkB (1:500), Anti-TrkB (1:1000) (Signalway Antibody (USA)), Anti-ProBDNF (1:400) (Alomone Labs (Israel)), Anti-Furin (1:1000) (SantaCruz technologies (USA)), Anti-Phospho(Ser133) CREB (1:500) and mouse monoclonal Anti-CREB (1:1000)(CST(USA)), mouse monoclonal Anti-beta-Actin (1:5000)(SantaCruz technologies (USA) over night at 4°C. Afterwards, membranes were incubed 30 minutes with secondary antibody (related to species of first antibody) coupled HRP. Protein bands were revealed, images were acquired with FX Fusion (Vilber) and analysed with ImageJ (US NIH (Bethesda) (Schneider, Rasband & Eliceiri, 2012).

For Peer Review

Measurement of hippocampal neurogenesis

Twenty-four hours after the BrdU injection (120 mg per kg of body weight in a 300 µl bolus), mice were euthanized and transcardially perfused with 4% cold paraformaldehyde. Serial brain sections were cut (40 µm) throughout the entire hippocampus on a vibratome (Leica). Every sixth section throughout the hippocampus was processed for BrdU or doublecortin (DCX) immunohistochemistry, as previously described (Heurteaux et al., 2006a). For each immunodetection, slides were first incubated overnight at 4°C with a mouse monoclonal anti-BrdU antibody (1:200; Becton-Dickinson) or a goat anti-DCX (1:400, Santa Cruz Laboratories). For chromogenic immunodetection, sections were then incubated for 1 hour in biotin-conjugated species-specific secondary antibodies (1:100; Vector Laboratories) followed by a peroxidase-avidin complex solution according to the manufacturer's protocol. The peroxidase activity of immune complexes was visualized with DAB staining using the VectaStain ABC kit (Vector Laboratories). For fluorescent double labeling, that were performed to determine the cell phenotype, sections were incubated overnight at 4°C with anti-sheep BrdU (1:200, Interchim), anti-goat DCX (1:200, Santa Cruz Laboratories), or an anti-GFAP (Glial Fibrillary acidic protein, marker for astrocytes, 1:250, Dako). Antibodies were revealed with anti-IgG Alexa 488 or 594-coupled antibodies (1:400; Molecular Probes). All BrdU-labeled cells in the granular cell layer and subgranular zone (SGZ) were counted in each section (n = 10 and 5 mice per group) at 400x and 1000x magnification under a light microscope (Olympus) by an experimenter blinded to the study code. The total number of BrdU-positive cells per section was multiplied by 6 to obtain the total number of cells per dentate gyrus. The counting of BrdU/DCX labeled cells was performed using a Laser Scanning Confocal Microscope (TCS SP, Leica) equipped with a DMIRBE inverted microscope.

Extracellular unitary recordings of DRN 5-HT neurons. Single-barreled glass micropipettes (recording electrodes) were filled with a 2 M NaCl solution saturated with Fast Green FCF,

For Peer Review

resulting in an impedance of 2–5 MΩ. Mice were anaesthetized with chloral hydrate (400 mg/kg, *i.p.*, using a 2% solution), and placed in a stereotaxic frame equipped with the Stoelting mouse adapter. Electrodes were positioned 0.5–1 mm posterior to the interaural line on the midline, and were then lowered into the dorsal raphe nucleus (DRN) at a depth of 2.5 mm from the brain surface. 5-HT neurons were then encountered over a maximal distance of 1 mm. They were identified using the following criteria: a slow (0.5–2.5 Hz) and regular firing rate and long-duration (0.8 – 1.2 ms) action potentials, with a positive-negative spike (Heurteaux et al., 2006a). Spikes were computed by using the Spike 2 software. Firing rates were calculated as the mean number of events occurring within a 10 s period. For each neuron, discharges were monitored during 60 seconds. Each mouse received either spadin (10^{-5} M in a 100 µl bolus) or its vehicle. Starting 30 min after the injection, 3 to 4 successive descents were performed along the DRN, for a total of 4–8 cells recorded per animal. Recordings were performed for a maximal duration of 4 hours post-injection.

For Peer Review

Results

Sort1$^{-/-}$ mice behavior in depression and anxiety tests

In the aim to confirm the existence of sortilin/TREK-1 complexes and the role of the TREK-1 channel in depression, we first investigated the behavior of *Sort1*$^{-/-}$ mice in a series of behavioral tests related to depression and anxiety.

Depression tests

The forced swimming test (FST) performed directly on both WT and *Sort1*$^{-/-}$ mice groups indicated that *Sort1*$^{-/-}$ mice presented a significant lower immobility time (100.3±13.5 sec) than WT mice (151.4±7.8 sec) (Figure 1A). FST was validated on WT mice by the use of the novel AD spadin (0.1 µM) which after *iv* injection decreased the immobility time from 162.9±12 sec to 104.4±12.5 sec (One way ANOVA, $F(3, 52) = 10.43$) (Figure 1B). Interestingly, the immobility time of vehicle injected *Sort1*$^{-/-}$ mice was 81.6±10.1 sec and injection of spadin had no effect on these mice (86.1±11.6 sec) (Figure 1B). This result prompted us to perform two other tests, the tail suspension test (TST) and the novelty supressed feeding test (NSF). The TST confirmed that *Sort1*$^{-/-}$ mice had an immobility time (65.9±11.2 sec) significantly reduced when compared to WT mice (133.2±14.4 sec, n = 20) (Figure 1C). Finally, in the NSF test, the latency time measured for WT mice (231.4±29.2 sec) was also significantly decreased in *Sort1*$^{-/-}$ mice (158.5±19.1 sec) (Figure 1D). Taken together, these results indicate that *Sort1*$^{-/-}$ mice appear to display a depression-resitant behavior resembling to that of *Kcnk2*$^{-/-}$ mice (Heurteaux et al., 2006b).

Anxiety tests

In the light dark test, the time of spent in the light zone for WT mice was 294.9±14.9 sec, time significantly higher than that of *Sort1*$^{-/-}$ mice (156.9±15.1 sec) (Figure 2A). Therefore, we tested the two groups of mice in the elevated-plus Maze test by measuring the ratio of the time and the number of entries in the open arm. As observed in Figure 2B, the time ratio in the open arm of WT mice (0.239±0.031) was significantly reduced in *Sort1*$^{-/-}$ mice (0.148±0.023) (Figure 2B). In the same way the ratio in the number of entries of WT mice (0.322±0.021) was decreased in *Sort1*$^{-/-}$

For Peer Review

mice (0.194±0.022) (Figure 2C). Finally, we tested the ability of WT and *Sort1*$^{-/-}$ mice to bury glass marbles, a test able to detect anxiety and obsessive compulsive disorders related phenotypes (Deacon, 2006). Figure 2D and E showed that WT mice were able to bury 72.7±2.9 % of marbles whereas *Sort1*$^{-/-}$ mice buryed 85.5±7.3 % of marbles suggesting again an aniety-like behavior of *Sort1*$^{-/-}$ mice as previously observed (Ruan, Yang, Li, Luo, Bobrovskaya & Zhou, 2016). The serum concentration of corticosterone in basal conditions remained unchanged between WT and *Sort1*$^{-/-}$ mice (Figure 2F) indicating that the anxiety-like behavior of *Sort1*$^{-/-}$ mice was not the consequence of the hormone increase.

Depression resistant phenotype of *Sort-1*$^{-/-}$ mice could be associated with TREK-1 modified membrane expression and function

The depression-resistant behavior of *Sort1*$^{-/-}$ mice may suggest some dysfunction of the TREK-1 channel for which its blockade or its deletion results in a depression-resistance phenotype. We first investigated the subcellular location of TREK-1 performed on sub-cellular fractionation from WT and *Sort1*$^{-/-}$ mouse brains. Surprisingly, the amount of TREK-1 channels present at the plasma membrane (PM) was significantly decreased by 36% in *Sort1*$^{-/-}$ mice when compared to WT mice (Figure 3A). The loss of TREK-1 at the PM appeared to be compensated by an increase of the protein at the level of high and low density vesicles (H/LDM) although not significant (Figure 3B). The total amount of TREK-1 was not modified between WT and *Sort1*$^{-/-}$ mice (Figure 3C). The loss of the TREK-1 channel at the cell surface without modification of total TREK-1 expression is in agreement with the role of sortilin in the channel cell sorting as already observed (Mazella et al., 2010).

To determine the consequence of the TREK-1 expression loss at the PM, we performed electrophysiological experiments on neurons prepared from WT and *Sort1*$^{-/-}$ mice. As shown in Figure 4A, the membrane potential measured on neurons from *Sort1*$^{-/-}$ mice was 44.7 ± 1.3 mV consisting to a significant increase of membrane potential of 18.21 mV when compared to neurons

For Peer Review

from WT mice (62.9 ± 3.6 mV). This result indicated that the decrease of TREK-1 channels at the cell surface of *Sort1*$^{-/-}$ neurons leads to an increase of membrane potential very similar to that obtained with the channel blocker spadin on WT neurons (Devader et al., 2015).

Previous studies have shown that the blockade (Mazella et al., 2010) or the deletion (Heurteaux et al., 2006b) of TREK-1 enhance midbrain 5-HT neuron firing rate, a key parameter predictive of AD efficacy. Therefore, we performed unitary extracellular recordings of 5-HT neurons in the DRN in anesthetized animals. The basal firing activities were recorded in both WT and *Sort1*$^{-/-}$ mice by successive tracks along the DRN. 5-HT neurons found in WT mice discharged within a normal frequency range (1.5-2 Hz) with an average that was more than two fold lower than in *Sort1*$^{-/-}$ mice (1.46 ± 0.09 Hz versus 3.42 ± 0.21 Hz, $p < 0.001$) (Figure 4B).

The hippocampus is known to be involved in emotional responses and depression is associated with the suppression of dentate gyrus neurogenesis. It is also established that chronic AD treatments, including fluoxetine but also the new rapid antidepressant spadin, induce neurogenesis in the hippocampus of rodents visualized by an increase of progenitor cells that incorporate 5-bromo-2'-deoxyuridine (BrdU). WT mice treated with spadin (100 µg per kg body weight) for 4days showed a significant increase in the number of hippocampal BrdU-positive cells compared with WT mice treated with vehicle (1919±134 cells/hippocampus vs 1218±105 cells/hippocampus, respectively, one-way ANOVA, $F(3.16) = 19.94$, $p<0.001$) (Figure 4C). In *Sort1*$^{-/-}$ mice, although the number of BrdU-positive cells was slightly lower in basal conditions, the effect of spadin remained efficient with a lower but significant increase of hippocampal newborn cells from 887±82 in WT hippocampus to 1306±37 in *Sort1*$^{-/-}$ hippocampus ($p < 0.05$) (Figure 4C).

The hippocampal neurogenesis is known to be concomitantly increased with the activation the transcription factor cAMP response element-binding protein (CREB) in response to chronic AD treatment, but not to non-antidepressant psychotic drugs (Carlezon, Duman & Nestler, 2005). These observations strongly suggest that CREB regulates hippocampal neurogenesis. Therefore we analyzed the phosphorylation state of CREB in the hippocampus of both WT and *Sort1*$^{-/-}$ and

For Peer Review

showed that the immunoreactive band of 46 kDa corresponding to phospho-CREB was significantly enhanced in the *Sort1*$^{-/-}$ hippocampus when compared to the WT whereas the amount of total CREB remained unchanged (Figure 4D).

Constitutive activition of BDNF release in *Sort1*$^{-/-}$ mice.

BDNF displays a potential role as a marker of treatment response in patients with major depressive disorder although its effects on mood variations remain unclear. The release of BDNF to the regulated pathway has been shown to be dependent on the presence of sortilin (Chen et al., 2005). For these reasons and because *Sort1*$^{-/-}$ mice display a depressive resistant phenotype, we evaluated the expression profiles of BDNF and its precursor proBDNF in the brain of WT and *Sort1*$^{-/-}$ mice. Western blot analyses of BDNF content from WT or *Sort1*$^{-/-}$ mouse brains clearly demonstrated that the neurotrophin amount was strongly increased in *Sort1*$^{-/-}$ mice vs WT ($p < 0.001$) (Figure 5A). By contrast, no change in amount of proBDNF was observed (Figure 5B). The increase of BDNF prompted us to examine the expression of the active phosphorylated form of the BDNF receptor TrkB. As shown in Figure 5C, the p-TrkB expression was significantly enhanced in *Sort1*$^{-/-}$ mice when compared with WT mouse brain.

To determine which of BDNF secretion pathway was affected in *Sort1*$^{-/-}$ mice we examined both the expression of furin, responsible for the intracellular maturation of proBDNF to the constitutive secretion pathway, and the expression of the complex plasmin/tPA, responsible for the extracellular maturation of the regulated secretion of proBDNF (Lu, Pang & Woo, 2005). Interestingly in *Sort1*$^{-/-}$ mice, the brain expression of furin was strongly enhanced ($p < 0.01$) (Figure 6A) whereas the expression of tPA, the plasmin activator, was significantly decreased in *Sort1*$^{-/-}$ mice (Figure 6B). Plasmin expression was not modified (Figure 6C).

The increase in the expression of BDNF and its activated receptor TrkB was certainly responsible for the over-expression of the phosphorylated form CREB observed in *Sort1*$^{-/-}$ mice suggesting a constitutive activity of the BDNF signaling system.

For Peer Review

Discussion

The present work shows for the first time that the cellular localization and function of the TREK-1 channel were altered in mice lacking sortilin. The TREK-1 dysfunction led to a depression resistant phenotype in *Sort1*$^{-/-}$ mice compared to wild-type mice in three different behavioral tests (Figure 1). Interestingly, this phenotype was comparable to that of *Kcnk2*$^{-/-}$ mice (lacking TREK-1) which behaved as wild-type mice treated with classical ADs. However and paradoxically, *Sort1*$^{-/-}$ mice displayed an anxiety-like behavior in several anxiety-related tests including the light dark and the marbles burying tests (Figure 2). This latter observation that appears not to be due to an elevated level of serum corticosterone, is in agreement with a recent study relating that *Sort1*$^{-/-}$ mice displayed elevated anxiety-like behavior and that chronically stressed wild-type mice showed an increase in the sortilin expression in neocortex and hippocampus leading to an increased depression-like behavior (Ruan, Yang, Li, Luo, Bobrovskaya & Zhou, 2016). Since the increase of sortilin expression is associated with depression, our results describing a resistance to depression in *Sort1*$^{-/-}$ mice could be the consequence of the absence of sortilin.

The TREK-1 expression decrease within the brain plasma membrane of *Sort1*$^{-/-}$ mice compared to WT mice (Figure 3A-C) highly suggests a crucial role of sortilin in the correct sorting of the TREK-1 channel. The involvement of sortilin in the TREK-1 targeting has previously been documented in a heterologeous expression system by cotransfection of the two proteins (Mazella et al., 2010). TREK-1 is not the only membrane protein that is regulated by its interaction with sortilin. In particular, sortilin displays important action in the function of several receptors including the proNGF receptor p75NTR (Nykjaer et al., 2004), the BDNF receptor TrkB (Yang, Lim, Li, Zhong & Zhou, 2011), and the neurotensin receptors NTSR1 (Martin, Navarro, Vincent & Mazella, 2002) and NTSR2 (Beraud-Dufour, Coppola, Massa & Mazella, 2009). In the present work, the absence of sortilin allowed us to definitively determine that either the dysfunction by alteration of its sorting or the inhibition by spadin of TREK-1 leads to a common result : the resistance to depression behavior.

For Peer Review

The neuronal consequences resulting from the decreased cell surface TREK-1 expression led to several observations : i) the membrane potential meassured on *Sort1*$^{-/-}$ neurons was strongly increased when compared to WT neurons (Figure 4A), and ii) the firing rate activity of 5-HT neurons from the dorsal raphe nucleus was twofold increased indicating an accelerated efficacy of 5-HT neurotransmission (Figure 4B). Both observations were very similar to those obtained with the blocking of TREK-1 activity by spadin (Devader et al., 2015; Mazella et al., 2010) and by fluoxetine (Heurteaux et al., 2006b) or when kcnk2 gene was deleted in TREK-1 null mice (Heurteaux et al., 2006b). These properties are in agreement with the observation that clinical pharmacological and electroconvulsive AD treatments enhance activation of hippocampal postsynaptic 5-HT$_{1A}$ receptors (Haddjeri, Blier & de Montigny, 1998).

While the number of hippocampal progenitor cells remained unchanged between *Sort1*$^{-/-}$ and WT mice, surprisingly, the two strains responded similarly to a 4day-spadin treatment with a significant increase in the number of BrdU-positive cells. This result suggests that 1/ despite the lower level of TREK-1 membrane expression measured in *Sort1*$^{-/-}$ mice, the remaining functional channels are sufficient to trigger neurogenesis under spadin exposure (note that the response to spadin was quite lower in *Sort1*$^{-/-}$ mice) or 2/ TREK-1 is not the only membrane protein responsible for the response to the peptide. In neurogenesis experiments *Sort1*$^{-/-}$ mice were still able to respond to spadin (Figure 3F). Similar observations were obtained from *Kcnk2*$^{-/-}$ mice in which basal hippocampal neurogenesis was identical to that measured from WT mice but *Kcnk2*$^{-/-}$ mice remained able to respond to fluoxetine (Heurteaux et al., 2006b).

Finally, we observed that the level of brain BDNF, as well as its activated receptor TrkB, was significantly increased in *Sort1*$^{-/-}$ mice whereas the level of its precursor form proBDNF remained unchanged (Figure 5A-C). This finding can be explained by the brain over-expression in *Sort1*$^{-/-}$ mice of the convertase furin involved in the regulated pathway of BDNF secretion (Figure 5A). Concomitantly, the plasmin and tPA expression involved in the constitutive secretion pathway, appeared slightly decreased (Figure 5B and C). The increase in both BDNF secretion and

For Peer Review

expression has been already observed in *Sort1*$^{-/-}$neurons (Chen et al., 2005) that have been prepared slightly differently than those used in this study (Devader et al., 2016). The elevated levels of BDNF and of its activated receptor TrkB in the *Sort1*$^{-/-}$ brains added to the increased active form of CREB, could be responsible for the depression-resistant phenotype.

In conclusion, data presented in this work could explain the molecular and physiological mechanisms that are responsible for the depression-resistant phenotype observed when the expression of TREK-1 was decreased or totaly absent.

Conflict of Interest

We declare to have no financial conflict of interest

Author contributions

SM, CD, MP and JM performed the experiments

MB, CH and JM conceived and designed the experiments

MB, CH and JM contributed reagents/materials/analysis tools

MB, CH and JM wrote the paper

For Peer Review

References

Beraud-Dufour S, Coppola T, Massa F, & Mazella J (2009). Neurotensin receptor-2 and -3 are crucial for the anti-apoptotic effect of neurotensin on pancreatic beta-TC3 cells. Int J Biochem Cell Biol 41**:** 2398-2402.

Carlezon WA, Jr., Duman RS, & Nestler EJ (2005). The many faces of CREB. Trends Neurosci 28**:** 436-445.

Carlo AS, Nykjaer A, & Willnow TE (2014). Sorting receptor sortilin-a culprit in cardiovascular and neurological diseases. J Mol Med (Berl) 92**:** 905-911.

Chen ZY, Ieraci A, Teng H, Dall H, Meng CX, Herrera DG*, et al.* (2005). Sortilin controls intracellular sorting of brain-derived neurotrophic factor to the regulated secretory pathway. J Neurosci 25**:** 6156-6166.

Clancy BM, & Czech MP (1990). Hexose transport stimulation and membrane redistribution of glucose transporter isoforms in response to cholera toxin, dibutyryl cyclic AMP, and insulin in 3T3-L1 adipocytes. The Journal of biological chemistry 265**:** 12434-12443.

Crawley JN (1999). Behavioral phenotyping of transgenic and knockout mice: experimental design and evaluation of general health, sensory functions, motor abilities, and specific behavioral tests. Brain Res 835**:** 18-26.

Cryan JF, Mombereau C, & Vassout A (2005). The tail suspension test as a model for assessing antidepressant activity: review of pharmacological and genetic studies in mice. Neurosci Biobehav Rev 29**:** 571-625.

Curtis MJ, Bond RA, Spina D, Ahluwalia A, Alexander SP, Giembycz MA*, et al.* (2015). Experimental design and analysis and their reporting: new guidance for publication in BJP. Br J Pharmacol 172**:** 3461-3471.

Deacon RM (2006). Digging and marble burying in mice: simple methods for in vivo identification of biological impacts. Nat Protoc 1**:** 122-124.

Devader C, Khayachi A, Veyssiere J, Moha Ou Maati H, Roulot M, Moreno S*, et al.* (2015). In vitro and in vivo regulation of synaptogenesis by the novel antidepressant spadin. Br J Pharmacol 172**:** 2604-2617.

Devader C, Moreno S, Roulot M, Deval E, Dix T, Morales CR*, et al.* (2016). Increased Brain Neurotensin and NTSR2 Lead to Weak Nociception in NTSR3/Sortilin Knockout Mice. Front Neurosci 10**:** 542.

Dube JB, Johansen CT, & Hegele RA (2011). Sortilin: an unusual suspect in cholesterol metabolism: from GWAS identification to in vivo biochemical analyses, sortilin has been identified as a novel mediator of human lipoprotein metabolism. Bioessays 33**:** 430-437.

Gross C, Zhuang X, Stark K, Ramboz S, Oosting R, Kirby L*, et al.* (2002). Serotonin1A receptor acts during development to establish normal anxiety-like behaviour in the adult. Nature 416**:** 396-400.

For Peer Review

Haddjeri N, Blier P, & de Montigny C (1998). Long-term antidepressant treatments result in a tonic activation of forebrain 5-HT1A receptors. J Neurosci 18**:** 10150-10156.

Hamill OP, Marty A, Neher E, Sakmann B, & Sigworth FJ (1981). Improved patch-clamp techniques for high-resolution current recording from cells and cell-free membrane patches. Pflugers Arch 391**:** 85-100.

Heurteaux C, Lucas G, Guy N, El Yacoubi M, Thümmler S, Peng X*, et al.* (2006a). Deletion of TREK-1, a background potassium channel, results in a depression-resistant phenotype. Nature Neurosci 9**:** 1134-1141.

Heurteaux C, Lucas G, Guy N, El Yacoubi M, Thummler S, Peng XD*, et al.* (2006b). Deletion of the background potassium channel TREK-1 results in a depression-resistant phenotype. Nat Neurosci 9**:** 1134-1141.

Hu F, Padukkavidana T, Vaegter CB, Brady OA, Zheng Y, Mackenzie IR*, et al.* (2010). Sortilin-mediated endocytosis determines levels of the frontotemporal dementia protein, progranulin. Neuron 68**:** 654-667.

Kandror KV, & Pilch PF (2011). The sugar is sIRVed: sorting Glut4 and its fellow travelers. Traffic 12**:** 665-671.

Kilkenny C, Browne W, Cuthill IC, Emerson M, Altman DG, National Centre for the Replacement R*, et al.* (2011). Animal research: reporting in vivo experiments--the ARRIVE guidelines. J Cereb Blood Flow Metab 31**:** 991-993.

Kjolby M, Andersen OM, Breiderhoff T, Fjorback AW, Pedersen KM, Madsen P*, et al.* (2010). Sort1, encoded by the cardiovascular risk locus 1p13.3, is a regulator of hepatic lipoprotein export. Cell Metab 12**:** 213-223.

Lefrancois S, Zeng J, Hassan AJ, Canuel M, & Morales CR (2003). The lysosomal trafficking of sphingolipid activator proteins (SAPs) is mediated by sortilin. EMBO J 22**:** 6430-6437.

Lu B, Pang PT, & Woo NH (2005). The yin and yang of neurotrophin action. Nat Rev Neurosci 6**:** 603-614.

Martin S, Navarro V, Vincent JP, & Mazella J (2002). Neurotensin receptor-1 and -3 complex modulates the cellular signaling of neurotensin in the HT29 cell line. Gastroenterology 123**:** 1135-1143.

Mazella J, Petrault O, Lucas G, Deval E, Beraud-Dufour S, Gandin C*, et al.* (2010). Spadin, a sortilin-derived peptide, targeting rodent TREK-1 channels: a new concept in the antidepressant drug design. PLoS Biol 8**:** e1000355.

Mazella J, Zsurger N, Navarro V, Chabry J, Kaghad M, Caput D*, et al.* (1998). The 100-kDa neurotensin receptor is gp95/sortilin, a non-G-protein-coupled receptor. The Journal of biological chemistry 273**:** 26273-26276.

McGrath JC, & Lilley E (2015). Implementing guidelines on reporting research using animals (ARRIVE etc.): new requirements for publication in BJP. Br J Pharmacol 172**:** 3189-3193.

For Peer Review

Musunuru K, Strong A, Frank-Kamenetsky M, Lee NE, Ahfeldt T, Sachs KV*, et al.* (2010). From noncoding variant to phenotype via SORT1 at the 1p13 cholesterol locus. Nature 466**:** 714-719.

Nykjaer A, Lee R, Teng KK, Jansen P, Madsen P, Nielsen MS*, et al.* (2004). Sortilin is essential for proNGF-induced neuronal cell death. Nature 427**:** 843-848.

Porsolt RD, Le Pichon M, & Jalfre M (1977). Depression: a new animal model sensitive to antidepressant treatments. Nature 266**:** 730-732.

Ruan CS, Yang CR, Li JY, Luo HY, Bobrovskaya L, & Zhou XF (2016). Mice with Sort1 deficiency display normal cognition but elevated anxiety-like behavior. Exp Neurol 281**:** 99-108.

Samsom JN, & Wong AH (2015). Schizophrenia and Depression Co-Morbidity: What We have Learned from Animal Models. Front Psychiatry 6**:** 13.

Santarelli L, Saxe M, Gross C, Surget A, Battaglia F, Dulawa S*, et al.* (2003). Requirement of hippocampal neurogenesis for the behavioral effects of antidepressants. Science 301**:** 805-809.

Schneider CA, Rasband WS, & Eliceiri KW (2012). NIH Image to ImageJ: 25 years of image analysis. Nat Methods 9**:** 671-675.

Tall AR, & Ai D (2011). Sorting out sortilin. Circ Res 108**:** 158-160.

Welch JM, Lu J, Rodriguiz RM, Trotta NC, Peca J, Ding JD*, et al.* (2007). Cortico-striatal synaptic defects and OCD-like behaviours in Sapap3-mutant mice. Nature 448**:** 894-900.

Yang M, Lim Y, Li X, Zhong JH, & Zhou XF (2011). Precursor of brain-derived neurotrophic factor (proBDNF) forms a complex with Huntingtin-associated protein-1 (HAP1) and sortilin that modulates proBDNF trafficking, degradation, and processing. The Journal of biological chemistry 286**:** 16272-16284.

Zeng J, Racicott J, & Morales CR (2009). The inactivation of the sortilin gene leads to a partial disruption of prosaposin trafficking to the lysosomes. Exp Cell Res 315**:** 3112-3124.

For Peer Review

Figures legends

Figure 1 : Antidepressant-like behavior in *Sort1*$^{-/-}$ mice.

(A) FST, *Sort1*$^{-/-}$ mice had a shorter immobility time than WT mice ($F(3, 52) = 10.43$, $p < 0.01$). (B) WT spadin-treated mice had also a shorter immobility time than vehicle-treated mice. Spadin had no effect on *Sort1*$^{-/-}$ mice. (C) TST, *Sort1*$^{-/-}$ mice had a significant reduced immobility time than WT mice. (D) NSF, the latency time for *Sort1*$^{-/-}$ mice was shorter than that measured for WT mice. Values are expressed as mean ± SEM. * $p< 0.05$, ** $p< 0.01$, *** $p< 0.001$.

Figure 2 : Anxiety-like behavior in *Sort1*$^{-/-}$ mice.

(A) Light-dark test, the time spent in the light zone was shorter for *Sort1*$^{-/-}$ mice compared to WT mice. (B and C) Elevated-plus Maze test, the ratio of the time spent in the open arm was reduced in *Sort1*$^{-/-}$ mice compared to WT mice. The ratio in the number of entries was also reduced in *Sort1*$^{-/-}$ mice. (D and E) Glass marbles burying test, the percent of marbles buried by WT mice was significantly increased by *Sort1*$^{-/-}$ mice as shown in E. (F) Serum corticosterone level in WT and *Sort1*$^{-/-}$ mice remained unchanged. Values are expressed as mean ± SEM. * $p< 0.05$, ** $p< 0.01$, *** $p< 0.001$, ns, non significant.

Figure 3 : Sub-cellular location of the TREK-1 channel protein in the brain of *Sort1*$^{-/-}$ and WT mice. (A) The expression of TREK-1 was decreased by 36% (histogram, left panel) in the plasma membrane (PM) prepared from *Sort1*$^{-/-}$ mouse brain when compared to PM prepared from WT mouse brain as visualized by Western blots (right panel). (B) the expression of TREK-1 channels remained unchanged in high and low densitiy vesicles (H/LDM) prepared from brains of *Sort1*$^{-/-}$ and WT mice, as well as in total brain extracts (C). The sub-cellular compartments were identified by specific markers : NaKATPase for plasma membranes (A), TGN38 for H/LDM (B) and actin for total brain extracts (C). * $p< 0.05$, ns, non significant.

For Peer Review

Figure 4 : Relationships with the 5-HT system in *Sort1*$^{-/-}$ mice.

(A) Membrane potential mean values obtained on primary cortical neurons prepared from *Sort1*$^{-/-}$ and WT mice showed an important depolarization in *Sort1*$^{-/-}$ neurons when compared with WT neurons (ΔmV = 18.21 mV).

(B) Dorsal Raphe Nucleus 5-HT neuronal firing activity recorded from WT and *Sort1*$^{-/-}$ mice . *** p< 0.001.

(C) 4 day spadin treatment increased the number of BrdU cells in hippocampus from WT and *Sort1*$^{-/-}$ mice (n = 5 per genotype), expressed as mean ± SEM. ***p< 0.001 versus vehicle injected WT mice and *p < 0.05 versus vehicle-injected *Sort1*$^{-/-}$ mice (vehicle-or-spadin-injected, Tukey's multiple comparison test).

(D) Western blot analysis of pCREB expression in the hippocampus from WT and *Sort1*$^{-/-}$ mice.

Figure 5 : Effect of deletion of *Sort1*$^{-/-}$ gene on BDNF system.

Western blot analyses and their corresponding histogram quantification of the expression of proteins involved in the BDNF system in brain extracts from WT and *Sort1*$^{-/-}$ mice. (A) BDNF, (B) proBDNF, (C) phospho-TrkB.

Figure 6 : Effect of deletion of *Sort1*$^{-/-}$ gene on BDNF releasing pathways.

Western blot analyses and their corresponding histogram quantification of the expression of proteins involved in the BDNF releasing pathways in brain extracts from WT and *Sort1*$^{-/-}$ mice. (A) Furin, (B) Plasmin and (C) tPA. Histograms represented mean ± SEM of protein quantification from indicated number of brain samples. Mann-Whitney test, *p< 0.05 ; **p< 0.01, ns, non significant.

For Peer Review

Figure 1

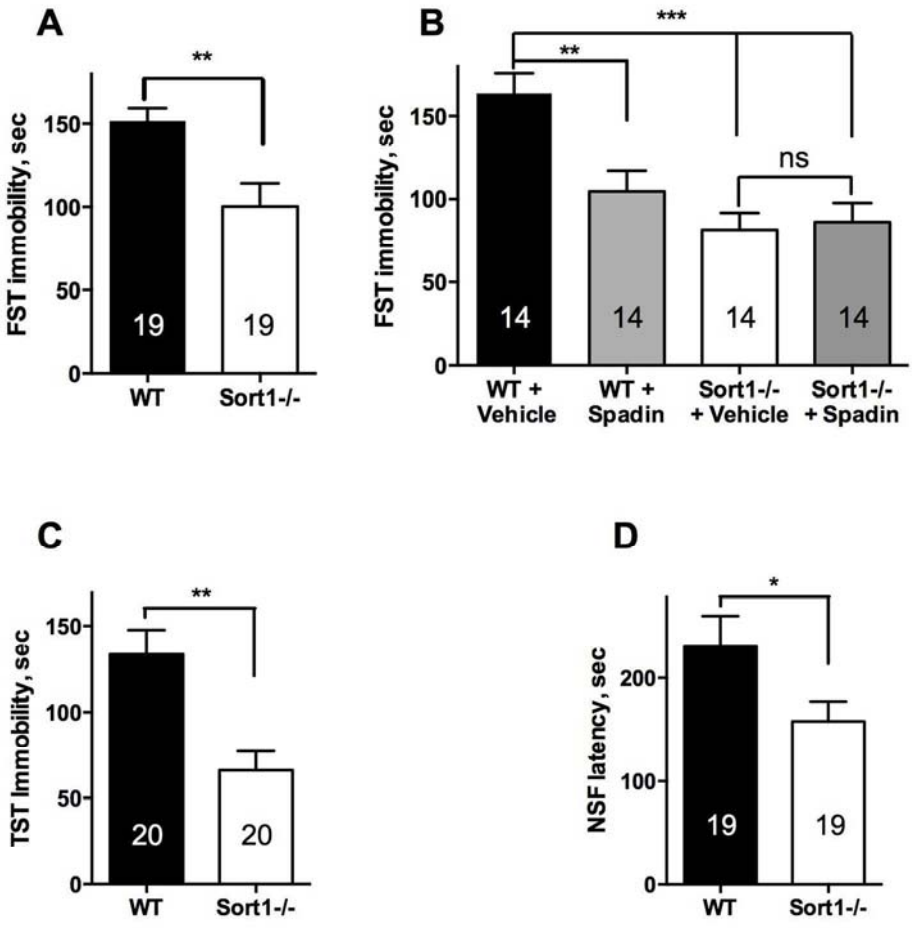

Figure 1

134x148mm (300 x 300 DPI)

Figure 2

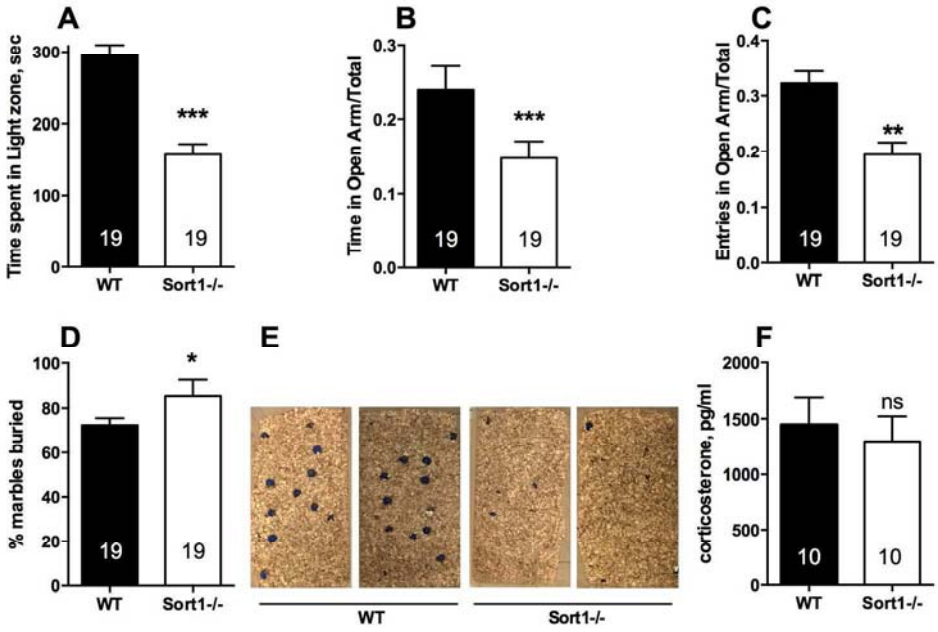

Figure 2

164x128mm (300 x 300 DPI)

For Review

Figure 3

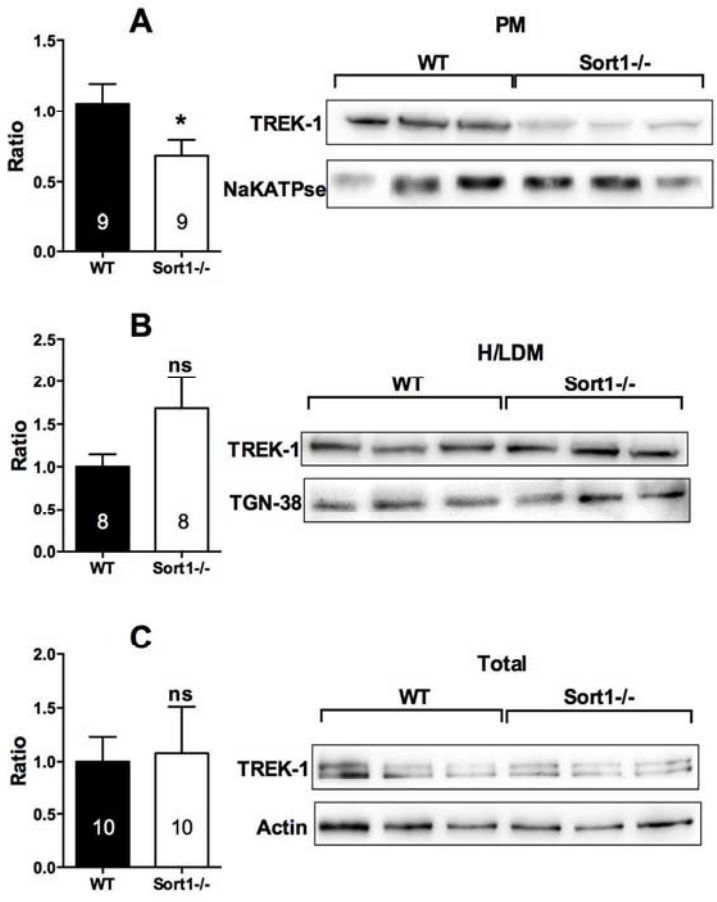

Figure 3

97x157mm (300 x 300 DPI)

Figure 4

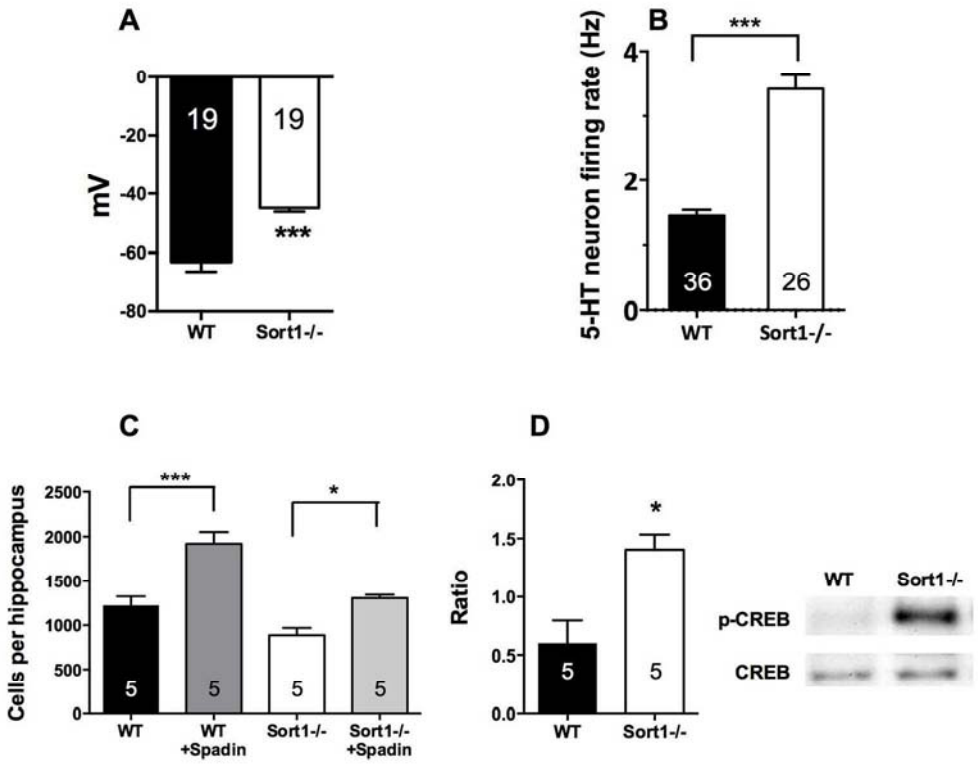

Figure 4

146x148mm (300 x 300 DPI)

Figure 5

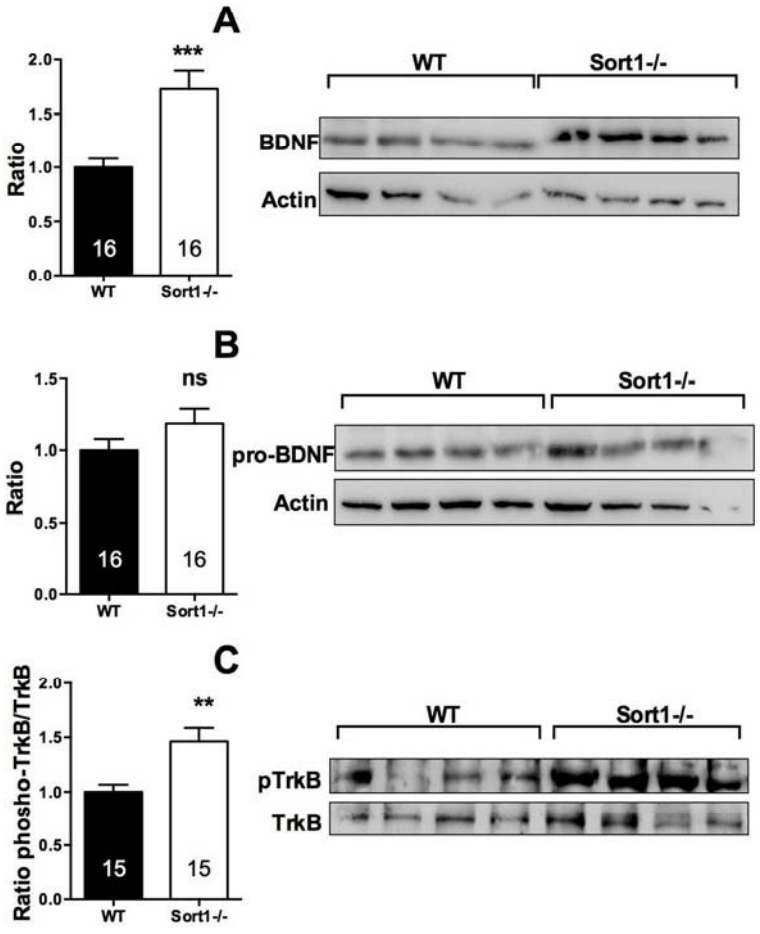

Figure 5

102x157mm (300 x 300 DPI)

Figure 6

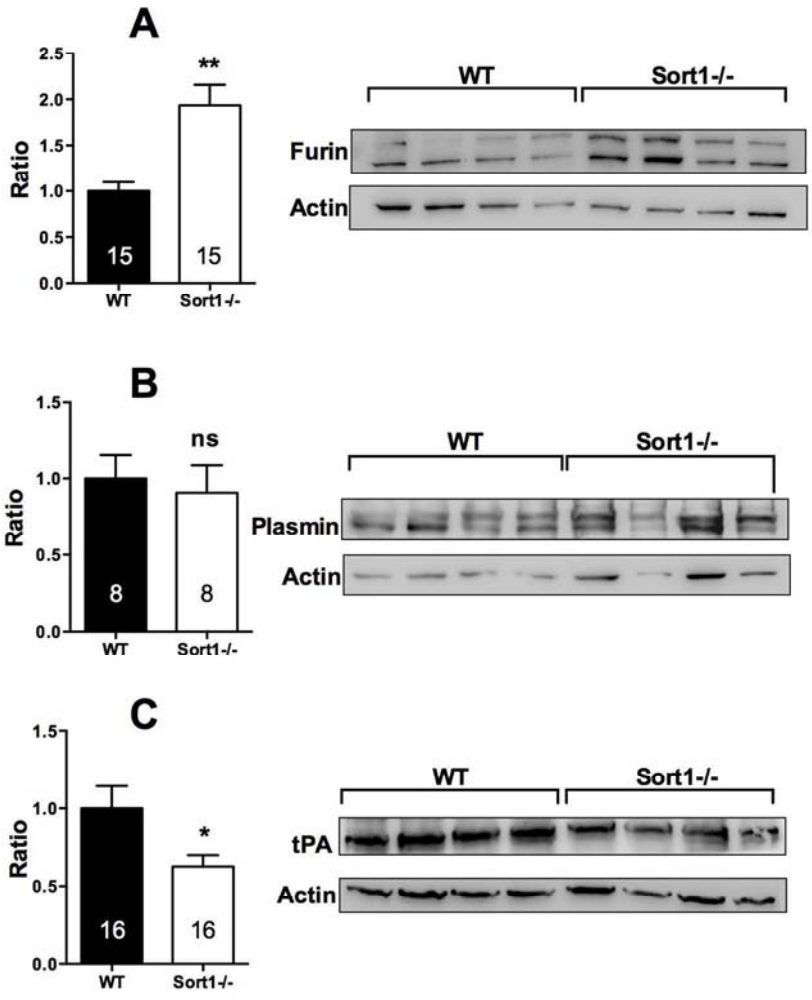

Figure 6

101x144mm (300 x 300 DPI)

Développement d’outils pour l’analyse du comportement chez le rongeur.

Article 2: *Behavior Trial Trigger*: Free standalone software using keyboard keys with possibility to connect serial device (Arduino ®) for timing and analysis rodents during behavioral tests.

***Sebastien MORENO**, Marc BORSOTTO and Jean MAZELLA*

*Submitted for publication in the **Journal of Neuroscience Methods (Under Review)***

Une importante partie de mon travail de thèse a été de réaliser des tests comportementaux chez la souris. De façon général, ce genre de tests demande un investissement important, tant pour la mise en place, le conditionnement et l'enregistrement des données, que pour l'analyse post expérience. Dans la plupart des cas, nous nous contentons de relever des données de type temps ou occurrence, qui peuvent s'effectuer soit pendant la durée du test, soit après un enregistrement vidéo. Il y a différentes façons de mesurer les données pendant les tests comportementaux, la plus simple et abordable est la méthode manuelle qui nécessite un chronomètre et un support d'écriture. Cette approche, relativement accessible, exige cependant un temps relativement important pour collecter le plus de données possibles, nécessitant parfois d'évaluer plusieurs fois un même enregistrement vidéo. Il existe maintenant des outils plus performants et complets pour mesurer et analyser le comportement. Ces logiciels sont capables, à partir d'une source vidéo ou de capteurs, de suivre l'activité du sujet analysé et de fournir un nombre conséquent de différentes données. Cependant, la prise en main de ces logiciels peut être assez fastidieuse, le coût des licences parfois onéreux, et même s'il existe des alternatives gratuites, logiciels open-source, l'installation et l'ergonomie ne sont inéluctablement pas intuitives.

C'est à partir de ces constats, et pour m'aider dans mon travail, que j'ai développé mon propre outil de mesure pour le comportement chez le rongeur. Nommé « Behavior Trial Trigger » (**BTT**), le logiciel se base sur l'utilisation des touches du clavier pour associer et déclencher des événements dont les durées seront mesurées et compilées dans un fichier fournissant un maximum d'éléments. La fenêtre principale arbore uniquement deux onglets, un pour l'expérience en cours (**Figure 24A**), l'autre pour les données déjà enregistrées (**Figure 24B**). Chaque onglet ne dispose que de quelques fonctions. L'onglet expérience possède une fonction pour créer le protocole, une fonction pour enregistrer, une fonction pour passer directement au sujet suivant sans réinitialiser les paramètres du protocole et une fonction pour connecter un appareil externe (**Figure 24A**). En effet, il tout à fait possible de connecter un dispositif par l'intermédiaire du port série de l'ordinateur et d'y associer des événements. Cette fonction permet de mettre au point, par exemple, son propre système de capteurs.

A

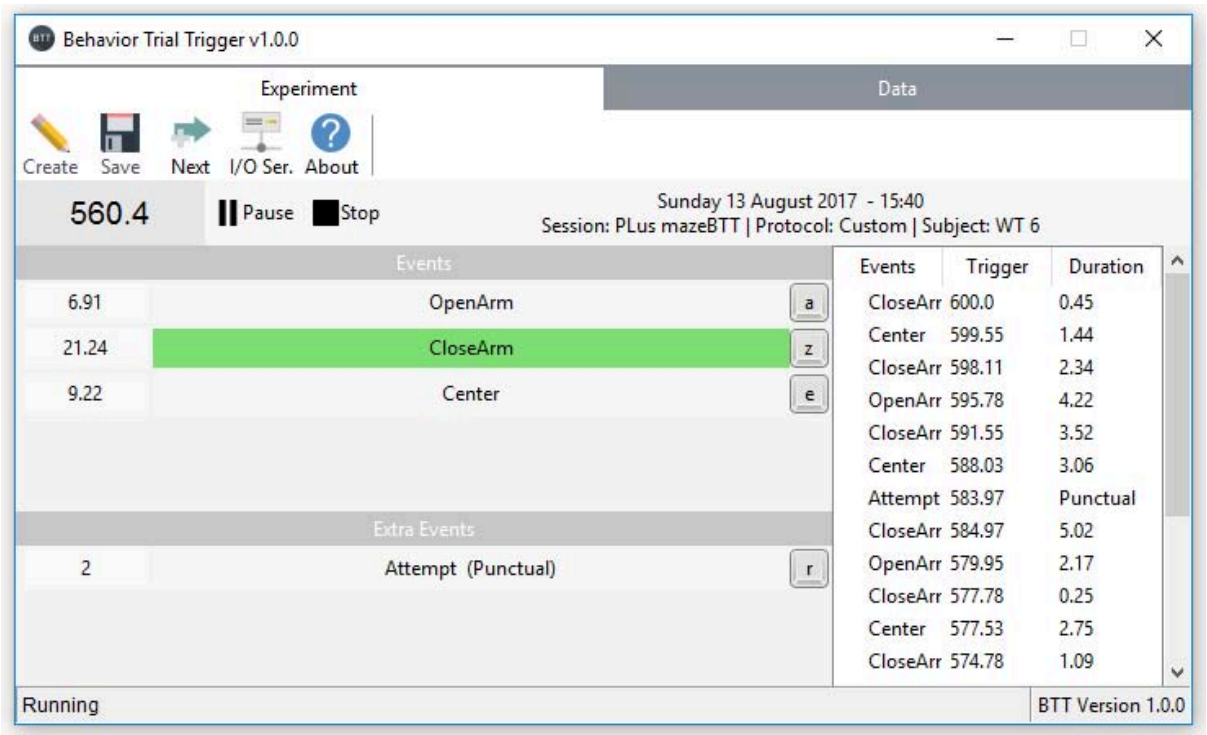

B

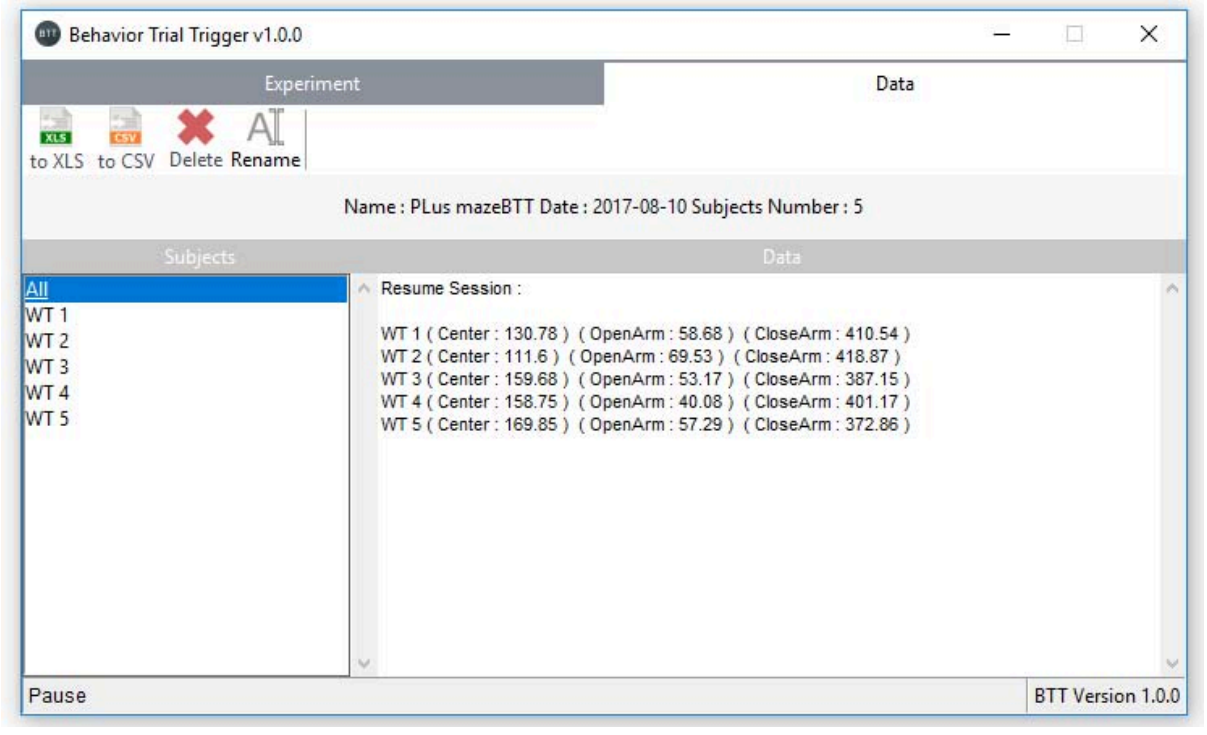

*Figure 24: Interface de Behavior Trial Trigger v1.0. **A)** Onglet 'Experiment' de la fenêtre principale. **B)** Onglet 'Data' de la fenêtre principale.*

La fonction principale du logiciel est de pouvoir associer des touches du clavier à des événements et d'en déclencher le chronomètre ou d'en comptabiliser les occurrences. Il est possible ensuite d'enregistrer soit individuellement, soit la totalité des sujets sous un format Excel ou CSV (Comma-separated values). Un autre avantage de BTT est qu'il a développé dans un langage multiplateforme, Python 3, ce qui veut dire que des versions Mac OS ou linux pourront être disponibles. Par ailleurs, et au-delà de son faible encombrement de stockage (>10 Mo), ce logiciel a été compilé de manière à ne nécessiter aucune installation préalable de la part de l'utilisateur (standalone), autrement dit, il peut tout à fait être exécuté à partir d'un support de stockage externe (ex : clé USB).

BTT a pu être testé en condition réelle au laboratoire dans le test de la croix surélevée et dans le paradigme de la boite clair-obscur. A partir des données récupérées, il a été facile d'accéder à une analyse plus fine des comportements observés chez les souris testées. La fonctionnalité de la connexion en série a pu être testée grâce à l'utilisation d'un capteur de proximité, le TCRT 5000, relié à une carte de programmation Arduino® pour faire l'interface avec l'ordinateur, dans le test d'anxiété de la boite claire obscure (**Figure 25**). Le capteur était disposé sur la face interne du compartiment obscure de la boite et envoyait un signal dès que la souris était présente dans ce compartiment. Ce signal déclenchait par la suite le chronomètre de l'événement associé. L'avantage d'une telle procédure a été d'automatiser le test comportemental ainsi que d'augmenter la précision des résultats. Un capteur électronique peut communiquer à une vitesse inférieure au 100éme de la seconde et être donc plus réactif que le déclenchement manuel tout en limitant les erreurs de déclenchements inappropriés.

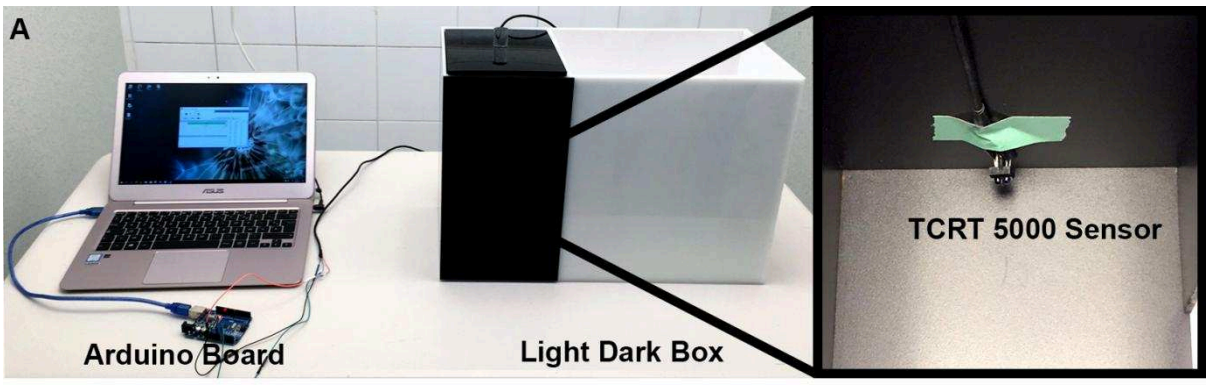

Figure 25 : Système de connexion en série dans le test de la boite clair-obscur

Au final, cet outil est disponible gratuitement au téléchargement sous une licence MIT et il est prévu d'en améliorer les fonctionnalités, notamment avec un système de *tracking* vidéo (en cours de développement avec préversion déjà utilisée) ou encore d'analyse statistique.

Behavior Trial Trigger: Free standalone software using keyboard keys with possibility to connect serial device (Arduino ®) for timing and analysis rodents during behavior tests.

Sebastien MORENO[1]#, Jean MAZELLA[1]

1, Université Côte d'Azur, CNRS, IPMC[**], France

Correspondence author:

Dr Jean Mazella; phone: +33 (0)4 93 95 77 61, Fax: +33 (0)4 93 95 77 08;

e-mail: smoreno@ipmc.cnrs.fr

**, IPMC, UMR7275, 660 route des Lucioles, Sophia Antipolis 06560 Valbonne France.

Abstract

Recording and analyze animal behaviors through specific test require an important personal investment and therefore, a lot a time. Behavior Trial Trigger, a free standalone software, provide an interesting solution to timing and collect many outcomes from behavioral test. The software use keyboard keys to facilitate the recording of events during experiment and generate data under Excel or CSV format including multiple values to perform accurate data analysis. A specific part has been coded to access to serial communication and lets the possibility to develop external trigger devices. Develop in Python 3 language and compile in a standalone software, it does not require any prior installation and can be use with at least Windows 7 and above, providing a versatile tool easily implementable.

Keywords: Behavior Trial Trigger, Software, Behavioral test, Arduino, Rodents, Timing records.

1. INTRODUCTION

Study of behavior in rodents is a complex and large field which requires major investments and time. This area provides a number of tests widely used to investigate specific context such as normal or pathological neuronal function. Behavior is a measurable phenotype (Walhlsten & Crabbe, 2007) and the outcomes of experiment are often numerical data: time, numbers of occurrence, etc. Even if methods to perform trials aren't slightly different between researchers, data acquisition can be provided by a wide range of tools of measure and analyze. In most case, acquisition is carry out after video recording to retrieve as many variables as possible, using specific software such video tracker (i.e. Ethovision (Noldus) (Spink et al., 2001 ; Noldus, Spink and Tegelenbosch, 2001), or quite

simply stopwatch and manually analyze. Software can provide multiple parameters, like distance travelled, speed of movement, position, and some specific occurrence (i.e. Ethovision (Noldus) (Spink et al., 2001 ; Noldus, Spink and Tegelenbosch, 2001) although it can be very complete, it isn't quite affordable, and even in open-source or free case, it's need, sometimes, dependencies and require a certain adaptation and implementation time. In the other hand, manually acquisition is the simple basic approach, but with the inconvenient fact that it need to observe several times the same record to track down most of the behavior parameters and therefore increase analysis length.

In this paper, we introduce a light standalone software that use keyboard keys code to follow different events and measure times, delays or occurrences. It provides a light interface and can be launch without prior installation, allowing utilization with external support (USB Key) on any computer with, a least, Windows 7 last update. The advantage of such application is to bring a versatile tool, quickly and easily usable. Another interesting point is the possibility to connect serial device, such an Arduino® board. This microcontroller has appeared as an interesting tool to create lab instrument (Besson et al., 2016) and record different signals, such optical or mechanical sensors (Devarakonda, Nguyen and Kravitz, 2015). Behavior Trial Trigger can communicate with this board in serial communication and record signals activities to allow the possibility of mounting its own test system.

2. MATERIALS and METHODS

2.1 General

Behavior Trial Trigger application was developed in Python 3.5 language (Python Software Foundation) and packaged into stand-alone executable, under Windows, using

PyInstaller (http://www.pyinstaller.org ; David Cortesi, based on structure by Giovanni Bajo & William Caban, based on Gordon McMillan's manual).). The user can run the packaged application without installing a Python interpreter or any modules. This program was successfully tested on different computer, from Windows 7 to Windows 10, with CPU range from Intel Atom z3735f (tablet) to Intel i7-4790.

The main interesting function is to be able to associate keyboard keys code to move easily and quickly from one state to another or trigger unique event during another. Every run session is automatically save in '.sb' file at each experiment end and it's possible to save the outputs data in Excel or CVS file.

2.2 Interface and Setting

The main window displays 2 panels: 'Experiment' and 'Data'. Experiment panel show the current session setting with keys code set, information of the session, main timer, a resume of events already triggered, and provides functions for create and load experiment, saving in excel file, changing subject and switching state for serial connection (Fig 1A).

Otherwise, data panel show the outcomes of the current session, with the number of subjects, details and function to saving in excel or csv file, rename or delete each (Fig 1B).

Before performing test, user needs to configure parameter in the 'New Experiment' window after selecting a new or existing session ('Create' function) (Fig 1C). Time is set in second, and events can be divided in two sections; main events and extra events (Fig 1D). Main events provide a simply way to measure duration in unique zone and are dependent on each other; when one start, others stop. Conversely, extra events are defined as events occurring during main events and are independent (can be start and stop whenever it's need). There are 3 different types of extra events that can be use: Punctual (count numbers of occurrence), Standard

(independent timer, press once to start and once again to stop), Maintain (same as 'Standard' except that the key code need to be maintain and release to start and stop the timer). Protocol parameters can be save, re-use, and are automatically save in the session file.

Once set up is complete, any keys code or spacebar pressed start the timer.

The 'Next Subject' function allows the user to change the subject without reset all protocol parameters.

2.3 Data files

The outputs data can be save in Excel or CSV file. It's possible to save all subject in one or individually file. The generated file displaying sums, orders and times of main events, and extra events are arranged in a table providing the time release, the zone where is triggered and the duration. For Excel format, when saving all, each subject is ordered in a different sheet and the first one show a resume of the experiment.

2.3 Serial communication

The application includes a part to read serial device through port connection and assign signal to events. A configuration file is available in the root folder and editable to configure the communication between the interface and the device.

2.3.1 Configuration

Prior to use serial communication, configuration file (serial.cfg) need to be edited to allowing the application to connect and read the device. Three parameters are available, port, baud rate and delay.

For better results and avoiding issues, baud rate need to be set at the same value between the device and the software and delay will be adjust depending on the latency of the device.

Once the file is ready, parameters are set in the 'Serial/COM' panel in 'New Experiment' window (Fig 1E). First, the device is connected by using 'Connect' function then, if the connection is ready, reading function allowing to retrieve the different values sent through the port. Each value can be link to the key code already configure previously.

2.3.2 Example with Arduino® UNO board

Arduino® UNO R3 is a development board using the ATmega328 microcontroller chip and providing 14 digital Inputs/Outputs pin, 6 analog inputs pins, a 16-MHz crystal oscillator and In Circuit Serial Programming header. It can be powered through USB connection or external supply on 5 to 12 volts. The Arduino® board can easily support many sensors and allowing fast input response with a good reliability, that make it an accurate platform for prototyping different lab projects (D'Ausilio, 2011).

For a quick example, a reflective optical sensor with transistor output (TCRT5000; VISHAY) is used to detect the presence of an object (in this case, mouse) in a closet space like light dark box paradigm. The sensor is installed in the dark compartment, against one of the walls perpendicular to the exit (Fig 2A) and connected to an analogic pin (A0) on the Arduino® UNO R3 board. The TCRT5000 is wiring with a 100 Ohm resistor apply to the LED (IR emitter) and a 10 kOhm resistor apply to the Phototransistor and then powered in +5V from the board (Fig 2B).

A simple code is loaded into the Arduino® UNO R3 to control and receive the analogic values from the sensor. Depending on values received, the two compartments are defined and software is configured.

The sensor uses a range value between 0 and 1024 depending on the distance of the object (the closer it is, the lower the value). Considering a value below 1000 correspond to the

presence of the animal in the box (the dark one in this case), the Arduino® board will send '1' to the software (link to the dark part), in the other case, '0' will be sent (link to the light part) (code provided in supplementary data).

2.5 Behavioral testing

Behavioral experiments were performed with naïve mice for all the tests used, and first isolated 30 minutes in neutral room before tests.

2.5.1 Animals

Mice used in this study were adult male from 8-10 weeks old, housed under controlled laboratory conditions according to the FELASA guidelines and recommendations (6 mice/cage with a 12 h dark-light cycle, a temperature of 21 ± 2°C, and a humidity of 40–60%). They have free access to standard rodent diet and tap water. C57Bl/6J male mice are from Janvier Labs (St Berthevin, France). Experimental procedures and animal care were approved by the local Ethics Committee (CIEPAL) (protocol number 00893.02) and in accordance with the policies on the care and use of laboratory animals of European Community legislation 2010/63/EU.

2.5.2 Elevated Plus Maze

Use of Elevated Plus Maze allowed to determinate an anxiety response from rodents. The apparatus consisted of central platform (5x5cm), two open arms and two closed arms across from each other and perpendicular, with the same size (45x5cm) and 15 cm high walls for the latter. It’s placed at 45 cm height above the floor. Mice were placed in the central platform facing one open arms and are allowed to freely move for 10 minutes. During this period, number of entries and time spent in both arm are measured.

2.5.3 Light Dark

Mice were placed in box divided into two compartments by a black partition with a small opening that allows mouse to move from one compartment to the other. One compartment, comprising one-third of the surface area, was made of white plastic and was brightly illuminated. The adjoining smaller compartment was black and dark. Mice were placed in the white compartment and allowed to move freely between the two chambers for 5 minutes. Time spent in the white chamber, and latency to the first transition were recorded.

3. RESULTS AND DISCUSSION

Two tests were performed to collect data from BTT software; Elevated Plus Maze, to set up multiple incomes variables, and Light Dark, to test serial device, using an Arduino® UNO R3.

In Elevated Plus Maze, the parameters set up were the open arm, the close arm, the center and attempts to enter in open arm, by this configuration, file generated provide each time duration in different zones, and more precisely, the time spent before switch to another zone and the order of displacement. After this, it can be easy to obtain the number of time a zone was enter and in which order.

Five mice were used in this test, and results were analyzed and show in table 1A. The values obtained for this C57BL/6J mice are in accordance with general common results for this strain (Komada, Takao and Miyakawa, 2008): ratio of time spent in the open arms: 9.29 ± 0.79%, ratio of time spent in the closed arms: 66.35 ± 1.37% ($p = 0.0079$) (Fig 3A); % open arm entries: 21.72 ± 1.80, % closed arms entries: 78.28 ± 1.80 ($p = 0.0079$) (Fig 3B). The fact that values were arranged depending the order provided a fine analyze to understand the behavior throughout the experiment. For examples, outcomes data can be analyzed to obtain cumulative times (Fig 3C), number of entries, or also, if the attempt to enter in open arm lead to an entry or

not by looking at the following entry zone (Fig 3D) (numbers of tries were recorded with the time and the zone triggered).

In the Light Dark paradigm, the sensor has allowed to collect data with a suitable performance and reproducibility. Indeed, mice show similar and constant results provided by the strain (Heredia et al., 2014; Simon et al., 2013): 63.6 ± 5.26 % in dark chamber ($p = 0.0079$) (Fig 3E), 19.2 ± 3.3 transitions and 22.1 ± 11.5 seconds latency to enter the dark chamber.

Behavior Trial Trigger software ensure a free, good reliability and flexible method to collect time data from experimental behavior tests, with the advantage to be easily use without prior installation. The accuracy of timer depends specifically of the input device such keyboards but not computing power. It was first design to fit for animal experiment but it can be easily use for other purpose that need duration analyze. Serial reading implementation, not limited to Arduino® board, lets the user the possibility to develop external trigger and design its own experiment to respond to his project. Also, Python 3 language open the possibility to update and enhance quickly the software for a better experience user.

Finally, this software can be an interesting tool for many different purposes that need a quick and accurate duration analyze.

References

Besson, T., Debayle, D., Diochot, S., Salinas, M. and Lingueglia, E. (2016). Low cost venom extractor based on Arduino® board for electrical venom extraction from arthropods and other small animals. Toxicon, 118, pp.156-161. doi: 10.1016/j.toxicon.2016.05.001.

D'Ausilio, A. (2011). Arduino: A low-cost multipurpose lab equipment. Behavior Research Methods, 44(2), pp.305-313. doi:10.3758/s13428-011-0163-z.

Devarakonda, K., Nguyen, K. and Kravitz, A. (2015). ROBucket: A low cost operant chamber based on the Arduino microcontroller. Behavior Research Methods, 48(2), pp.503-509. doi: 10.3758/s13428-015-0603-2.

Heredia, L., Torrente, M., Colomina, M. and Domingo, J. (2014). Assessing anxiety in C57BL/6J mice: A pharmacological characterization of the open-field and light/dark tests. Journal of Pharmacological and Toxicological Methods, 69(2), pp.108-114. doi: 10.1016/j.vascn.2013.02.010.

Komada, M., Takao, K. and Miyakawa, T. (2008). Elevated Plus Maze for Mice. Journal of Visualized Experiments, (22):1088. doi: 10.3791/1088.

Noldus, L., Spink, A. and Tegelenbosch, R. (2001). EthoVision: A versatile video tracking system for automation of behavioral experiments. Behavior Research Methods, Instruments, & Computers, 33(3), pp.398-414.doi : 10.3758/BF03195394.

Simon, M. M., Greenaway, S., White, J. K., Fuchs, H., Gailus-Durner, V., Wells, S., . . . Brown, S. D. (2013). A comparative phenotypic and genomic analysis of C57BL/6J and C57BL/6N mouse strains. Genome Biology, 14(7). doi:10.1186/gb-2013-14-7-r82.

Spink, A., Tegelenbosch, R., Buma, M., & Noldus, L. (2001). The EthoVision video tracking system—A tool for behavioral phenotyping of transgenic mice. Physiology & Behavior, 73(5), 731-744. doi:10.1016/s0031-9384(01)00530-3.

Wahlsten, D., Crabbe, J.C.(2007). Behavioral testing. In J.G Fox, S. Barthold, M. T. Davisson, C. Newcomer, F. Quimby, & A. Smith (Eds.).The mouse in biomedical research, vol 3, Normative biology, husbandry, and models (pp. 513-534). Amsterdam: Elsevier

Figures

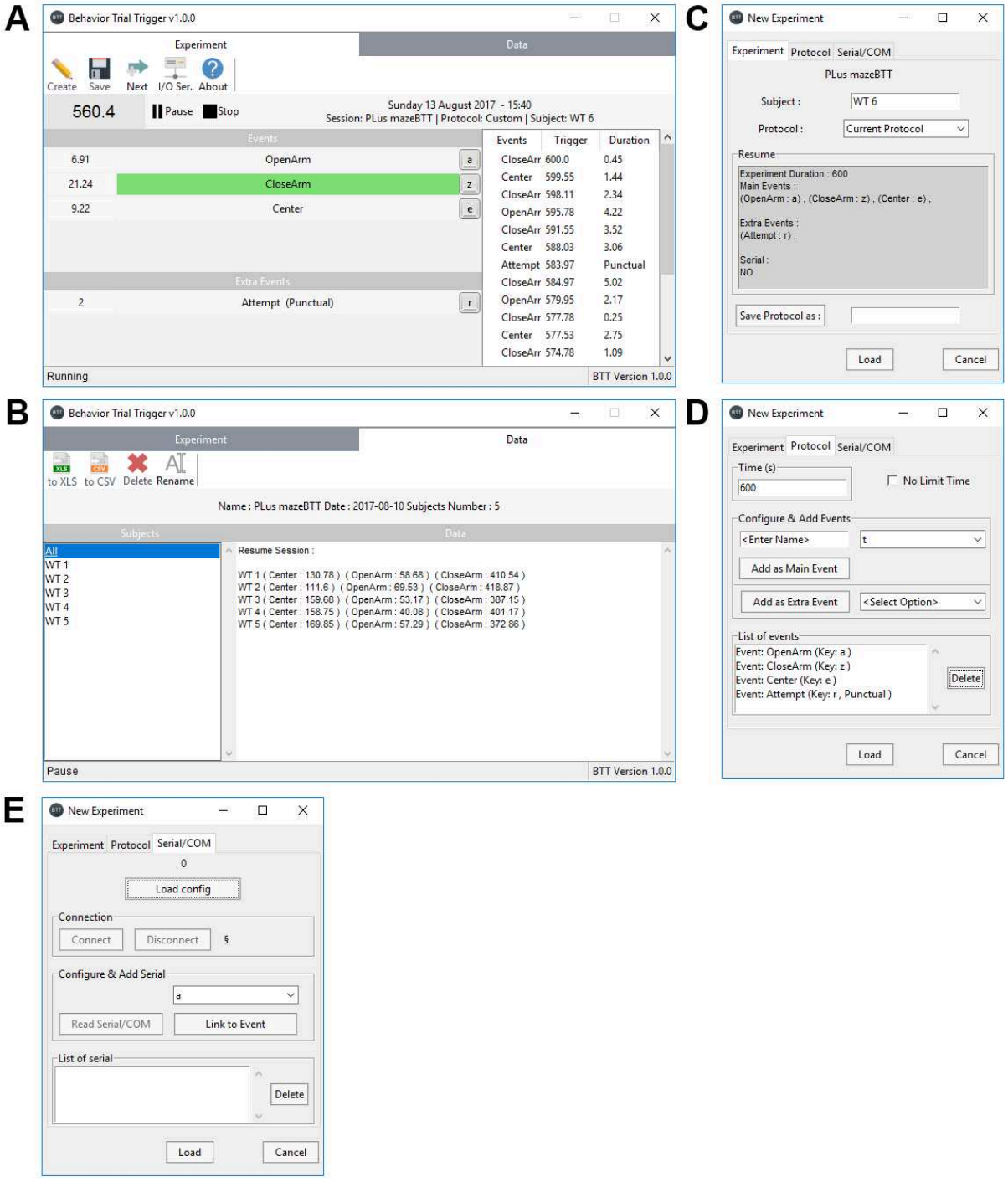

Figure 1. Interface of Behavior Trial Trigger. A) Main window. B) Data panel. C) Experiment panel, D) Protocol panel and E) Serial/COM panel on 'New Experiment' window.

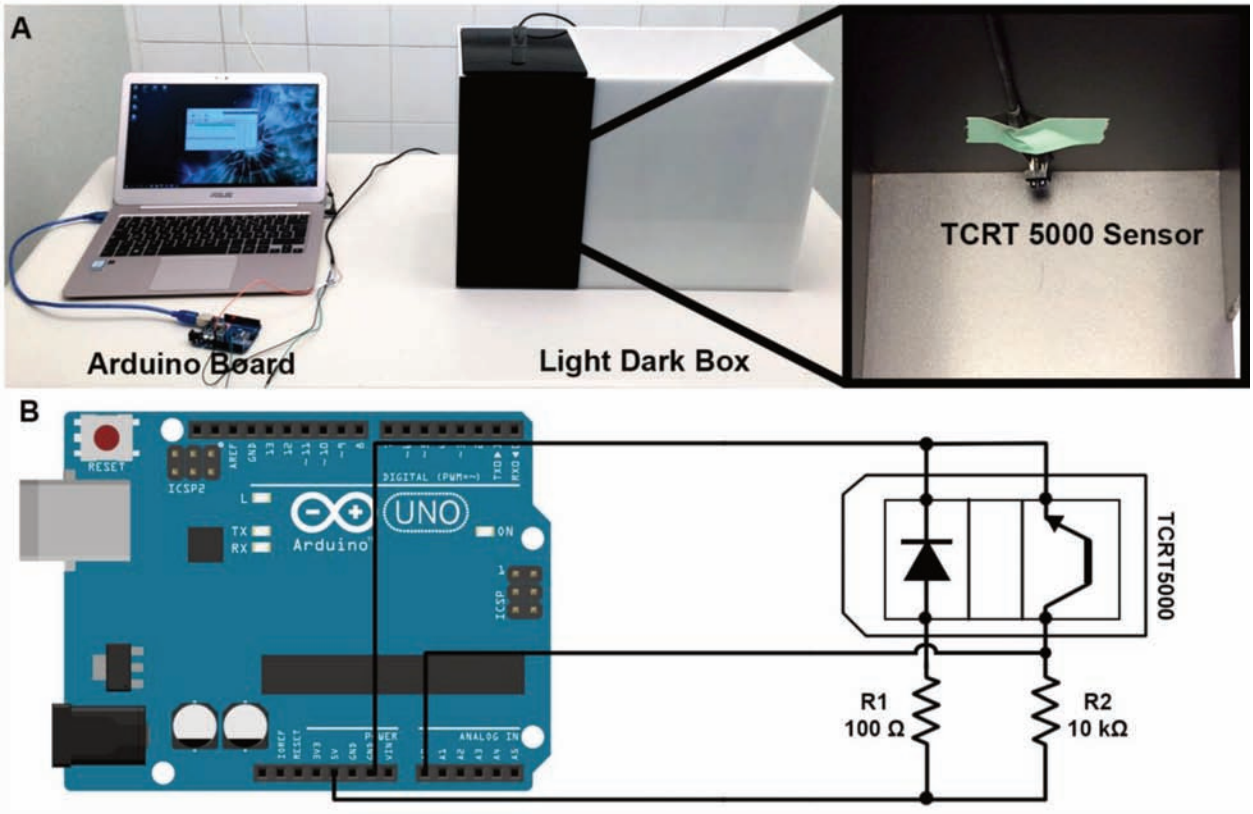

Figure 2. Serial system and installation. A) General installation with Arduino® UNO R3 board and position of sensor in dark chamber. B) Electronic scheme of device and sensor.

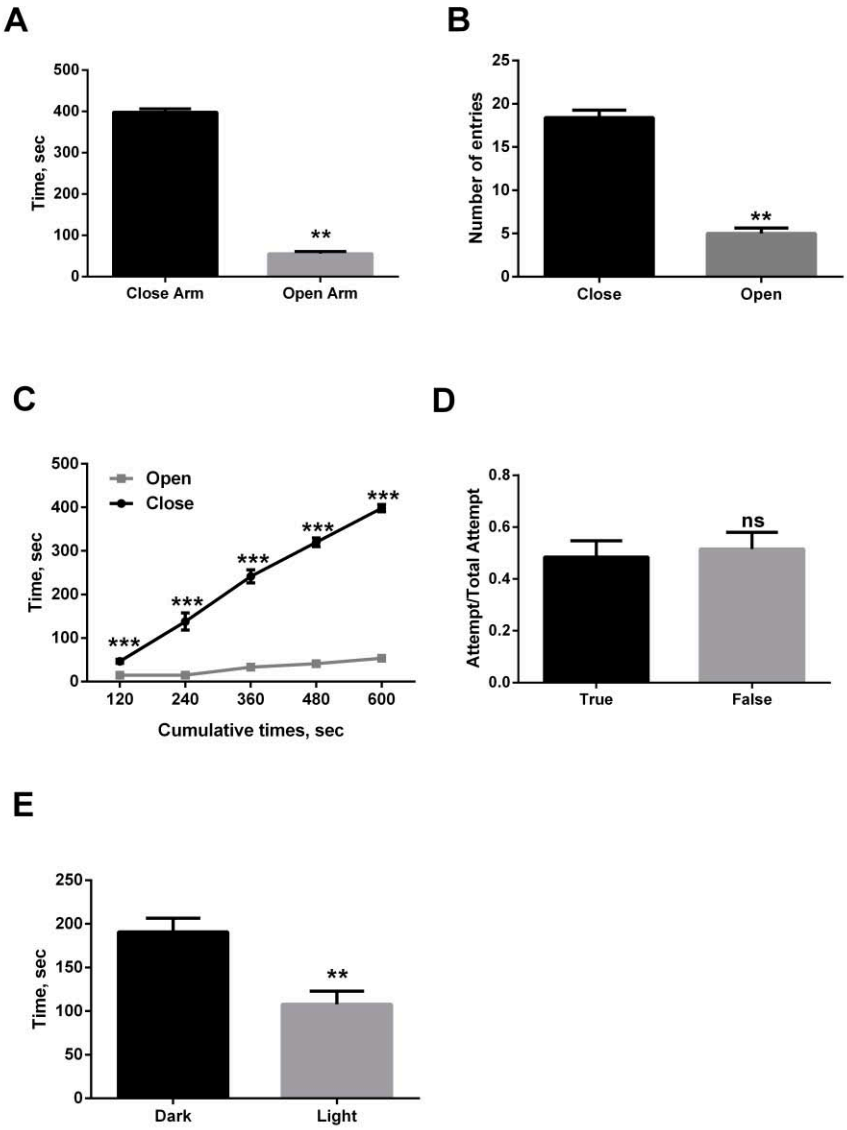

Figure 3. Results of behavioral test; plus maze (A, B, C, D) and light dark test (E) on C57Bl6J mice (n=5). A) Time in second spent in close and open arms. B) Numbers of entries in close and open arms. C) Cumulative duration for close and open arms. D) Number of attempts that lead (true) or not (false) to the enter in open arm. E) Time in second spent in dark and light chambers. Statistic: Mann & Whitney, with p value > 0,05(*), 0,005(**) and 0,001(***).

Etude de la délétion du NTSR3/Sortiline dans le système neurotensinergique.

Article 3: Increased Brain Neurotensin and NTSR2 Lead to Weak Nociception in NTSR3/Sortilin Knockout Mice.

*Christelle Devader, **Sebastien Moreno**, Morgane Roulot, Emmanuel Deval, Thomas Dix, Carlos R. Morales and Jean Mazella*

***Front Neurosci**. 2016; 10: 542. 24 November 2016 doi: 10.3389/fnins.2016.00542*

1. Contexte de l'étude

Le NTSR3/Sortiline a d'abord été identifié comme un récepteur de la neurotensine (NTS). Ce peptide endogène est impliqué dans de nombreuses fonctions biologiques que ce soit au niveau central ou périphérique. On lui reconnait des effets sur la transmission dopaminergique, l'analgésie, l'hypothermie ou encore la régulation de l'activité hormonale. Il existe deux autres récepteurs identifiés de ce peptide qui diffèrent du NTSR3/Sortiline par leurs structures ; le récepteur 1 (NTSR1) et 2 (NSTR2). Le NTSR1 et le NTSR2 sont des récepteurs couplés aux protéines G (RCPG), tandis que NTSR3/Sortiline est un récepteur à un seul domaine transmembranaire de type I. L'utilisation d'agonistes et d'antagonistes sélectifs ainsi que la génération de souris déficientes pour le NTSR1 et NTSR2 ont permis de déterminer le rôle de ces deux récepteurs dans les effets centraux induits par la NTS. En premier lieu, il existe une différence d'affinité entre ces deux récepteurs, le NTSR1 est caractérisé comme le récepteur de haute affinité pour la NTS, alors que le NTSR2 représente celui de faible affinité. De façon intéressante, la lévocabastine, un composé antihistaminique H1, est capable de se lier sélectivement, par compétition avec la NTS, au récepteur NTSR2 sans affecter la liaison de la NTS au NTSR1. On distingue pour le NTSR1 une implication dans le comportement antipsychotique (Mechanic et al., 2009), l'inhibition de la mémoire de peur (Yamada et al., 2010) et la signalisation nociceptive dans un modèle de douleur tonique induit par le formaldéhyde (Roussy et al., 2008) . Pour le NTSR2, sa délétion chez la souris entraîne la perte de la nociception thermique (Maeno et al., 2004) et de la nociception tonique de la NTS (Roussy et al., 2009).

S'il existe bien un certain nombre de recherches qui évaluent les effets de la délétion fonctionnelle du NTSR1 et du NTSR2, en revanche, rien n'est encore établi en ce qui concerne la perte du NTSR3/Sortiline au sein du système neurotensinergique. Sachant que le NTSR3/Sortiline est capable d'interagir avec le NTSR1, en modulant la signalisation de la NTS dans les cellules HT29 (Martin et al., 2002) et avec le NTSR2, en contribuant à l'effet protecteur de la NTS dans les cellules

bêta pancréatiques (Béraud-Dufour et al., 2009), nous nous sommes donc intéressés aux conséquences d'une délétion fonctionnelle du NTSR3/Sortiline sur l'expression et les effets du NTSR1, NTSR2 et de la neurotensine.

2. Résultats et discussion

Dans cette étude, je me suis concentré sur la partie biochimie des récepteurs neurotensinergique ainsi que le dosage sérique et cérébral de la neurotensine.

En premier lieu, nous nous sommes intéressés à la quantité de sites de liaison de la NTS correspondant aux NTSR1 et NTSR2 dans le cerveau de souris sauvages (WT) et de souris déficientes en NTSR3/Sortiline (KO-NTSR3). Pour cela, nous avons effectué des expériences de saturation de liaison avec de la NTS iodée sur les différents homogénats de cerveaux, en présence ou non de l'inhibiteur sélectif du NTSR2, la lévocabastine. En absence de lévocabastine, la courbe de saturation chez les WT atteint une capacité maximale de liaison (Bmax) de 200 fmol/mg, alors qu'en présence du bloqueur sélectif, ce Bmax descend autour de 65-70 fmol/mg, ce qui correspond aux sites de liaison de la NTS insensibles à la lévocabastine attribués au NTSR1. En revanche, chez les KO-NTSR3, que l'on soit en présence ou non de lévocabastine, le Bmax reste identique et d'une valeur maximale de 200 fmol/mg, suggérant une insensibilité à ce composé. Cela se traduit par une augmentation de la quantité de sites de liaison insensibles à la lévocabastine chez les KO-NTSR3 par rapport aux sauvages, qui va de pair avec une diminution des sites de liaisons sensibles à la lévocabastine, suggérant peut-être une augmentation des récepteurs NTSR1 et une diminution des récepteurs NTSR2 chez les KO-NTSR3 (**Figure 17**).

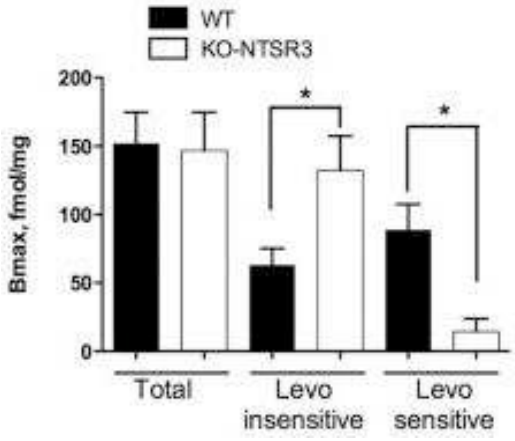

Figure 17 : Représentation de la moyenne ± SEM des sites de liaison totales et des sites de liaison sensibles et insensibles à la lévocabastine, calculée à partir de 5 expériences indépendantes réalisées triplets. p < 0,05 à l'aide d'un Student t-Test.

De façon logique, nous avons regardé l'expression génique et protéique des récepteurs NTSR1 et NTSR2. De manière surprenante, les niveaux d'ARNm de NTSR1, mesurés par PCR quantitative, ne révèlent aucun changement, alors que la quantité d'ARNm du NTSR2 a significativement augmenté dans les cerveaux des souris KO-NTSR3. Ces résultats semblent contradictoires avec les précédents. Par conséquent, nous avons vérifié l'expression protéique des deux récepteurs après fractionnement sub-cellulaire en analyse Western blot. Il n'existe aucun changement significatif d'expression protéique de NTSR1 que ce soit sur extrait total, à la membrane plasmique ou dans les vésicules de haute et de basse densité dans les extraits de cerveau des KO-NTSR3 par rapport aux WT. En revanche, la quantité de NTSR2 a significativement augmenté dans les membranes plasmiques des KO-NTSR3, alors qu'il n'apparait pas de changement de l'expression totale et entre les KO-NTSR3 et les sauvages.

L'augmentation du récepteur NTSR2 à la surface membranaire nous a emmené à vérifier si l'expression de son ligand, la NTS, pouvait être également modifié chez les souris KO-NTSR3. D'abord, il apparait une augmentation de l'expression des ARNm du peptide chez ces souris comparativement aux WT. Ce niveau plus élevé d'ARNm de NTS mesuré dans le cerveau des souris NTSR3/Sortiline KO nous a incité à quantifier la teneur en peptides dans les extraits cérébraux et le sérum des deux souris. Pour réaliser ces expériences, nous avons développé des outils (anticorps spécifiques et NST biotinylé) à utiliser selon la méthode AlphaLisa™ (Perkin). Nous avons observé une augmentation significative du peptide dans le sérum (de 12 nM en WT à 18 nM chez les souris KO) et des extraits de cerveau (de 21 nM en WT à 45 nM en KO) (**Figure 18**).

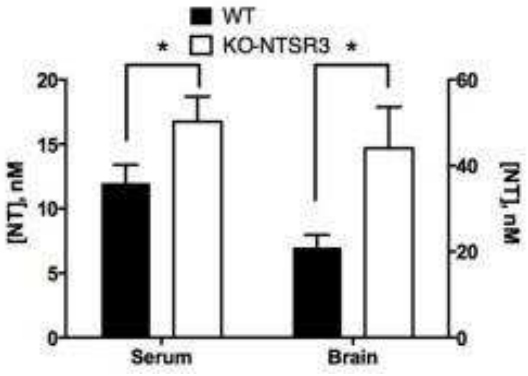

*Figure 18 : Concentrations de NTS dans les sérums et dans le cerveau de souris WT et KO-NTSR3 mesurées à l'aide de la technique AlphaLisa™. Chaque barre représente la valeur moyenne ± SEM des concentrations de NST mesurées dans le sérum (n = 19) et dans les extraits cérébraux (n = 3). *p < 0.05.*

Etant donné l'augmentation de la NTS et de son récepteur NTSR2 chez les KO-NTSR3 et le fait que l'effet analgésiant induit par la NTS est dépendant de ce NTSR2, nous avons vérifié la

fonctionnalité du NTSR2 dans des tests de douleur aigüe, comprenant des tests chimiques (crambes abdominales) et thermiques nociceptifs (léchage de la patte) chez les KO-NTSR3. Lorsque les souris ont été placées sur la plaque chauffante, la latence pour le léchage des pattes est passée de 8,9 ± 0,85 s pour les souris WT à 17,3 ± 0,95 s pour les souris KO. De même, la latence du saut était de 30,9 ± 1,5 s pour les souris WT et augmentée à 39,4 ± 3,7 s pour les souris KO, ce qui suggère une résistance à la douleur chez les souris KO-NTSR3. En ce qui concerne le test chimique, après injection d'acide acétique pour déclencher une douleur aigüe et induire les crampes abdominales, les souris KO-NTSR3 étaient sujettes à un nombre significativement plus faible de crampes que les souris sauvages. Par ailleurs, l'utilisation d'un analogue de la NTS, le JT212, qui permet de passer la barrière hémato encéphalique et d'induire l'effet analgésiant dépendant de la NTS, a bien démontré une diminution des crampes chez les sauvages alors qu'il n'avait pas d'effet chez les souris KO-NTSR3, confirmant que ces souris semblent avoir perdu la sensibilité à la douleur (**Figure 19**).

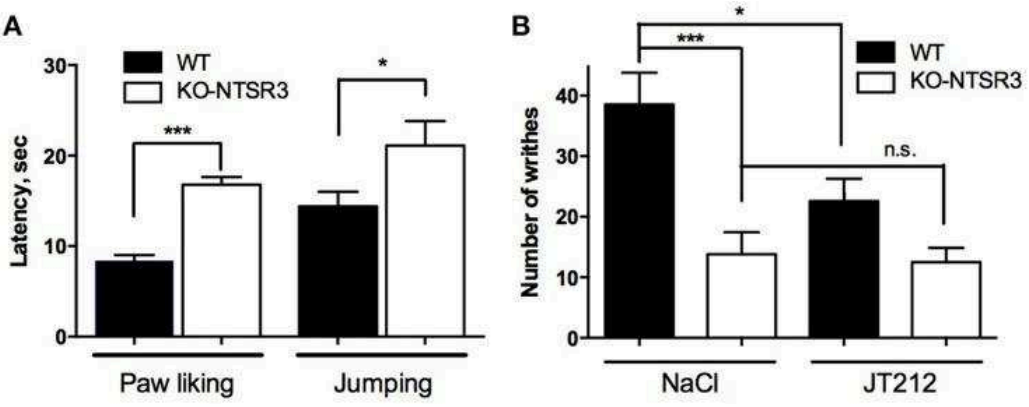

Figure 19 : Réponses analgésiques des souris WT et KO-NTSR3. **(A)** Test de la plaque chauffante, les souris ont été placées sur une plaque à une température de 55 °C. Les barres représentent la moyenne ± SEM des latences de léchage des pattes et de saut. Latence de léchage des pattes, ***p < 0,001, n = 20; latence de saut, *p < 0,05, n = 20. **(B)** Les crampes ont été comptées sur une période de 15 minutes après l'injection intrapéritonéale d'acide acétique à 0,5 % et après l'injection intrapéritonéale d'un contrôle (NaCl) ou de 100 µl de JT212 (1 µM).

Tous ces résultats apportent la preuve que l'absence de NTSR3/Sortiline conduit à une modification du système neurotensinergique, engendrant en conséquence une diminution de la sensibilité à la douleur. Ce comportement particulier découle probablement de l'augmentation du NTSR2, le récepteur principalement impliqué dans l'effet analgésique de la NTS (Dubuc et al., 1999), et de la NTS elle-même.

Cependant, dans la série d'expériences de liaison pour analyser la quantité de sites sensibles et insensibles à la lévocabastine provenant de cerveaux de souris WT et KO, nous avons obtenu des résultats contradictoires. Des expériences de liaison ont révélé que dans le cerveau de souris KO, la

quantité de sites de liaison sensibles à la lévocabastine, prévue pour être NTSR2 (Kitabgi et al., 1987 ; Mazella et al., 1996), a diminué de façon importante alors que les sites de liaison insensibles à la lévocabastine semblaient être augmentés (**Figure 17**). Par contre, les analyses de qPCR et Western blot n'ont révélé aucun changement dans la quantité de NTSR1 et une augmentation significative de NTSR2 au niveau des membranes plasmiques. L'explication possible peut provenir du fait que la sensibilité du NTSR2 à la lévocabastine ainsi que sa relativement faible affinité à la NTS sont probablement dues à son interaction avec le NTSR3/Sortiline, comme déjà observé dans les cellules bêta et pour le NTSR1 dans les HT29 (Beraud-Dufour et al., 2009; Martin et al., 2003). En l'absence de NTSR3/Sortiline, le NTSR2 pourrait être moins retenu par voie intracellulaire et la conformation de la protéine NTSR2 pourrait empêcher la liaison de la lévocabastine et augmenter aussi son affinité pour la NTS. De plus, il existe de nombreuses preuves de l'implication de l'homodimérisation et l'hétérodimérisation des RCPG dans la reconnaissance des récepteurs, le trafic cellulaire et la signalisation (Fuxe et al., 2014). Pour ce qui est du système neurotensinergique, il a été démontré que le NTSR1 est fonctionnellement associé au récepteur D2 de la dopamine pour moduler son activité (Borroto-Escuela et al., 2013) et qu'il existe une hétérodimérisation entre le NTSR1 et le NTSR2, qui entraine des modifications de la distribution, du trafic et de la fonctionnalité du NTSR1 intracellulaire (Hwang et al., 2010; Perron et al., 2007). Dans le cas présent, l'augmentation de l'expression du NTSR2 pourrait conduire à un dysfonctionnement général du système neurotensinergique en diminuant également l'activité du NTSR1.

Enfin, il semblerait que l'effet de désensibilisation à la douleur chez les souris KO-NTSR3 serait la conséquence d'une augmentation de la neurotensine et du NTSR2, ce qui concorde avec des résultats retrouvés chez des souris avec une forte quantité de neurotensine (Kleczkowska and Lipkowski, 2013). Tout ceci souligne l'importance du système neurotensinergique dans la modulation de la douleur.

En conclusion, la délétion du NTSR3/Sortiline a permis de mettre en évidence un concept physiologique nouveau dans la régulation de la douleur, montrant qu'une augmentation de NTS dans le cerveau, en concomitance avec l'augmentation de l'expression de NTSR2, semble suffisante pour réduire la sensibilité des animaux à la douleur, permettant ainsi de dégager des perspectives dans le développement d'analogues de la NTS pour le traitement de la douleur.

frontiers in Neuroscience

ORIGINAL RESEARCH
published: 24 November 2016
doi: 10.3389/fnins.2016.00542

Increased Brain Neurotensin and NTSR2 Lead to Weak Nociception in NTSR3/Sortilin Knockout Mice

Christelle Devader[1], Sébastien Moreno[1], Morgane Roulot[1], Emmanuel Deval[1], Thomas Dix[2,3], Carlos R. Morales[4] and Jean Mazella[1]**

[1] CNRS, Institut de Pharmacologie Moléculaire et Cellulaire, UMR 7275, Université de Nice Sophia Antipolis, Valbonne, France, [2] Department of Drug Discovery and Biomedical Sciences, College of Pharmacy, Medical University of South Carolina, Charleston, SC, USA, [3] JT Pharmaceuticals, Inc., Mount Pleasant, SC, USA, [4] Department of Anatomy and Cell Biology, McGill University, Montreal, QC, Canada

The neuropeptide neurotensin (NT) elicits numerous pharmacological effects through three different receptors (NTSR1, NTSR2, and NTSR3 also called sortilin). Pharmacological approaches and generation of NTSR1 and NTSR2-deficient mice allowed to determine the NT-induced antipsychotic like behavior, the inhibitory of weak fear memory and the nociceptive signaling in a rat formalin tonic pain model to NTSR1. Conversely, the effects of NT on thermal and tonic nociceptions were mediated by NTSR2. However, the role of NTSR3/sortilin on the neurotensinergic system was not investigated. Here, by using C57Bl/6J mouse model in which the gene coding for NTSR3/sortilin has been inactivated, we observed a modification of the expression of both NTSR2 and NT itself. Quantitative PCR and protein expression using Western blot analyses and AlphaLisa^{TM} technology resulted in the observation that brain NTSR2 as well as brain and blood NT were 2-fold increased in KO mice leading to a resistance of these mice to thermal and chemical pain. These data confirm that NTSR3/sortilin interacts with other NT receptors (i.e., NTSR2) and that its deletion modifies also the affinity of this receptor to NT.

Keywords: neurotensin, receptor, sortilin, knockout gene, nociception

OPEN ACCESS

Edited by:
Pascal Bonaventure, Janssen Research and Development, LLC, USA

Reviewed by:
Andrew L. Gundlach, Florey Institute of Neuroscience and Mental Health, Australia
Dasiel Oscar Borroto-Escuela, Karolinska Institutet, Sweden

****Correspondence:***
Christelle Devader
devader@ipmc.cnrs.fr
Jean Mazella
mazella@ipmc.cnrs.fr

Specialty section:
This article was submitted to Neuropharmacology, a section of the journal Frontiers in Neuroscience

Received: *15 September 2016*
Accepted: *08 November 2016*
Published: *24 November 2016*

Citation:
Devader C, Moreno S, Roulot M, Deval E, Dix T, Morales CR and Mazella J (2016) Increased Brain Neurotensin and NTSR2 Lead to Weak Nociception in NTSR3/Sortilin Knockout Mice. Front. Neurosci. 10:542. doi: 10.3389/fnins.2016.00542

INTRODUCTION

The endogenous neuropeptide NT is involved in numerous biological functions both in the brain and in periphery organs (for review see Kleczkowska and Lipkowski, 2013). These processes include dopamine transmission (Kitabgi et al., 1989), analgesia (Dobner, 2006), hypothermia (Popp et al., 2007) and hormonal activity regulation (Rostene and Alexander, 1997; Beraud-Dufour et al., 2010). The effects of NT are the consequence of its interaction with three different NT receptors (NTSRs). NTSR1 and NTSR2 are both seven transmembrane (TM) domain G protein-coupled receptors (GPCR) whereas NTSR3 is a single TM domain type I receptor that displays 100% homology with the sorting protein, sortilin (Petersen et al., 1997; Mazella et al., 1998; Mazella, 2001).

The use of selective agonists and antagonists as well as the generation of NTSR1 and NTSR2-deficient mice permitted the determination of the role of these two GPCRs in the NT-induced central effects. The high affinity NTSR1, insensitive to levocabastine, is involved in a series of actions of NT including the antipsychotic like behavior (Mechanic et al., 2009), the inhibition of weak fear memory (Yamada et al., 2010) and the nociceptive signaling in a

rat formalin tonic pain model (Roussy et al., 2008). The deletion in mice of the low affinity NTSR2, sensitive to levocabastine, results in the loss of thermal (Maeno et al., 2004) and tonic nociception of NT (Roussy et al., 2009). Levocabastine is a well characterized compound able to selectively bind by competition with NT to the low affinity NT receptor (i.e., NTSR2) without affecting the binding of NT to NTSR1 in murine brain (Kitabgi et al., 1987; Mazella et al., 1998).

At the level of the neurotensinergic system, NTSR3/sortilin has been shown to interact with NTSR1 to modulate NT signaling in HT29 cells (Martin et al., 2002) and with NTSR2 to contribute to the protective effect of NT in pancreatic beta cells (Beraud-Dufour et al., 2009). NTSR3/sortilin is a protein that belongs to the Vps10p protein family (Marcusson et al., 1994) and displays multiple functions and may act as a receptor or a co-receptor as well as a sorting partner to trigger proteins either to the degradation pathway or to the plasma membrane (reviewed in Mazella, 2001; Hermey, 2009; Carlo et al., 2014; Wilson et al., 2014). Two different NTSR3/sortilin deficient mice have been generated (Nykjaer et al., 2004; Zeng et al., 2009). These mice have been mainly used to study the sorting functions of NTSR3/sortilin including rapid endocytosis of progranulin to lysosomes (Hu et al., 2010; Tall and Ai, 2011).

However, nothing is known about the consequence of NTSR3/sortilin deletion on the neurotensinergic system in mice. Therefore, we investigated the fate of NTSR1, NTSR2 and NT expression in the NTSR3/sortilin-deficient mice developed by the Morales's group (Zeng et al., 2009; Musunuru et al., 2010). In the present study, we observed that the lack of NTSR3/sortilin led to the increase of NTSR2 and NT expression in the adult mouse brain. The higher levels of both NTSR2 and NT in the brain of NTSR3/sortilin-deficient mice resulted, as expected, in the loss of sensitivity of pain measured with thermal and chemical nociceptive tests.

MATERIALS AND METHODS

Materials

Neurotensin (NT) was purchased from Peninsula Laboratories. ^{125}I-Tyr$_3$-NT was prepared and purified as described (Sadoul et al., 1984). The brain permeant JT212 (formerly called ABS212) was kindly provided by Dr. Thomas Dix (Charleston, USA). Levocabastine was generously provided by A. Schotte (Belgium). Bovine Serum Albumin (BSA), mammalian protease and phosphatase inhibitor cocktails were from Sigma France. Rabbit polyclonal antibodies against NTSR1 and NTSR2 were from SantaCruz technologies (USA). The monoclonal antibody against NTSR3 was from BD Bioscience. HRP conjugated goat anti-rabbit and anti-mouse were from Cell Signaling. Sortilin (sort1; Uniprot number: Q6PHU5) knockout mice were kindly provided by Dr. Carlos Morales (Montreal, Canada).

Binding Experiments

Binding experiments were carried out on brain homogenates prepared as previously described (Zsurger et al., 1994). ^{125}I-NT (2000 Ci/mmol) has been prepared and purified as described (Sadoul et al., 1984). Homogenates (60 μg of protein) were incubated in 250 μl of 50 mM Tris-HCl, pH 7.5, containing 0.2% BSA and 1 mM MgCl2 at 25°C for 30 min with increasing concentrations of ^{125}I-NT alone (from 50 to 400 pM) or isotopically diluted by unlabeled NT (from 0.1 to 25 nM) in the absence or in the presence of levocabastine (1 μM). Binding experiments were terminated by addition of 2 ml ice-cold buffer. Radioactivity bound to homogenate was separated from free ligand by filtration under reduced pressure through cellulose acetate Sartorius filters (SM11107, 0.2 μm pore size). Filters and tubes were rapidly washed twice with 2 ml of incubation buffer. Radioactivity retained on filters was counted with a Packard g-counter. Binding parameters (dissociation constant Kd and maximal binding capacities Bmax) were determined by computerized Scatchard analysis.

Primer Design and Real-Time qPCR

Mice were killed by cervical dislocation. The brain was dissected and immediately frozen in liquid nitrogen. Total RNA was extracted following the Tri Reagent method (Sigma). 2 μg of total RNA was digested with Turbo Dnase (Ambion) and used as template in the reverse transcription reaction with the SuperScript III Reverse Transcriptase and Random Primers (Invitrogen). Primers (Eurogentec) were specific for sequences of NT, NTSR1 (Uniprot number: O88319), NTSR2 (Uniprot number: P70310), GAPDH and CycloD (**Table 1**).

Real-time qPCR was performed on the LightCycler™ 480 (Roche) using the LightCycler™ 480 SYBR Green 1 Master mix (Roche). PCR reactions were performed in 20 μl volume containing 16 ng cDNA, 10 μl 2x LightCycler™ 480 SYBR Green 1 Master mix and 1 μl of primer mix (10 μM forward primer, 10 μM reverse primer). The PCR profile was as follows: 5 min at 95°C, followed by 45 cycles of 10 s at 95°C, 10 s at 60°C and 10 s at 72°C.

The Ct value of each gene of interest was normalized to the Ct of the reference genes as follows: DC = Ct_{goi}-Ct_{ref} with Ct_{ref} = (Ct_{GAPDH} x Ct_{CycloD})$^{(1/2)}$ with $_{goi}$ = gene of interest, and $_{ref}$ = reference gene. DDCT = DCT experimental condition - DCT control condition. Values were expressed as 2^{-DDCt} normalized using C57Bl/6J as a control.

Animals

Adult male mice, weighing 20–25 g (8–10 weeks old) were used in this study. The animals were housed under controlled laboratory

TABLE 1 | Oligonucleotides used for qPCR.

mGAPDH-qPCR-F : AAGAGGGATGCTGCCCTTA
mGAPDH-qPCR-R : TTTTGTCTACGGGACGAGGA
mCycloD-qPCR-F : AAGGATGGCAAGGATTGAAA
mCycloD-qPCR-R : GCAATTCTGCCTGGATAGCTT
mNTs-qPCR-F : TGACTCTCCTGGCTTTCAGC
mNTs-qPCR-R : TCCAGGGCTCTCACATCTTC
mNTR1-qPCR-F2 : GGCAATTCCTCAGAATCCATCC
mNTR1-qPCR-R2 : ATACAGCGGTCACCAGCAC
mNTR2-qPCR-F : TGCACGGTGCTAGTAAGTCG
mNTR2-qPCR-R : AAGGAGACCAGCACGTTCAC

conditions (in accordance with the FELASA guidelines and recommendations), 6 mice/cage with a 12 h dark-light cycle, a temperature of 21 ± 2°C, and a humidity of 40–60%. Mice had free access to standard rodent diet and tap water. The NTSR3/sortilin homozygous KO mice were generated by the Morales's laboratory by incorporation of a GFP cassette after exon 1 (Zeng et al., 2009) and the controls were C57Bl/6J male mice from Janvier Labs (St Berthevin, France). All animal care and experimental procedures complied with the policies on the care and use of laboratory animals of European Community legislation 2010/63/EU and were approved by the local Ethics Committee (CIEPAL) (protocol number 00893.02).

Pain Behavioral Tests

The writhing test was performed as follows: 20 min prior to acetic acid injection, mice were injected intraperitoneally with either 100 µl of saline or 100 µl of a solution containing 1 µM of JT212, a NT analog able to cross the blood-brain-barrier (Hughes et al., 2010). Writhes were counted over a 15 min period starting from the fifth min after intraperitoneal injection of a 0.5% acetic acid solution (10 µl/g).

The Hot plate test was performed with a hot plate apparatus (Ugo Basile) at 55°C. We measured the time (in seconds) to paw licking and jumping latency in response to heat.

Determination of Blood and Central NT Concentration

Serum samples were collected in the morning by retroorbital puncture in mice anesthetized by isoflurane 4%. Brain NT was recovered after acid extraction of brain homogenates as described (Kokko et al., 2005). The amount of NT was measured from serum and brain using a method adapted to AlphaScreen technology (Perkin Elmer, France). The technique necessitated the preparation of a biotinylated NT on one hand, and of an antibody against the C-terminus of NT on the other hand.

Rabbit polyclonal antibodies against the C-terminus of NT (2-13) were prepared by Agro Bio (La Ferté St Aubin, France). NT (2-13) (5.4 mg, 3.6 mmol) was solubilized in 1.5 ml of 25 mM phosphate buffer, pH 6.7. N-hydroxysuccinimide biotin (13.5 mmol) resuspended in 700 µl of 70% acetonitrile, 30% dimethyl formamide was added to the peptide solution and incubated overnight at room temperature. Biotin-NT (2-13) was purified by HPLC using a Waters apparatus equipped with a semi-preparative RP18 Lichrosorb column. Biotin-NT (2-13) (eluted at 35 min), identified by mass spectrometry, was collected, quantified by its absorption at 280 nm and lyophylised in aliquots.

According to the principles of AlphaScreen technology, streptavidin-donor microbeads were recognized by biotin-NT (2-13) and the anti-rabbit IgG-acceptor microbeads were bound by anti-NT (2-13) antibodies. The signal was produced when the two microbeads (acceptor and donor) were drawn into proximity by a molecular interaction occurring between the binding partners captured on the beads. The peptide present in the sample was able to interfere with this interaction leading to competition. Standard curves were obtained by incubation in 96-well plaque of 1 nM biotin-NT (2-13) with the anti-NT (2-13) antibody (1:5000) in the AlphaLisa™ buffer in the absence or in the presence of increasing concentrations of NT (2-13) (from 10^{-11} to 10^{-6} M) for 1 h at room temperature. After addition of acceptor and donor beads and further incubation for 2 h at room temperature, the plaque was read using the Enspire apparatus (Perkin). Note that non-apparented peptides like somatostatin or spadin were unable to interfere with the dosing method. For sera measurements, the same volume of serum was added instead of unlabeled NT (2-13). The amount of NT was determined from its percent of signal inhibition and calculated using the standard curve.

Sub-cellular Fractionation

In order to quantify the amount of NTSRs expressed at the cell surface and intracellularly, we performed sub-cellular fractionation from brain homogenates. Plasma membranes were prepared from brain homogenates of WT or KO-NTSR3/Sortilin mice according to the protocol previously described (Clancy and Czech, 1990). 30 µg of crude homogenates, purified plasma membranes and high and low density vesicles (H/LDM) were submitted to Western blot analysis using the rabbit polyclonal antibodies against NTSR1 or NTSR2 (1:500) (SantaCruz Technologies (USA)). Proteins detected with these antibodies were normalized using antibodies specific for each intracellular compartment (NaKATPase for plasma membranes, TGN38 for H/LDM and tubulin for total extracts) from SantaCruz technologies (USA).

Statistics

Results are expressed as mean ± standard error mean (SEM). Statistical analyses were performed using GraphPad (version 6.0). Student *t*-tests were used when appropriate to evaluate differences in quantitative variables whereas analysis of variance (ANOVA) was used to compute possible differences between groups.

RESULTS

Binding of NT to Brain Homogenates from Wild Type and NTSR3/Sortilin KO Mice

In order to quantify the amount of NT binding sites corresponding to NTSR1 and NTSR2 in the brain of wild type (WT) and NTSR3/sortilin deficient mice (KO-NTSR3), we first performed saturation binding experiments of iodinated NT on homogenates prepared from the indicated brains in the absence or in the presence of the NTSR2 selective blocker levocabastine (1 µM) (Kitabgi et al., 1987). In brain homogenates from WT mice, in the absence of levocabastine, the saturation curve obtained from a typical experiment indicated a maximal binding capacity (Bmax) of about 200 fmol/mg (**Figure 1A**). In the presence of levocabastine, the Bmax decreased to 65–70 fmol/mg (**Figure 1A**), a binding capacity corresponding to the levocabastine insensitive NT binding sites attributed to NTSR1. Interestingly, in brain homogenates from KO-NTSR3 mice, saturation experiments performed in the absence or in the

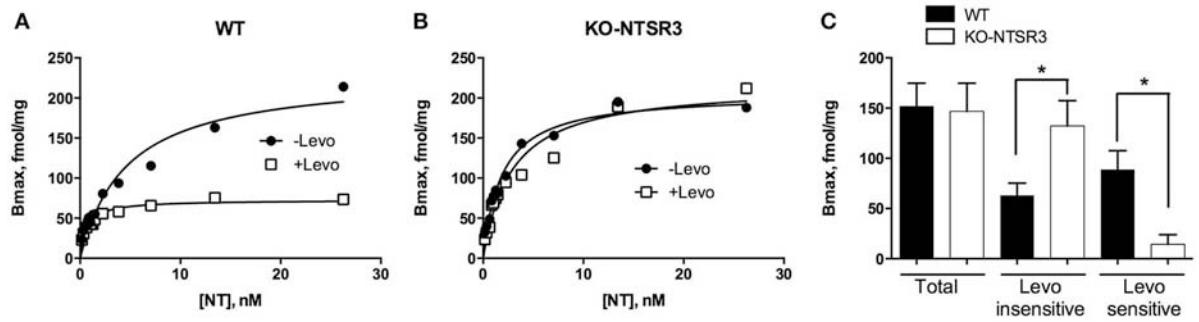

FIGURE 1 | Binding of ^{125}I-NT to brain homogenates from WT and NTSR3/sortilin KO mice. (A,B) Brain homogenates from WT **(A)** or from NTSR3/sortilin KO mice **(B)** (60 μg of proteins) were incubated with increasing concentrations of ^{125}I-NT alone or isotopically diluted with unlabeled NT in the absence (closed symbols) or in the presence (open symbols) of 1 μM levocabastine. Saturation curves were made from specific binding using GraphPad analysis. **(C)** Representation of the mean ± SEM of total binding and levocabastine-sensitive and -insensitive binding sites calculated from 5 independent experiments performed in triplicate. *$p < 0.05$ using Student *t*-Test.

presence of levocabastine revealed the same Bmax (**Figure 1B**), demonstrating that in KO-NTSR3 mice, the binding of NT is insensitive to the drug. **Figure 1C** which summarized the Bmax mean values obtained from 5 independent experiments, clearly indicated that the amount of levocabastine-insensitive NT binding sites increased in KO mice (from 63 ± 12 fmol/mg in WT mice to 124 ± 30 fmol/mg in KO mice, $p = 0.029$). As expected, the amount of levocabastine-sensitive NT binding sites was decreased in brain from KO mice from 88 ± 19 fmol/mg in WT to 14 ± 9 fmol/mg in KO ($p = 0.028$).

Measurement of the Expression of NTSR1, NTSR2 in Brain Homogenates from Wild Type and NTSR3/Sortilin KO Mice

Binding experiments performed above suggested a loss of levocabastine-sensitive NT binding sites (i.e., NTSR2) and an increase of levocabastine-insensitive NT binding sites (i.e., NTSR1) in the brain of KO-NTSR3 mice. For this reason, we further analyzed the expression of both receptors at the mRNA and protein levels.

Intriguingly, quantitative PCR (qPCR) determination indicated that the mRNA of NTSR1 remained unchanged whereas the amount of NTSR2 mRNA was significantly increased in the brain of KO mice ($p < 0.001$) (**Figure 2A**). This increase of NTSR2 mRNA was in contradiction with the loss levocabastine-sensitive NT binding sites. The similar mRNA level of NTSR1 between WT and KO mice did not correspond to the increase of levocabastine-sensitive NT binding sites observed in the brain of KO mice. Therefore, we verified the protein expression of both receptors after subcellular fractionation and Western blot analysis. The quantification determined from 5 independent experiments indicated that the protein level of NTSR1-like remained similar at the plasma membranes (PM), in the high and low density vesicles (H/LDM) and in the total extracts from brain from WT and KO mice (**Figure 2B**). However, the amount of NTSR2-like protein was significantly increased by a factor 2 ($p < 0.05$) at the plasma membranes prepared from KO mouse brain but was similar between WT and KO mice in H/LDM and total extracts (**Figures 2C,D**).

Increased Expression of NT in Brain and Serum from NTSR3/Sortilin KO Mice

As we observed an important increase of NTSR2 expression at the plasma membrane, we wondered whether the expression of its ligand may also be modified in NTSR3/sortilin KO mice by using the dosing method developed for NT. We first observed that the amount of NT mRNA was also significantly enhanced in the brain of KO mice ($p < 0.05$) (**Figure 3A**). The higher level of NT mRNA measured in the brain from NTSR3/sortilin KO mice prompted us to quantify the peptide content in brain extracts and serum from both mice. To perform these experiments, we developed tools (specific antibodies and biotinylated NT) to be used according to the AlphaLisa™ method (Perkin). The **Figure 3B** illustrated the competition curve between biotinylated NT and unlabeled NT. The amount of NT present in the serum or in the brain extracts was determined from this curve (**Figure 3C**). We observed a significant increase of the peptide in serum (from 12 nM in WT to 18 nM in KO mice) and brain extracts (from 21 nM in WT to 45 nM in KO) (**Figure 3C**).

NTSR3/Sortilin KO Mice Are Resistant to Pain

Since we observed an increase of both NT and NTSR2 in NTSR3/sortilin KO mice and that NTSR2 is mainly involved in NT-induced analgesia (Dubuc et al., 1999), we wondered whether NTSR2 is still functional using acute pain tests including chemical (writhing test) and thermal (paw licking) nociceptive tests. When mice were placed on the hot plate, the latency for paw licking increased from 8.9 ± 0.85 s for WT mice to 17.3 ± 0.95 s for KO mice ($p < 0.001$) (**Figure 4A**). Similarly, the latency to jump was 30.9 ± 1.5 s for WT mice and increased to 39.4 ± 3.7 s for KO mice ($p = 0.038$) (**Figure 4A**), suggesting a

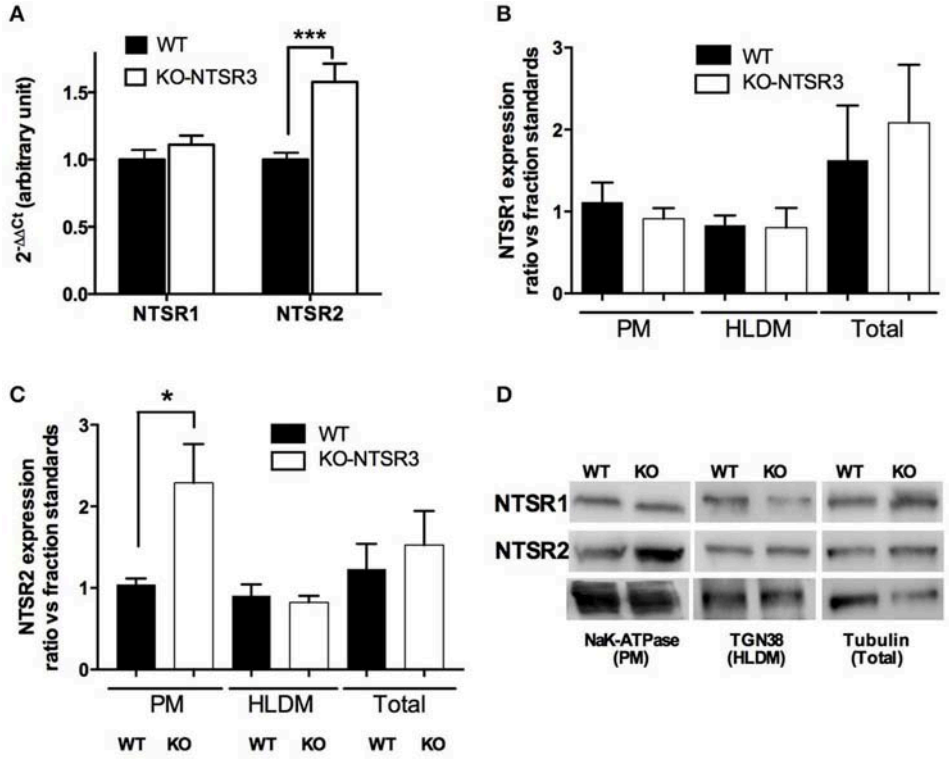

FIGURE 2 | Quantification of NT receptors from WT and NTSR3/sortilin KO mice (A) Quantitative PCR of NTSR1 and NTSR2 from WT and NTSR3/sortilin KO mouse brains, $^{***}p < 0.001$. **(B,C)** Protein expression of NTSR1-like and NTSR2-like in plasma membranes (PM), high and low density vesicles (HLDM) and total homogenates prepared from brains from WT and NTSR3/sortilin KO mice. Each bar in the graphs represents the mean ± SEM of bands intensitiy quantified using the corresponding compartment markers from 5 independent experiments. $^{*}p < 0.05$ using Mann and Whitney Student *t*-test. **(D)** Representative Western blot analysis of NTSR1-like and NTSR2-like proteins expressed in plasma membranes (PM), high and low density vesicles (HLDM) and total homogenates prepared from brains from WT and NTSR3/sortilin KO mice. NaK-ATPase; Sodium Potassium-ATPase, TGN38; Trans-Golgi Network protein of 38 kDa.

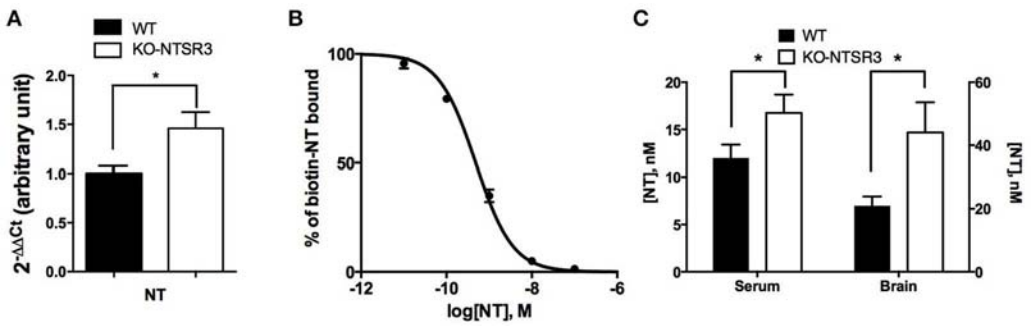

FIGURE 3 | Measurement of brain and blood NT content in WT and NTSR3/sortilin KO mice (A) Quantitative PCR of NT from WT and NTSR3/sortilin KO mouse brains. **(B)** Competitive inhibition of biotinylated NT by unlabeled NT, the standard curve was the mean ± SEM from 3 independent experiments performed in triplicate, the corresponding IC50 was 0.48 nM. **(C)** NT concentrations in sera and in brain from WT and NTSR3/sortilin KO mice measured using AlphaLisa^{TM} technique. Each bar in the graphs represents the mean value ± SEM of NT concentrations determination in serum ($n = 19$) and in brain extracts ($n = 3$). $^{*}p < 0.05$.

resistance to pain for KO-NTSR3 mice. When WT mice were subjected to the writhing test, the number of writhes/15 min was 38.5 ± 5.2 (**Figure 4B**). In KO-NTSR3 mice, the number of writhes was 13.8 ± 3.6, a value significantly different to that obtained in WT mice ($p < 0.001$). Therefore, we tested the effect of IP injection of JT212 (100 µl of a 1 µM solution) on the pain writhing test and as expected, JT212 significantly decreased the number of writhes to 22.6 ± 3.7 in WT mice (One way ANOVA, $p = 0.028$) (**Figure 4B**). In KO mice, the injection of the peptide was without significant effect on the number of writhes (12.5 ±

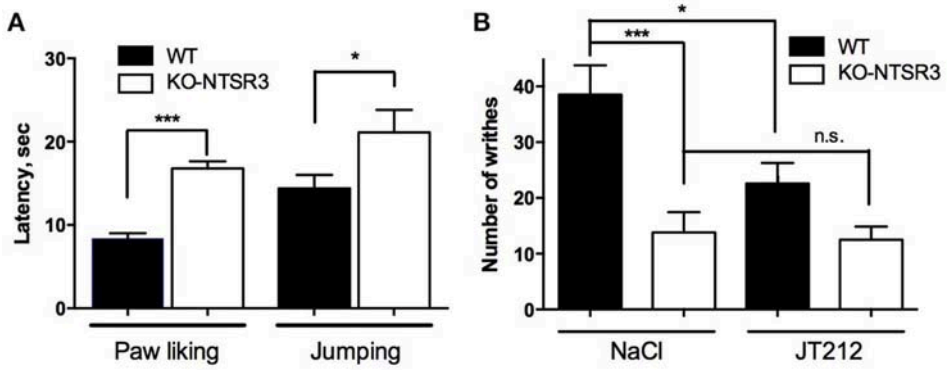

FIGURE 4 | Analgesic responses of WT and NTSR3/sortilin KO mice (A) Hot plate test, mice were placed on a plate at a temperature of 55°C. Bars represent mean ± SEM of paw licking and jumping latencies. Paw licking latency, ***$p < 0.001$, $n = 20$; jumping latency, *$p < 0.05$, $n = 20$. **(B)** Writhes were counted over a 15 min period after intraperitoneal injection of 0.5% acetic acid after intraperitoneal injection of either vehicle (NaCl) or 100 μl of 1 μM JT212. The number of indicated writhes is the mean ± SEM from groups of 10–12 mice. ***$p < 0.001$, *$p < 0.05$, n.s: non-significant.

2.4 ($p = 0.99$) (**Figure 4B**) indicating that no further analgesic action of JT212 was measurable when animals were already desensitized.

DISCUSSION

In the present work, we provide evidence that the absence of NTSR3/sortilin leads to modificiation of the neurotensinergic system with the consequence that these mice are less sensitive to pain as clearly shown by the two different tests (**Figure 4**). This particular behavior is likely due to the increase of both NTSR2, the NT receptor mainly involved in the analgesic effect of NT (Dubuc et al., 1999), and NT itself.

However, in the first series of experiments we performed to analyze the amount of levocabastine-sensitive and -insensitive NT binding sites from WT and KO mice brains, we obtained contradictory results. Binding experiments revealed that in the brain from KO mice, the amount of levocabastine-sensitive binding sites, predicted to be NTSR2 (Kitabgi et al., 1987; Mazella et al., 1996), was dramatically decreased whereas levocabastine-insensitive binding sites appeared to be enhanced (**Figure 1**). By constrast, qPCR and Western blot analyses indicated no change in the NTSR1 content and a significant increase of NTSR2 at the plasma membranes prepared from NTSR3/sortilin KO mouse brain (**Figure 2**). A possible explanation is that the sensitivity of NTSR2 to levocabastine as well as its relatively low affinity to NT are likely due to its interaction with NTSR3/sortilin as already observed in beta cells (Beraud-Dufour et al., 2009). In the absence of NTSR3/sortilin, NTSR2 could be less retained intracellularly and the conformation of NTSR2 protein could prevent the binding of levocabastine and could increase its affinity for NT. Growing evidences have demonstrated that homo and heterodimerizations of GPCRs are involved in receptor recognition, cellular trafficking and signaling (for review see Fuxe et al., 2014). Concerning the neurotensinergic system, NTSR1 has been shown to be functionally associated with dopamine D2 receptor to modulate its activity (Borroto-Escuela et al., 2013). Heterodimerization between NTSR1 and NTSR2 was also observed leading to modifications of intracellular NTSR1 distribution, trafficking and functionality (Perron et al., 2007; Hwang et al., 2010). In the present case, the increase of NTSR2 expression could lead to a general dysfunction of the neurotensinergic system by decreasing also the activity of NTSR1. A similar interaction between NTSR3/sortilin and NT receptors has been already demonstrated for NTSR1 expressed in the colonic adenocarcinoma cell line HT29 in which its physical association with NTSR3/sortilin led to a decrease of both the affinity of NT for NTSR1 and the NTSR1-mediated biological response (i.e., IPs turnover) (Martin et al., 2002).

Another interesting finding was the increase in the expression of NTSR2 concomittant to an increase of NT content both in the brain and in the blood from NTSR3/sortilin KO mice (**Figure 3**). The higher level of NT in the brain was correlated with the higher mRNA content for the peptide whereas the origin of the higher amount of NT measured in the serum from NTSR3/sortilin KO mice remains to be elucidated.

From the latter observations, we hypothesized that NTSR3/sortilin KO mice would likely behave differently than WT mice when subjected to pain, with modified sensitivity to thermal and chemical stimuli. As expected, there is a lower sensitivity of KO mice vs. WT mice to high temperatures as measured by paw licking and jump latency, and to intraperitoneal injection of acetic acid as measured by the number of writhes, corresponding to expected results from mice with a high content of NT (Kleczkowska and Lipkowski, 2013). These results confirm the importance of the neurotensinergic system in the control of pain modulation. The involvement of both NTSR1 and NTSR2 in the effect of NT on analgesia has been largely demonstrated in the literature either by using ligands selective for each receptor (Sarret et al., 2005; Smith et al., 2012) or by using mice in which NTSR1 or NTSR2 genes have been deleted (Maeno et al., 2004; Roussy et al., 2010).

In conclusion, the work presented here incorporated a new physiological concept that should be taken into account for further investigations for the development of

NT analogs to be used in pain treatment. This concept is that a small increase of NT production in the brain, associated with an increase of NTSR2 expression, appears to be sufficient to reduce the sensitivity of animals to pain.

ETHICS STATEMENT

The local Ethics Committee (CIEPAL) (protocol number 00893.02).

AUTHOR CONTRIBUTIONS

CD and JM designed study concept and supervised acquisition of the results. Acquisition of data by CD, SM, MR, and ED. JM wrote the manuscript with the help of CD, TD, and CM.

ACKNOWLEDGMENTS

This work was supported by the Centre National de la Recherche Scientifique.

REFERENCES

Beraud-Dufour, S., Abderrahmani, A., Noel, J., Brau, F., Waeber, G., Mazella, J., et al. (2010). Neurotensin is a regulator of insulin secretion in pancreatic beta-cells. *Int. J. Biochem. Cell Biol.* 42, 1681–1688. doi: 10.1016/j.biocel.2010.06.018

Beraud-Dufour, S., Coppola, T., Massa, F., and Mazella, J. (2009). Neurotensin receptor-2 and -3 are crucial for the anti-apoptotic effect of neurotensin on pancreatic beta-TC3 cells. *Int. J. Biochem. Cell Biol.* 41, 2398–2402. doi: 10.1016/j.biocel.2009.04.002

Borroto-Escuela, D. O., Ravani, A., Tarakanov, A. O., Brito, I., Narvaez, M., Romero-Fernandez, W., et al. (2013). Dopamine D2 receptor signaling dynamics of dopamine D2-neurotensin 1 receptor heteromers. *Biochem. Biophys. Res. Commun.* 435, 140–146. doi: 10.1016/j.bbrc.2013.04.058

Carlo, A. S., Nykjaer, A., and Willnow, T. E. (2014). Sorting receptor sortilin-a culprit in cardiovascular and neurological diseases. *J. Mol. Med.* 92, 905–911. doi: 10.1007/s00109-014-1152-3

Clancy, B. M., and Czech, M. P. (1990). Hexose transport stimulation and membrane redistribution of glucose transporter isoforms in response to cholera toxin, dibutyryl cyclic AMP, and insulin in 3T3-L1 adipocytes. *J. Biol. Chem.* 265, 12434–12443.

Dobner, P. R. (2006). Neurotensin and pain modulation. *Peptides* 27, 2405–2414. doi: 10.1016/j.peptides.2006.04.025

Dubuc, I., Sarret, P., Labbe-Jullie, C., Botto, J. M., Honore, E., Bourdel, E., et al. (1999). Identification of the receptor subtype involved in the analgesic effect of neurotensin. *J. Neurosci.* 19, 503–510.

Fuxe, K., Agnati, L. F., and Borroto-Escuela, D. O. (2014). The impact of receptor-receptor interactions in heteroreceptor complexes on brain plasticity. *Expert Rev. Neurother.* 14, 719–721. doi: 10.1586/14737175.2014.922878

Hermey, G. (2009). The Vps10p-domain receptor family. *Cell. Mol. Life Sci.* 66, 2677–2689. doi: 10.1007/s00018-009-0043-1

Hu, F., Padukkavidana, T., Vægter, C. B., Brady, O. A., Zheng, Y., Mackenzie, I. R., et al. (2010). Sortilin-mediated endocytosis determines levels of the frontotemporal dementia protein, progranulin. *Neuron* 68, 654–667. doi: 10.1016/j.neuron.2010.09.034

Hughes, F. M. Jr., Shaner, B. E., May, L. A., Zotian, L., Brower, J. O., Woods, R. J., et al. (2010). Identification and functional characterization of a stable, centrally active derivative of the neurotensin (8–13) fragment as a potential first-in-class analgesic. *J. Med. Chem.* 53, 4623–4632. doi: 10.1021/jm100092s

Hwang, J. R., Baek, M. W., Sim, J., Choi, H. S., Han, J. M., Kim, Y. L., et al. (2010). Intermolecular cross-talk between NTR1 and NTR2 neurotensin receptor promotes intracellular sequestration and functional inhibition of NTR1 receptors. *Biochem. Biophys. Res. Commun.* 391, 1007–1013. doi: 10.1016/j.bbrc.2009.12.007

Kitabgi, P., Herve, D., Studler, J. M., Tramu, G., Rostene, W., and Tassin, J. P. (1989). [Neurotensin/dopamine interactions]. *Encephale* 15(Spec No), 91–94.

Kitabgi, P., Rostene, W., Dussaillant, M., Schotte, A., Laduron, P. M., and Vincent, J. P. (1987). Two populations of neurotensin binding sites in murine brain: discrimination by the antihistamine levocabastine reveals markedly different radioautographic distribution. *Eur. J. Pharmacol.* 140, 285–293. doi: 10.1016/0014-2999(87)90285-8

Kleczkowska, P., and Lipkowski, A. W. (2013). Neurotensin and neurotensin receptors: characteristic, structure-activity relationship and pain modulation–a review. *Eur. J. Pharmacol.* 716, 54–60. doi: 10.1016/j.ejphar.2013.03.004

Kokko, K. P., Hadden, M. K., Price, K. L., Orwig, K. S., See, R. E., and Dix, T. A. (2005). *In vivo* behavioral effects of stable, receptor-selective neurotensin[8-13] analogues that cross the blood-brain barrier. *Neuropharmacology* 48, 417–425. doi: 10.1016/j.neuropharm.2004.10.008

Maeno, H., Yamada, K., Santo-Yamada, Y., Aoki, K., Sun, Y. J., Sato, E., et al. (2004). Comparison of mice deficient in the high- or low-affinity neurotensin receptors, Ntsr1 or Ntsr2, reveals a novel function for Ntsr2 in thermal nociception. *Brain Res.* 998, 122–129. doi: 10.1016/j.brainres.2003.11.039

Marcusson, E. G., Horazdovsky, B. F., Cereghino, J. L., Gharakhanian, E., and Emr, S. D. (1994). The sorting receptor for yeast vacuolar carboxypeptidase Y is encoded by the VPS10 gene. *Cell* 77, 579–586. doi: 10.1016/0092-8674(94)90219-4

Martin, S., Navarro, V., Vincent, J. P., and Mazella, J. (2002). Neurotensin receptor-1 and -3 complex modulates the cellular signaling of neurotensin in the HT29 cell line. *Gastroenterology* 123, 1135–1143. doi: 10.1053/gast.2002.36000

Mazella, J. (2001). Sortilin/neurotensin receptor-3: a new tool to investigate neurotensin signaling and cellular trafficking? *Cell. Signal.* 13, 1–6. doi: 10.1016/S0898-6568(00)00130-3

Mazella, J., Botto, J. M., Guillemare, E., Coppola, T., Sarret, P., and Vincent, J. P. (1996). Structure, functional expression, and cerebral localization of the levocabastine-sensitive neurotensin/neuromedin N receptor from mouse brain. *J. Neurosci.* 16, 5613–5620.

Mazella, J., Zsurger, N., Navarro, V., Chabry, J., Kaghad, M., Caput, D., et al. (1998). The 100-kDa neurotensin receptor is gp95/sortilin, a non-G-protein-coupled receptor. *J. Biol. Chem.* 273, 26273–26276. doi: 10.1074/jbc.273.41.26273

Mechanic, J. A., Sutton, J. E., Berson, A. E., Wu, X., Kwan, J., Schreiber, R., et al. (2009). Involvement of the neurotensin receptor 1 in the behavioral effects of two neurotensin agonists, NT-2 and NT69L: lack of hypothermic, antinociceptive and antipsychotic actions in receptor knockout mice. *Eur. Neuropsychopharmacol.* 19, 466–475. doi: 10.1016/j.euroneuro.2009.01.004

Musunuru, K., Strong, A., Frank-Kamenetsky, M., Lee, N. E., Ahfeldt, T., Sachs, K. V., et al. (2010). From noncoding variant to phenotype via SORT1 at the 1p13 cholesterol locus. *Nature* 466, 714–719. doi: 10.1038/nature09266

Nykjaer, A., Lee, R., Teng, K. K., Jansen, P., Madsen, P., Nielsen, M. S., et al. (2004). Sortilin is essential for proNGF-induced neuronal cell death. *Nature* 427, 843–848. doi: 10.1038/nature02319

Perron, A., Sharif, N., Sarret, P., Stroh, T., and Beaudet, A. (2007). NTS2 modulates the intracellular distribution and trafficking of NTS1 via heterodimerization. *Biochem. Biophys. Res. Commun.* 353, 582–590. doi: 10.1016/j.bbrc.2006.12.062

Petersen, C. M., Nielsen, M. S., Nykjaer, A., Jacobsen, L., Tommerup, N., Rasmussen, H. H., et al. (1997). Molecular identification of a novel candidate sorting receptor purified from human brain by receptor-associated protein affinity chromatography. *J. Biol. Chem.* 272, 3599–3605. doi: 10.1074/jbc.272.6.3599

Popp, E., Schneider, A., Vogel, P., Teschendorf, P., and Bottiger, B. W. (2007). Time course of the hypothermic response to continuously administered neurotensin. *Neuropeptides* 41, 349–354. doi: 10.1016/j.npep.2007.06.002

Rostene, W. H., and Alexander, M. J. (1997). Neurotensin and neuroendocrine regulation. *Front. Neuroendocrinol.* 18, 115–173. doi: 10.1006/frne.1996.0146

Roussy, G., Beaudry, H., Lafrance, M., Belleville, K., Beaudet, N., Wada, K., et al. (2010). Altered morphine-induced analgesia in neurotensin type 1 receptor null mice. *Neuroscience* 170, 1286–1294. doi: 10.1016/j.neuroscience.2010.08.016

Roussy, G., Dansereau, M. A., Baudisson, S., Ezzoubaa, F., Belleville, K., Beaudet, N., et al. (2009). Evidence for a role of NTS2 receptors in the modulation of tonic pain sensitivity. *Mol. Pain* 5:38. doi: 10.1186/1744-8069-5-38

Roussy, G., Dansereau, M. A., Dore-Savard, L., Belleville, K., Beaudet, N., Richelson, E., et al. (2008). Spinal NTS1 receptors regulate nociceptive signaling in a rat formalin tonic pain model. *J. Neurochem.* 105, 1100–1114. doi: 10.1111/j.1471-4159.2007.05205.x

Sadoul, J. L., Mazella, J., Amar, S., Kitabgi, P., and Vincent, J. P. (1984). Preparation of neurotensin selectively iodinated on the tyrosine 3 residue. Biological activity and binding properties on mammalian neurotensin receptors. *Biochem. Biophys. Res. Commun.* 120, 812–819. doi: 10.1016/S0006-291X(84)80179-5

Sarret, P., Esdaile, M. J., Perron, A., Martinez, J., Stroh, T., and Beaudet, A. (2005). Potent spinal analgesia elicited through stimulation of NTS2 neurotensin receptors. *J. Neurosci.* 25, 8188–8196. doi: 10.1523/JNEUROSCI.0810-05.2005

Smith, K. E., Boules, M., Williams, K., and Richelson, E. (2012). NTS1 and NTS2 mediate analgesia following neurotensin analog treatment in a mouse model for visceral pain. *Behav. Brain Res.* 232, 93–97. doi: 10.1016/j.bbr.2012.03.044

Tall, A. R., and Ai, D. (2011). Sorting out sortilin. *Circ. Res.* 108, 158–160. doi: 10.1161/RES.0b013e31820d7daa

Wilson, C. M., Naves, T., Saada, S., Pinet, S., Vincent, F., Lalloue, F., et al. (2014). The implications of sortilin/vps10p domain receptors in neurological and human diseases. *CNS Neurol. Disord. Drug Targets* 13, 1354–1365. doi: 10.2174/1871527313666141023151642

Yamada, D., Wada, E., Amano, T., Wada, K., and Sekiguchi, M. (2010). Lack of neurotensin type 1 receptor facilitates contextual fear memory depending on the memory strength. *Pharmacol. Biochem. Behav.* 96, 363–369. doi: 10.1016/j.pbb.2010.06.007

Zeng, J., Racicott, J., and Morales, C. R. (2009). The inactivation of the sortilin gene leads to a partial disruption of prosaposin trafficking to the lysosomes. *Exp. Cell Res.* 315, 3112–3124. doi: 10.1016/j.yexcr.2009.08.016

Zsurger, N., Mazella, J., and Vincent, J. P. (1994). Solubilization and purification of a high affinity neurotensin receptor from newborn human brain. *Brain Res.* 639, 245–252. doi: 10.1016/0006-8993(94)91737-X

Conflict of Interest Statement: The authors declare that the research was conducted in the absence of any commercial or financial relationships that could be construed as a potential conflict of interest.

Copyright © 2016 Devader, Moreno, Roulot, Deval, Dix, Morales and Mazella. This is an open-access article distributed under the terms of the Creative Commons Attribution License (CC BY). The use, distribution or reproduction in other forums is permitted, provided the original author(s) or licensor are credited and that the original publication in this journal is cited, in accordance with accepted academic practice. No use, distribution or reproduction is permitted which does not comply with these terms.

Etude du niveau circulant de propeptide dans l'affect dépressif.

Article 4: Serum sortilin-derived propeptides concentrations are decreased in major depressive disorder patients.

*Christelle Devader, Morgane Roulot, **Sebastien Moreno**, Alessandra Minelli, Marco Bortolomasi, Chiara Congiu, Massimo Gennarelli, Marc Borsotto, Catherine Heurteaux, Jean Mazella*

***Journal of Affective Disorders** - Volume 208, 15 January 2017, Pages 443-447*

1. Contexte de l'étude

La polymodalité du trouble dépressif rend le diagnostic complexe à établir. En résulte alors une difficulté à octroyer une médication adéquate en vue d'une rémission optimale. En effet, l'efficacité des traitements antidépresseurs s'appuie grandement sur la spécificité du trouble caractérisé, c'est pour cela qu'il est important d'établir la symptomatologie la plus exacte possible. La plupart des diagnostics apposés en maladie psychologique se fondent principalement sur l'analyse comportementale et psychique des patients. Souvent basé sur des échelles d'évaluation psychiatrique, il existe peu de marqueurs biologiques suffisants pour supporter le diagnostic. Des études cliniques et précliniques ont identifié un certain nombre de facteurs qui peuvent servir de biomarqueurs présumés pour diagnostiquer et traiter le trouble dépressif majeur. Cependant, ces marqueurs se heurtent à leur manque de sensibilité et de spécificité.

Le BDNF a récemment été identifié comme potentiel biomarqueur de la dépression. Le niveau sérique de BDNF est significativement réduit chez les personnes atteintes d'un trouble dépressif majeur (Allen et al., 2015; Nase et al., 2016). Comme décrit précédemment, le NTSR3/Sortiline est un régulateur de cette neurotrophine et des études récentes ont mis en évidence une corrélation entre le NTSR3/Sortiline soluble et le BDNF circulant dans la dépression (Belzeaux et al., 2010; Buttenschøn et al., 2015). L'équipe a récemment mis en évidence des propriétés antidépressives du propeptide issu de la maturation du récepteur. Ces effets sont induits par le blocage du canal TREK-1, cependant, pour qu'un tel mécanisme soit efficace sur le plan fonctionnel dans des conditions physiologiques *in vivo*, le propeptide doit être libéré dans la circulation sanguine. Cette assertion a pu être validée grâce à l'utilisation de la technique d'Alpha Screen (Amplified Luminescent Proximity Homogenous Assay) qui a permis de doser le propeptide ou la Spadine dans des échantillons de sérum de souris (Mazella et al., 2010).

À la vue de ces données, l'hypothèse a été de savoir s'il pouvait il y avoir une corrélation entre le propeptide circulant et l'état pathologique dépressif chez l'humain. Dans un premier temps,

il a fallu valider la spécificité de l'anticorps pour la forme humaine du propeptide, puis, dans un second temps, mesurer le niveau sérique circulant entre des sujets sains et diagnostiqués dépressifs.

2. Résultats et discussion

Lors de cette étude, j'ai principalement réalisé le dosage des échantillons de sérum humain à l'aide la technique d'AlphaLisa.

L'anticorps utilisé dans la méthode de dosage a été validé pour reconnaitre le propeptide humain. Nous avons d'abord conçu une série de séquences partielles du propeptide humain pour caractériser la spécificité des anticorps utilisés (**Figure 15A**). L'analyse de reconnaissance structurelle de ces peptides (**Figure 15B et 15C**) a permis d'observer que le propeptide, la Spadine, le propeptide 12-27 et 14-25 étaient reconnus par les anticorps avec des affinités identiques, alors que le propeptide 1-16 et 22-28 n'étaient pas reconnus. A noter que les peptides non apparentés comme la neurotensine ou la somatostatine n'interféraient pas avec la méthode de dosage (Fig. 1B et C). Ces résultats nous ont permis d'identifier l'épitope des anticorps utilisés, la séquence WSGPI. L'activité antidépresseur de ces analogues a été ensuite testée à l'aide du FST et il apparait que tous les peptides portant la séquence épitope (PE, Spadine, PE 12-27 et PE 14-25) ont démontré une activité antidépressive similaire à celle de la Spadine.

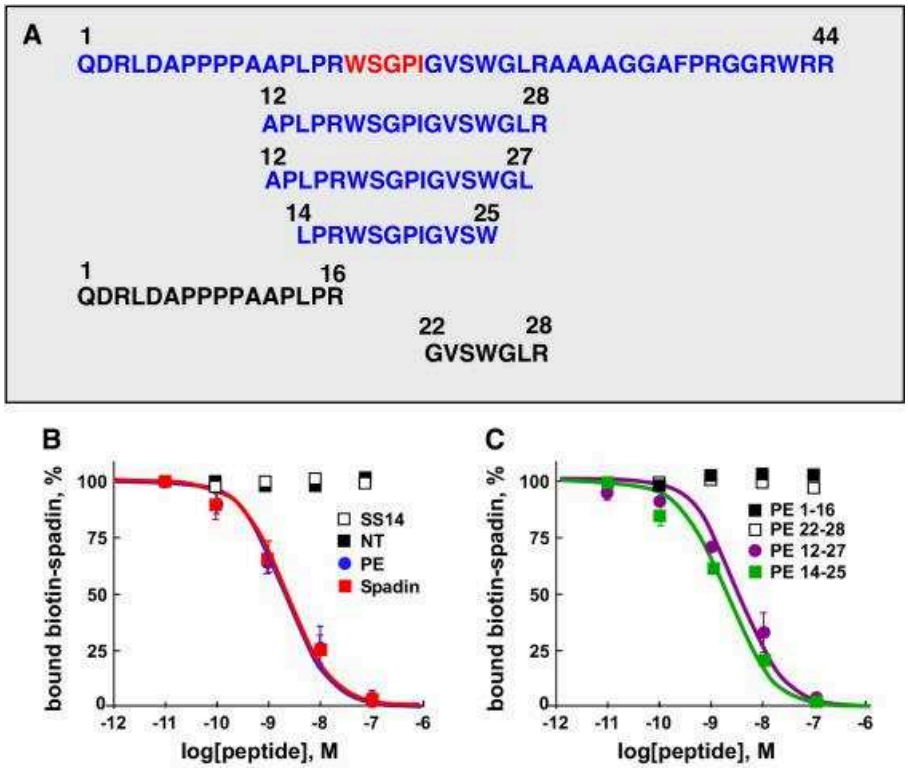

Figure 15 : Peptides synthétisés et affinités. ***A)*** *Représentation schématique des peptides conçus pour l'étude. La séquence épitope est en rouge.* ***B*** *et* ***C)*** *Affinités relatives de la Spadine, du propeptide et*

des analogues récupérés pour la méthode de détection. Chaque point correspond à la moyenne±SEM pour 3-6 expériences indépendantes.

Ensuite, afin d'évaluer les variations de niveau sérique de propeptide dans la pathologie de la dépression, nous avons collecté un ensemble de sérums humains dans un centre clinique italien. Dans cette cohorte, nous avons observé que la concentration de propeptide était significativement plus faible chez les patients dépressifs (18,9±1,3 nM) que chez les témoins sains (23,7±1,5 nM) (z=-2,11, p=0,035) (**Figure 16**). Étant donné que les analyses comparatives des variables sociodémographiques ont révélé des différences dans l'éducation et le pourcentage de fumeurs entre les patients atteints d'un trouble dépressif majeur et les témoins, nous avons effectué d'autres analyses pour nous assurer que cette différence significative entre les groupes n'était pas influencée par ces deux variables. Aucune corrélation significative n'a été observée entre l'éducation ou le pourcentage de fumeurs et les concentrations de propeptide, tant chez les témoins que chez les patients, et en tenant compte de l'ensemble des échantillons de sujets utilisés. De façon intéressante, nous avons pu observer une augmentation subtile et significative de la concentration de propeptide entre les personnes dépressives après un traitement antidépresseur de 12 semaines et avant le traitement (21.0±1.5 nM) (z=−1.98, p=0.047) (**Figure 16**). L'efficacité du traitement a été confirmée par la diminution significative du score MADRS. Par ailleurs, il n'existe aucune corrélation significative entre cette cotation clinique et l'évolution des concentrations de propeptide (r=0,18, p=0,27).

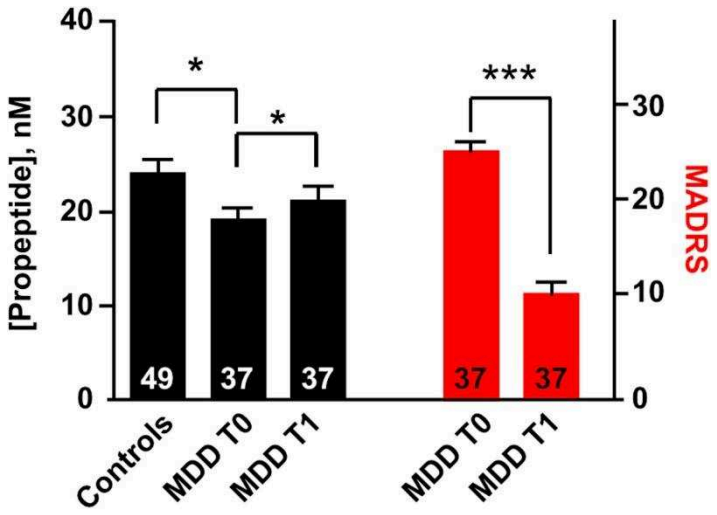

Figure 16 : Concentrations de propeptide dans les sérums de patients sains (Controls) et patients atteints d'un trouble dépressif majeur (MDD) non traités (T0) et traités (T1) pendant 12 semaines. Analyses statistiques : Mann-Whitney entre les patients (MDD T0, n =37) et les témoins (n =49), et test des rangs signés de Wilcoxon entre les non traités (T0) et les traités (T1). p<0,05. Moyenne±SEM des MADRS pour les patients atteints d'un MDD avant (T0) et après (T1) un traitement de 12 semaines (barres en rouge). *** p<0.001.*

Cette étude a permis d'abord de caractériser un anticorps pour la forme humaine du propeptide issu de la maturation du NTSR3/Sortiline dans le sérum. Seulement quelques peptides dérivés du propeptide et le propeptide lui-même sont reconnus par l'anticorps et non des peptides non apparentés comme la neurotensine ou la somatostatine. De façon intéressante, les peptides identifiés par les anticorps ont démontré également une activité antidépressive dans le test de nage forcée chez la souris. Suite à cette caractérisation, nous avons pu mettre en évidence deux constations pertinentes. D'une part, qu'il existe une diminution significative de la concentration en propeptide chez les sujets dépressifs par rapport aux sujets sains et d'autre part, qu'il existe un retour à une concentration normale de propeptide chez les patients dépressifs dont les niveaux sont plus faibles, corrélée à l'évolution clinique après un traitement antidépresseur. Ces résultats peuvent suggérer le propeptide comme un marqueur potentiel du trouble dépressif et peut être complémentaire à l'analyse sérique de BDNF montré comme diminuée chez les patients dépressifs (Molendijk et al., 2014). L'hypothèse explicative admet que le propeptide est capable de lier au NTSR3/Sortiline et de réduire l'activité du récepteur pour internaliser le pro-BDNF, un processus qui peut engendrer une augmentation de la production de BDNF.

Le propeptide mesuré dans le sérum étant dépendant de la maturation du NTSR3/Sortiline, il parait judicieux de se demander s'il existe également des variations d'expression du récepteur. Plusieurs études ont mis en évidence des différences d'expression du NTSR3/Sortiline chez les patients atteints d'un trouble dépressif majeur. Il a été reporté une diminution de l'expression génique du récepteur dans les cellules mononucléaires sanguines corrélée avec l'amélioration clinique (Belzeaux et al., 2010), alors qu'il existe une surexpression de celui-ci chez les patients déprimés, en particulier chez les non-répondants (Belzeaux et al., 2012). Dernièrement, c'est une augmentation de la forme soluble du NTSR3/Sortiline qui a été observée chez les patients dépressifs (Buttenschøn et al., 2015). Ces derniers résultats semblent rentrer en contradiction avec nos observations. En effet, s'il existe bien une augmentation de l'expression et libération du NTSR3/Sortiline chez les patients dépressifs, comment est-il possible d'obtenir une diminution de son produit de maturation, le propeptide ? C'est sur les mécanismes de production du NTSR3/Sortiline que l'on peut émettre des éléments de réponses. La diminution observée dans les cellules mononucléaires sanguines peut dépendre des étapes de transcription/traduction de l'expression du gène, alors que l'augmentation du récepteur soluble est dépendant d'un clivage par des métalloprotéases de la matrice qui se produit uniquement à la membrane. En ce qui concerne le propeptide, sa quantité est dépendante, d'une part, du clivage du précurseur du NTSR3/Sortiline et d'autre part, de la capacité de la protéine mature à atteindre la membrane plasmatique. A noter que 90% du récepteur est intracellulaire au sein du Réseau Trans-Golgien, seulement 10 % se retrouve

exprimé à la surface membranaire. Cet adressage à la membrane plasmique peut être induit par divers effecteurs, comme cela a déjà été démontré dans les cellules cibles de l'insuline et, en particulier, dans les vésicules Glut4 du transporteur de glucose (Kandror, 2003). En effet, ces vésicules peuvent être transférées à la membrane plasmatique lors de l'activation de l'insuline (Huang et al., 2013) où elles peuvent libérer du propeptide dans la circulation.

Le facteur limitant de cette étude repose sur un nombre relativement restreint d'échantillons de patients. Cela pourrait avoir une incidence négative sur la probabilité qu'un résultat statistiquement significatif reflète un réel effet.

Néanmoins, ce travail de recherche amène le concept que la variation de concentration sérique de propeptide peut fluctuer en fonction de l'humeur et, par extension, pourrait être un biomarqueur adéquat dans le diagnostic d'un état dépressif majeur chez l'homme. S'ajoute à cela, le potentiel de la Spadine comme antidépresseur dont il est possible de mesurer également son niveau sérique circulant, amenant ainsi des perspectives de nouvelles stratégies dans la prise en charge et le traitement de cet affect psychologique.

Journal of Affective Disorders 208 (2017) 443–447

Contents lists available at ScienceDirect

Journal of Affective Disorders

journal homepage: www.elsevier.com/locate/jad

Short communication

Serum sortilin-derived propeptides concentrations are decreased in major depressive disorder patients

Christelle Devader[a], Morgane Roulot[a], Sébastien Moréno[a], Alessandra Minelli[b], Marco Bortolomasi[c], Chiara Congiu[b], Massimo Gennarelli[b,d], Marc Borsotto[a], Catherine Heurteaux[a], Jean Mazella[a,*]

[a] CNRS, Institut de Pharmacologie Moléculaire et Cellulaire, UMR 7275, Université Côte d'Azur, 660 route des Lucioles, 06560 Valbonne, France
[b] Department of Molecular and Translational Medicine, Biology and Genetic Division, University of Brescia, Brescia, Italy
[c] Psychiatric Hospital "Villa Santa Chiara", Verona, Italy
[d] Genetic Unit, IRCCS Istituto Centro San Giovanni di Dio Fatebenefratelli, Brescia, Italy

ARTICLE INFO

Keywords:
Sortilin
Depression
Propeptide
Biomarker
TREK-1
Diagnosis

ABSTRACT

Background: Despite intense research on mechanisms underlying the depressive pathophysiology, reliable biomarkers to assess antidepressant treatment response are still lacking. Since the sortilin-derived propeptide (PE) displays potent antidepressant activities and can be measured in the blood of rodents, we wondered whether in human its seric level can vary between patients affected by major depressive disorder (MDD) and healthy controls and after antidepressant treatment.

Methods: By using a specific dosing method, characterized by structure-recognition analysis with various synthesized PE analogues, we conducted a translational study to test whether blood levels of PE are under pathophysiological regulation and could serve as biomarkers of the depression state.

Results: The serum concentration of PE, a peptide displaying potent antidepressant activities in rodents, is decreased in patients affected by major depressive disorder (MDD) when compared to healthy non-psychiatric controls cohort (p=0.035). Interestingly, pharmacological antidepressant treatments restore normal PE levels.

Limitations: The limitation of the study concerns the relatively small patient samples that could negatively affect the likelihood that a nominally statistically significant finding actually reflects a true effect.

Conclusions: The longitudinal quantification of the serum PE concentration could assist psychiatrists in the diagnosis of antidepressant response efficacy, and the need to modify the therapeutic strategy.

1. Introduction

Major depressive disorder (MDD) episodes are treated with different drug classes. However any first-line of treatment currently leads, after several weeks, to a remission of about 35%, and approximately 30% of MDD patients are classified as having treatment resistant depression (TRD) (Bentley et al., 2014; Thomas et al., 2013; Wong and Licinio, 2001). Despite significant research efforts aimed at understanding the neurobiological underpinnings of MDD, treatments are still based solely on relatively subjective assessment of symptoms. Due to the low rate of remission, the identification of robust biological markers predicting the clinical evolution of MDD and characterizing the extent of the treatment outcome is therefore mandatory (Nestler et al., 2002). Clinical and preclinical studies have identified a number of factors that may serve as putative biomarkers for diagnosing and treating MDD. However, the utility of any given marker to serve as a clinically useful biomarker of MDD is limited by a lack of sensitivity and specificity (Jani et al., 2015; Schmidt et al., 2011).

Recent studies have pointed out the Brain Derived Neurotrophic Factor (BDNF) as a potential biomarker for clinical response under antidepressive pharmacotherapy and clinical outcome (Allen et al., 2015; Nase et al., 2016). Interestingly, sortilin is known to control intracellular sorting of BDNF to the regulated secretory pathway (Chen et al., 2005). Moreover, increased serum levels of sortilin are associated with MDD and correlated with BDNF (Belzeaux et al., 2010; Buttenschon et al., 2015). Recently, we have identified spadin, which is a partial peptide (12–28) of the 44 amino-acid propeptide (PE) generated from the maturation of sortilin (Munck Petersen et al., 1999), also called neurotensin receptor-3 (Mazella et al., 1998). When injected *iv* or *ip* in mice both spadin and PE display potent anti-

* Corresponding author.
E-mail address: mazella@ipmc.cnrs.fr (J. Mazella).

http://dx.doi.org/10.1016/j.jad.2016.10.049
Received 4 July 2016; Received in revised form 26 September 2016; Accepted 16 October 2016
Available online 04 November 2016
0165-0327/ © 2016 Elsevier B.V. All rights reserved.

depressant (AD) activities through inhibition of the potassium channel TREK-1 activity (Mazella et al., 2010), a target for depression treatment (Heurteaux et al., 2006). We originally developed a method to measure the PE level in mouse (Mazella et al., 2010). To undertake the dosing in human, we characterized the ability of the antibody directed against spadin to recognize peptides derived from the human sequence of PE. We demonstrated that both human peptides (PE and spadin) can be measured from human sera samples and we addressed the possibility that these peptides represent biological markers of MDD. Then, we measured the serum PE concentrations in a cohort of 37 patients with MDD treated with a pharmacological protocol and compared to 49 healthy non-psychiatric subjects.

2. Methods

2.1. Animals

All experiments were carried out on 20–25 g C57Bl/6 J males of 8–10 week old (Janvier France Breeding) according to policies on the care and use of laboratory animals of European Community legislation 2010/63/EU. The local Ethics Committee (CIEPAL) approved the protocols used in this study (protocol number 00893.02).

2.2. Antibodies and biotinylated peptide preparation

Peptides were synthesized by Genecust (Dudelange, Luxemburg). Rabbit polyclonal antibodies against spadin (YAPLPRWSGPIG-VSWGLR) were prepared by Eurogentec (Seraing, Belgium). Spadin (5.4 mg; 2.7 mmol) was solubilized in 1.5 mL of 25 mM phosphate buffer, pH 6.7. N-hydroxysuccinimide biotin (13.5 mmol) resuspended in 700 µl of 70% acetonitrile, 30% dimethyl formamide was added to the spadin solution and incubated overnight at room temperature. Spadin-biotinylated was purified by HPLC using a Waters apparatus equipped with a semi-preparative RP18 Lichrosorb column. Spadin-biotinylated (eluted at 27 min), identified by mass spectrometry, was collected, quantified by its absorption at 280 nm and lyophilized in aliquots.

2.3. Alpha-Lisa™ test

According to the principles of AlphaScreen™ technology (Perkin Elmer), streptavidin-donor microbeads were recognized by biotin-spadin, whereas anti-rabbit IgG-acceptor microbeads were bound by anti-spadin antibodies. When the two microbeads (acceptor and donor) were into proximity, the signal was produced by a molecular interaction occurring between the binding partners bound on the beads. The propeptide present in the serum sample was able to interfere with this interaction leading to competition. Standard curves were obtained by incubation in 96-well plates of 10 nM biotin-spadin with the anti-spadin antibody (1:1000) in the AlphaLisa™ buffer in the absence or in the presence of increasing concentrations of spadin (from 10^{-11} to 10^{-6} M) for 1 h at room temperature. After addition of acceptor and donor beads and further incubation for 2 h at room temperature, the plaques were read using the Enspire apparatus (Perkin). For serum measurements, the same volume of serum was added instead of unlabeled spadin. The amount of propeptide was determined from its percent of signal inhibition and calculated using the standard curve.

2.4. Porsolt forced swim test (FST)

After *iv* injection of either saline or various tested peptides, mice (n =10–12 per group) were placed individually in a cylinder (height: 30 cm, diameter: 15 cm) filled with water to a depth of 12 cm (temperature: 22 ± 1 °C) for 6 min. The total period of immobility was recorded during the last 4 min (Porsolt et al., 1977).

2.5. Human blood samples

The control cohort consisted of 49 unrelated healthy volunteers who were screened for DSM-IV Axis I disorder diagnoses by expert psychologists using the Mini-International Neuropsychiatric Interview (MINI) (Sheehan et al., 1998). Only healthy volunteers without history of drug or alcohol abuse or dependence and without a personal or first-degree family history of psychiatric disorders were enrolled in the study. Furthermore, the absence of relevant neurological diseases *i.e.* epilepsy, Parkinson's syndrome, was mandatory for inclusion into the study. Finally, subjects who obtained a score lower than 27/30 at the Mini Mental State Examination (MMSE) were excluded from the study.

The patient cohort was made of 37 MDD patients with moderate to severe depression who met Diagnostic and Statistical Manual of Mental Disorders-IV (DSM-IV) classification system criteria. Diagnosis of unipolar depression was confirmed using the Structured Clinical Interview for DSM-IV Axis I Disorders (SCID-I). The exclusion criteria were: a) mental retardation or cognitive disorder; b) a lifetime history of schizophrenic, schizoaffective, or bipolar disorder; c) personality disorder, substance abuse, alcohol abuse or dependency, obsessive compulsive disorder, or post-traumatic stress disorder as the primary diagnosis; and d) comorbidity with an eating disorder.

No patients showed psychotic symptoms; 11 (29.7%) showed current comorbidity in Axis I (generalized anxiety disorder (GAD), panic attacks, panic disorders or anxiety disorder not otherwise specified (NOS)), 2 (5.4%) showed symptoms of Axis II disorders (dependent personality disorder) and no alcohol abuse, as a secondary diagnosis (the total number exceeded the number of subjects due to the presence of comorbidities).

All patients were either 'drug naïve', and had never received previous treatment with any antidepressant drug, or 'drug free'. They have been previously treated with one or two antidepressants but had a washout period lasting at least 2 weeks before starting with the new antidepressant treatment. All patients were treated in monotherapy: thirty-five patients were treated with selective serotonin reuptake inhibitors (SSRIs), and the other patients were treated with selective serotonin-norepinephrine reuptake inhibitors (SNRIs), tricyclics (TCAs) or noradrenergic and specific serotoninergic antidepressants (NASSAs).

Illness severity was assessed by the Montgomery and Asberg Depression Rating Scale (MADRS) before the start of the new antidepressant treatment (T0) and after 12 weeks of treatment (T1). All of the socio-demographical, clinical and pharmacological treatment characteristics of patients are shown in Table 1.

For both patients and controls, venous blood samples were collected between 8:00 and 9:00 a.m. after an overnight fast in anticoagulant-free tubes. Serum was separated by centrifugation (1620*g* for 15 min). Blood samples for PE measurements were collected at each timepoint.

Studies were approved by the Local Ethics Committees (CEIOC IRCCS Istituto Centro San Giovanni di Dio Fatebenefratelli, Brescia N: 50/2008 and Ethics Committee of the province of Verona N: 4997/09.11.01), and written informed consent was obtained.

2.6. Statistics

Results are expressed as mean ± standard error mean (SEM). Statistical analyses were performed using GraphPad (version 6.0). Analysis of variance (ANOVA) was used to compute differences in time immobility for the different peptides used in the FST (Fig. 1D). Demographic and clinical characteristics in our patient samples were described either in quantitative term of mean ± standard deviation (SD) or as proportions. Chi-square ($\chi 2$) tests were conducted to evaluate the association between groups and categorical variables, while analysis of variance (ANOVA) was used to compute possible differences in age, education and BMI between groups (Table 1). Due to

Table 1
Demographic and clinical characteristics of control and MDD patient groups.

Characteristics	Controls (N=49)	MDD (N=37)	*p*-value
Age (years), mean (SD)	45.1 (12.1)	44.9 (13.1)	0.95
Gender (%F)	65.3	75.7	0.30
Education (years), mean (SD)	13.8 (5.1)	11.9 (2.8)	0.04*
BMI (Body Mass Index)	23.6 (3.1)	24.4 (2.8)	0.26
% Smokers	16.3	37.8	0.02*
Age of onset (years), mean (SD)		40.9 (11.1)	
% of MADRS at T0, mean (SD)		25.5 (5.2)	
% of ΔMADRS at T1, mean (SD)		−60.1 (33.1)	
% of recurrent MDD		27.0	
% of severe vs. moderate MDD		8.1	
% comorbidity with personality disorders		5.4	
% comorbidity with anxiety disorders		29.7	
% comorbidity with alcohol abuse		0.0	
% administration of SSRIs* (Escitalopram)		75.7	
% administration of SNRIs* (Venlafaxine)		5.4	
% administration of SNRIs* (Duloxetine)		2.7	
% administration of TCAs* (Nortriptyline)		10.8	
% administration of NaSSAs* (Mirtazapine)		5.4	

[a]the total number could exceed the number of subjects due to the presence of multiple drugs administration

* Indicates significant *p*-values (< 0.05)

the relative small size of groups more conservative statistical analyses were used to investigate possible involvement of PE in MDD. Thus, Mann-Whitney *U* and Wilcoxon Signed Ranks non-parametric tests were used to evaluate differences of PE levels between groups, and the effect of AD treatment in MDD sample. The Pearson coefficient was used to evaluate bivariate correlations.

3. Results

To verify that we were able to detect the peptides derived from the human sequence with our aim to compare its levels in the serum from MDD and healthy controls, we investigated on the specificity of the antibodies used in the dosing method. We first designed a series of partial sequences from human PE to characterize the specificity of the antibodies used (Fig. 1A). From the structure-recognition analysis of these peptides (Fig. 1B and C), we observed that PE, Spadin, PE 12–27 and PE 14–25 were recognized by the antibodies with identical affinities, whereas PE 1–16 and PE 22–28 were not recognized. Note that non-apparented peptides like neurotensin or somatostatin were unable to interfere with the dosing method (Fig. 1B and C). These results allowed us to identify the epitope of antibodies used, the sequence WSGPI. The AD activity of these analogues was tested using FST. As shown in Fig. 1D, all the peptides bearing the epitope sequence (PE, Spadin, PE 12–27 and PE 14–25) displayed in the Porsolt swim test AD activity similar to that of spadin itself. Relative affinities and range amount for detection of tested peptides were summarized in the Table S1. These results indicated that both PE, spadin and major partial sequences of PE corresponded to active peptides that can be quantified (spadin-like immunoreactivity, SLI). Therefore, the stability of the measured SLI up to 24 h at room temperature (Fig. S1) validated further measurements in mouse and human.

To gain insight into the variations of PE levels in the pathology of depression, we collected a set of human sera from a clinical center from Italy.

In the cohort we observed that PE concentration was significantly lower in MDD patients (18.9 ± 1.3 nM) than in healthy controls (23.7 ± 1.5 nM) (z=−2.11, p=0.035) (Fig. 2). Since, comparative analyses of sociodemographical variables (Table 1), have shown differences in education and percentage of smokers between MDD patients and controls, we carried out further analyses for assuring that the significant difference in PE levels between groups is not being influenced by these two variables. No significant correlations were found between education or percentage of smokers and PE concentrations both in controls than in patients, and also considering the whole sample of subjects used.

Interestingly, MDD treated for 12 weeks with ADs showed a PE level significantly higher than before treatment (21.0 ± 1.5 nM) (z=−1.98, p=0.047) (Fig. 2). The increase of PE concentration after treatment was very subtle. We confirmed the efficacy of the treatment by the significant decrease of MADRS (Fig. 2). No significant correlation was found between clinical scoring and PE concentration evolution (r=0.18, p=0.27).

4. Discussion

The present work indicates that the antibody used during this study recognizes only a series of peptides derived from the human PE as well as PE itself and not non-apparented peptides like neurotensin or somatostatin. Interestingly, the peptides recognized by the antibody display AD activities as shown with the forced swimming test in mice (Fig. 1D). From this characterization, results obtained in human indicate two relevant findings. First, the serum PE concentration is down-regulated in MDD patients when compared with healthy subjects. Second, MDD patients with lower PE levels may recover a normal concentration of peptide in correlation with clinical evolution following AD treatments. Therefore, serum PE concentrations may be an additional marker to BDNF serum level which has been shown to be significantly decreased in MDD patients (for review see (Molendijk et al., 2014)). The decrease of BDNF as well as the dysfunction of BDNF signaling can be the consequence of the sortilin-induced anterograde trafficking of its precursor pro-BDNF then decreasing the production of BDNF. We already observed that spadin enhanced BDNF mRNA and protein (Devader et al., 2015). One explanation could be that since spadin and/or PE are able to bind sortilin, this binding may decrease the potency of sortilin to internalize pro-BDNF, a process which can lead to an increase of BDNF production.

The serum PE concentration is significantly lower in MDD patients, and taking into account that peptides measured in the present work were generated from sortilin, we wondered whether this observation was correlated with sortilin level and/or expression. Interestingly, the variation of sortilin expression in the blood has been already observed in MDD patients. First, in blood mononuclear cells, the genetic expression of sortilin is decreased with the clinical improvement (Belzeaux et al., 2010) whereas sortilin is over-expressed in MDD patients, particularly in non-responders (Belzeaux et al., 2012). Second, in the human serum, the increase in the level of sortilin is associated with the depression state (Buttenschon et al., 2015). The latter observations appear in contradiction with our results. How the level of sortilin propeptides can decrease when both the expression and release of sortilin itself are increased in MDD patients? A probable explanation is that the amount of sortilin recovered in mononuclear cells likely depends on transcription/translation gene expression steps, whereas the recovery of soluble sortilin in the blood is the consequence of the shedding of the membrane-bound protein as already observed from several cell types (Navarro et al., 2002). In the present study, we quantified the serum concentration of sortilin-derived propeptides whose amounts depend first on the effective cleavage of the protein precursor by the furin protein convertase (Munck Petersen et al., 1999), and second, on the ability of the matured protein to reach the plasma membrane. Indeed, about 90% of sortilin is intracellularly located within the Trans-Golgi Network (Mazella et al., 1998; Petersen et al., 1997) and its sorting to the cell surface can be induced by various

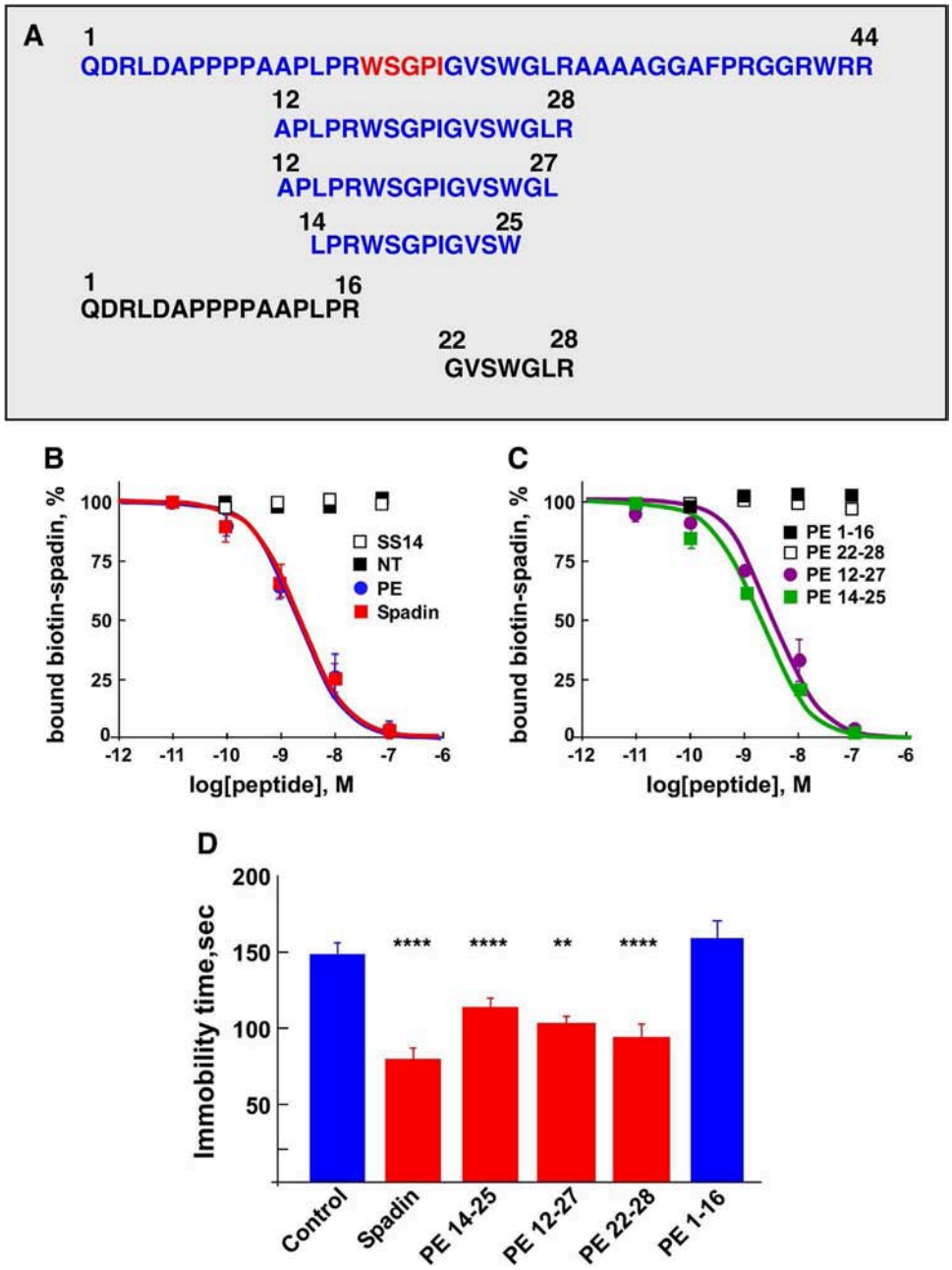

Fig. 1. A) Schematic representation of peptides designed for the study. The epitope sequence is in red. B and C) Relative affinities of spadin, PE and analogues recovered for the detection method. B) Both spadin and the entire PE were recognized by anti-spadin antibodies with IC50 of 2.50 nM (95% CI: 1.85–3.37; n =6) and of 2.18 nM (95% CI: 1.53–3.09; n =3), respectively, neurotensin (NT, black squares) and somatostatin-14 (SS14, white squares) were not recognized by antibodies. (C) PE 14–25 bound to antibodies with an IC50 of 1.73 nM, whereas the IC50 of PE 12–27 was of 3.44 nM, PE 22–28 (white squares) and PE 1–16 (black squares) were not recognized by antibodies. Each point corresponds to mean ± SEM. for 3–6 independent experiments. D) Porsolt forced swim test (FST). Spadin or partial peptides-treated mice had a shorter time of immobility comparable to those obtained with saline. (Ordinary one way ANOVA, $F_{5,54}$ =20.21, ****$p < 0.0001$ for spadin, PE 12–27 and PE 22–28 versus saline-treated mice, **p=0.0026 for PE 14–25 versus saline; error bars, mean ± SEM.

effectors as already demonstrated in insulin target cells and, particularly, in glucose transporter Glut4 vesicles (Kandror, 2003). Indeed, these vesicles can be translocated to the plasma membrane upon insulin activation (Huang et al., 2013) where they can release PE within the circulation.

The limitation of the study concerns the relatively small patient samples that could negatively affect the likelihood that a nominally statistically significant finding actually reflects a true effect.

Nevertheless, taken together, the data presented in this work indicate a proof of concept that the serum PE concentration can vary as a function of the mood symptoms in human, and can be an additional biomarker of the depression like BDNF and VEGF (Buttenschon et al., 2015). In addition, the possible further use of spadin as a potent therapy against the pathology, a peptide for which the serum level could also be controlled, will certainly greatly enhance the perspectives of new strategies to efficiently manage depression in the world.

Funding sources

The work performed by JM, CD, MR, SM, CH and MB was funded by grants obtained from the Agence Nationale de la Recherche (ANR-13-SAMA-0002 and ANR-13-RPIB-0002). All authors declare no financial interests or potential conflict of interest.

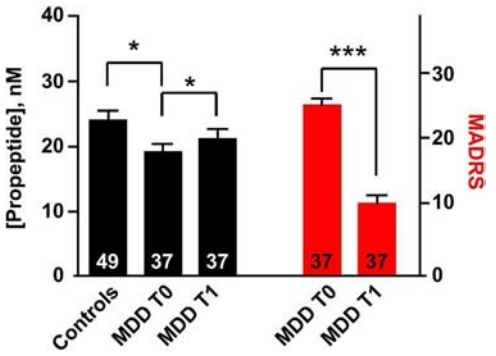

Fig. 2. PE concentrations in sera from healthy, untreated (T0) and treated (T1) MDD patients for 12 weeks. Statistical analysis was performed using Mann-Whitney Test between patients (MDD T0, n =37) and controls (n =49), and using Wilcoxon Signed Rank Test between untreated (T0) and treated (T1) MDD. * $p < 0.05$; n.s. non significant. Mean ± SEM of MADRS for MDD patients before (T0) and after (T1) a 12 week treatment (bars in red). *** $p < 0.001$.

Author contributions

CD, MR, SM and JM performed the experiments. MB, CH and JM conceived and designed the experiments. MB, CH and JM contributed reagents/materials/analysis tools. AM enrolled and screened controls and patients performed statistical analyses from Italian cohort. MBort enrolled and screened patients from Italian cohort. AM, CC, MG, MBort provided human blood serum from Italian cohort, and contributed to the final manuscript. JM wrote the paper with the contribution of AM, CC and CH.

Acknowledgements

This work was supported by the Centre National de la Recherche Scientifique and the Agence Nationale de la Recherche. We also thank the French Government for the “Investments for the Future” LABEX ICST.

Appendix A. Supplementary material

Supplementary data associated with this article can be found in the online version at http://dx.doi.org/10.1016/j.jad.2016.10.049.

References

Allen, A.P., Naughton, M., Dowling, J., Walsh, A., Ismail, F., Shorten, G., Scott, L., McLoughlin, D.M., Cryan, J.F., Dinan, T.G., Clarke, G., 2015. Serum BDNF as a peripheral biomarker of treatment-resistant depression and the rapid antidepressant response: a comparison of ketamine and ECT. J. Affect. Disord. 186, 306–311.

Belzeaux, R., Bergon, A., Jeanjean, V., Loriod, B., Formisano-Treziny, C., Verrier, L., Loundou, A., Baumstarck-Barrau, K., Boyer, L., Gall, V., Gabert, J., Nguyen, C., Azorin, J.M., Naudin, J., Ibrahim, E.C., 2012. Responder and nonresponder patients exhibit different peripheral transcriptional signatures during major depressive episode. Transl. Psychiatry 2, e185.

Belzeaux, R., Formisano-Treziny, C., Loundou, A., Boyer, L., Gabert, J., Samuelian, J.C., Feron, F., Naudin, J., Ibrahim, E.C., 2010. Clinical variations modulate patterns of gene expression and define blood biomarkers in major depression. J. Psychiatr. Res. 44, 1205–1213.

Bentley, S.M., Pagalilauan, G.L., Simpson, S.A., 2014. Major depression. Med. Clin. North Am. 98, 981–1005.

Buttenschon, H.N., Demontis, D., Kaas, M., Elfving, B., Molgaard, S., Gustafsen, C., Kaerlev, L., Petersen, C.M., Borglum, A.D., Mors, O., Glerup, S., 2015. Increased serum levels of sortilin are associated with depression and correlated with BDNF and VEGF. Transl. Psychiatry 5, e677.

Chen, Z.Y., Ieraci, A., Teng, H., Dall, H., Meng, C.X., Herrera, D.G., Nykjaer, A., Hempstead, B.L., Lee, F.S., 2005. Sortilin controls intracellular sorting of brain-derived neurotrophic factor to the regulated secretory pathway. J. Neurosci. 25, 6156–6166.

Devader, C., Khayachi, A., Veyssiere, J., Moha Ou Maati, H., Roulot, M., Moreno, S., Borsotto, M., Martin, S., Heurteaux, C., Mazella, J., 2015. In vitro and in vivo regulation of synaptogenesis by the novel antidepressant spadin. Br. J. Pharm. 172, 2604–2617.

Heurteaux, C., Lucas, G., Guy, N., El Yacoubi, M., Thummler, S., Peng, X.D., Noble, F., Blondeau, N., Widmann, C., Borsotto, M., Gobbi, G., Vaugeois, J.M., Debonnel, G., Lazdunski, M., 2006. Deletion of the background potassium channel TREK-1 results in a depression-resistant phenotype. Nat. Neurosci. (9), 1134–1141.

Huang, G., Buckler-Pena, D., Nauta, T., Singh, M., Asmar, A., Shi, J., Kim, J.Y., Kandror, K.V., 2013. Insulin responsiveness of glucose transporter 4 in 3T3-L1 cells depends on the presence of sortilin. Mol. Biol. Cell 24, 3115–3122.

Jani, B.D., McLean, G., Nicholl, B.I., Barry, S.J., Sattar, N., Mair, F.S., Cavanagh, J., 2015. Risk assessment and predicting outcomes in patients with depressive symptoms: a review of potential role of peripheral blood based biomarkers. Front Hum. Neurosci. 9, 18.

Kandror, K.V., 2003. A long search for Glut4 activation. Sci. STKE 2003, PE5.

Mazella, J., Petrault, O., Lucas, G., Deval, E., Beraud-Dufour, S., Gandin, C., El-Yacoubi, M., Widmann, C., Guyon, A., Chevet, E., Taouji, S., Conductier, G., Corinus, A., Coppola, T., Gobbi, G., Nahon, J.L., Heurteaux, C., Borsotto, M., 2010. Spadin, a sortilin-derived peptide, targeting rodent TREK-1 channels: a new concept in the antidepressant drug design. PLoS Biol. 8, e1000355.

Mazella, J., Zsurger, N., Navarro, V., Chabry, J., Kaghad, M., Caput, D., Ferrara, P., Vita, N., Gully, D., Maffrand, J.P., Vincent, J.P., 1998. The 100-kDa neurotensin receptor is gp95/sortilin, a non-G-protein-coupled receptor. J. Biol. Chem. 273, 26273–26276.

Molendijk, M.L., Spinhoven, P., Polak, M., Bus, B.A., Penninx, B.W., Elzinga, B.M., 2014. Serum BDNF concentrations as peripheral manifestations of depression: evidence from a systematic review and meta-analyses on 179 associations (N=9484). Mol. Psychiatry 19, 791–800.

Munck Petersen, C., Nielsen, M.S., Jacobsen, C., Tauris, J., Jacobsen, L., Gliemann, J., Moestrup, S.K., Madsen, P., 1999. Propeptide cleavage conditions sortilin/neurotensin receptor-3 for ligand binding. EMBO J. 18, 595–604.

Nase, S., Kohler, S., Jennebach, J., Eckert, A., Schweinfurth, N., Gallinat, J., Lang, U.E., Kuhn, S., 2016. Role of serum brain derived neurotrophic factor and central N-acetylaspartate for clinical response under antidepressive pharmacotherapy. Neurosignals 24, 1–14.

Navarro, V., Vincent, J.P., Mazella, J., 2002. Shedding of the luminal domain of the neurotensin receptor-3/sortilin in the HT29 cell line. Biochem. Biophys. Res. Commun. 298, 760–764.

Nestler, E.J., Barrot, M., DiLeone, R.J., Eisch, A.J., Gold, S.J., Monteggia, L.M., 2002. Neurobiology of depression. Neuron 34, 13–25.

Petersen, C.M., Nielsen, M.S., Nykjaer, A., Jacobsen, L., Tommerup, N., Rasmussen, H.H., Roigaard, H., Gliemann, J., Madsen, P., Moestrup, S.K., 1997. Molecular identification of a novel candidate sorting receptor purified from human brain by receptor-associated protein affinity chromatography. J. Biol. Chem. 272, 3599–3605.

Porsolt, R.D., Le Pichon, M., Jalfre, M., 1977. Depression: a new animal model sensitive to antidepressant treatments. Nature 266, 730–732.

Schmidt, H.D., Shelton, R.C., Duman, R.S., 2011. Functional biomarkers of depression: diagnosis, treatment, and pathophysiology. Neuropsychopharmacology 36, 2375–2394.

Sheehan, D.V., Lecrubier, Y., Sheehan, K.H., Amorim, P., Janavs, J., Weiller, E., Hergueta, T., Baker, R., Dunbar, G.C., 1998. The Mini-international neuropsychiatric interview (M.I.N.I.): the development and validation of a structured diagnostic psychiatric interview for DSM-IV and ICD-10. J Clin Psychiatry 59 (Suppl 20), S22–S33, quiz 34-57.

Thomas, L., Kessler, D., Campbell, J., Morrison, J., Peters, T.J., Williams, C., Lewis, G., Wiles, N., 2013. Prevalence of treatment-resistant depression in primary care: cross-sectional data. Br. J. Gen. Pr. 63, e852–e858.

Wong, M.L., Licinio, J., 2001. Research and treatment approaches to depression. Nat. Rev. Neurosci. 2, 343–351.

DISCUSSION GENERALE et CONCLUSION

Durant ces trois années de thèse, mon travail s'est consacré sur l'étude et la compréhension d'un récepteur multifonctionnel dans la régulation de l'état émotionnel. De façon intéressante, la démarche originelle de ce projet se base sur les conséquences comportementales de l'absence ou du blocage d'un de ses partenaires, le canal potassique TREK-1. La protéine NTSR3/Sortiline a été identifiée par plusieurs approches, ce qui a permis de rendre compte de l'existence de fonctionnalités qui ne se limitent pas qu'à un rôle de récepteur. Caractérisée comme une protéine d'adressage grâce à son homologie structurelle avec le complexe VPS10p, c'est en identifiant ses partenaires que l'on peut potentiellement définir son rôle au sein de l'organisme. En effet, face à sa localisation cérébrale abondante et la formation de complexe avec des éléments du système neurotrophique, comme le BDNF ou encore p75NTR, il n'est pas incohérent d'émettre l'hypothèse d'une fonction centrale dans la régulation neuronale. L'observation d'une interaction entre le NTSR3/Sortiline et le canal TREK-1, impliqué dans la régulation de l'humeur, a été le point de départ pour étudier les différents aspects du récepteur dans l'affect dépressif. Son produit de maturation, le propeptide qui interagit avec le canal en bloquant son activité est responsable des effets antidépressifs chez la souris. En découle alors l'idée que ce produit de maturation du NTSR3/Sortiline, molécule endogène, pouvait alors être mesuré afin de déterminer s'il existe une corrélation entre son taux sanguin et l'état dépressif chez des patients.

Dans l'étude sur le niveau circulant du propeptide, les résultats amènent un concept intéressant. Il existe bien une différence entre des personnes atteintes d'épisode dépressif majeur (EDM) et des patients diagnostiqués sains. Hormis le fait qu'il faille élever le nombre d'échantillons de patients pour augmenter la robustesse de ce résultat, il tient bon de noter qu'il existe également une variation lorsque le patient déprimé répond à un traitement antidépresseur mais qu'il n'y a pas de corrélation entre le score MADRS et la quantité circulante de propeptide. Ce dernier point met en avant le fait que les variations de propeptide semblent spécifiques du degré de l'état dépressif et qu'il se pourrait qu'il ne soit pas significativement possible de voir une différence sur des symptômes plus légers. Cependant, le niveau sérique de propeptide se place comme un outil complémentaire dans la détection des cas sévères de dépression et permet de préciser le caractère épisodique de l'affect pour une meilleure prise en charge thérapeutique.

Les résultats précédents suggèrent qu'une diminution du propeptide peut être le reflet d'une dégradation de l'état émotionnel d'un individu. En prenant en considération l'origine de ce

peptide, et ses propriétés d'amélioration sur l'humeur qui résultent de l'activité du canal TREK-1, il existe une certaine évidence à poser le NSTR3/Sortiline comme régulateur important du système nerveux central. L'approche la plus intéressante pour accéder, de manière complète, aux fonctions d'une protéine, réside en l'analyse phénotypique d'un modèle dépourvu de cette dernière. Dans le cas présent, la délétion du NTSR3/Sortiline a permis d'évaluer non seulement ses partenaires connus, comme TREK-1 et le BDNF, mais également les conséquences sur la régulation du comportement et du système dont il fait partie, le système neurotensinergique. En effet, il semblerait que le récepteur prend une part importante dans la régulation du système neurotensinergique. De par la modulation de l'expression du NTSR2, qui résulte en une perte de sensibilité nociceptive chez les souris délétées du NTSR3/Sortiline. De façon remarquable, l'absence de NTSR3/Sortiline résulte en une augmentation de la production de neurotensine cérébrale et sérique, mais également en un possible changement d'affinité du peptide pour le récepteur NTSR2. Les mécanismes sous-jacents à ce changement d'affinité n'ont pas encore été résolus, mais il est probable que l'interaction avec le NTSR3/Sortiline permet des changements conformationnels nécessaires au fonctionnement adéquat de ces récepteurs.

Les propriétés d'adressage du NTSR3/Sortiline représentent une fonction clé dans la régulation de ces partenaires. En identifiant le canal potassique TREK-1 comme une des protéines associées au récepteur, il a été intéressant de caractériser cette perte fonctionnelle chez notre modèle murin *Sort-/-* dans l'état dépressif. En reprenant l'hypothèse que TREK-1 est un modulateur de l'humeur, les premiers tests établis sur ces souris ont été des tests comportementaux relatifs à la dépression, comme le FST et le TST, qui mesurent la résignation, et le NSF, qui permet d'évaluer la propension à l'exploration dans un milieu aversif. De façon étonnante, le phénotype de résistance des souris KO-NTSR3 se révèle être semblable à celui des souris KO-TREK-1. Cela suggère que l'expression tissulaire ou cellulaire du canal semble être altérée. Cette assertion a été vérifiée d'abord par western blot, qui révèle que le niveau d'expression de TREK-1 est significativement diminué à la membrane plasmique où il est pleinement fonctionnel, sans modification de son expression totale. Par électrophysiologie, nous avons confirmé que le potentiel de membrane des neurones est fortement modifié.

L'autre partenaire essentiel identifié est le BDNF. Cette neurotrophine nécessite une maturation dépendante du NTSR3/Sortiline, plus particulièrement dans sa voie régulée. En effet, ce complexe NTSR3/Sortiline proBDNF n'est présent que dans la voie régulée du BDNF, et il est nécessaire pour le repliement correct du domaine mature pour sa maturation par la furine. Cela suggère que le NTSR3/Sortiline est un acteur prépondérant dans le contrôle de la sécrétion de la

neurotrophine et que son absence crée un déséquilibre entre les voies de libération. Dans une lignée cellulaire dérivée d'un phéochromocytome, les PC12, il a pu être montré qu'en présence d'une forme tronquée du NTSR3/Sortiline au niveau du site de liaison avec le proBDNF, il y avait une augmentation de libération de BDNF dans la voie constitutive (Chen et al., 2005). Le BDNF est une protéine clé dans la viabilité et la croissance neuronale, par ailleurs, son niveau sérique et cérébral peut être un indicateur dans certains états dépressifs. C'est de façon cohérente que l'évaluation de ce système neurotrophique s'est posée comme une hypothèse de travail dans notre modèle de souris Sort-/-. Les résultats confirment l'existence d'une augmentation de BDNF dans les homogénats de cerveaux des souris KO-NTSR3, qui résulte d'une augmentation de la maturation intracellulaire par la furine, aboutissant également à une augmentation de l'activité de son récepteur TrkB.

En associant ces derniers résultats avec une augmentation du taux de décharges des neurones sérotoninergiques, nous avons pu mettre en évidence le rôle important du NSTR3/Sortiline dans la régulation de l'humeur et plus particulièrement dans l'affect dépressif, suggérant le récepteur comme une cible potentiel dans le traitement de cette maladie psychologique.

Cependant, il existe chez les souris KO-NTSR3 un phénotype d'anxiété révélé par des tests comportementaux comme le paradigme de la boite clair-obscur ou encore la croix surélevée. L'anxiété fait partie du spectre de l'affect dépressif, ce qui rend ce résultat assez paradoxal par rapport au phénotype antidépressif de ces souris. Ces tests mesurent la prédisposition des souris à l'exploration dans un environnement aversif. De manière intéressante, ils sont assez proches de celui du NSF, à la différence que les souris n'ont pas été soumises à une suppression de nourriture pendant 24h. Il semblerait possible que la sensation de faim ait eu un impact sur l'issue de ce test. D'un point de vue métabolique, des résultats non publiés ont apporté des éléments intéressants. Le poids des souris KO-NTSR3 est sensiblement plus faible celui des souris sauvages ainsi que la prise alimentaire. Il pourrait donc y avoir une régulation différente dans le système alimentaire. Pour revenir au phénotype anxieux, il n'est pas corrélé à une dérégulation de l'hormone du stress, la corticostérone. D'autres tests de résistance à la dépression ont été réalisés, mettant en jeux la résignation acquise. La résignation acquise est une sensation d'impuissance permanente générée par le fait d'être plongé, de façon durable ou répétée, dans une situation à laquelle on ne peut s'échapper ou contrôler. Le test chez la souris consiste en une série de chocs électriques d'où il n'est pas possible de s'échapper, durant plusieurs jours afin de provoquer une résignation. Le dernier jour, les souris ont la possibilité de s'échapper pour mettre fin à la situation stressante, permettant ainsi d'évaluer leur degré d'envie d'éviter l'environnement aversif. Les antidépresseurs classiques ainsi

que la Spadine permettent un comportement positif à l'égard de ce test. De façon étonnante, les souris KO-NTSR3 échouent le plus souvent pour s'échapper et lorsqu'elles s'échappent, la latence pour sortir de l'environnement aversif est beaucoup plus importante par rapport aux souris sauvages (**Figure 26A**). Ce résultat est assez contradictoire avec le phénotype antidépressif mais peut corréler à l'état anxieux. Mais alors, comment expliquer ce phénomène opposé ? La réponse peut se trouver dans la régulation du BDNF. Cette neurotrophine est très importante dans l'apprentissage et notamment la mémoire. Dans des tests, non encore publiés, nous avons regardé l'apprentissage des souris KO-NTSR3 dans la piscine de Morris. Ce test consiste, dans un premier temps, en une phase d'apprentissage où il faut repérer une plateforme immergée pour sortir de l'eau, puis, dans un second temps, la plateforme est supprimée et les souris sont évaluées sur le temps passé dans la zone antérieure de cette plateforme. Dans ce test, les souris KO-NTSR3 n'ont pas de meilleurs résultats lors de la phase d'apprentissage par rapport aux souris sauvages, cependant, de façon étonnante, dans la phase de rappel, effectué après 10 jours, les souris KO-NTSR3 ont une meilleure trace mnésique (**Figure 26B**). On a ici un résultat assez intéressant, qui peut être la conséquence de l'augmentation d'expression du BDNF. Des études ont montré que cette neurotrophine est impliquée dans la consolidation de la mémoire à long terme dans l'hippocampe (Bekinschtein et al., 2007) et qu'il existe également un soutien de l'amygdale dans cet apprentissage, facilité par le BDNF. En particulier, des preuves de plus en plus nombreuses indiquent maintenant un rôle pour la signalisation du BDNF dans les noyaux basal et latéral de l'amygdale (Rattiner et al., 2004), régions connues pour être nécessaires à la formation de l'apprentissage lié à la peur (LeDoux, 2000). Récemment, des études ont montré que le BDNF était nécessaire à la consolidation de l'apprentissage de la peur conditionnée dans l'amygdale (Chou et al., 2014; Harris et al., 2016). Cela pourrait expliquer le comportement que l'on retrouve chez les souris KO-NTSR3, qui présentent une quantité cérébrale de BDNF significativement supérieure à celle des souris sauvages.

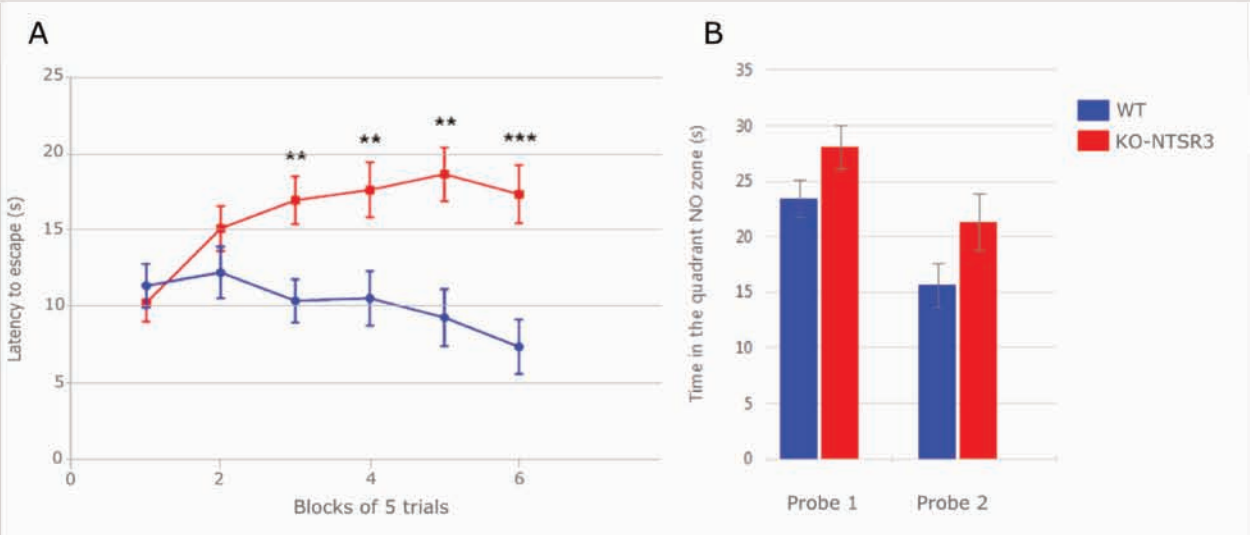

Figure 26 : Comportement des souris KO-NTSR3 dans la résignation acquise et la mémoire spatiale. ***A)*** *Test du Learn Helpness, latences d'échappement subdivisées en 5 blocs d'essais (n=30). Le test se compose de 30 essais séparés par un intervalle de 30 secondes. Un essai est défini par l'administration d'un choc électrique soutenu qui s'accompagne de l'ouverture de la porte de communication, permettant à la souris de fuir. Le choc électrique (et donc l'essai) se termine soit lorsque la souris change de compartiment, soit 24 sec après le début du choc.* ***B)*** *Morris Maze, temps passé dans la zone où se situé la plateforme, 10 (probe 1) et 11 (probe 2) jours après l'entrainement (n=20).*

En conclusion, ces travaux ont permis de mettre en lumière le rôle du NTSR3/Sortiline au sein de l'état dépressif. D'une part, un propeptide considéré comme un possible biomarqueur de la dépression majeure et qui possède également des propriétés antidépressives puissantes chez la souris et d'autre part, le récepteur NTSR3/Sortiline impliqué dans la régulation de l'humeur dépendante du canal potassique TREK-1 mais également du BDNF.

En parallèle, j'ai eu l'opportunité de travailler sur les analogues de la Spadine. Dans ces études, j'ai caractérisé d'une part l'effet sur la neurogénèse sur des neurones corticaux primaires et d'autre part, évalué la biodisponibilité dans le sérum ou le cerveau des souris, après injection. Ces articles sont disponibles en annexes du manuscrit.

PERSPECTIVES

Ces travaux de thèse ont apporté de nombreux résultats concernant le NSTR3/Sortiline dans le système nerveux central, tant au niveau comportemental que biochimique et électrophysiologique. Néanmoins, il est nécessaire d'approfondir certains des aspects observés.

Dans la mesure du propeptide circulant, il serait intéressant d'étendre ce dosage sérique au diffèrent degrés du trouble dépressif pour essayer de corréler et d'affiner le diagnostic établi. De plus, le stress jouant sur l'expression de BDNF, il pourrait être intéressant de regarder les variations du propeptide dans des tests de stress chronique chez le rongeur, sachant déjà, que ce test induit une diminution de l'expression de NTSR3/Sortiline.

En ce qui concerne l'étude sur la délétion du NTSR3/Sortiline dans le système neurotensinergique, il conviendrait d'approfondir les mécanismes sous-jacents à la modification d'expression et d'affinité du NTSR2 (internalisation, changement de conformation), responsable de la perte de sensibilité nociceptive, ainsi que d'élucider les processus qui induisent une augmentation de neurotensine dans le sérum.

Enfin, la perte de NSTR3/Sortiline aboutit à une altération de la fonction du canal potassique TREK-1 et du système neurotrophique du BDNF. Les souris KO-NTSR3 montrent un comportement similaire aux souris KO-TREK-1 à la différence que l'on observe une augmentation de l'anxiété. Ce dernier résultat nécessite de regarder les fonctions qui régulent cet état émotionnel, notamment lié à des structures comme l'amygdale et l'hippocampe. Premièrement, s'intéresser à des tests comportementaux liés à la mémoire (reconnaissance d'objet, fear conditionning, labyrinthe) étant donnée la place du BDNF dans l'apprentissage. Puis, d'un point de vue biochimique, régionaliser l'expression des différentes protéines modifiées par la perte du NTSR3/Sortiline. En effet, les résultats obtenus se sont concentrés sur l'étude du cerveau entier, il serait donc judicieux de regarder si, par exemple, l'augmentation de BDNF varie en fonction des régions cérébrales, ainsi, il sera possible, en fonction des régions localisées, de mieux comprendre les conséquences sur le comportement. Enfin, l'augmentation de l'activité de TrkB provoque une augmentation de phoshpoCREB pouvant aboutir à la synthèse de protéines. Situé dans le cerveau, le complexe BDNF/TrkB est connu pour favoriser l'amélioration de la libération présynaptique de neurotransmetteurs par : 1) l'activation des MAPK 2) l'augmentation de l'expression du récepteur au glutamate AMPA post-synaptique (AMPAR) et 3) la maturation des épines dendritiques et l'augmentation de l'expression des protéines (Park and Poo, 2012). Partant de ce constat, il serait donc intéressant d'évaluer l'expression et l'activité des neurotransmetteurs mais également de leurs récepteurs AMPA et NMDA.

ANNEXES

Hindawi Publishing Corporation
Journal of Diabetes Research
Volume 2016, Article ID 3142175, 9 pages
http://dx.doi.org/10.1155/2016/3142175

Research Article

Potentiation of Calcium Influx and Insulin Secretion in Pancreatic Beta Cell by the Specific TREK-1 Blocker Spadin

Céline Hivelin,[1] Sophie Béraud-Dufour,[1] Christelle Devader,[1] Amar Abderrahmani,[2] Sébastien Moreno,[1] Hamid Moha ou Maati,[3] Alaeddine Djillani,[1] Catherine Heurteaux,[1] Marc Borsotto,[1] Jean Mazella,[1] and Thierry Coppola[1]

[1]*CNRS, Inserm, IPMC, Université Côte d'Azur, Valbonne, France*
[2]*CNRS, CHU Lille, Institut Pasteur de Lille, UMR 8199-EGID, Université Lille, 59000 Lille, France*
[3]*Département de Physiologie, Institut de Génomique Fonctionnelle (IGF), CNRS/INSERM UMR5203, Université de Montpellier, Montpellier, France*

Correspondence should be addressed to Thierry Coppola; coppola@ipmc.cnrs.fr

Received 3 August 2016; Revised 21 November 2016; Accepted 29 November 2016

Academic Editor: Eusebio Chiefari

Copyright © 2016 Céline Hivelin et al. This is an open access article distributed under the Creative Commons Attribution License, which permits unrestricted use, distribution, and reproduction in any medium, provided the original work is properly cited.

Inhibition of the potassium channels TREK-1 by spadin (SPA) is currently thought to be a promising therapeutic target for the treatment of depression. Since these channels are expressed in pancreatic β-cells, we investigated their role in the control of insulin secretion and glucose homeostasis. In this study, we confirmed the expression of TREK-1 channels in the insulin secreting MIN6-B1 β-cell line and in mouse islets. We found that their blockade by SPA potentiated insulin secretion induced by potassium chloride dependent membrane depolarization. Inhibition of TREK-1 by SPA induced a decrease of the resting membrane potential ($\Delta V_m \sim 12$ mV) and increased the cytosolic calcium concentration. In mice, administration of SPA enhanced the plasma insulin level stimulated by glucose, confirming its secretagogue effect observed in vitro. Taken together, this work identifies SPA as a novel potential pharmacological agent able to control insulin secretion and glucose homeostasis.

1. Introduction

Insulin secretion by pancreatic β-cells is critical for glucose homeostasis. Glucose-induced insulin secretion relies on potassium (K^+) current-dependent plasma membrane depolarization [1, 2]. Indeed high glucose concentration causes the closure of the ATP-sensitive K^+ channel (K_{ATP} channel) preventing potassium efflux and leads to β-cell membrane depolarization [3–5]. As a consequence, the voltage-dependent calcium channels open, thus allowing calcium influx responsible for the fusion of insulin-containing granules to finally release insulin into the bloodstream [6]. The search for innovative therapeutic strategies improving the β-cell function is a key issue for the treatment of diabetes. The first oral antidiabetic agents, metformin and sulfonylureas, were developed in the 1950s and continue to be used effectively. Since 2008, two other very promising therapeutic classes have been placed on the market: dipeptidyl peptidase-4 (DPP-4) inhibitors and glucagon like peptide 1 (GLP-1) analogues to promote insulin secretion without the risk of hypoglycemia. These two drug therapies take advantage of the incretin effect which is a decrease in blood glucose levels. Incretins promote an increase in the amount of insulin released from islets of Langerhans after a meal [7, 8]. Sulfonylureas stimulate insulin secretion by selectively inhibiting β-cell K_{ATP} channels [9]. Beside inducing intracellular signaling, GLP-1 also regulates glucose stimulated insulin secretion by the changes in membrane potential [10].

In pancreatic β-cells, it is thought that the two-pore potassium channels (K_2P) participate in regulating cell membrane potential [11–13]. Among K_2P channels, TREK-1, TREK-2, and TRAAK belong to a subfamily of channels that are opened by mechanical and chemical stimuli [14–16]. TREK-1, the first mechanosensitive K^+ channel to be identified [17], is activated by polyunsaturated fatty acids and

volatile anesthetics [15, 16]. TREK-1 is efficiently inhibited through an intracellular increase of cAMP that leads to the protein kinase A (PKA) activation. Therefore, PKA phosphorylates the serine 333 in the cytoplasmic C-terminal region of the channel [18, 19]. This inhibitory effect is also observed after agonist stimulation of the β-adrenergic receptors known to increase intracellular cAMP contents [20]. Incretin hormones like GLP1 and gastric inhibitory polypeptide (GIP) are also able to increase cAMP by activation of PKA [21]. The role of incretins in insulin secretion can therefore be the consequence of both an increase of cAMP and the activation of the phosphorylation of key proteins involved in regulation of insulin exocytosis [22].

Recently, we identified a peptide named spadin (SPA), a partial sequence of the propeptide (PE) released during the maturation of sortilin, as a new class of highly effective and fast acting antidepressants (AD). Sortilin is a class 1 receptor involved in the sorting of several transmembrane proteins including TREK-1 [23]. The AD action of SPA is triggered through the blockade of the TREK-1 channel activity. Since we previously observed that TREK-1 was expressed in the pancreatic β-cell line β-TC3 [23], we wondered whether TREK-1 and SPA play a physiological role in the regulation of insulin secretion by maintaining the membrane potential of pancreatic cells. In the present work, we demonstrate that SPA by specifically blocking TREK-1 channels depolarizes pancreatic β-cell membranes, increases Ca^{2+} influx, and contributes to insulin secretion.

2. Materials and Methods

2.1. Animals for In Vivo Experiments. All experiments were performed according to policies on the care and use of laboratory animals of European Community Legislation. The local Ethics Committee approved the experiments (protocol number 00893.02).

All efforts were made to minimize animal suffering and reduce the number of animals used. Adult male C57/Bl6 mice, weighing 24–28 g (8–10 weeks old), were used in this study. The animals housed under controlled laboratory conditions with a 12 h dark-light cycle, a temperature of 21 ± 2°C, and a humidity of 60–70% for at least one week prior to drug treatment. Mice had free access to standard rodent diet and tap water.

2.2. Cell Culture. Mouse insulin secreting MIN6-B1 cells (passages 35–45) were cultured at 37°C in a humidified atmosphere containing 5% CO_2 in DMEM medium supplemented with 5% foetal calf serum, 1 mM sodium pyruvate, 2 mM glutamate, 50 mM 2-mercaptoethanol, 100 units/ml penicillin, and 100 mg/ml streptomycin. For Fura-2AM experiments, cells were plated at a density of 1.5×10^5/ml, onto 25 mm poly-D Lysine-coated glass coverslips. For the electrophysiological experiments MIN6-B1 cells were seeded at a density of 20,000 cells/35 mm dishes. Then, cell membrane potential measurements were recorded after 2–6 days of culture.

2.3. Whole Cell Patch Clamp Recordings and Membrane Potential Measurements. Whole cell patch clamp recordings were performed in MIN6-B1 cells in a bath solution containing a cocktail of K^+ channel blockers to record specifically the TREK-1 current. This solution contains 10 mM tetraethyl ammonium (TEA), 3 mM 4-aminopyridine (4-AP), 50 nM charybdotoxin, 10 mM glibenclamide (Glib), and 100 nM apamin.

Membrane potentials were measured in MIN6-B1 cells incubated during 45 min in control conditions in the presence of SPA (1 μM) or Glib (10 μM) or both. Each experimental group was tested in the presence of glucose (2 mM or 10 mM). After the incubation period, cells were patched and membrane potentials were immediately measured using the whole cell patch clamp technique [24]. Each membrane potential was evaluated by using a RK 400 patch clamp amplifier (Axon Instruments, USA), low-pass filtered at 3 kHz and digitized at 10 kHz using a 12-bit analogue-to-digital converter Digidata (1322 series, Axon Instruments, USA). Patch clamp pipettes were pulled using vertical puller (PC-10, Narishige) from borosilicate glass capillaries and had a resistance of 3–5 MΩ. The bath solution contained (in mM) 150 NaCl, 5 KCl, 3 $MgCl_2$, 1 $CaCl_2$, and 10 HEPES adjusted to pH 7.4 with NaOH. The pipette solution contained (in mM) 155 KCl, 3 $MgCl_2$, 5 EGTA, and 10 HEPES adjusted to pH 7.2 with KOH. All experiments were performed at room temperature (21-22°C). Data acquisition was carried out using a microcomputer (Dell Pentium) witch used commercial software and hardware (pClamp 8.2). All values of membrane potentials are expressed in mV as mean ± standard error of the mean (SEM).

2.4. Measurement of Cytosolic Calcium Concentrations. The cytosolic calcium variations were measured using the Fura-2AM loading protocol as previously described [25]. Loaded cells were visualized under an inverted epi-fluorescence microscope (AxioObserver, Carl Zeiss, France) using a Fluar 40x/1.3 oil immersion objective. The intracellular Fura-2AM was sequentially excited at 340 and 380 nm with a Xenon lamp through a high-speed multifilter wheel. For each excitation wavelength, the fluorescence emission was discriminated by the same 400 LP dichroic mirror and a 510/40 bandpass filter. Fluorescence images were acquired every 10 sec on an EMCCD camera (Cascade 512, Roper Scientific, Evry, France). Calcium image analyses were made using MetaMorph, MetaFluor (Universal Imaging). Fura-2 fluorescence intensities were expressed as changes relative to the initial fluorescence ratio (F340/380).

2.5. Islets Preparation. Mouse islets were isolated by hand-picking after collagenase digestion of pancreas as described previously [26] and were maintained overnight in DMEM supplemented with 10% FCS, 10 mM HEPES, pH 7.4, 1 mM sodium pyruvate, 100 units/ml penicillin-streptomycin, 50 μM β-mercaptoethanol, and 11 mM glucose.

2.6. Measurement of Insulin Secretion and Cellular Content. For insulin secretion and cellular content, MIN6-B1 cells (5×10^5 per well) or isolated pancreatic islets (20 islets per well) were incubated with 0.1 μM SPA for 45 min at 37°C in control conditions (2.8 mM glucose, 5 mM KCl) or in stimulating

conditions (30 mM KCl and 16.7 mM glucose). The amount of insulin was measured using an ELISA kit (Mercodia) as already described [27].

2.7. Western Blot Analysis. Solubilized proteins were separated on SDS-PAGE (10% acrylamide) and then transferred to a nitrocellulose membrane that was probed simultaneously with the following primary antibody: a mouse monoclonal sortilin (1 : 1000, BD Transduction Laboratories) and a rabbit polyclonal TREK-1 (1 : 1000, Millipore).

2.8. Immunocytochemistry. MIN6-B1 cells were plated on glass coverslips coated with 2 mg/mL poly-L-Lysine. Cells were preincubated for 10 min in Phosphate-Buffered Saline (PBS) and then fixed for 20 min with 4% paraformaldehyde in PBS at room temperature. Coverslips were rinsed twice with PBS and incubated with 50 mM NH_4Cl in PBS for 10 min to quench excess of free aldehyde groups. After incubation for 20 min in PBS containing 3% Horse Serum (HS) and 0.1% Triton X100, cells were incubated with a rabbit polyclonal anti-TREK1 (1/200, Millipore #AB5860) or a mouse monoclonal anti-chromogranin (1/400, Santa Cruz) for 2 h at room temperature in PBS containing 0.5% HS and 0.1% Triton-X100. Cells were rinsed three times in PBS and incubated for 45 min at room temperature with a Texas-Red-conjugated donkey anti-rabbit antibody (1/400, Invitrogen) or a FITC-conjugated donkey anti-mouse antibody (1/400, Invitrogen) in PBS containing 0.5% HS and 0.1% Triton-X100.

Immunohistochemistry was performed on mouse pancreas slices from wild type and TREK-1 invalidated mice using goat antibodies against insulin (1/400, Santa Cruz Technologies, sc-7838) and rabbit polyclonal anti-TREK1 (1/200, Millipore #AB5860). Briefly, adult male mice were transcardially perfused with 4% paraformaldehyde in PBS and then sacrificed. Pancreas was removed, postfixed in 4% paraformaldehyde in PBS for 2 h at 4°C, and transferred into a 20% sucrose/PBS solution. After freezing of the pancreas in isopentane, 35 μm sections were cut in a cryostat. Sections were stored at −20°C. Labeling was performed as described above for cells.

After two washes with PBS and one with water, coverslips were mounted on glass slides with Mowiol for confocal microscopy examination. Immunofluorescence of confocal images was analysed using ImageJ 1.4.3.67 (WS Rasband, National Institute of Health, https://imagej.nih.gov/ij/).

2.9. Intraperitoneal Glucose Tolerance Tests. Intraperitoneal glucose tolerance tests (IPGTTs) were performed on mice after an overnight (16 h) fast. 20 min prior to injection of glucose mice were injected (i.v.) with 100 μl of a saline solution (0.9% NaCl) in the absence or in the presence of 10^{-6} M SPA (8 μg/kg). Glucose administration was performed via intraperitoneal injection (2 g/kg) in 6 to 8 mice for each experimental group. Blood samples (100 μl) were collected from the tail vein before (basal glycemia) and after 10, 20, 30, 60, 90, and 120 min following injection and glucose. Insulin levels were then measured using an ELISA kit as described above.

2.10. Statistical Analysis. Data are given as means ± SEM. Statistical significance was evaluated with Student's t-test performed using GraphPad Prism.

3. Results

3.1. SPA Modulates Insulin Secretion in β-Cells. Previous studies indicated the presence of sortilin in β-cell lines and in mouse islets and of TREK-1 in β-TC3 cells [23, 28]. We therefore verified, using immunocytochemical and immunohistological approaches, that the channel TREK-1 was also expressed in our models (islets and MIN6-B1 cells). Figure 1(a) indicated that TREK-1 was expressed in mouse islets visualized by insulin immunoreactivity staining. Control experiments performed on pancreatic slices from TREK-1 KO mice confirmed the specificity of the antibody used (Figure 1(b)). Figure 1(c) confirmed the expression of TREK-1 in the insulin producing MIN6-B1 cells, particularly at the level of plasma membrane. The specificity of the TREK-1 antibodies used was also confirmed by Western blot analyses of islets proteins from WT and KO-TREK-1 mice (Figure 1(d)).

The expression of both TREK-1 and sortilin (the precursor of the PE) in β-cells and in islets prompted us to investigate the role of the PE related peptide SPA on insulin secretion. Under basal conditions (5 mM KCL, 2.8 mM glucose), incubation of isolated mouse islets and MIN6-B1 cells with 0.1 μM of SPA for 45 min did not modify the amount of secreted insulin (Figures 2(a) and 2(c)). By contrast, SPA potentiated KCl-induced insulin secretion both in islets (from 19.2 ± 0.72 μg/L to 27.47 ± 0.35 μg/L, $p < 0.001$) (Figure 2(a)) and in MIN6-B1 cells (from 297.5 ± 2.92 μg/L to 427.7 ± 20.58 μg/L, $p < 0.01$) (Figure 2(b)). Interestingly, SPA also increased the glucose-induced insulin secretion in mice islets (from 37.8 ± 0.73 μg/L to 47.2 ± 0.9 μg/L, $p < 0.01$) (Figure 2(c)) and in MIN6-B1 cells (from 144.7 ± 18.6 μg/L to 241 ± 30 μg/L, $p < 0.01$) (Figure 2(d)).

3.2. SPA Modulates Resting Membrane Potential. The resting membrane potential of neuronal cells (i.e., GABA neurons) was known to be maintained in part by TREK-1 channels on which SPA exerted a potent effect [29]. Furthermore, in other cell types such as embryonic atrial myocytes [30] and human osteoblasts [31], TREK-1 contributes to setting the resting membrane potential. Interestingly, it was recently reported that two members of the K_2P family (TALK-1 and TASK-1) are expressed in pancreatic islets [32, 33] in which they modulate electrical activity. We therefore postulated that these background K^+ channels could function as modulators of β-cell excitability. To answer this question we tested the effects of SPA on K^+ current recorded on whole MIN6-B1 cell patch. As shown in Figure 3(a), TREK-1 current was potentiated by 10 μM arachidonic acid (AA) and application of SPA (10^{-6} M) inhibited the AA activated TREK-1 current. This SPA effect was summarized in Figure 3(b) where the difference of membrane potential of SPA-treated versus control cells ($E_{mSPA} - E_{mC}$) ΔE_m was 12.6 ± 2.0 mV ($n = 15$, $p < 0.001$). As a control we observed that glibenclamide induced a depolarization up to −47.07 ± 2.33 mV ($p < 0.001$) ($\Delta E_m = 17 \pm 2.3$ mV, $p < 0.001$) (Figure 3(b)). We have

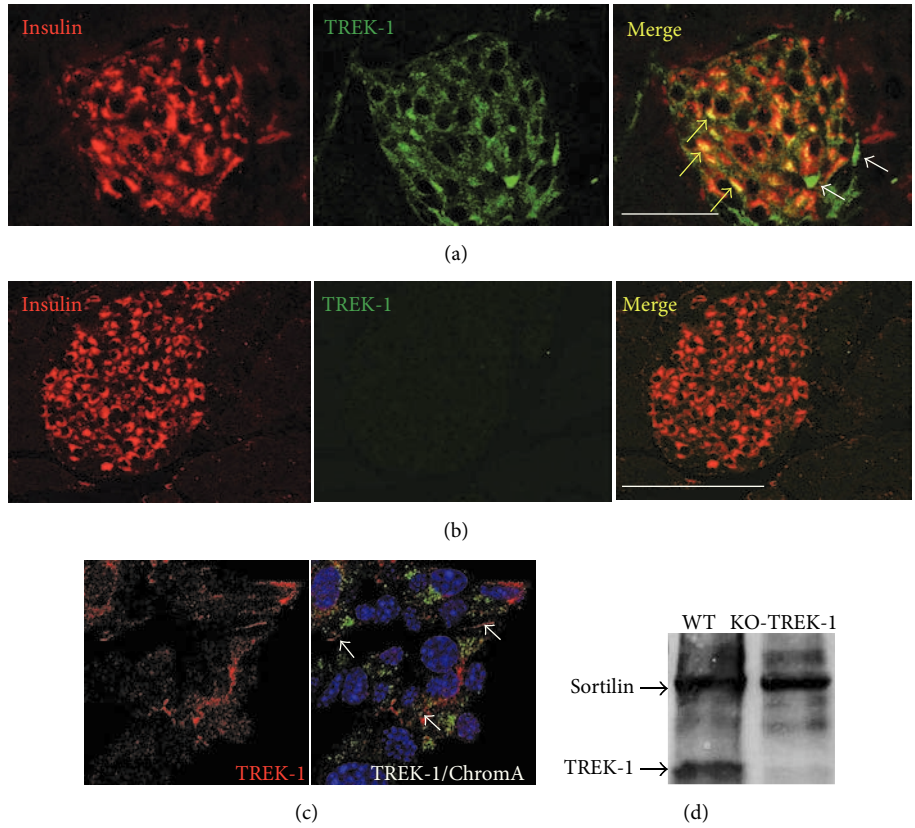

Figure 1: TREK-1 channels are expressed in insulin-containing cells. Immunofluorescent labeling of TREK-1 channels endogenously expressed in mouse pancreatic islets ((a) and (b)) and MIN6-B1 β-cells (c). (a) Immunohistochemistry of mouse pancreas sections stained for TREK-1 channels (Alexa-594) and insulin (Alexa-488) as described in Section 2. The merged image indicated colocalization of TREK-1 and insulin (yellow arrows), some peripheral cells were labeled only with TREK-1 antibodies (white arrows). (b) Immunohistochemistry of mouse pancreas sections from TREK-1 KO mice stained for TREK-1 channels (Alexa-594) and insulin (Alexa-488) clearly showed the absence of TREK-1 labeling. (c) Immunocytochemistry of MIN6-B1 cells was performed using anti-chromogranin A (labeling of secretory granules) and anti-TREK-1 antibodies followed by anti-mouse Alexa-488 and anti-rabbit Alexa-594 secondary antibodies and DAPI for nucleus labeling. Merged image showed the expression of TREK-1 at the plasma membrane (white arrows) (scale bar: 100 μm). (d) Immunoblotting of membrane homogenates from islets from WT and KO-TREK-1 mice, with anti-sortilin and anti-TREK-1, reveals a protein of 50 kDa for TREK-1 and 95 kDa for sortilin, respectively.

also tested the SPA effect when added to glucose 20 mM. As expected, we observed a strong and robust depolarization when the MIN6-B1 cells were incubated in the presence of 20 mM glucose, -60 ± 1.0 mV (2 mM glucose) versus -48.71 ± 2.378 mV (20 mM glucose) (Figure 3(c)). Addition of the GLP-1R agonist exendin4 (ex4) (10^{-7} M) induced a significant additive effect to reach -37.60 ± 2.50 mV ($p < 0.05$). Interestingly, SPA effects were also additive to reach -32 ± 1.826 mV ($p < 0.001$) when coincubated with 20 mM glucose (Figure 3(c)).

3.3. Effect of SPA on Intracellular Calcium Content. After recording of cultured MIN6-B1 β-cells, we observed that, as in INS1E β-cells [25], SPA (10^{-7} M) induced an increase in intracellular calcium level (ratio 340/380 value: 1.15 ± 0.16), which did not return at the basal level after withdrawal (value: 0.46 ± 0.01 versus 0.69 ± 0.032, before and after SPA, resp.) (Figure 4(a)). Since SPA increased the glucose-induced insulin release like incretins, we compared the effect of ex4 with that of SPA. Ex4 induced an increase of intracellular calcium level (value: 1.29 ± 0.1, $p < 0.001$) as well as SPA (1.30 ± 0.14, $p < 0.001$) when compared with the basal level (value: 0.61 ± 0.02). As controls, we measured the effect of KCl (25 mM) and glucose (20 mM) on intracellular calcium levels and obtained ratio values of 2.05 ± 0.11 ($p < 0.001$) and 2.0 ± 0.11 ($p < 0.001$), respectively (Figure 4(b)). To verify the involvement of intracellular cAMP on the SPA effect, we used various concentrations of the stable analogue 8-Br-cAMP. At low dose (5 μM) the cAMP analogue increased calcium levels from a ratio of 0.8 ± 0.03 to 1.25 ± 0.06 ($p < 0.001$) (Figure 4(c)). However, addition of SPA (10^{-7} M) enhanced the signal values up to 1.87 ± 0.07 ($p < 0.001$ versus 5 μM 8Br-cAMP alone) (Figure 4(c)). A higher dose of 8-Br-cAMP (50 μM) induced an increase of cytosolic calcium (from 0.75 ± 0.02 to 1.44 ± 0.14, $p < 0.001$) that was not significantly modified by addition of SPA (ratio of 1.39 ± 0.1) (Figure 4(d)).

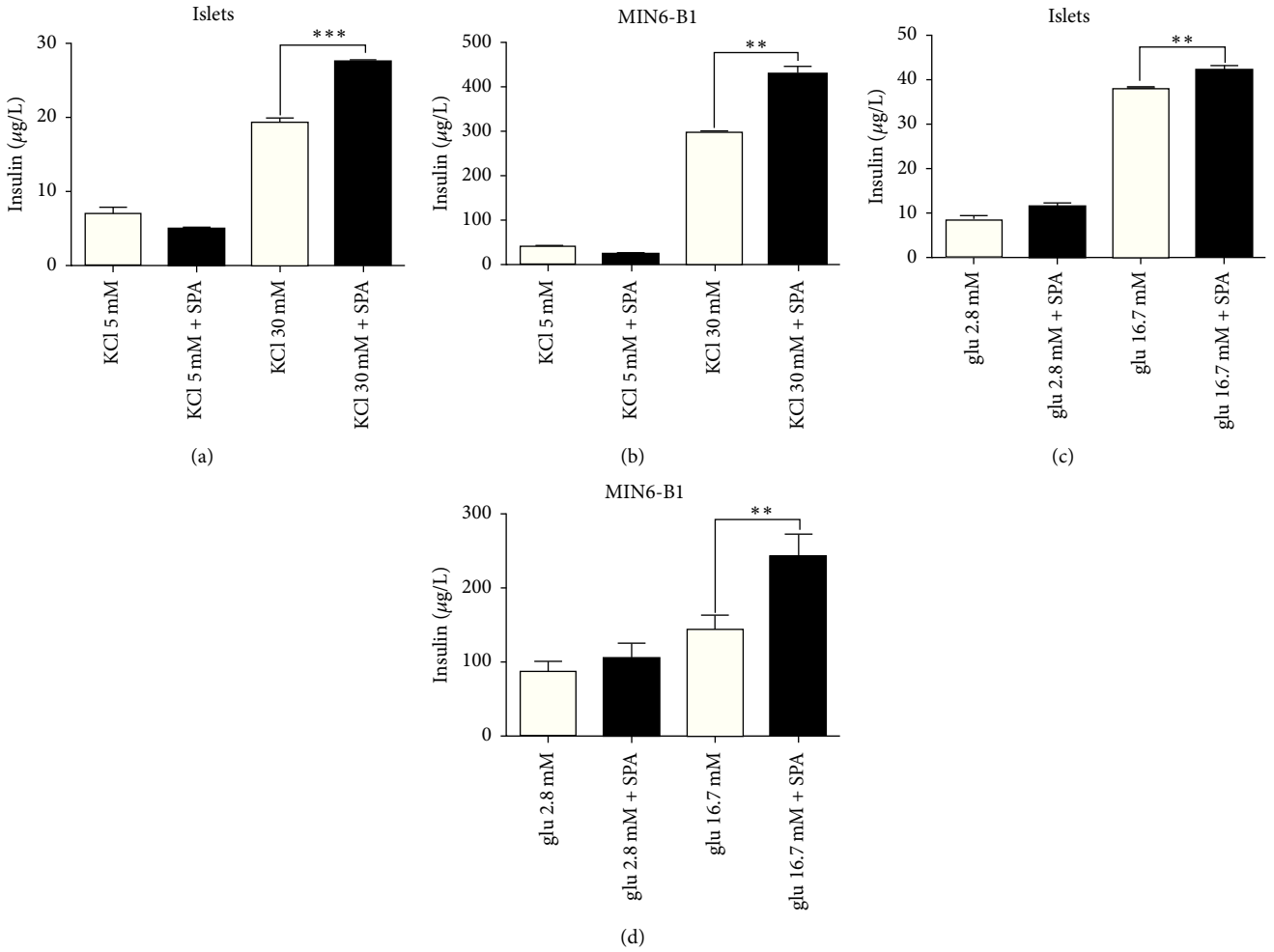

Figure 2: Effects of SPA on insulin secretion from isolated islets and MIN6-B1 cells. Mouse islets (a) or MIN6-B1 cells (b) were incubated at 5 mM (Cont) or stimulating concentration of 30 mM KCl in the presence or in the absence of 10^{-7} M SPA for 45 min. Mouse islets (c) and MIN6-B1 cells (d) were incubated under basal (2.8 mM glucose) or under stimulating (16.7 mM glucose) conditions in the presence or in the absence of 10^{-7} M of SPA for 45 min. The amount of secreted insulin was normalized using the intracellular insulin concentration and was expressed in μg/L. Each value represents the mean ± SEM from 3 independent experiments ($^{**}p < 0.01$ and $^{***}p < 0.001$).

Interestingly, the PKA inhibitor H89 inhibited the ex4 effect but not the SPA effect on calcium levels (Figure 4(e)). This indicates that the action of SPA on intracellular calcium levels is not dependent on PKA activity.

3.4. SPA Improves Plasma Insulin Level and Leads to Hypoglycemia in Mice. To investigate the role of SPA on glycemia in mice, we challenged the action of i.v. injection of SPA (100 μL of 1 μM, 8 μg/kg) during the glucose tolerance test. We followed the glucose serum concentration up to 120 min after i.p. injection of a high glucose solution (2 g/kg). In control conditions (injection of 100 μL saline), we observed a typical response with a blood glucose concentration that increased from the injection time up to 20–30 min after injection followed by the return to the basal level after 120 min (Figure 5(a)). In mice injected with SPA 20 min before the test, the increase in blood glucose concentration was smaller to reach a maximal concentration of 332.6 ± 31.26 mg/dL (n = 7) compared to 404.1 ± 16.32 mg/dL (n = 9) in the control condition ($p < 0.05$) (Figure 5(a)) at 30 min. At 60 min, the glycemia remained statistically lower in SPA-injected mice (314.8 ± 26.04 mg/dL, n = 9 versus 229.3 ± 20.55 mg/dL, n = 7, $p < 0.05$) (Figure 5(a)). These differences were illustrated by the smaller area under the curve (AUC) decreased by 28.46% in the presence of SPA (20205 ± 1449 arbitrary unit (AU), n = 9 for control versus 14455 ± 2015 AU, n = 7 for SPA) ($p < 0.05$) (Figure 5(b)). In order to investigate the correlation between the SPA-induced effect on glycemia and the amount of insulin released in the blood, we measured both glucose and insulin from blood samples collected before and 20 min after glucose injection. We confirmed that SPA significantly decreased glycemia 20 min after glucose injection (503 ± 12.9 mg/dL (n = 13) for saline versus 450.4 ± 10.15 mg/dL (n = 13) for SPA) ($p < 0.005$) (Figure 5(c)). In parallel,

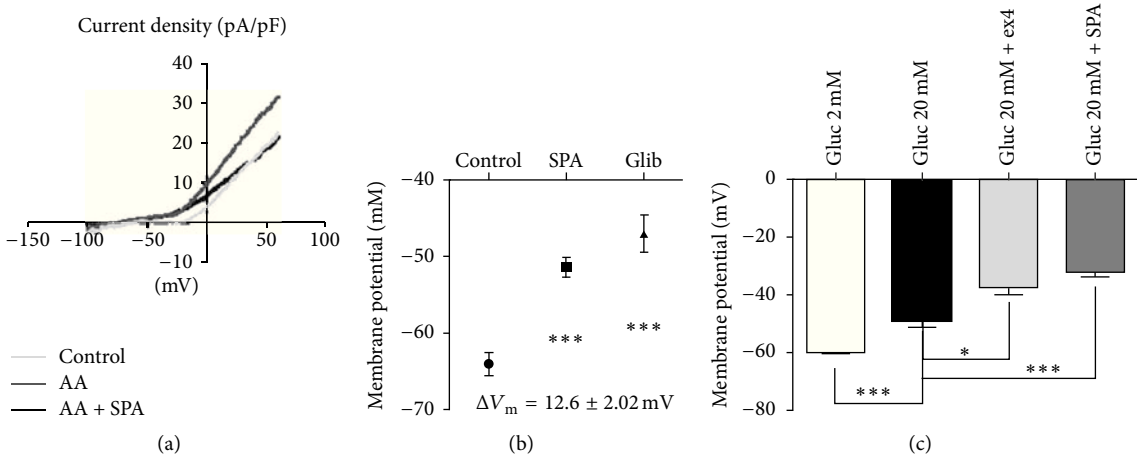

Figure 3: TREK-1 channel current recorded from pancreatic MIN6-B1 cells. (a, b) Whole cell currents measured in MIN6-B1 cells. (a) *IV* curves and membrane potentials recorded after 1 h of incubation in control conditions (grey line), after stimulation of TREK-1 current by 10 μM of arachidonic acid (AA) (dark grey line) and in the presence of 1 μM SPA (dark line). (b) Membrane potential mean values obtained from these conditions; the difference between potential values was $\Delta V_m = 12.6 \pm 2.02$ mV ($n = 15$) between control and SPA ($^{***}p < 0.001$) and $\Delta V_m = 17 \pm 2.02$ mV ($n = 15$) between control and glibenclamide ($^{***}p < 0.001$). (c) Membrane potential mean values obtained from three different groups of cells incubated at low (2 mM) and high (20 mM) glucose concentrations in the absence or in the presence of 1 μM ex4 or 1 μM SPA. $^{*}p < 0.05$ and $^{***}p < 0.001$.

SPA significantly increased glucose-induced serum insulin content (from 0.31 ± 0.03 μg/L ($n = 13$) to 0.59 ± 0.13 μg/L ($n = 12$) ($p = 0.029$) (Figure 5(d)).

4. Discussion

The present work describes the effect of SPA in the regulation of both glucose homeostasis and glucose-induced insulin secretion. Although SPA displays an effect similar to those of incretins, its mechanism of action is quite different since it is not controlled by the intracellular levels of cAMP.

Developing safer drugs and drug candidates for the treatment of diabetes is one of the major goals of the pharmaceutical industry, and its importance has been intensified by the withdrawal of many drugs from the market due to side effects and a decrease of new chemical entities introduced into the market [34]. We initially developed SPA as a TREK-1 channel blocker that could be used for the treatment against mood disorders. In that perspective, we have established that SPA, designed from an endogenous peptide, is a safer choice for a new pharmacological concept due to its absence of toxicity and long lasting central side effects [35, 36]. Since TREK-1 is expressed in β-cells, we investigated the role of SPA in the glucose homeostasis to verify that this compound does not display any deleterious peripheral action [35]. In the present work, we showed that SPA could have further interesting functions in the regulation of glucose homeostasis.

Endocrine pancreatic islets can be compared in some instance to neurons. Indeed, like neurons, β-cells secrete insulin after depolarization of plasma membrane upon stimulation. The secretion process is controlled by ATP-dependent potassium channels that are already a target in the development of type 2 antidiabetic drugs. The background two-pore potassium channel TREK-1 could also be an actor in the regulation of membrane potential. In neurons, TREK-1 channels are important regulators in the signaling of serotonin (5-HT) or gamma amino butyric acid (GABA), two neurotransmitters involved in brain pathophysiology [37]. Therefore, SPA, as a TREK-1 blocker, is able to improve brain functions [29]. In the present work, we demonstrated that TREK-1 channels are expressed in endocrine pancreas (Figure 1) and that SPA enhances stimulated insulin secretion both in islets and in MIN6-B1 cells (Figure 2). Deciphering the effect of SPA on β-cells by using the MIN6-B1 cell line, we observed that the peptide is able to induce the depolarization of the plasma membrane with the same potency than glibenclamide (a K_{ATP} channel blocker) and ex4 (a GLP1 receptor agonist) (Figure 3). This plasma membrane depolarization likely facilitates the exocytosis process through the enhancement of intracellular calcium concentration (Figure 4). SPA does not induce insulin secretion at low glucose concentration, because it does not reach the threshold of depolarization necessary to induce exocytosis. β-cell does not induce an action potential even though more than 90% of the K_{ATP} channels are closed [6]. We hypothesize that TREK-1 depolarization is not enough to induce a robust calcium entry. As insulin secretion is a calcium dependent process, exocytosis needs a stronger increase in calcium concentrations to trigger fusion of insulin granules membrane with the plasma membrane. Since SPA increases the glucose-induced insulin secretion, we hypothesized that this peptide could function like an incretin hormone. However, as expected, H89 inhibits the effects of ex4 on calcium influx but not those of SPA, indicating that its action is not mediated by PKA and likely results only from the blocking of K^+ currents. We propose that TREK-1 currents can be blocked by SPA or by PKA dependent phosphorylation. In this way, we can hypothesize a direct blocking effect of SPA on TREK-1

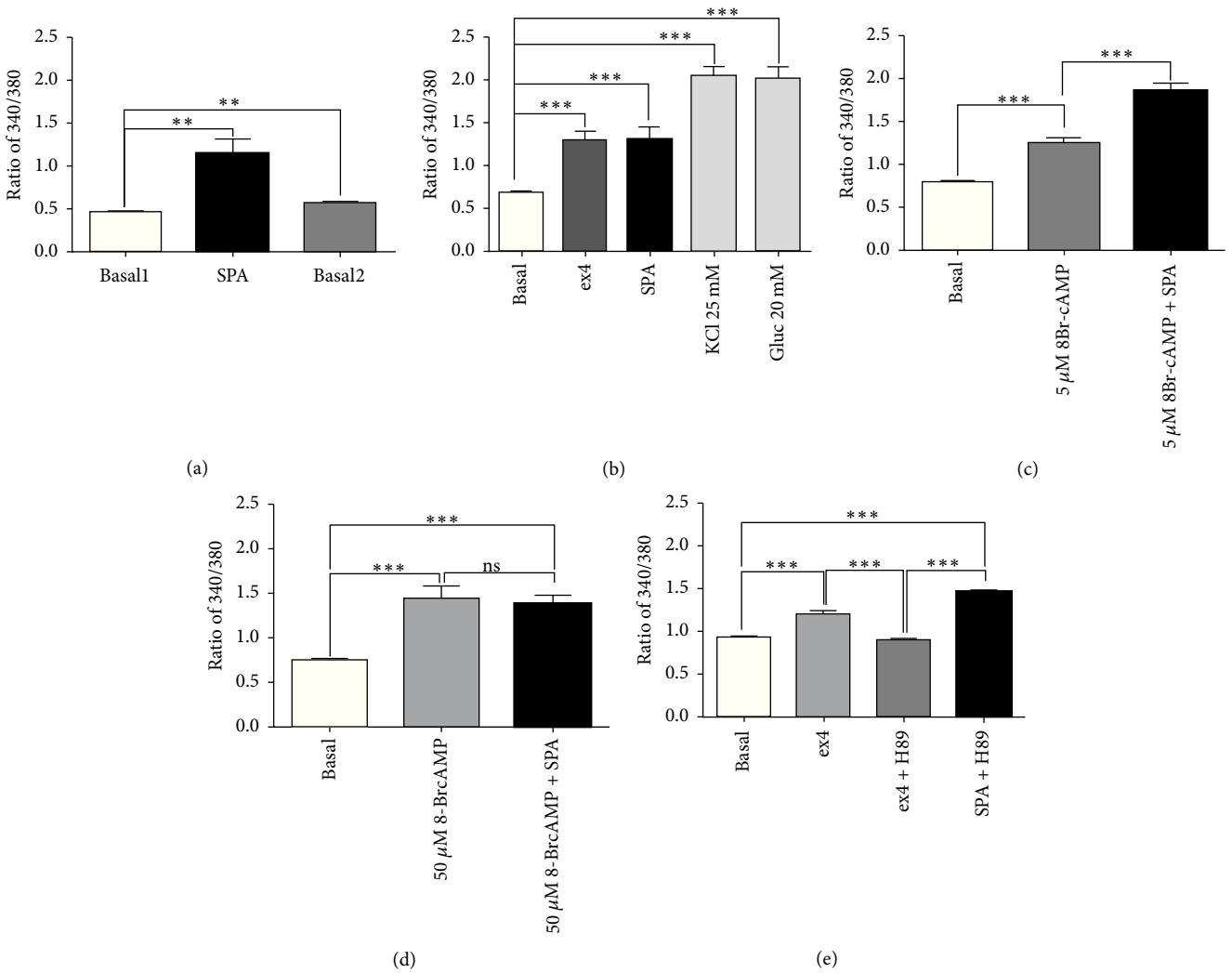

Figure 4: Effects of SPA on cytosolic calcium concentrations. Cytosolic calcium variations were measured using the Fura-2AM in the mouse MIN6-B1 β-cell line. Fura2-AM absorbance ratio (340/380) was given for the time point with the maximal signal. (a) At low glucose concentration (5 mM), SPA (10^{-7} M) induced a significant cytosolic calcium rise ($n = 18$, $p < 0.01$) that did not return to basal level after washing out ($p < 0.01$). (b) Comparing SPA and ex4 effects, controls were performed using either KCl (25 mM) or glucose (20 mM) ($n = 17$). (c) Preincubation of MIN6-B1 cells with 5 mM 8Br-cAMP did not prevent the stimulating effect of SPA on calcium rise ($n = 48$). (d) When MIN6-B1 cells were preincubated with 50 mM 8Br-cAMP, SPA was not able to increase intracellular calcium ($n = 12$). (e) Preincubation of MIN6-B1 cells in the presence of 1 μM H89 significantly inhibited the ex4 effect but not that of SPA ($n = 38$). n indicates the number of responding cells in each of three experiments. Results are expressed as mean ± SEM; $^{**}p < 0.01$, $^{***}p < 0.001$, and ns: nonsignificant.

activity whereas GLP1 agonists blocking action on these channels are the consequence of their effects on PKA activation.

Finally, in vivo, we clearly observe an action of SPA on glycemia since the glucose level is always lower in mice treated with the peptide during IPGTT experiments. During the glucose tolerance tests, SPA significantly increases plasma insulin concentration indicating that the lower level of glycemia is likely the consequence of insulin amount.

In conclusion, this work constitutes the first report on the involvement of TREK-1 channels in the function of β-cells particularly the secretion of insulin. Interestingly, the activity of these channels can be modulated by SPA leading to an incretin like action independent from the activation of PKA. Therefore, this peptide could be the basis for the development of new therapeutic strategies for the treatment of diabetes.

Competing Interests

The authors declare that they have no competing interests.

Authors' Contributions

Céline Hivelin and Sophie Béraud-Dufour contributed equally to this work.

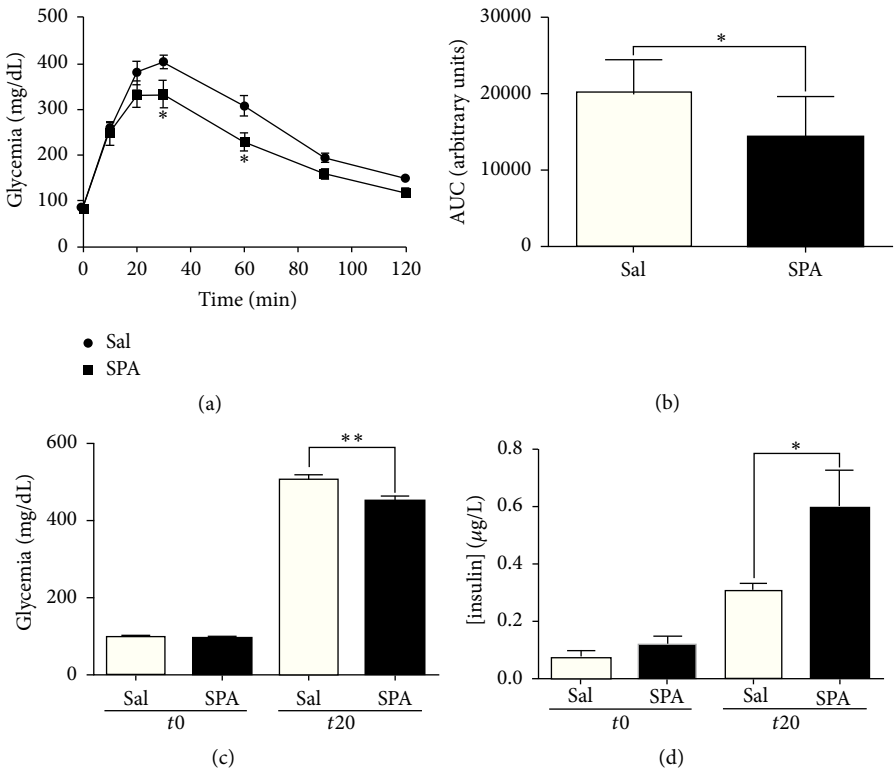

Figure 5: SPA modulates insulin secretion in mice. (a) IPGTT challenge (2 g/kg glucose i.p.) is performed onto two groups of C57Bl6 mice. 20 minutes before glucose injection, mice were injected (i.v.) with SPA (8 μg/kg) (square dots) or saline (round dots). Glycemia was measured at time 0 (before injection) and 10, 20, 30, 60, 90, and 120 minutes after glucose injection, from blood samples collected from the caudal vein tail ($n = 9$ for saline and $n = 7$ for SPA). (b) The areas under curve (AUC) were calculated using GraphPad Prism from the mean of individual AUC obtained for each mouse. (c) Glycemia was measured from blood samples collected before i.v. injection of SPA ($n = 12$) or saline ($n = 13$) ($t0$) and 20 minutes after i.p. glucose injection ($t20$). (d) Plasma insulin concentration was measured from the same blood samples as above ($^{**}p < 0.01$, $^{*}p < 0.05$).

Acknowledgments

This work was supported by the Centre National de la Recherche Scientifique, a grant from the Société Francophone du Diabète (SFD 2011) to Thierry Coppola and a grant from the Agence Nationale de la Recherche (ANR-13-SAMA-0002) to Jean Mazella. Amar Abderrahmani is supported by "European Genomic Institute for Diabetes" (EGID, ANR-10-LABX-46), European Commission, the Regional Council Nord Pas de Calais and the European Regional Development Fund. Alaeddine Djillani is supported by ICST LabEx.

References

[1] G. J. Félix-Martínez and J. R. Godínez-Fernández, "Mathematical models of electrical activity of the pancreatic β-cell: a physiological review," *Islets*, vol. 6, no. 3, Article ID e949195, 2014.

[2] C. G. Nichols and M. S. Remedi, "The diabetic β-cell: hyperstimulated vs. hyperexcited," *Diabetes, Obesity and Metabolism*, vol. 14, no. 3, pp. 129–135, 2012.

[3] M. Prentki, K. Tornheim, and B. E. Corkey, "Signal transduction mechanisms in nutrient-induced insulin secretion," *Diabetologia*, vol. 40, no. 2, pp. S32–S41, 1997.

[4] J. S. McTaggart, R. H. Clark, and F. M. Ashcroft, "The role of the KATP channel in glucose homeostasis in health and disease: more than meets the islet," *Journal of Physiology*, vol. 588, no. 17, pp. 3201–3209, 2010.

[5] J. C. Koster, M. A. Permutt, and C. G. Nichols, "Diabetes and insulin secretion: the ATP-sensitive K+ channel (KATP) connection," *Diabetes*, vol. 54, no. 11, pp. 3065–3072, 2005.

[6] S.-N. Yang, Y. Shi, G. Yang, Y. Li, J. Yu, and P.-O. Berggren, "Ionic mechanisms in pancreatic β cell signaling," *Cellular and Molecular Life Sciences*, vol. 71, no. 21, pp. 4149–4177, 2014.

[7] C. F. Deacon and H. E. Lebovitz, "Comparative review of dipeptidyl peptidase-4 inhibitors and sulphonylureas," *Diabetes, Obesity and Metabolism*, vol. 18, no. 4, pp. 333–347, 2016.

[8] G. Cantini, E. Mannucci, and M. Luconi, "Perspectives in GLP-1 research: new targets, new receptors," *Trends in Endocrinology & Metabolism*, vol. 27, no. 6, pp. 427–438, 2016.

[9] S. Seino, "Cell signalling in insulin secretion: the molecular targets of ATP, cAMP and sulfonylurea," *Diabetologia*, vol. 55, no. 8, pp. 2096–2108, 2012.

[10] G. G. Holz IV, C. A. Leech, and J. F. Habener, "Activation of a cAMP-regulated Ca^{2+}-signaling pathway in pancreatic β-cells by the insulinotropic hormone glucagon-like peptide-1," *Journal of Biological Chemistry*, vol. 270, no. 30, pp. 17749–17757, 1995.

[11] D. Kang, C. Choe, and D. Kim, "Functional expression of TREK-2 in insulin-secreting MIN6 cells," *Biochemical and Biophysical Research Communications*, vol. 323, no. 1, pp. 323–331, 2004.

[12] P. K. Dadi, N. C. Vierra, and D. A. Jacobson, "Pancreatic β-cell-specific ablation of TASK-1 channels augments glucose-stimulated calcium entry and insulin secretion, improving glucose tolerance," *Endocrinology*, vol. 155, no. 10, pp. 3757–3768, 2014.

[13] N. C. Vierra, P. K. Dadi, I. Jeong, M. Dickerson, D. R. Powell, and D. A. Jacobson, "Type 2 diabetes-associated K^+ channel TALK-1 modulates β-cell electrical excitability, second-phase insulin secretion, and glucose homeostasis," *Diabetes*, vol. 64, no. 11, pp. 3818–3828, 2015.

[14] D. Kang, C. Choe, and D. Kim, "Thermosensitivity of the two-pore domain K+ channels TREK-2 and TRAAK," *Journal of Physiology*, vol. 564, no. 1, pp. 103–116, 2005.

[15] A. J. Patel, E. Honoré, F. Maingret et al., "A mammalian two pore domain mechano-gated S-like K^+ channel," *EMBO Journal*, vol. 17, no. 15, pp. 4283–4290, 1998.

[16] A. J. Patel, E. Honoré, F. Lesage, M. Fink, G. Romey, and M. Lazdunski, "Inhalational anesthetics activate two-pore-domain background K+ channels," *Nature Neuroscience*, vol. 2, no. 5, pp. 422–426, 1999.

[17] F. Maingret, A. J. Patel, F. Lesage, M. Lazdunski, and E. Honoré, "Mechano- or acid stimulation, two interactive modes of activation of the TREK-1 potassium channel," *Journal of Biological Chemistry*, vol. 274, no. 38, pp. 26691–26696, 1999.

[18] J. Murbartián, Q. Lei, J. J. Sando, and D. A. Bayliss, "Sequential phosphorylation mediates receptor- and kinase-induced inhibition of TREK-1 background potassium channels," *Journal of Biological Chemistry*, vol. 280, no. 34, pp. 30175–30184, 2005.

[19] J. Chemin, C. Girard, F. Duprat, F. Lesage, G. Romey, and M. Lazdunski, "Mechanisms underlying excitatory effects of group I metabotropic glutamate receptors via inhibition of 2P domain K+ channels," *EMBO Journal*, vol. 22, no. 20, pp. 5403–5411, 2003.

[20] C. Terrenoire, I. Lauritzen, F. Lesage, G. Romey, and M. Lazdunski, "A TREK-1-like potassium channel in atrial cells inhibited by β-adrenergic stimulation and activated by volatile anesthetics," *Circulation Research*, vol. 89, no. 4, pp. 336–342, 2001.

[21] T. Shibasaki, T. Takahashi, H. Takahashi, and S. Seino, "Cooperation between cAMP signalling and sulfonylurea in insulin secretion," *Diabetes, Obesity and Metabolism*, vol. 16, supplement 1, pp. 118–125, 2014.

[22] H. Yang and L. Yang, "Targeting cAMP/PKA pathway for glycemic control and type 2 diabetes therapy," *Journal of Molecular Endocrinology*, vol. 57, no. 2, pp. R93–R108, 2016.

[23] J. Mazella, O. Pétrault, G. Lucas et al., "Spadin, a sortilin-derived peptide, targeting rodent TREK-1 channels: a new concept in the antidepressant drug design," *PLOS Biology*, vol. 8, no. 4, Article ID e1000355, 2010.

[24] O. P. Hamill, A. Marty, E. Neher, B. Sakmann, and F. J. Sigworth, "Improved patch-clamp techniques for high-resolution current recording from cells and cell-free membrane patches," *Pflügers Archiv European Journal of Physiology*, vol. 391, no. 2, pp. 85–100, 1981.

[25] S. Béraud-Dufour, A. Abderrahmani, J. Noel et al., "Neurotensin is a regulator of insulin secretion in pancreatic beta-cells," *International Journal of Biochemistry and Cell Biology*, vol. 42, no. 10, pp. 1681–1688, 2010.

[26] R. Sutton, M. Peters, P. McShane, D. W. R. Gray, and P. J. Morris, "Isolation of rat pancreatic islets by ductal injection of collagenase," *Transplantation*, vol. 42, no. 6, pp. 689–691, 1986.

[27] T. Coppola, C. Frantz, V. Perret-Menoud, S. Gattesco, H. Hirling, and R. Regazzi, "Pancreatic β-cell protein granuphilin binds Rab3 and Munc-18 and controls exocytosis," *Molecular Biology of the Cell*, vol. 13, no. 6, pp. 1906–1915, 2002.

[28] S. Béraud-Dufour, T. Coppola, F. Massa, and J. Mazella, "Neurotensin receptor-2 and -3 are crucial for the anti-apoptotic effect of neurotensin on pancreatic β-TC3 cells," *International Journal of Biochemistry and Cell Biology*, vol. 41, no. 12, pp. 2398–2402, 2009.

[29] C. Devader, A. Khayachi, J. Veyssière et al., "In vitro and in vivo regulation of synaptogenesis by the novel antidepressant spadin," *British Journal of Pharmacology*, vol. 172, no. 10, pp. 2604–2617, 2015.

[30] H. Zhang, N. Shepherd, and T. L. Creazzo, "Temperature-sensitive TREK currents contribute to setting the resting membrane potential in embryonic atrial myocytes," *The Journal of Physiology*, vol. 586, no. 15, pp. 3645–3656, 2008.

[31] S. Hughes, J. Magnay, M. Foreman, S. J. Publicover, J. P. Dobson, and A. J. El Haj, "Expression of the mechanosensitive 2PK+ channel TREK-1 in human osteoblasts," *Journal of Cellular Physiology*, vol. 206, no. 3, pp. 738–748, 2006.

[32] P. K. Dadi, N. C. Vierra, and D. A. Jacobson, "Pancreatic β-cell-specific ablation of TASK-1 channels augments glucose-stimulated calcium entry and insulin secretion, improving glucose tolerance," *Endocrinology*, vol. 155, no. 10, pp. 3757–3768, 2014.

[33] N. C. Vierra, P. K. Dadi, I. Jeong, M. Dickerson, D. R. Powell, and D. A. Jacobson, "Type 2 diabetes–associated K^+ channel TALK-1 modulates β-cell electrical excitability, second-phase insulin secretion, and glucose homeostasis," *Diabetes*, vol. 64, no. 11, pp. 3818–3828, 2015.

[34] P. J. Edwards and C. Sturino, "Managing the liabilities arising from structural alerts: a safe philosophy for medicinal chemists," *Current Medicinal Chemistry*, vol. 18, no. 20, pp. 3116–3135, 2011.

[35] H. Moha Ou Maati, J. Veyssiere, F. Labbal et al., "Spadin as a new antidepressant: absence of TREK-1-related side effects," *Neuropharmacology*, vol. 62, no. 1, pp. 278–288, 2012.

[36] J. Veyssiere, H. Moha Ou Maati, J. Mazella et al., "Retroinverso analogs of spadin display increased antidepressant effects," *Psychopharmacology*, vol. 232, no. 3, pp. 561–574, 2015.

[37] G. Sandoz, J. Levitz, R. H. Kramer, and E. Y. Isacoff, "Optical control of endogenous proteins with a photoswitchable conditional subunit reveals a role for TREK1 in $GABA_B$ signaling," *Neuron*, vol. 74, no. 6, pp. 1005–1014, 2012.

BJP British Journal of Pharmacology

DOI:10.1111/bph.13083
www.brjpharmacol.org

RESEARCH PAPER

In vitro and *in vivo* regulation of synaptogenesis by the novel antidepressant spadin

C Devader, A Khayachi, J Veyssière, H Moha ou Maati*, M Roulot, S Moreno, M Borsotto, S Martin, C Heurteaux and J Mazella

CNRS, Institut de Pharmacologie Moléculaire et Cellulaire, UMR 7275, Université de Nice-Sophia Antipolis, Valbonne, France

Correspondence
Jean Mazella, Institut de Pharmacologie Moléculaire et Cellulaire, UMR 7275, Université de Nice-Sophia Antipolis, 660 route des Lucioles, 06560 Valbonne, France. E-mail: mazella@ipmc.cnrs.fr

*Present address: Institut de Génomique Fonctionnelle, UMR 5203 CNRS/INSERM/UM1/UM2, 141 rue de la Cardonille, 34095 Montpellier Cedex 5, France.

Received
24 June 2014
Revised
10 December 2014
Accepted
8 January 2015

BACKGROUND AND PURPOSE

We have described a novel antidepressant peptide, spadin, that acts by blocking the TWIK-related-potassium channel, type 1 (TREK-1). Here, we examined possible mechanisms of action of spadin at both molecular and cellular levels.

EXPERIMENTAL APPROACHES

Effects of spadin were measured in primary cultures of neurons or tissues from mice injected i.v. with spadin. Western blots, qPCR, histochemical and electrophysiological techniques were used.

KEY RESULTS

In vitro, spadin increased neuronal membrane potential and activated both the MAPK and PI3K signalling pathways, in a time- and concentration-dependent manner. The latter pathway was involved in the protective effect of spadin against staurosporine-induced apoptosis. Also, spadin enhanced both mRNA expression and protein of two markers of synaptogenesis, the post-synaptic density protein of 95 kDalton (PSD-95) and synapsin. We confirmed these effects on synaptogenesis by the observation that spadin treatment significantly increased the proportion of mature spines in cortical neurons. Finally, *in vivo* injections of spadin led to a rapid increase in both mRNA expression and protein level of brain-derived neurotrophic factor (BDNF) in the hippocampus, confirming the antidepressant action of the peptide. We argue for a new role of spadin in synaptogenesis as both PSD-95 and synapsin mRNA expression and protein levels were further enhanced in the hippocampus, following treatment *in vivo* with the peptide.

CONCLUSIONS AND IMPLICATIONS

These findings provide new mechanisms of action for the rapidly acting antidepressant peptide spadin by stimulating expression of BDNF and synaptic proteins, both *in vitro* and *in vivo*.

Abbreviations

BDNF, brain-derived neurotrophic factor; LY294002, 2-morpholin-4-yl-8-phenylchromen-4-one; mTOR, mammalian target of rapamycin; NTSR3, neurotensin receptor-3; PD98059, 2′-amino-3′-methoxyflavone; PSD-95, post-synaptic density protein of 95 kDalton; TREK-1, TWIK-related-potassium channel, type 1

© 2015 The British Pharmacological Society

Tables of Links

TARGETS
Ion channel[a]
TREK-1,. K_{2P}2.1 channel
Enzymes[b]
Akt
Caspase-3
ERK1/2
mTOR
PI3K

LIGANDS
BDNF
Fluoxetine
Ketamine
LY294002
PD98059
Staurosporine

These Tables list key protein targets and ligands in this article which are hyperlinked to corresponding entries in http://www.guidetopharmacology.org, the common portal for data from the IUPHAR/BPS Guide to PHARMACOLOGY (Pawson *et al.*, 2014) and are permanently archived in the Concise Guide to PHARMACOLOGY 2013/14 ([a,b]Alexander *et al.*, 2013a,b).

Introduction

The origins and causes of depression are diverse, and therefore do not facilitate the diagnosis of the pathology. Molecules developed to treat depression include the tricyclic antidepressants, inhibitors of MAO-A or 5-HT selective reuptake inhibitors (see Berton and Nestler, 2006). Nevertheless, many other atypical antidepressant drugs were also developed such as mianserine, tradozone (Boschmans *et al.*, 1987; Fagiolini *et al.*, 2012), mirtazapine (Dolder *et al.*, 2012), agomelatine (Srinivasan *et al.*, 2012), tianeptine (McEwen and Olie, 2005), scopolamine (Drevets *et al.*, 2013), ketamine or lanicemine (Zarate *et al.*, 2006; Sanacora *et al.*, 2014).

The antidepressant drugs do not provide a fully satisfactory treatment, for several important reasons: (i) one-third of patients are resistant to the drugs (Pacher and Kecskemeti, 2004); (ii) there is a delayed onset of antidepressant drug action (Fava and Kendler, 2000; Nestler *et al.*, 2002); and (iii) antidepressant drug treatments have numerous deleterious side effects (Sicouri and Antzelevitch, 2008; Thase and Denko, 2008).

Taking into account the mental health of millions of people worldwide and the associated economic burden, it is now crucial to develop alternative strategies aimed at developing novel antidepressants that could potentially show higher rates of efficacy and lower rates of side effects. We previously reported that an endogenous peptide of 44 amino acids (PE) released from the maturation of the neurotensin receptor-3 (NTSR3) (Mazella *et al.*, 1998; Munck Petersen *et al.*, 1999), also called sortilin (Petersen *et al.*, 1997), displays potent antidepressant effects in several tests performed in mice (Mazella *et al.*, 2010). We isolated an active sequence of 17 amino acids from this peptide, named spadin, which exerts its antidepressant properties through the blockade of the TWIK-related-potassium channel, type 1 (TREK-1) (K_{2P}2.1; Mazella *et al.*, 2010). TREK-1 channels are activated by stretch, polyunsaturated fatty acids, warm temperatures, internal acidosis and volatile anaesthetics (Honore, 2007). They are inhibited by fluoxetine and blocked by phosphorylation processes. Deletion of the TREK-1 gene (*kcnk2*) leads to mice that display a depression-resistant phenotype, which mimics treatment with antidepressants (Heurteaux *et al.*, 2006b). Spadin binds to TREK-1 with an affinity of 10 nM, blocks its activity and induces its sequestration into cells. The interaction of spadin with TREK-1 does not show any striking side effects and does not interfere with any known TREK-1-controlled functions (Moha Ou Maati *et al.*, 2012). *In vivo*, spadin increases the firing rate of serotonergic neurons from the dorsal raphe nucleus and activates hippocampal neurogenesis (Mazella *et al.*, 2010). Moreover, NTSR3/sortilin directly interacts with TREK-1 to regulate its plasma membrane localization (Mazella *et al.*, 2010). Both proteins are colocalized in neurons within the dorsal raphe nucleus and have been previously shown to be expressed in several brain areas known to be involved in depression including the prefrontal cortex, amygdala, hippocampus, nucleus accumbens, dorsal raphe and hypothalamus (Hervieu *et al.*, 2001; Sarret *et al.*, 2003).

Spadin exhibits antidepressant properties, when injected in mice (Mazella *et al.*, 2010), and induced a rapid hippocampal neurogenesis after a 4 day treatment. However, its cellular mechanisms of action as well as the demonstration that new neurons are functional have not yet been characterized. Moreover, the rapid onset of action of spadin, which can be compared with the rapidly acting antidepressant ketamine (Li *et al.*, 2011; Dwyer and Duman, 2013), prompted us to evaluate the effect of spadin on the induction of synaptogenesis and spine maturation. The mechanisms of action of spadin were determined in primary cultures of neurons from embryonic and post-natal mice. We performed electrophysiological and biochemical experiments to study the membrane function and the intracellular signalling of the peptide followed by qPCR and Western blot analyses of proteins involved in synaptogenesis and whose expression is altered in mood disorders such as post-synaptic density protein of 95 kDalton (PSD-95), synapsin and brain-derived neurotrophic factor (BDNF). Neuronal spine maturation has been visualized using confocal imaging of GFP-transfected neurons. We confirmed the effects we observed *in vitro*, on synaptic proteins by *in vivo* injection of spadin followed by protein analysis in samples of hippocampus and prefrontal cortex.

Methods

Animals

All animal care and experimental procedures complied with the policies on the care and use of laboratory animals of European Community legislation 2010/63/EU and were approved by the local Ethics Committee (CIEPAL) (protocol number 00893.02). All studies involving animals are reported in accordance with the ARRIVE guidelines for reporting experiments involving animals (Kilkenny *et al.*, 2010; McGrath *et al.*, 2010). A total of 100 animals were used in the experiments described here. We used C57Bl/6J male mice (20–25 g) from Janvier Labs (St Berthevin, France).

Primary neuronal cultures

Mice were anaesthetized by inhalation of 2% isoflurane mixed with 30% oxygen and 70% nitrous oxide and then killed. Embryos (E14) were removed and brain cortices dissected in PBS containing 1% glucose. Neurons were also prepared from cerebral cortices of 3-day-old mice, as described by Brewer and Torricelli (2007). Dissociated neurons were plated on poly-L-lysine-treated dishes and cultured up to 18 days in neurobasal medium containing 2% B27 and 50 $\mu g \cdot mL^{-1}$ gentamycin at 37°C under 5% CO2.

Spadin iodination

Spadin (2 nmol) was iodinated with [^{125}I]NaI (0.5 nmol) using lactoperoxidase as oxidant. Monoiodinated spadin (on Tyr-0) was purified by HPLC using a Waters apparatus equipped with a RP18 Lichrosorb column (Macherey-Nagel, Düren, Germany). Elution was carried out at a flow rate of 1 $mL \cdot min^{-1}$ with a linear gradient of increasing concentration from 30 to 60% of acetonitrile in water containing 0.1% TFA in 36 min. The iodinated peptide was eluted at 24 min.

Binding assays

Cultures of cortical neurons were incubated with 0.4 nM [^{125}I]-spadin (400 000 cpm in 250 µL). Incubations were performed in Earle's-Tris-HEPES buffer pH 7.4, containing 140 mM NaCl, 5 mM KCl, 1.8 mM $CaCl_2$, 3.6 mM $MgCl_2$ and 0.1% BSA in the presence of increasing concentrations of non-radioactive spadin (from 10^{-10} to 10^{-5}M). Incubations were terminated by washing cells twice with 2 mL of Earle's-Tris-HEPES buffer. The radioactivity bound to neurons was recovered with 1 M NaOH (1 mL) and counted with a gamma-counter.

Electrophysiological experiments

Whole cell current recordings were performed on primary cortical mouse neurons seeded at a density of 1 200 000 cells per 35 mm dish 10 days before testing. Membrane potentials were measured on cortical neurons after 1 h of incubation in control conditions (water for the vehicle), in the presence of 1 µM of spadin. Cells were then patched and membrane potentials immediately measured using the whole-cell, patch-clamp configuration. All membrane potentials values are expressed in mV as mean ± SEM. IV curves were realized for each cell in control conditions and in the presence of 1 µM of spadin. Global current was recorded using the whole-cell configuration of the patch-clamp technique. Each current was calculated using an RK 400 patch-clamp amplifier (Axon Instrument, Sunnyvale, CA, USA), low-pass filtered at 3 kHz and digitized at 10 kHz using a 12-bit analogue-to-digital converter digidata (1322 series, Axon Instrument). The bath solution contained (in mM) 150 NaCl, 5 KCl, 3 $MgCl_2$, 1 $CaCl_2$ and 10 HEPES adjusted to pH 7.4 with NaOH. The pipette solution contained (in mM) 155 KCl, 3 $MgCl_2$, 5 EGTA and 10 HEPES adjusted to pH 7.2 with KOH. Stimulation protocols and data acquisition were carried out at room temperature using a microcomputer (Dell Pentium, Montpellier, France) and the pClamp 8.2 commercial software (Molecular Devices, Wokingham, UK). Cells were clamped at –80 mV and voltage changes applied by step of 20 mV (from –100 to +60 mV). Duration of depolarization pulses was 0.825 ms and the pulse cycling rate was 5 s. Current amplitudes were calculated at the end of stimulation pulses. Current amplitudes were expressed in current densities.

Western blotting

Mouse cortical neurons treated with the indicated effectors for various times were homogenized in Laemmli buffer and analysed using 10% SDS PAGE gels. Separated proteins were then transferred from gels onto nitrocellulose membranes (VWR, Fontenay-sous-Bois, France) and blocked either with 5% skim milk or 5% BSA as indicated in PBS for 30 min at room temperature. Membranes were incubated with antibodies directed against PSD-95, synapsin or BDNF overnight at 4°C. Tubulin contents were determined after stripping using a 1/1000 dilution anti-tubulin antibodies (Sigma-Aldrich, Saint-Quentin Fallavier, France). After four washes in 0.1% Tween/PBS, secondary anti-mouse or anti-rabbit HRP-conjugated antibodies (Amersham Biosciences, Orsay, France; 1/10000) were incubated for 1 h at room temperature. Proteins were detected with the ECL plus detection reagents (Amersham Biosciences) using an LAS-3000 imaging system (Fujifilm, Düsseldorf, Germany). Relative intensities of the labelled bands were analysed by densitometric scanning using ImageJ software (Wayne Rasband, National Institute of Health, Bethesda, MD, USA). Protein activation was normalized using total tubulin as indicated.

Caspase-3 activity measurements

Neurons were plated in 12-well dishes for 10–14 days before experiments. Neurons were incubated for 2–4 h with 1 µM staurosporine (Sigma-Aldrich) in the absence or in the presence of 1 µM spadin. Caspase-3 activity was measured using Ac-DEVD-7-AMC (Sigma-Aldrich) as a substrate (Coppola *et al.*, 2008).

Primer design and real-time qPCR

Primers (Eurogentec, Angers, France), designed as previously described (Dingemans *et al.*, 2010), were specific for sequences of PSD-95, synapsin, BDNF and GAPDH and CycloD as reference genes (Table 1). Real-time qPCR was performed on the LightCycler™ 480 (Roche, Meylan, France) using the LightCycler™ 480 SYBR Green 1 Master mix (Roche). PCR reactions were performed in 20 µL volume containing 16 ng cDNA, 10 µL 2× LightCycler™ 480 SYBR Green 1 Master mix and 1 µL of primer mix (10 µM forward primer, 10 µM reverse primer).

Table 1
Primers used in qPCR experiments

	Forward	Reverse
PSD-95	5′-CGCTACCAAGATGAAGACACG-3′	5′-CAATCACAGGGGGAGAATTG-3′
Synapsin	5′-GGAAGGGATCACATTATTGAGG-3′	5′-TGCTTGTCTTCATCCTGGTG-3′
BDNF	5′-AGTCTCCAGGACAGCAAAGC_3′	5′-TGCAACCGAAGTATGAAATAACC_3′
Gapdh	5′-GAACATCATCCCTGCATCC-3′	5′-CCAGTGAGCTTCCCGTTCA-3′
CycloD	5′-AAGGATGGCAAGGATTGAAA-3′	5′-GCAATTCTGCCTGGATAGCTT-3′

The PCR profile was as follows: 5 min at 95°C, followed by 45 cycles of 10 s at 95°C, 10 s at 60°C and 10 s at 72°C.

The Ct value of each gene of interest was normalized to the Ct of the reference genes: $\Delta Ct = Ct_{goi} - Ct_{ref}$ with $Ct_{ref} = (Ct_{GAPDH} \times Ct_{CycloD})^{(1/2)}$ with $_{goi}$ = gene of interest, and $_{ref}$ = reference gene. $\Delta\Delta CT$ = ΔCT experimental condition – ΔCT control condition. Values were expressed as $2^{-\Delta\Delta Ct}$ normalized using saline solution-injected animals as control. For experiments performed from newborn cerebral cortex values are expressed as $2^{-\Delta Ct}$.

Analysis of spine morphology

Primary cortical neurons were treated every day for 18 days with spadin (2 µL; final concentrations 10 nM or 1 µM). Half of the medium was changed every 3 days. Neurons were then transduced with attenuated Sindbis virus (Martin *et al.*, 2008) expressing GFP for 22 h before use. For imaging experiments, neurons were fixed at 19 days *in vitro* in PBS containing 3.7% formaldehyde and 5% sucrose for 1 h at room temperature. Fixed neurons were then rinsed twice with PBS at room temperature and mounted in Mowiol (Sigma) before confocal examination.

Sequential confocal images (1024 × 1024 pixels) were acquired with a 63× oil-immersion lens with Numerical Aperture, 1.4 on an inverted TCS-SP5 confocal microscope (Leica Microsystems, Nanterre, France). Z-series of six to eight images of randomly selected GFP-expressing dendrites were compressed into two dimensions using the maximum projection algorithm of the Leica software. We analysed ~3500 spines per condition from secondary dendrites (~3 dendrites per neuron, 20 neurons per condition). At the time of acquisition, laser power was adjusted so that all spines were below the threshold of saturation. To analyse dendritic protrusions, projection images were imported into Neuronstudio software (Rodriguez *et al.*, 2008), which allows for the automated detection of dendrites, immature and mature spines. The length of individual spines was automatically measured and data were imported in GraphPad Prism software for statistical analysis.

In vivo *injection of spadin*

Prior to injection, 8- to 12-week-old male C57BL/6J were warmed for 5–10 min with an overhead heat lamp to dilate the veins. Then, they were placed in a constrained box and injected in the caudal vein with 100 µL of either 1 µM spadin or 0.9% NaCl solution. For mRNA expression and protein content of PSD-95 and synapsin, mice were injected once a day for 4 days, then groups of mice (six per group) were killed on days 7, 14 and 21, after the first day of injection. The brain was removed and the indicated cerebral regions were dissected and analysed by qPCR or Western blotting, as described earlier.

Data analysis

Results are presented as means ± SEM from four to six determinations. However, statistical significance was calculated from median values obtained using the non-parametric Kruskal–Wallis test. For spine morphogenesis experiments, values represent means ± SEM. All experiments were repeated at least three times. Statistical significance for group comparisons was analysed by ANOVA with a Newman–Keuls post-test. Normality for all groups was verified using the Shapiro-Wilk test. According to the Levene variance test, variances were homogenous for the percentage of mature spines and for the length of immature spines ($F = 0.25$; $P = 0.77$ and $F = 0.42$; $P = 0.65$ respectively). Cumulative plot data were analysed by the Kolmogorov–Smirnov test (K–S test). $P < 0.05$ was considered significant.

Materials

The peptide, spadin, with the following amino acid sequence: Y-APLPRWSGPIGVSWGLR (GenBank NM_019972 for mouse) was synthetized by Genecust (Dudelange, Luxemburg). Neurobasal medium and complementary medium B27 were from Invitrogen (Fisher Scientific, Illkirch, France). Gentamycin, 1–10-phenanthroline, Bovine Serum Albumin (BSA), fluoxetine, mammalian protease and phosphatase inhibitor cocktails were from Sigma France. Antibodies against the phosphorylated or total forms of ERK 1/2 and Akt were from Santa Cruz Laboratory, Inc. (Heidelberg, Germany). The antibodies against phospho-Akt, PSD-95, phospho-mammalian target of rapamycin (mTOR), BDNF and synapsin were from Cell Signaling (Ozyme, Montigny-le-Bretonneux, France).

Results

Spadin binding to neurons leads to neuronal depolarization

To characterize the cellular effects of the antidepressant spadin on mouse cortical neurons, we first performed direct binding experiments using a radiolabelled spadin peptide on living cells (Figure 1A). Competition experiments between [^{125}I]-spadin and unlabelled spadin indicated that spadin bound specifically to cortical neurons. The displacement curve

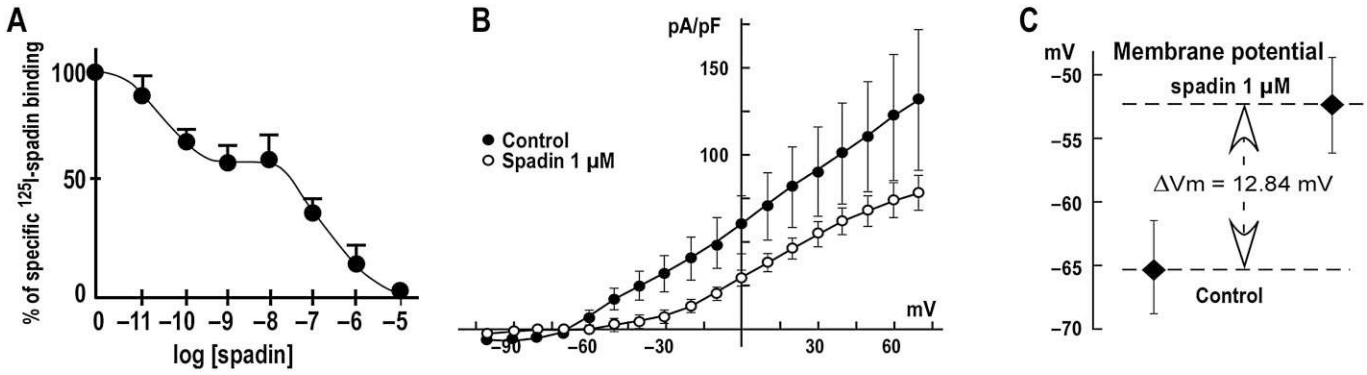

Figure 1

Spadin binding to neurons in culture triggers neuronal depolarization and drives endocytosis. (A) Competition between ^{125}I-spadin and unlabelled spadin for binding to mouse cortical neurons. Each point represents the mean ± SEM of duplicate determinations from three independent experiments. (B and C) I-V curves and membrane potentials on primary cortical embryonic mouse neurons recorded after 1 h incubation in control conditions (vehicle) and in the presence of spadin 1 µM. (B) I-V curves obtained in control conditions and in the presence of spadin 1 µM. (C) membrane potential mean values obtained in the two different conditions.

revealed the existence of two binding sites with corresponding IC_{50} values of 0.05 nM for the binding component representing 40% of the total binding, and of 100 nM for the 60% remaining binding (Figure 1A). Electrophysiological recordings on whole cells confirmed that the binding of spadin to neurons was functional. Indeed, I-V curves (Figure 1B) and membrane potentials (Figure 1C) recorded on cortical neurons 1 h after spadin (1 µM) incubation indicated that the peptide efficiently depolarized neurons, as expected from a blocking action on TREK-1 channels. Consequently, spadin induced an increase in the membrane potential with a ΔVm of 12.84 mV ± 2.28 (Figure 1C). We also confirmed that spadin dynamically regulates the membrane levels of both TREK-1 and sortilin in cortical neurons (Supporting Information Fig. S1).

To perform signalling and protein expression experiments *in vitro* and *in vivo*, we first needed to know the half-life time of the peptide when exposed to neuronal cultures, and second, its ability to cross the blood–brain barrier and to reach the brain following i.v. injection. The stability of spadin was measured on reverse-phase HPLC after incubation for various times with the cultured neuronal medium or mouse serum (Supporting Information Fig. S2). After 60 min of incubation on neurons, about half of the initial spadin remained intact whereas almost all the peptide was degraded after 60 min in mouse serum indicating that spadin is more stable at the vicinity of neurons than in serum. These results allowed us to determine how frequently spadin should be added to the primary neurons to maintain its activity.

To differentiate spadin recovered in the brain after i.v. injection, from other endogenous peptides present in the brain, we incorporated a fluorophore on the peptide (Atto 488 from Atto-Tec GmbH, Siegen, Germany) exhibiting a high e_{max} at 500 nm (9×10^4 $M^{-1} \cdot cm^{-1}$). This allowed us to determine, using HPLC, that about 1% of the labelled peptide was recovered in the brain in its intact form 30 min after i.v. injection (Supporting Information Fig. S2). This observation is in line with our initial finding that peripheral administration of spadin can induce central antidepressant effects (Mazella *et al.*, 2010).

Functional signalling of spadin in cortical neurons

We investigated the intracellular signalling pathways activated by spadin in cultured neurons from embryos. Spadin (100 nM) rapidly stimulated the phosphorylation of ERK1/2 and Akt, but not of mTOR (Figure 2A) whereas ketamine, used as a positive control, induced phosphorylation of mTOR (Figure 2A). The latter observation is in agreement with the mTOR-dependent antidepressant effects of ketamine (Li *et al.*, 2010). We confirmed that spadin was able to activate the same signalling pathways (i.e. ERK1/2 and Akt) in neurons prepared from new-born mice (Figure 2B). Standardization of signalling pathways using antibodies against non-phosphorylated proteins indicated a twofold stimulation from 15 to 60 min for phospho-ERK1/2 (Figure 2C), a two- to threefold stimulation up to 60 min for phospho-Akt (Figure 2D), and an absence of spadin effect on phospho-mTOR (Figure 2E). ERK phosphorylation was maximum for 100 nM spadin (Figure 2F). We confirmed that ERK1/2 activation in response to spadin was blocked in the presence of the MAPK inhibitor PD98059 (Figure 2F). Similarly to ERK phosphorylation, the concentration of spadin that maximally increased Akt phosphorylation was 100 nM (Figure 2G). As expected, when neurons were pretreated with the PI3K inhibitor LY294002, the phosphorylation of Akt in spadin-treated neurons was abolished (Figure 2G).

As the PI3K pathway is involved in cell survival, we investigated the effect of spadin on protection against staurosporine-induced caspase-3 activation in neuronal cultures. We found that a 4 h incubation of cortical neurons with 1 µM staurosporine significantly increased caspase-3 activity (Figure 2H) and spadin inhibited 70% of the staurosporine-induced caspase-3 activation (Figure 2I). This effect was dependent on PI3K, as LY294002, a specific inhibitor of this pathway, reversed the protective effect of spadin but the MAPK inhibitor PD98059 was not effective (Figure 2I). These results therefore demonstrated that spadin

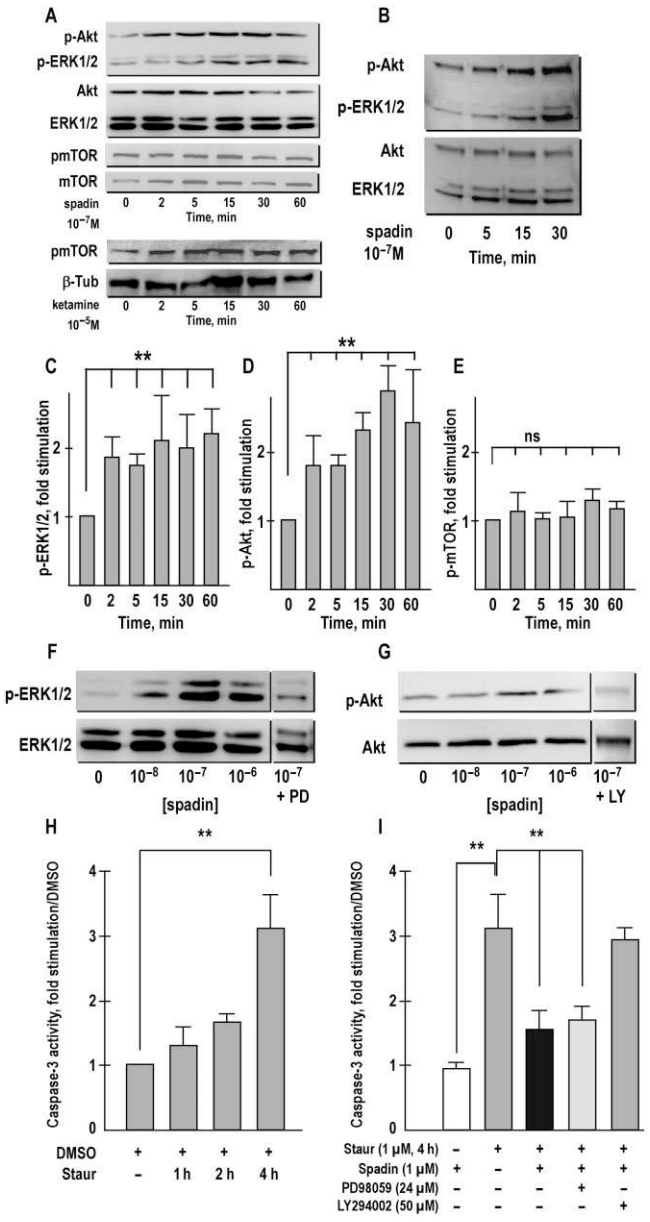

Figure 2

Effect of spadin on ERK1/2 and Akt phosphorylation in cortical neurons. (A) Neurons prepared from 14-day-old embryos were incubated with 10^{-7}M spadin or 10 μM ketamine (1 μL of a 1000× solution) for various times at 37°C. The phosphorylation of ERK, Akt and mTOR was determined by immunoblotting using antibodies directed against the phosphorylated active forms of both kinases. (B) Neurons prepared from 3-day-old mice were stimulated with 10^{-7}M spadin for indicated times at 37°C. The phosphorylation of Erk, Akt was determined by immunoblotting using antibodies directed against the phosphorylated active forms of both kinases. (C–E) Data were standardized from three to five different experiments using the labelling obtained on the same blot with antibodies directed against the total forms of ERK1/2, Akt and mTOR and expressed as means ± SEM. $^{**}P < 0.05$, significantly different as indicated. ns, non-significant. (F and G) Neurons were incubated with various concentrations of spadin for 15 min at 37°C. Phosphorylation of ERK1/2 (F) and Akt (G) was determined as described in A. PD98059 and LY294002 are specific inhibitors of ERK and Akt kinases respectively. (H) Effect of staurosporine on caspase-3 activity in cortical neurons. Neurons were incubated for the indicated times with 1 μM staurosporine. Samples were processed for capsase-3 activity as described. Data are means ± SEM from three independent experiments and are expressed in arbitrary units. $^{**}P < 0.05$, significantly different as indicated. (I) Effect of spadin on staurosporine-induced caspase-3 activity. Neurons were treated for 4 h with 1 μM staurosporine in the absence or in the presence of 1 μM spadin with or without 24 μM PD98059 or 50 μM LY294002. Caspase-3 activity was measured as earlier. Data are means ± SEM from three experiments. $^{**}P < 0.05$, significantly different as indicated.

was a potent protector of neurons against cytotoxicity, through the activation of the PKB/Akt signalling pathway.

Spadin increases content of synaptic marker proteins and promotes the maturation of dendritic spines

We previously determined that a subchronic treatment with spadin in mice resulted in a rapid (4 days) activation of neurogenesis in the dentate gyrus through the phosphorylation of the transcription factor CREB (Mazella *et al.*, 2010), a factor known to be involved in neurogenesis (Carlezon *et al.*, 2005; Krishnan and Nestler, 2008). As synaptic alterations have been observed in depression and could therefore be a potential target for therapeutic intervention (Duman and Aghajanian, 2012), we explored the role of spadin on synaptogenesis. We first measured the effect of spadin on mRNA expression levels and protein content of two protein markers of synaptogenesis, PSD-95 and synapsin. Spadin transiently increased the mRNA expression levels of both PSD-95 and synapsin with a maximum expression observed 8 h after exposure to spadin (Figure 3A and B). We also analysed the mRNA expression of BDNF whose levels are known to be down-regulated during depression and up-regulated by antidepressants (Airan *et al.*, 2007). We observed a weak and transient increase of its mRNA expression, 5 h after spadin incubation (Figure 3C). At the protein levels, PSD-95 immunoreactivity was significantly increased 5 h post-treatment while the increase in synapsin protein occurred 36 h post-spadin treatment (Figure 3D and E). Despite the slight increase in BDNF mRNA expression levels, we were not able to detect any significant increase in the corresponding protein level (Figure 3F).

Synaptic dysfunction is generally correlated with deleterious alterations of spine morphology, which play crucial roles in major depressive disorders (Shansky *et al.*, 2009; Lin and Koleske, 2010; Duman and Aghajanian, 2012). Some antidepressant drugs are able to restore the density of dendritic spines (Norrholm and Ouimet, 2001). The various shapes of spines (thin, filopodia and mushroom) are associated with different stages of dendritic maturation, consequent on functional neuronal circuits (McKinney, 2010). Therefore, we tested the effect of spadin on the frequency and the morphology of dendritic spines in cultured neurons. We treated neurons *in vitro* for 18 days instead of only 4 days during the last 4 days of neuronal differentiation, in order to ensure assessments of the effects of spadin, over the whole

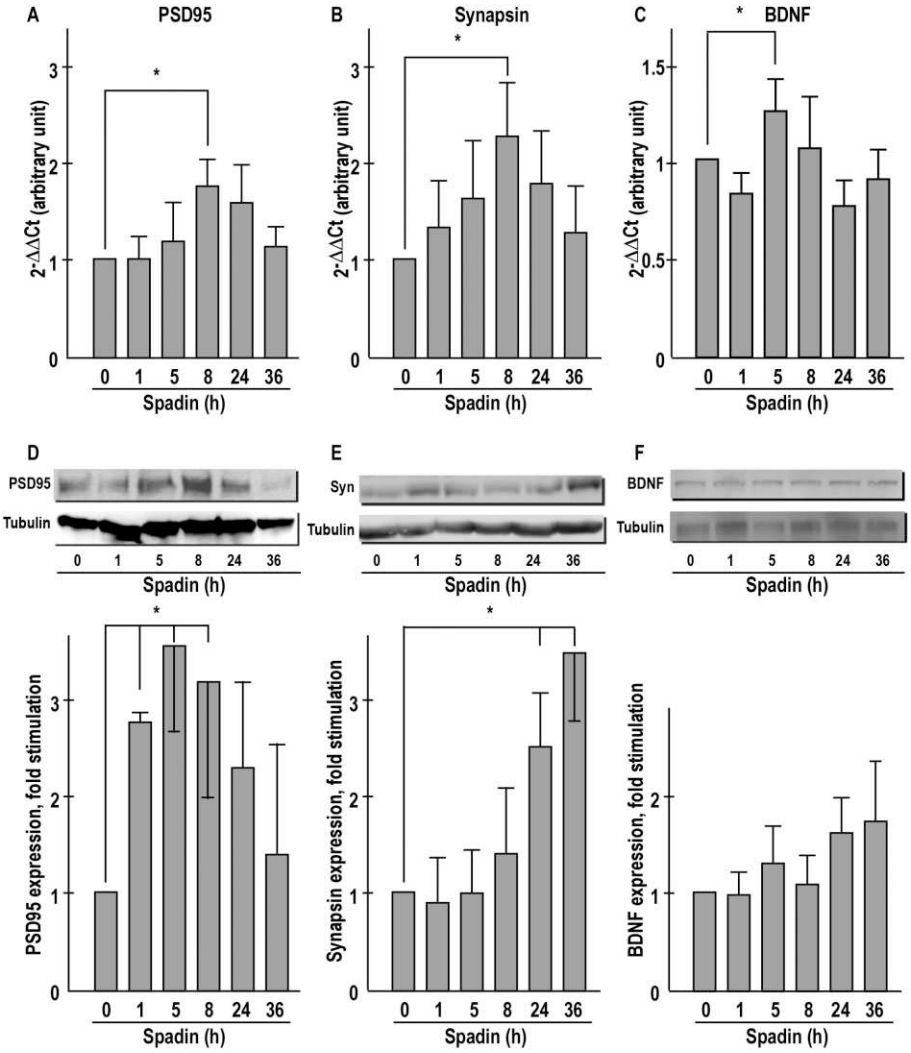

Figure 3

Spadin increases the expression of synaptic proteins in cortical neurons. (A–C) Neurons were incubated with 10^{-7}M spadin for the indicated times at 37°C. RNAs extracted from neurons were subjected to quantitative PCR. Bar graphs showing the mRNA expression of PSD-95 (A), synapsin (B) and BDNF (C) were normalized with the control condition (0). Histograms are mean ± SEM from three independent determinations, *$P < 0.05$, significantly different as indicated. (D–F) Neurons were incubated with 10^{-7}M spadin for indicated times at 37°C. The amount of PSD-95, synapsin and BDNF was determined by immunoblotting and using the labelling of the same blot with antibodies against β-tubulin. Immunoblots shown are representative of a typical experiment. The representation of the amount of each protein was expressed as fold increase compared with control conditions. Data are means ± SEM from three independent experiments. *$P < 0.05$, significantly different as indicated.

maturation period of neurons and not only the last 4 days, when neurons are already matured. Moreover, this longer treatment showed the lack of toxicity of the peptide when compared with identical treatment with either ketamine (10 μM) or fluoxetine (1 μM), which induced cell death after 1 week application (J. Mazella, unpubl. obs.). Figure 4A and B show dendrites from GFP-expressing neurons treated for 18 days with vehicle (PBS) or with 10 nM or 1 μM spadin. Spadin, at either concentration, did not affect the number of protrusions (Figure 4C), with the same protrusion frequencies of about 5 spines per 10 μm in all three conditions (control, 10nM or 1mM spadin). From these experiments, we measured the proportion of mature spines (mushroom and cup shaped) and immature spines (thin and filopodia) (Figure 4B) and observed that spadin significantly increased the proportion of mature spines at either 10 nM or 1 μM, compared with control conditions (Figure 4D). Concurrently, the amount of immature spines was significantly decreased by either concentration of spadin (Figure 4E).

Spadin incubation also decreased the immature spine length, compared with that under control, untreated, conditions (Figure 5A and B). We quantified the length of mature spines and observed that spadin had no effect on this parameter (Figure 5C and D). However, analysis of mushroom head sizes showed that spadin increased this parameter, compared with control conditions (Figure 5E and F). These data indicated that spadin promoted the maturation of dendritic spines.

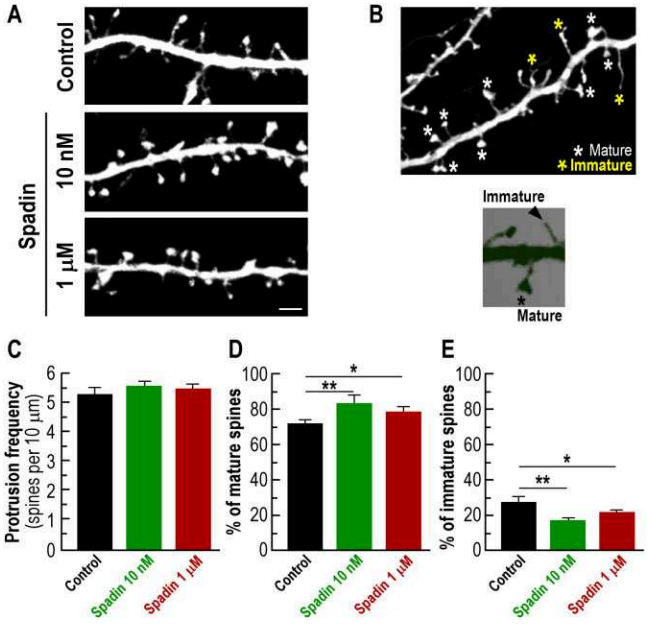

Figure 4

Spadin promotes spine maturation. (A) Representative images of dendrites from eGFP-transduced mouse cortical neurons either untreated (control) or treated with spadin 10 nM or 1 µM for 18 days. Scale bar, 2 µm. (B) Examples of mature and immature spines used in the analyses. (C) Histograms show quantification of protrusion frequency indicating that spadin does not affect spine density. (D and E) Bars show the percentage of mature or immature spines from dendrites of neurons revealing that spadin treatments significantly increase spine maturation. *P < 0.05, **P < 0.01, significantly different from control.

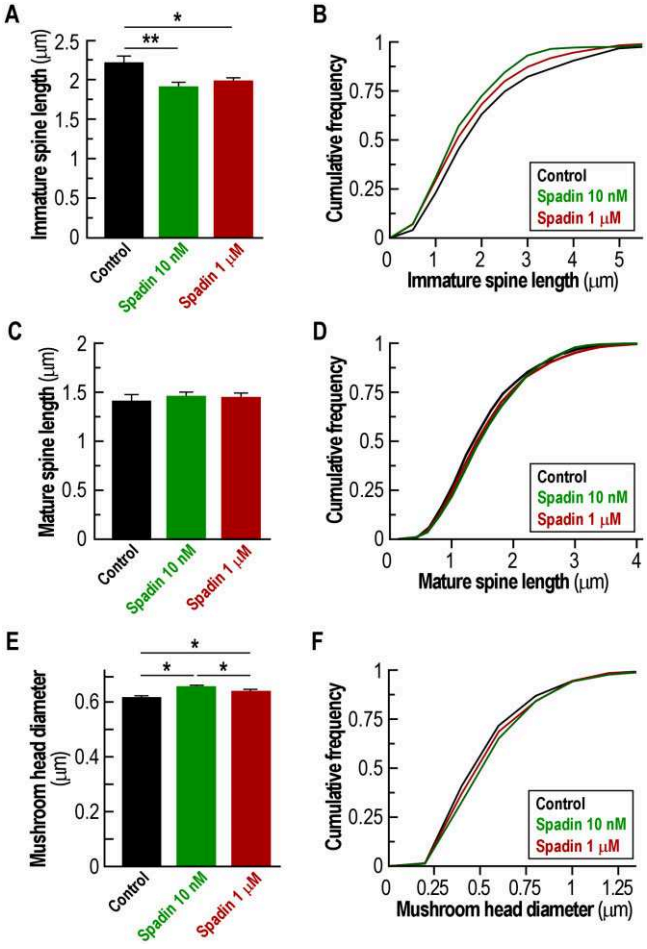

Figure 5

Spadin modifies spine length and mushroom head diameter. (A and B) Analysis of immature spine length. Graphs show quantification of immature spine length on neurons treated with 10 nM or 1 µM spadin. *P < 0.01, **P < 0.001, significantly different from control, K–S test. (C and D) Histograms show quantification of mature spine length and indicate that spadin did not affect spine density. Analysis of mature spine length. Graphs show quantification of mature spine length on neurons treated with 10 nM or 1 µM spadin. (E and F) Spine head diameter is increased in spadin-treated neurons. Graphs show quantification of mushroom type head diameter on neurons treated with 10 nM or 1 µM spadin for 18 days. *P < 0.05, significantly different from control, K–S test.

Spadin promotes synaptogenesis in vivo

We also examined the effect of spadin *in vivo* and specifically in cerebral areas involved in depression (i.e. prefrontal cortex and hippocampus) following i.v. administration of the peptide. We gave a daily i.v. injection of 100 µL of 1 µM spadin for 4 days, to assess the effect of spadin *in vivo* on synaptogenesis. Brain structures were dissected and analysed 7, 14 and 21 days after the first injection. Within the prefrontal cortex, spadin significantly increased the mRNA expression level of BDNF after 21 days, but not those of PSD-95 and synapsin (Figure 6A). By contrast, analysis of mRNA levels of PSD-95, synapsin and BDNF in the hippocampus revealed a significant increase in both synaptic markers (PSD-95 and synapsin; P < 0.05) and increased BDNF was more rapidly detected 7 and 14 days after the first spadin injection (P < 0.05; Figure 6B). We also observed that the protein levels of PSD-95 and synapsin were not modified within the prefrontal cortex (Figure 6C), but were significantly increased in the hippocampus 21 days after the first injection of spadin (Figure 6D). Interestingly, the BDNF protein content was enhanced from 7 to 21 days, but only in the hippocampus (Figure 6D). To compare results obtained from *in vitro* and *in vivo* studies, we performed qPCR experiments to determine the expression levels of synaptic proteins and BDNF from post-natal day 1 to adult mouse brain and observed that both PSD-95 and synapsin were expressed in all stages analysed, with a slight increase of their expression from days 1 to 15 (Supporting Information Fig. S3). By contrast, the level of BDNF was weak between days 1 and 6 and reached its peak expression at day 15. These results indicated that synaptic proteins and BDNF are expressed during embryonic and post-natal development, as well as in adult mice.

Altogether, our data confirmed that spadin was able to cross the blood–brain barrier and to trigger effects in the CNS, after injection in the periphery. These effects were correlated with a significant activation of synaptogenesis and an increase in BDNF content by spadin, particularly in the hippocampus.

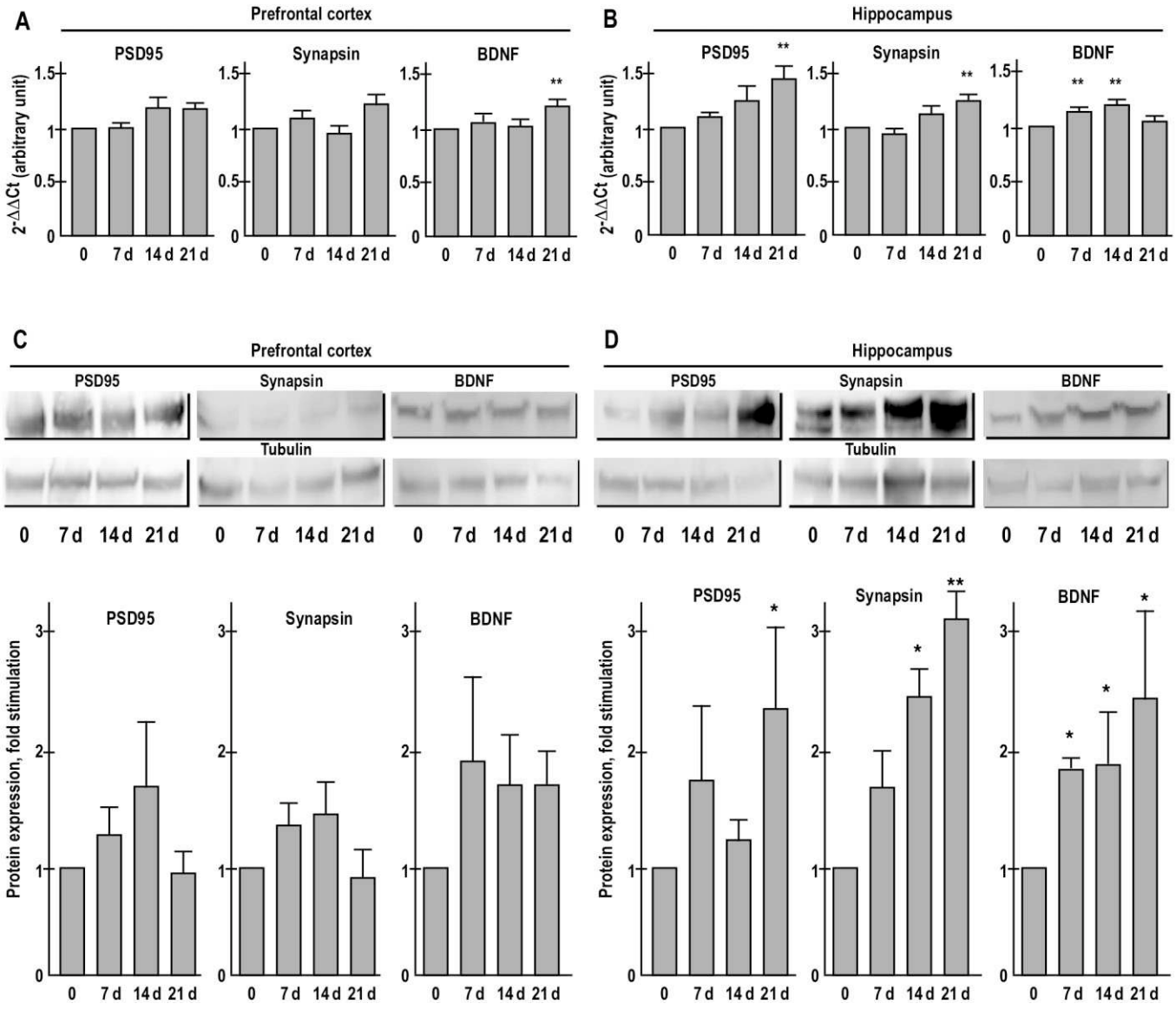

Figure 6

In vivo effects of spadin on synaptic proteins. Males C57BL/6J mice were injected in the caudal vein with 100 μL of 1 μM spadin once daily, for four days, then groups of mice were killed on days 7, 14 and 21 after the first injection. The brain was removed and prefrontal cortices and hippocampi were dissected and analysed by qPCR (A and B) and Western blotting (C and F). (A and B) RNA extracted from the prefrontal cortex (A) or the hippocampus (B) at the indicated day was subjected to quantitative PCR. Bar graphs showing the mRNA expression of PSD-95, synapsin and BDNF were normalized with the control condition (0) and compared with mice treated for 21 days with fluoxetine. Histograms are mean ± SEM from five independent determinations. *$P < 0.05$, significantly different from control (day 0). (C and D) Proteins extracted from the prefrontal cortex (C) or the hippocampus (D) recovered at the indicated day were subjected to Western blot analysis. Immunoblots shown are from a typical experiment. The amount of PSD-95, synapsin and BDNF expressed in the prefrontal cortex (C) and in the hippocampus (D) was represented as fold increase compared with control conditions. Data are means ± SEM from five independent experiments. *$P < 0.05$, **$P < 0.01$, significantly different from control (day 0).

Discussion and conclusions

Here we have investigated the *in vitro* and *in vivo* actions of spadin, a new type of antidepressant compound, at both molecular and cellular levels. Spadin binding to neurons caused neuronal depolarization and to the activation of MAP and PI3K signalling pathways. The latter pathway was involved in the protective effect of spadin against staurosporine-induced neuronal apoptosis. Furthermore, spadin treatment increased the expression of the synaptic markers PSD-95 and synapsin and led to dendritic spine maturation. Injection (i.v.) of spadin for 4 days increased PSD-95 and synapsin protein levels in the hippocampus sampled after 21 days whereas increased BDNF expression was apparent only after 7 days. Our results suggested two phases to spadin action. The first rapid antidepressant effect is

triggered by the increase of BDNF and associated with the release of 5-HT from the dorsal raphe and with hippocampal neurogenesis (Mazella *et al.*, 2010). The second phase is likely to correspond to the maturation of new neurons identified by the increase of synaptic markers as well as an increase in spinogenesis (the present study).

The efficacy of spadin as an antidepressant derives from its biological characteristics as well as its mode of action. Indeed, the peptide sequence of spadin is part of the endogenous peptide of 44 amino acids (PE) released from the precursor form of the NTSR3/sortilin receptor (Munck Petersen *et al.*, 1999). The antidepressant action of spadin is observed after an acute injection and its action on neurogenesis appears only after a 4 day treatment (Mazella *et al.*, 2010) whereas existing antidepressant drugs need 21 days to induce neurogenesis. The antidepressant properties of spadin are due to its ability to block the K^+ channel TREK-1 (Mazella *et al.*, 2010) without any detectable side effect related to this channel (Moha Ou Maati *et al.*, 2012). Although we had already identified the potent antidepressant action of spadin associated with hippocampal neurogenesis, its pharmacological, molecular and cellular modes of action remained unknown.

Functional interaction of spadin with neurons

The biochemical and electrophysiological properties of spadin were initially characterized using heterologous transfected cells (Mazella *et al.*, 2010; Moha ou Maati *et al.*, 2011). Here, we used a more physiologically relevant system to investigate the molecular and cellular mechanisms of action of spadin. In neurons, spadin clearly binds to two binding components with affinities of 0.05 and 100 nM respectively. Taking into account the concentration of PE detected in the brain (about 10 nM), spadin is likely to triggers cellular effects through its high-affinity binding site. We previously identified two targets of spadin, one of them is NTSR3/sortilin, the protein from which the peptide is released after maturation, and the second one is TREK-1 (Mazella *et al.*, 2010). The binding of spadin to TREK-1 blocks the related K^+ current and induces cell-membrane depolarization (Figure 1C). This process is compatible with the inhibition of TREK-1 channels (Fink *et al.*, 1996) (Hughes *et al.*, 2006). Moreover, we observed that spadin affects the plasma membrane distribution of TREK-1 and sortilin as it binds and induces their internalization (Supporting Information Fig. S1). One known function of NTSR3/sortilin is the sorting of proteins, this observation strongly suggests that sortilin not only targets TREK-1 channels to the plasma membrane (Mazella *et al.*, 2010), but also participates in their concomitant internalization. Spadin totally inactivates TREK-1 by blocking and internalizing the channel, a process crucial for the antidepressant effect in mice (Heurteaux *et al.*, 2006b).

Spadin protects neurons from apoptosis by a mechanism dependent on PI3K pathway

Spadin stimulates both ERK1/2 and PI3K signalling pathways in a time- and concentration-dependent manner (Figure 2). The level of phospho-Akt remains surprisingly high after 60 min. Usually, by that time, the level returns to the basal value. This finding could explain the prolonged effects of spadin *in vivo* on synaptic proteins and for the mTOR-independent Akt stimulation induced by the peptide. The ERK1/2 and PI3K pathways are known to be involved in cell growth and cell survival respectively. The expression of TREK-1 is known to be protective against ischaemia (Heurteaux *et al.*, 2004) (Buckler and Honore, 2005) and potent TREK-1 openers protect brain from ischaemia in rodents (Duprat *et al.*, 2000) (Blondeau *et al.*, 2002) (Heurteaux *et al.*, 2006a). In this scheme, spadin, which blocks TREK-1 activity, should decrease the protective action of the channel. We observed that spadin efficiently protected neurons from cell death by reversing staurosporine-induced caspase-3 activation (Figure 2H). This effect was mediated through a PI3K signalling pathway, but not via the MAPK pathway as only the PI3K inhibitor LY294002 reversed the protective action of spadin (Figure 2H). The involvement of the PI3K pathway in neuronal protection has already been reported in several studies including neuroprotection induced by nicotine against colchicine-induced apoptosis (Huang *et al.*, 2012) and the protective action of extracellular progranulin against toxic insults (Xu *et al.*, 2011).

Our finding that spadin acted as a protective agent on cortical neurons suggests that this regulatory system is not so simple. The membrane components responsible for the spadin-induced anti-apoptotic effects remain to be identified. One candidate is NTSR3/sortilin and further experiments performed on neurons prepared from sortilin-KO mice are required to verify this hypothesis.

In vitro *and* in vivo *effects of spadin on synaptogenesis*

Spadin has been described to initiate hippocampal neurogenesis, probably through the activation of CREB (Mazella *et al.*, 2010). This action, which was also observed with fluoxetine (Ohira *et al.*, 2013), does not indicate that new neurons generated by the treatment are functional. The modulation of neurogenesis in the aetiology of depression is still a matter of debate. Indeed, although it is well known that antidepressant drugs induce hippocampal and cortical neurogenesis, blocking neurogenesis does not alter the improving actions of antidepressant drugs on mood (Bessa *et al.*, 2009). Thus, the role of neurogenesis could be to buffer stress response and depressive behaviour (Snyder *et al.*, 2011). Our observation that spadin increases the ratio of mushroom spine types suggests a beneficial adjustment of synaptic function, which could lead a significant action of the peptide on neuron maturation and consequently on synaptic plasticity.

In vitro, we observed a rapid increase in the mRNA and protein expression levels of two synaptic markers; PSD-95 and synapsin, but not of BDNF upon incubation with spadin (Figure 3). The lack of spadin effect on BDNF protein expression is likely to be due to the low number of neuronal cells expressing the neurotrophic factor in our cultures. Acute exposure of neurons to spadin enhances the proportion of mature dendritic spines (mushrooms) without significant changes in the total number of spines (Figure 4). We analysed synaptic proteins up to 21 days because this time should be enough to show effects, taking into account that we showed that a 4 day treatment with spadin was enough to increase the phosphorylation of CREB in the hippocampus. Phospho-CREB is known to be crucial for full maturation of new

neurons (Fujioka *et al.*, 2004). When phospho-CREB is measured where immature new neurons are observed, the expression of phospho-CREB, correlated with maturation, is increased up to 14 days after proliferation. We therefore assumed that 21 days was enough time to observe variations. However, our observations were in agreement with the initial observation that overexpression of PSD-95 is involved in the maturation of spines (El-Husseini *et al.*, 2000). The regulation of spine morphology is generally correlated with changes in neuronal activity (Yuste and Bonhoeffer, 2001). Indeed, based on the structure–stability–function relationships, dendritic spines are classified in two categories, small and large (Kasai *et al.*, 2003). Small spines are usually unstable and non-functional whereas large spines (i.e. mushrooms) are much more stable and maintain strong synaptic connections. Moreover, increasing the proportion of large long-lasting spines in hippocampal neurons is likely to facilitate long-term memory (Lippman and Dunaevsky, 2005). Although dendritic spines are dynamic structures (Lippman and Dunaevsky, 2005), the change in morphology together with the up-regulation of synaptic markers strongly suggest that spadin is a potent up-regulator of neuronal functions.

We also analysed the effect of the peptide on the expression of the two synaptic proteins and BDNF in two cerebral regions involved in the regulation of mood disorders: the prefrontal cortex and the hippocampus (Figure 6). A 4 day treatment with spadin significantly increased the hippocampal expression of both PSD-95 and synapsin, 21 days after the first spadin injection, but not in the prefrontal cortex (Figure 6). These results confirmed the action of spadin on cultured neurons and indicated that the hippocampus is likely to be one of its main cerebral targets. Note that a 21 day administration of the 5-HT reuptake inhibitor fluoxetine was without any effect on synaptic protein mRNA expression levels (not shown). However, experiments carried out using intrahippocampal infusion of fluoxetine did increase PSD-95 expression and synaptogenesis (Mogha *et al.*, 2012). This discrepancy is probably due to the difference in the mode of administration. Interestingly, the same spadin treatment increased BDNF expression in the hippocampus more rapidly (after 7 days) than expression of PSD-95 and synapsin (after 21 days). This effect is compatible with our previous observation that a 4 day treatment with spadin induced a potent antidepressive action and a marked neurogenesis in the hippocampus (Mazella *et al.*, 2010). This result is also in agreement with the observation that a hippocampus-specific increase in BDNF activity is involved in the improvement of cognitive symptoms of depression and in the facilitation of hippocampal neurogenesis (Airan *et al.*, 2007).

To date, antidepressants that are able to reverse synaptic dysfunctions have a limited efficacy and a delayed response ranging from several weeks to months. The recent discovery that ketamine, a non-competitive NMDA receptor antagonist, rapidly enhanced synaptogenesis and reversed synaptic deficits (Duman and Aghajanian, 2012), as well as the discovery of the peptide spadin which bears key properties of a potent antidepressant, may open new fields for treatment of mood disorders. However, in contrast to ketamine, which activates the mTOR pathway through ERK and PI3K pathways (Licznerski and Duman, 2013), the spadin action appears independent of mTOR signalling. This is in agreement with the antidepressant effect of extracts of Radix polygalae (the dried root of *Polygala tenuifolia*) on the modulation of glutamatergic synapses, independently of mTOR activation (Shin *et al.*, 2014). Akt is usually placed downstream of mTORC2 and upstream of mTORC1 (Bhaskar and Hay, 2007). However, after deletion of mTORC2 activity, the phosphorylation of Akt was still observed suggesting that mTORC2 is not placed uptstream of Akt (Shiota *et al.*, 2006). In this case, Akt can phosphorylate other substrates than mTORC1, such as NF-κB or GSK3β that are involved in cell protection or cell cycle (Liu *et al.*, 2009). Further studies are necessary to identify the downstream pathways involved in spadin-induced neuronal activation.

The increase in the expression of synaptic proteins upon spadin treatment both *in vitro* and *in vivo* is a key property that could have considerable effects on therapy of depression. In addition to its ability to cross the blood–brain barrier and to stimulate neurogenesis, spadin appears to be a molecule able to potentiate dendritic spine maturation and synapse formation and, consequently, reinforces our concept that spadin is a novel potent antidepressant.

Acknowledgements

This work was supported by the Centre National de la Recherche Scientifique and the Agence Nationale de la Recherche (ANR, ANR-13-SAMA-0002-02 and ANR-11-EMMA-0050-01). SMa was supported by grants from the Fondation pour la Recherche Médicale (Equipe labellisée # DEQ20111223747) and the Agence Nationale de la Recherche (ANR-2011-JSV4-0031). We also thank the French government for the 'Investments for the Future' LABEX 'SIGNALIFE' # ANR-11-LABX-0028-01 to SMa and ICST # ANR-11 LABX 0015 to CH. JV was supported by a CIFRE fellowship.

Author contributions

C. D., A. K., J. V., H. M. M., M. R., S. M. and J. M. performed the experiments. M. B., S. Ma., C. H. and J. M. conceived and designed the experiments. M. B., S. Ma., C. H. and J. M. contributed reagents/materials/analysis tools. C. D. and J. M. wrote the paper.

Conflict of interest

Authors declare that there is no financial conflict of interest.

References

Airan RD, Meltzer LA, Roy M, Gong Y, Chen H, Deisseroth K (2007). High-speed imaging reveals neurophysiological links to behavior in an animal model of depression. Science 317: 819–823.

Alexander SPH, Benson HE, Faccenda E, Pawson AJ, Sharman JL, Catterall WA *et al.* (2013a). The Concise Guide to PHARMACOLOGY 2013/14: Ion Channels. Br J Pharmacol 170: 1607–1651.

Alexander SPH, Benson HE, Faccenda E, Pawson AJ, Sharman JL, Spedding M *et al.* (2013b). The Concise Guide to PHARMACOLOGY 2013/14: Enzymes. Br J Pharmacol 170: 1797–1867.

Berton O, Nestler EJ (2006). New approaches to antidepressant drug discovery: beyond monoamines. Nat Rev Neurosci 7: 137–151.

Bessa JM, Ferreira D, Melo I, Marques F, Cerqueira JJ, Palha JA *et al.* (2009). The mood-improving actions of antidepressants do not depend on neurogenesis but are associated with neuronal remodeling. Mol Psychiatry 14: 764–773, 739.

Bhaskar PT, Hay N (2007). The two TORCs and Akt. Dev Cell 12: 487–502.

Blondeau N, Lauritzen I, Widmann C, Lazdunski M, Heurteaux C (2002). A potent protective role of lysophospholipids against global cerebral ischemia and glutamate excitotoxicity in neuronal cultures. J Cereb Blood Flow Metab 22: 821–834.

Boschmans SA, Perkin MF, Terblanche SE (1987). Antidepressant drugs: imipramine, mianserin and trazodone. Comp Biochem Physiol C 86: 225–232.

Brewer GJ, Torricelli JR (2007). Isolation and culture of adult neurons and neurospheres. Nat Protoc 2: 1490–1498.

Buckler KJ, Honore E (2005). The lipid-activated two-pore domain K + channel TREK-1 is resistant to hypoxia: implication for ischaemic neuroprotection. J Physiol 562 (Pt 1): 213–222.

Carlezon WA Jr, Duman RS, Nestler EJ (2005). The many faces of CREB. Trends Neurosci 28: 436–445.

Coppola T, Beraud-Dufour S, Antoine A, Vincent JP, Mazella J (2008). Neurotensin protects pancreatic beta cells from apoptosis. Int J Biochem Cell Biol 40: 2296–2302.

Dingemans AM, van den Boogaart V, Vosse BA, van Suylen RJ, Griffioen AW, Thijssen VL (2010). Integrin expression profiling identifies integrin alpha5 and beta1 as prognostic factors in early stage non-small cell lung cancer. Mol Cancer 9: 152–160.

Dolder CR, Nelson MH, Iler CA (2012). The effects of mirtazapine on sleep in patients with major depressive disorder. Ann Clin Psychiatry 24: 215–224.

Drevets WC, Zarate CA Jr, Furey ML (2013). Antidepressant effects of the muscarinic cholinergic receptor antagonist scopolamine: a review. Biol Psychiatry 73: 1156–1163.

Duman RS, Aghajanian GK (2012). Synaptic dysfunction in depression: potential therapeutic targets. Science 338: 68–72.

Duprat F, Lesage F, Patel AJ, Fink M, Romey G, Lazdunski M (2000). The neuroprotective agent riluzole activates the two P domain K(+) channels TREK-1 and TRAAK. Mol Pharmacol 57: 906–912.

Dwyer JM, Duman RS (2013). Activation of mammalian target of rapamycin and synaptogenesis: role in the actions of rapid-acting antidepressants. Biol Psychiatry 73: 1189–1198.

El-Husseini AE, Schnell E, Chetkovich DM, Nicoll RA, Bredt DS (2000). PSD-95 involvement in maturation of excitatory synapses. Science 290: 1364–1368.

Fagiolini A, Comandini A, Catena Dell'Osso M, Kasper S (2012). Rediscovering trazodone for the treatment of major depressive disorder. CNS Drugs 26: 1033–1049.

Fava M, Kendler KS (2000). Major depressive disorder. Neuron 28: 335–341.

Fink M, Duprat F, Lesage F, Reyes R, Romey G, Heurteaux C *et al.* (1996). Cloning, functional expression and brain localization of a novel unconventional outward rectifier K+ channel. EMBO J 15: 6854–6862.

Fujioka T, Fujioka A, Duman RS (2004). Activation of cAMP signaling facilitates the morphological maturation of newborn neurons in adult hippocampus. J Neurosci 24: 319–328.

Hervieu GJ, Cluderay JE, Gray CW, Green PJ, Ranson JL, Randall AD *et al.* (2001). Distribution and expression of TREK-1, a two-pore-domain potassium channel, in the adult rat CNS. Neuroscience 103: 899–919.

Heurteaux C, Guy N, Laigle C, Blondeau N, Duprat F, Mazzuca M *et al.* (2004). TREK-1, a K+ channel involved in neuroprotection and general anesthesia. EMBO J 23: 2684–2695.

Heurteaux C, Laigle C, Blondeau N, Jarretou G, Lazdunski M (2006a). Alpha-linolenic acid and riluzole treatment confer cerebral protection and improve survival after focal brain ischemia. Neuroscience 137: 241–251.

Heurteaux C, Lucas G, Guy N, El Yacoubi M, Thummler S, Peng XD *et al.* (2006b). Deletion of the background potassium channel TREK-1 results in a depression-resistant phenotype. Nat Neurosci 9: 1134–1141.

Honore E (2007). The neuronal background K2P channels: focus on TREK1. Nat Rev Neurosci 8: 251–261.

Huang X, Cheng Z, Su Q, Zhu X, Wang Q, Chen R *et al.* (2012). Neuroprotection by nicotine against colchicine-induced apoptosis is mediated by PI3K–Akt pathways. Int J Neurosci 122: 324–332.

Hughes S, Magnay J, Foreman M, Publicover SJ, Dobson JP, El Haj AJ (2006). Expression of the mechanosensitive 2PK+ channel TREK-1 in human osteoblasts. J Cell Physiol 206: 738–748.

Kasai H, Matsuzaki M, Noguchi J, Yasumatsu N, Nakahara H (2003). Structure–stability–function relationships of dendritic spines. Trends Neurosci 26: 360–368.

Kilkenny C, Browne W, Cuthill IC, Emerson M, Altman DG (2010). Animal research: reporting *in vivo* experiments: the ARRIVE guidelines. Br J Pharmacol 160: 1577–1579.

Krishnan V, Nestler EJ (2008). The molecular neurobiology of depression. Nature 455: 894–902.

Li N, Lee B, Liu RJ, Banasr M, Dwyer JM, Iwata M *et al.* (2010). mTOR-dependent synapse formation underlies the rapid antidepressant effects of NMDA antagonists. Science 329: 959–964.

Li N, Liu RJ, Dwyer JM, Banasr M, Lee B, Son H *et al.* (2011). Glutamate *N*-methyl-D-aspartate receptor antagonists rapidly reverse behavioral and synaptic deficits caused by chronic stress exposure. Biol Psychiatry 69: 754–761.

Licznerski P, Duman RS (2013). Remodeling of axo-spinous synapses in the pathophysiology and treatment of depression. Neuroscience 251: 33–50.

Lin YC, Koleske AJ (2010). Mechanisms of synapse and dendrite maintenance and their disruption in psychiatric and neurodegenerative disorders. Annu Rev Neurosci 33: 349–378.

Lippman J, Dunaevsky A (2005). Dendritic spine morphogenesis and plasticity. J Neurobiol 64: 47–57.

Liu P, Cheng H, Roberts TM, Zhao JJ (2009). Targeting the phosphoinositide 3-kinase pathway in cancer. Nat Rev Drug Discov 8: 627–644.

Martin S, Bouschet T, Jenkins EL, Nishimune A, Henley JM (2008). Bidirectional regulation of kainate receptor surface expression in hippocampal neurons. J Biol Chem 283: 36435–36440.

Mazella J, Zsurger N, Navarro V, Chabry J, Kaghad M, Caput D *et al.* (1998). The 100-kDa neurotensin receptor is gp95/sortilin, a non-G-protein-coupled receptor. J Biol Chem 273: 26273–26276.

Mazella J, Petrault O, Lucas G, Deval E, Beraud-Dufour S, Gandin C *et al*. (2010). Spadin, a sortilin-derived peptide, targeting rodent TREK-1 channels: a new concept in the antidepressant drug design. PLoS Biol 8: e1000355.

McEwen BS, Olie JP (2005). Neurobiology of mood, anxiety, and emotions as revealed by studies of a unique antidepressant: tianeptine. Mol Psychiatry 10: 525–537.

McGrath J, Drummond G, McLachlan E, Kilkenny C, Wainwright C (2010). Guidelines for reporting experiments involving animals: the ARRIVE guidelines. Br J Pharmacol 160: 1573–1576.

McKinney RA (2010). Excitatory amino acid involvement in dendritic spine formation, maintenance and remodelling. J Physiol 588 (Pt 1): 107–116.

Mogha A, Guariglia SR, Debata PR, Wen GY, Banerjee P (2012). Serotonin 1A receptor-mediated signaling through ERK and PKCalpha is essential for normal synaptogenesis in neonatal mouse hippocampus. Transl Psychiatry 2: e66.

Moha ou Maati H, Peyronnet R, Devader C, Veyssiere J, Labbal F, Gandin C *et al*. (2011). A human TREK-1/HEK cell line: a highly efficient screening tool for drug development in neurological diseases. PLoS ONE 6: e25602.

Moha Ou Maati H, Veyssiere J, Labbal F, Coppola T, Gandin C, Widmann C *et al*. (2012). Spadin as a new antidepressant: absence of TREK-1-related side effects. Neuropharmacology 62: 278–288.

Munck Petersen C, Nielsen MS, Jacobsen C, Tauris J, Jacobsen L, Gliemann J *et al*. (1999). Propeptide cleavage conditions sortilin/neurotensin receptor-3 for ligand binding. EMBO J 18: 595–604.

Nestler EJ, Barrot M, DiLeone RJ, Eisch AJ, Gold SJ, Monteggia LM (2002). Neurobiology of depression. Neuron 34: 13–25.

Norrholm SD, Ouimet CC (2001). Altered dendritic spine density in animal models of depression and in response to antidepressant treatment. Synapse 42: 151–163.

Ohira K, Takeuchi R, Shoji H, Miyakawa T (2013). Fluoxetine-induced cortical adult neurogenesis. Neuropsychopharmacology 38: 909–920.

Pacher P, Kecskemeti V (2004). Trends in the development of new antidepressants. Is there a light at the end of the tunnel? Curr Med Chem 11: 925–943.

Pawson AJ, Sharman JL, Benson HE, Faccenda E, Alexander SP, Buneman OP *et al*.; NC-IUPHAR (2014). The IUPHAR/BPS Guide to PHARMACOLOGY: an expert-driven knowledge base of drug targets and their ligands. Nucl Acids Res 42 (Database Issue): D1098–D1106.

Petersen CM, Nielsen MS, Nykjaer A, Jacobsen L, Tommerup N, Rasmussen HH *et al*. (1997). Molecular identification of a novel candidate sorting receptor purified from human brain by receptor-associated protein affinity chromatography. J Biol Chem 272: 3599–3605.

Rodriguez A, Ehlenberger DB, Dickstein DL, Hof PR, Wearne SL (2008). Automated three-dimensional detection and shape classification of dendritic spines from fluorescence microscopy images. PLoS ONE 3: e1997.

Sanacora G, Smith MA, Pathak S, Su HL, Boeijinga PH, McCarthy DJ *et al*. (2014). Lanicemine: a low-trapping NMDA channel blocker produces sustained antidepressant efficacy with minimal psychotomimetic adverse effects. Mol Psychiatry 19: 978–985.

Sarret P, Krzywkowski P, Segal L, Nielsen MS, Petersen CM, Mazella J *et al*. (2003). Distribution of NTS3 receptor/sortilin mRNA and protein in the rat central nervous system. J Comp Neurol 461: 483–505.

Shansky RM, Hamo C, Hof PR, McEwen BS, Morrison JH (2009). Stress-induced dendritic remodeling in the prefrontal cortex is circuit specific. Cereb Cortex 19: 2479–2484.

Shin IJ, Son SU, Park H, Kim Y, Park SH, Swanberg K *et al*. (2014). Preclinical evidence of rapid-onset antidepressant-like effect in radix polygalae extract. PLoS ONE 9: e88617.

Shiota C, Woo JT, Lindner J, Shelton KD, Magnuson MA (2006). Multiallelic disruption of the rictor gene in mice reveals that mTOR complex 2 is essential for fetal growth and viability. Dev Cell 11: 583–589.

Sicouri S, Antzelevitch C (2008). Sudden cardiac death secondary to antidepressant and antipsychotic drugs. Expert Opin Drug Saf 7: 181–194.

Snyder JS, Soumier A, Brewer M, Pickel J, Cameron HA (2011). Adult hippocampal neurogenesis buffers stress responses and depressive behaviour. Nature 476: 458–461.

Srinivasan V, Zakaria R, Othman Z, Lauterbach EC, Acuna-Castroviejo D (2012). Agomelatine in depressive disorders: its novel mechanisms of action. J Neuropsychiatry Clin Neurosci 24: 290–308.

Thase ME, Denko T (2008). Pharmacotherapy of mood disorders. Annu Rev Clin Psychol 4: 53–91.

Xu J, Xilouri M, Bruban J, Shioi J, Shao Z, Papazoglou I *et al*. (2011). Extracellular progranulin protects cortical neurons from toxic insults by activating survival signaling. Neurobiol Aging 32: 2326, e2325–2316.

Yuste R, Bonhoeffer T (2001). Morphological changes in dendritic spines associated with long-term synaptic plasticity. Annu Rev Neurosci 24: 1071–1089.

Zarate CA Jr, Singh JB, Carlson PJ, Brutsche NE, Ameli R, Luckenbaugh DA *et al*. (2006). A randomized trial of an *N*-methyl-D-aspartate antagonist in treatment-resistant major depression. Arch Gen Psychiatry 63: 856–864.

Supporting information

Additional Supporting Information may be found in the online version of this article at the publisher's web-site:

http://dx.doi.org/10.1111/bph.13083

Figure S1 Immunoprecipitation of NTSR3/sortilin or TREK-1 with their corresponding antibodies from cortical neurons pretreated with Sulfo-NHS-biotin before incubation with spadin (1 μM) for the indicated times. Immunoprecipitated internalized proteins were revealed using HRP-streptavidin.

Figure S2 Degradation of spadin and analysis of blood–brain barrier transit. (A) Time course of disappearance of spadin after incubation with cortical neurons (open symbols) or mouse serum (closed symbols) for the indicated times. Incubations were terminated by acidification (HCl 1N) and the peptide contents were analysed by reverse-phase HPLC. Values represent the amount of intact spadin recovered after HPLC and expressed as the percentage of the initial amount of incubated peptide. Values are means ± SEM of three independent determinations obtained from three different neurons preparations or sera samples. (B) Fluorescent Atto488-spadin crosses the blood–brain barrier. HPLC profile

of Atto488- spadin recovered in the brain 30 min after i.v. injection. The brain was subjected to acidic extraction and the extracted peptide content was analysed by reverse-phase HPLC. The retention time for spadin-Atto488 is indicated by the arrow.

Figure S3 Expression of PSD-95, synapsin and BDNF during mouse brain development. The brain (from mice; ages as indicated) was removed and cortical cortices were dissected and analysed in qPCR experiments. Bar graphs showing the mRNA expression of PSD-95, synapsin and BDNF from 1 (D1), 3 (D3), 6 (D6) and 15-day-old (D15) mice were compared with the expression levels of adult (Adt) mice. Histograms are mean ± SEM from three independent determinations.

Psychopharmacology (2015) 232:561–574
DOI 10.1007/s00213-014-3683-2

ORIGINAL INVESTIGATION

Retroinverso analogs of spadin display increased antidepressant effects

Julie Veyssiere · Hamid Moha ou Maati · Jean Mazella · Georges Gaudriault · Sébastien Moreno · Catherine Heurteaux · Marc Borsotto

Received: 3 February 2014 / Accepted: 7 July 2014 / Published online: 2 August 2014
© The Author(s) 2014. This article is published with open access at Springerlink.com

Abstract
Rationale Although depression is the most common mood disorder, only one third of patients are treated with success. Finding new targets, new drugs, and also new drug intake way are the main challenges in the depression field. Several years ago, we identified a new target with the TWIK-related potassium channel-1 (TREK-1) potassium channel, and more recently, we have discovered a peptide of 17 amino acids with antidepressant properties. This peptide, that we called spadin, can be considered as a new concept in antidepressant drug design. Spadin derives from a larger peptide resulting to a posttranslational maturation of sortilin; consequently, spadin can be considered as a natural molecule. Moreover, spadin acts more rapidly than classical antidepressants and does not induce side effects.

Objectives In this work, we sought analogs of spadin displaying a better affinity on TREK-1 channels and an increased action duration.
Methods Analogs were characterized by electrophysiology measurements, by behavioral tests, and by their ability to induce neurogenesis.
Results We identified two retro-inverso peptides that have kept the antidepressant properties of spadin; particularly, they increased the hippocampal neurogenesis after a 4-day treatment. As spadin, these analogs did not induce side effects on either pain, epilepsy processes, or at the cardiac level.
Conclusions Together, our results indicated that spadin retro-inverso peptides could represent new potent antidepressant drugs. As exemplified by spadin in the field of depression, retro-inverso strategies could represent a useful technique for developing new classes of drugs in a number of pathologies.

Keywords Retro-inverso · Spadin · TREK-1 · Depression · Electrophysiology

Catherine Heurteaux and Marc Borsotto contributed equally to the project.

Dr. Georges Gaudriault is a board member and an employee of the Medincell SA company. Julie Veyssiere is a PhD student granted by Medincell SA company.

J. Veyssiere · H. Moha ou Maati · J. Mazella · S. Moreno · C. Heurteaux (✉) · M. Borsotto (✉)
Université de Nice Sophia Antipolis, IPMC, 06560 Sophia Antipolis, France
e-mail: heurteau@ipmc.cnrs.fr
e-mail: borsotto@ipmc.cnrs.fr

J. Veyssiere · H. Moha ou Maati · J. Mazella · S. Moreno · C. Heurteaux · M. Borsotto
CNRS, IPMC, 06560 Sophia Antipolis, France

H. Moha ou Maati
Institut de Génomique Fonctionnelle, 141 rue de la Cardonille, 34095 Montpellier Cedex 5, France

G. Gaudriault
Medincell SA, 1 rue Charles Cros, 34830 Jacou, France

Introduction

Depression is a devastating neuropsychiatric disorder and affects approximately 20 % of the population. Depression is predicted to be a major cause of morbidity worldwide in the next 10 years and will induce an important economic burden (Greenberg et al. 2003; Moussavi et al. 2007). Depression is a multifactorial and multigenic disease characterized by many symptoms like fatigue, anhedonia, pessimism, irritability, sleep troubles, increased or decreased appetite, guiltiness, and suicidal tendencies (Nestler et al. 2002). Sixty years ago, antidepressant treatments have been revolutionized by the discovery of tricyclic antidepressants and monoamine oxidase inhibitors. Later, a second generation of antidepressants was developed with the selective serotonin or

norepinephrine selective reuptake inhibitors. Despite their efficacy, around one third of patients remain unresponsive to these drugs. Moreover, they display some adverse side effects and have a long onset of action (Sicouri and Antzelevitch 2008). Consequently, it was necessary to develop new antidepressant molecules with new pharmacological targets.

We previously demonstrated that the inhibition of TREK-1 led to an antidepressant phenotype (Heurteaux et al. 2006b). Our researches led to the identification of a specific inhibitor of TREK-1 channel called spadin (Mazella et al. 2010). Spadin resulted from modification of the sortilin receptor (Mazella et al. 1998). Spadin is a 17 amino acid peptide which was designed from a 44 amino acid peptide (called PE) released by furin in the late Golgi apparatus during the posttranslational maturation of the sortilin receptor (Munck Petersen et al. 1999). Spadin is able to block the TREK-1 potassium channel current and displays antidepressant effects in different behavioral tests (Mazella et al. 2010). Additionally, like other antidepressant drugs, spadin is able to increase neurogenesis and serotoninergic transmission. More interestingly, unlike the most used antidepressants, which need 21 days to be efficient, spadin has a quicker onset of action since it is able to induce these improvements only after a 4-day treatment (Mazella et al. 2010). In the two pore (K_{2P}) potassium channel family, spadin is specific for TREK-1 channels (Moha ou Maati et al. 2011b). Moreover, the activation of TREK-1 channels was demonstrated to be beneficial in different functions such as general anesthesia, neuroprotection by the way of polyunsaturated fatty acids, pain, ischemia, and epilepsy (Alloui et al. 2006; Heurteaux et al. 2006a; Lauritzen et al. 2000; Noel et al. 2009). Nevertheless, blockade of TREK-1 channels by spadin does not interfere with these functions. In other words, spadin is devoid of side effects on TREK-1-controlled functions (Moha ou Maati et al. 2011b). Importantly, spadin does not induce any cardiac dysfunctions, and both systolic pressure and pulses are not affected by a 3-week spadin treatment. Additionally, spadin is unable to block the two most important repolarizing currents in the heart (I_{KR}, I_{KS}) (Moha ou Maati et al. 2011b). Taken together, these properties are strong evidences for considering spadin as an antidepressant drug of a new generation.

With the aim to identify new analogs displaying a better efficacy than spadin, we synthesized different portions of human sortilin either in natural L-configuration or retro-inverso configuration. This approach consists in synthesizing peptides in which not only the chirality of amino acid is inverted by replacing all L-amino acids by D-amino acids but also the amino acid sequence is reversed (Bonny et al. 2001; Chorev and Goodman 1995). In such a way, the side chains of amino acids are in a similar position to that of the native peptide (Bonny et al. 2001; Chorev and Goodman 1995; Van Regenmortel and Muller 1998). Very often, retro-inverso peptide properties are the same or close, sometimes better, than the parent L-peptides and, overall, retro-inverso peptides are more resistant to proteolysis (Taylor et al. 2010; Weeden et al. 2011).

We first screened 12 spadin analogs for their ability to block TREK-1 channel activity. The two most efficient were retained for further studies using behavioral tests and measurements of their effects on neurogenesis. Because the TREK-1 channel deletion was shown to be deleterious for epilepsy or pain (Alloui et al. 2006; Heurteaux et al. 2004; Noel et al. 2009), we studied the effects of analog treatments on these potential side effects. We also checked the analog harmlessness on the two main cardiac repolarizing currents I_{KR} and I_{KS} that are essential in cardiac function.

Materials and methods

Cell culture

The human-TREK-1/HEK293 cell line (h-TREK-1/HEK) (Moha ou Maati et al. 2011a) and HEK-IKS cell line (Ducroq et al. 2010) were grown in the presence of 0.5 mg/mL G418 in Dulbecco's modified Eagle's medium supplemented with 10 % (*v*/*v*) heat-inactivated fetal bovine serum containing 1 % (*v*/*v*) penicillin/streptomycin in an atmosphere of 95 % air/5 % CO_2 as previously described (Moha ou Maati et al. 2011a).

HEK-293 native cells were grown in serum in an atmosphere of 95 % air/5 % CO_2 in Dulbecco's modified Eagle's medium supplemented with 10 % (*v*/*v*) heat-inactivated fetal bovine containing 1 % (*v*/*v*) of penicillin/ streptomycin and Glutamax X 1. Cells were plated at a density of 20,000 cells/35 mm dish, and after 24 h, cells were transfected using the Jet PEI method (Polyplus, France) with 25 ng/35 mm dish of p-IRES-HERG channel vector. Patch clamp experiments were carried out 48 h after transfection.

Electrophysiology

All electrophysiological experiments were performed on h-TREK-1/HEK cells seeded at a density of 20,000 cells/35 mm dish after 2–6 days of culture. All electrophysiological recordings were performed in whole cell configuration of the patch clamp technique except for I_{KS} measures which were obtained by using the patch clamp perforated configuration (amphotericin B 0.9 mg/mL in the pipette medium) (Moha ou Maati et al. 2011b). Each current was evaluated by using a RK 400 patch clamp amplifier (Axon Instrument, USA), low-pass filtered at 3 kHz, and digitized at 10 kHz using a 12-bit analog-to-digital converter digidata (1322 series, Axon Instrument, USA). All current amplitudes are expressed in current densities. Results are expressed as mean±standard error of the mean (SEM). Patch clamp pipettes were pulled using vertical puller (PC-10, Narishige)

from borosilicate glass capillaries and had a resistance of 3–5 MΩ. The bath solution contained (in mM) 150 NaCl, 5 KCl, 3 $MgCl_2$, 1 $CaCl_2$, and 10 4-(2-hydroxyethyl)piperazine 1-ethane sulfonic acid (HEPES) adjusted to pH 7.4 with NaOH. The pipette solution contained (in mM) 155 KCl, 3 $MgCl_2$, 5 EGTA, and 10 HEPES adjusted to pH 7.2 with KOH. TREK-1 currents were evaluated at room temperature (21–22 °C) in the presence of a cocktail of potassium channel inhibitors (K^+ blockers, 3 mM 4-aminopyridine (4-AP), 10 mM tetraethylammonium (TEA), 10 μM glibenclamide, 100 nM apamin, and 50 nM charybdotoxin). Stimulation protocols and data acquisition were carried out using a microcomputer (Dell Pentium) with a commercial software and hardware (pClamp 8.2). Currents were recorded by voltage clamp steps to membrane potentials of −100 to +60 mV in 20-mV steps applied from a holding potential of −80 mV. The duration of depolarization pulses was 825 ms, and the pulse cycling rate was 5 s. TREK-1 current amplitudes were evaluated at the end of stimulation pulses. Cells were continuously superfused with microperfusion system. TREK-1 inhibitory effects of spadin or analogs were performed on arachidonic acid pre-activated currents. Spadin and analogs were tested at the unique dose of 100 nM on TREK-1 channel activity and at 10 μM on I_{KR} and I_{KS} currents. For both analogs 3 and 8, TREK-1 concentration-dependent inhibitions were performed by applying concentrations ranging between 1 nM and 1 μM.

I_{KS} currents were activated by voltage clamp steps of membrane potentials from −100 to +100 mV in 20-mV steps applied from a holding potential of −80 mV. Tail currents were generated by repolarization to −40 mV. Duration of both depolarization and repolarization pulses was 2.4 s, and the pulse cycling rate was 10 s. I_{KR} currents were activated by voltage clamp steps of membrane potentials from −100 to +100 mV in 10-mV steps applied from a holding potential of +80 mV, and tail currents were generated by a repolarization to +40 mV. The duration of both depolarization and repolarization pulses was 1 s, and the pulse cycling rate was 5 s. The amplitudes of I_{KS} and I_{KR} currents were calculated at both the end of the first pulse and the peak of the tail pulse.

Animals

Naïve male C57Bl/6J mice from 7 to 9 weeks old were used in all experiments (Janvier Laboratory, Saint Berthevin, France). Mice were housed (10 animals per cage) under a 12:12 light–dark cycle (light on at 8:00 am) in a ventilated room at a temperature of 22±1 °C. Animals had free access to water and food (A03; SAFE, Augy, France). All experiments were conducted according to policies on the care and use of laboratory animals of the Society for Neuroscience and also with respect to national laws on animal use. The local ethics committee (CIEPAL) approved the experimental protocols (authorization number 00736–02).

Treatments

Spadin was synthesized by Gencust (France). Other peptides (see Fig. 1) were synthesized by the American Peptide Company (Sunnyvale, CA, USA). Peptides were purified by the supplier, purity >80 %. The purity was verified by analytical high-performance liquid chromatography (HPLC) and mass spectral analysis.

Stock solutions were prepared at 10^{-3} M in distilled water, and before injection, spadin or analog solutions were diluted in NaCl 0.9 % to obtain the different concentrations used for treatments. Corticosterone (Sigma-Aldrich, France) was dissolved in drinking water at the concentration of 3.5 mg/L in the presence of 4.5 g/L of beta-cyclodextrin. The mixture was filled into opaque bottles to protect from the light and mice had a free access to this solution. Fluoxetine (Sigma-Aldrich, France) was dissolved in drinking water at the dose of 80 mg/L and administered during 21 days. For i.p. administration, fluoxetine (TEVA Santé, France) was dissolved in NaCl 0.9 % at a concentration of 0.75 mg/mL. The total amount injected was adjusted to obtain 3 mg/kg. Spadin and analogs were administered by intravenous (i.v.) injection. For acute treatment, drugs were administered in a single 100-μL bolus 30 min prior to the beginning of the behavioral tests. For subchronic treatment, drugs were injected during four consecutive days, and behavioral tests were performed on day 5, without additional injection.

Behavioral tests

Behavioral experiments were performed with naïve mice. The experimenter was blind to experimental groups. All mice were naïve to every behavioral test used.

Name	Sequence
Analog 1	YAPLPRWSGPIGVSWGLR
Analog 2	Ac-APLPRWSGPIGVSWGLR-NH2
Analog 3	Ac-rlGwsvGipGswrplpa-NH2
Analog 4	Ac-GVSWGLR-NH2
Analog 5	Ac-lGVSWGLR-NH2
Analog 6	Ac-rlGwsvGi-NH2
Analog 7	Ac-QDRLDAPPPPAAPLPRWSGPIGVSWGLR-NH2
Analog 8	Ac-rlGwsvGipGswrplpaappppadlrdq-NH2
Analog 9	Ac-APPPPAAPLPRWSGPIGVSWGLR-NH2
Analog 10	Ac-rlGwsvGipGswrplpaappppa-NH2
Analog 11	Ac-QDRLDAPPPPAAPLPRWSGPIGVSWGLRAAAAGGAFPRGGRWRR-NH2
Analog 12	Ac-rrwrGGrpfaGGaaaarlGwsvGipGswrplpaappppadlrdq-NH2

Fig. 1 Sequences of spadin analogs. Peptide sequences are presented using the *one-letter* nomenclature. Amino acids in L-configuration are shown in *capital letters*, while amino acids in D-configuration are shown as *lowercase letters*. *Ac* corresponds to acetyl group, *−NH2* to amide group, and spadin and PE correspond to sequences 1 and 11, respectively

Forced swimming test (FST) (Porsolt et al. 1977)

The animals were individually placed in a non-escapable cylinder (height 30 cm, diameter 15 cm) filled with 15-cm water at 22±1 °C. The trial was conducted for 6 min. The total period of immobility was manually measured during the last 4 min of the test. A mouse was considered immobile when it remained floating with only slight movements to keep its head above water.

Novelty suppressed feeding (NSF) (Santarelli et al. 2003)

The NSF paradigm is a 2-day test protocol. On day 1, mice were deprived from food. On day 2, mice were placed in a highly brightly lit area, in a plastic box (45×45×20 cm), with a floor covered with wooden bedding. The test was carried out during a 10-min period. During this time, the latency to eat was measured. During the test, a single pellet of food was placed in the center of the box, on a white platform.

Learned helplessness (LH) (Caldarone et al. 2000)

The learned helplessness test is divided in a 4-day training session and 1-day test session.

During the training session, mice were exposed to 360 inescapable 2-s footshocks, with an intertrial interval of 8 s.

The test consists in 30 trials separated by a 30-s interval. One trial was defined as a 5-s period before shock onset and was terminated when the mouse moved to the second compartment or at the end of the shock onset. During the test, the latency to escape for each mouse during every trial was recorded.

Tail immersion test (Alloui et al. 2006)

Mice were i.v. injected with 10 μg/kg of spadin in a bolus of 100 or 100 μL of a saline solution (0.9 % NaCl) 30 min before the beginning of the test. The tail was immersed in a water bath at 48 °C until withdrawal was observed (cutoff time 30 s). Two separate withdrawal latency time determinations were averaged (Alloui et al. 2006).

Seizure induced by kaïnate (Tsirka et al. 1995)

Kaïnate solutions were prepared in a solution of 140 mM NaCl (saline solution).

Spadin 10 μg/kg or vehicle was i.v. injected and, immediately after the injection, kaïnate, 25 mg/kg, was i.p injected in a bolus of 100 μL. Mice (n=10 per group) were monitored during 2 h for onset and extent of seizures. Six levels of seizure severity were defined: (1) immobility, (2) head/neck movements, (3) clonic unilateral activity, (4) clonic bilateral activity, (5) generalized convulsions, and (6) death. Seizure severity was blindly scored (Tsirka et al. 1995). The seizure index was calculated by averaging the points for seizure activity in each group (n=10 per treatment).

Mouse locomotor activity

To determine whether analog 3 induced a change in locomotor activity, mice (n=8 per group) were injected with the saline solution or analog 3 (10^{-5} M in 100 μL bolus, i.v.) 30 min before starting the test session. Locomotor activity was monitored individually for 24 h using an infrared photobeam activity monitoring system (Imetronic, Pessac, France), which measured consecutive horizontal beam breaks. Testing was in transparent plastic cages (43×20×20 cm^3) with fresh bedding in a grid of 8 cm horizontal infrared beams. Locomotor activity was defined as breaking of consecutive photobeams. Movements were recorded and totalized for each 10-min time section. Six periods were pooled to obtain data for 1 h of time. Different movements were monitored: the coming-and-going between the back and the front of the cage, climbing, and other movements in the back or the front of the cage. Mice were kept under standard laboratory conditions: 12:12 light–dark cycle with free access to food and water during the experiment. Data are the mean value of eight animals per condition, and bars represent SEM.

Spadin analog recovery in the brain after i.v. injection

Prior to injection, C57BL/6J males were warmed for 5–10 min with an overhead heat lamp to dilate the veins. Then, they were placed in a constrained box and injected in the caudal vein with 100 μL of either 100 μM spadin analog 3 or 0.9 % NaCl solution. The brain was removed either immediately or 30 and 60 min after injection, and the peptide content was recovered by acidic extraction and analyzed by HPLC using a Jasco apparatus equipped with an analytic RP18 Lichrosorb column as previously described (Checler et al. 1986). Elutions of HPLC products were carried out by means of a 50-min linear gradient of acetonitrile from 10 to 60 % at a flow rate of 1 mL/min. Under these conditions, the analog was eluted at 31.5 min. The analog recovered from the brain and identified by mass spectrometry was quantified using a standard curve made with increasing concentrations of analog 3 from 50 to 200 pmol.

Neurogenesis

One day after 5-bromo-2′-deoxyuridine (BrdU) injections, 12 mg per animal divided in four bolus of 300 μL injected every 2 h, mice were anesthetized with isoflurane and transcardially perfused with 20 mL of NaCl 0.9 % followed by 20 mL paraformaldehyde 4 %/NaCl 0.9 %. By using a vibratome (Leica), brains were cut into 40-μm sections, throughout the entire hippocampus. Eight slices, from bregma 3.3 to bregma 5.3, were retained to process the BrdU

immunohistochemistry as previously described (Heurteaux et al. 2006b). For each BrdU labeling, slices were first incubated with a mouse monoclonal anti-BrdU antibody (1/8,000, Becton Dickinson). For chromogenic immunodetection, sections were incubated during 2 h in biotin-conjugated species-specific secondary antibodies (1/400; Vector laboratories) followed by a peroxidase-avidin complex solution, to amplify the reaction. The peroxidase activity of immune complex was visualized with DAB staining using the VectaStain ABC kit according to the manufacturer's protocol (Vector Laboratories).

Statistics

Data were expressed as mean±SEM. Statistical analysis of differences between groups was performed by using Mann-Whitney test. In all analyses, the level of significance was set at $p<0.05$ (*), $p<0.01$ (**), and $p<0.001$ (***).

In the learned helplessness test, latencies to escape were recorded for each of the 30 trials. The average value was calculated for each of the five trials; thus, six blocks of values were obtained in addition to the overall average escape latency. A Mann-Whitney test was carried out on both overall latencies and blocks of trials.

Results

Electrophysiological characterization of spadin's analog on TREK-1 channel affinity

In order to identify analogs having a better affinity than spadin for TREK-1 channels, we first studied their ability to block the channel activity in the h-TREK-1/HEK cell line (Moha ou Maati et al. 2011a). TREK-1 channels expressed in this cell line have conserved all their modulating properties (Moha ou Maati et al. 2011a). By using the whole cell configuration of the patch clamp technique, analog 2 to analog 12 (Fig. 1) were tested at 100 nM ($n=10$ to 12) and the analog 1 corresponding to spadin (Mazella et al. 2010; Moha ou Maati et al. 2011a, b) was used as reference. Our data indicated that only two analogs, analogs 3 and 8, presented an increased blockade effect when compared to spadin (Fig. 2a, b). Analog 2 that corresponds to the N-terminal-acetylated and C-terminal amidated form of spadin displayed similar activity to spadin. IC_{50} values calculated from dose–response curves were of 11.5±0.59 and 9.95±0.85 nM for analogs 3 and 8, respectively (Fig. 2c). These values had to be compared to 56.39±0.01 nM determined for spadin on the same cell line (Moha ou Maati et al. 2011a), noting that analog 2 had an IC_{50} of 60±0.41 nM (Fig. 2c). These data indicated that both analogs 3 and 8 have a sixfold higher affinity for TREK-1 channels. We retained these analogs in order to investigate their potential antidepressant properties.

Antidepressant effect of spadin's analogs after an acute treatment

Because the FST is based on the immobility and influenced by molecules that spontaneously increase the general activity, we controlled the effect of analogs on mouse locomotion. By using an infrared photobeam activity monitoring system, we showed that there was no significant difference in locomotor activities between analog 3- and saline-treated mice within 24 h after the drug injection (Fig. 3). Coming-and-going (Fig. 3a), climbing (Fig. 3b), and total movements (Fig. 3c) were very similar in both conditions. These results indicate that the difference in the immobility time we further observed in the FST was really due to the effect of the analog treatment and not to a change in the locomotor activity.

The antidepressant effects of both analogs were first studied in the FST after an acute injection (Mazella et al. 2010). Here again, spadin was used as control. A 10-μg/kg acute i.v. injection of spadin or both analogs 3 and 8 significantly reduced the immobility time of mice compared to saline-injected mice (Fig. 4a). Values were 166.13±5.54, 107.40±5.05, 135.10±8.11, and 83.60±9.01 s for saline, spadin ($U=0$, $p<0.001$), analog 3 ($U=8$, $p=0.01$), and analog 8 ($U=0$, $p=0.001$), respectively ($n=10$ for each group).

Antidepressant effect of spadin's analogs after a subchronic treatment

The main goal of this study was to find a molecule that can be used in clinic. Thus, we needed a molecule that remained active after several days of administration. Consequently, as already performed with spadin (Mazella et al. 2010), we pursued our study after a subchronic administration of both analogs.

In the FST, subchronic treatments of 4 days (10 μg/kg i.v. injected once a day) with spadin or analogs induced a significant decrease of immobility times. Immobility times observed were of 161.80±8.12 s, 123.70±7.16 s ($U=10.5$, $p<0.01$), 114.9±9.82 s ($U=10.5$, $p<0.01$), and 124.1±10.53 s ($U=17.5$, $p<0.05$) for saline solution, spadin, analog 3, and analog 8, respectively (Fig. 4b).

Similar results were obtained in the novelty suppressed feeding test. Spadin and both analogs reduced the latency to feed. Values were of 305.00±62.47 s, 151.11±17.70 s ($U=13$, $p<0.05$), 143.88±23.42 s ($U=11$, $p<0.05$), and 167.00±22.96 s ($U=13$, $p<0.05$) for saline solution, spadin, analog 3, and analog 8, respectively (Fig. 4c). Although weaker, this antidepressant effect was also observed with learned helplessness test (LHT) (Fig. 4d, e).

Our data clearly indicated that, as spadin, analogs are efficient after only 4 days of treatment.

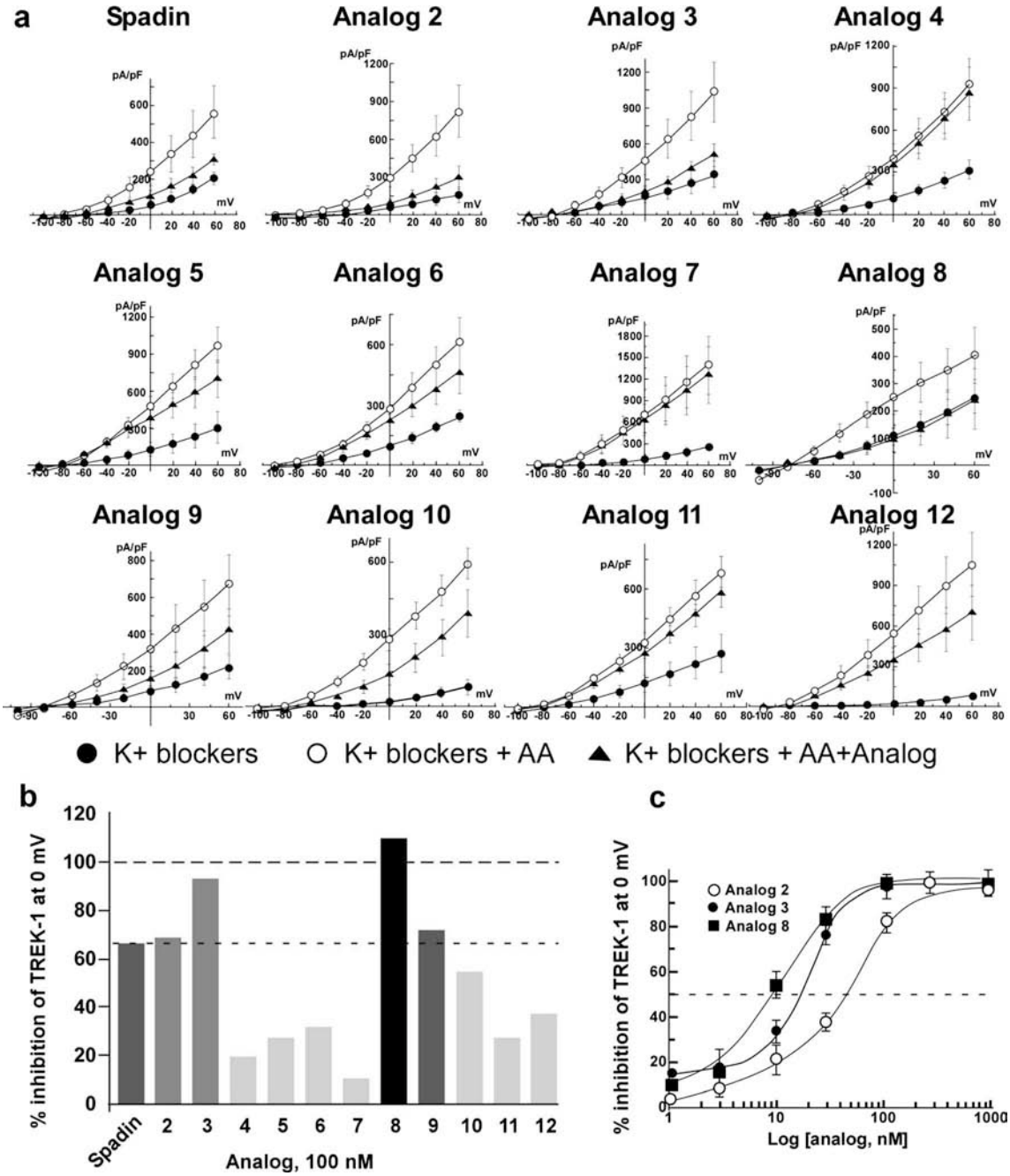

Fig. 2 *I–V* curves of spadin and its analogs. All experiments were performed on h-TREK-1/HEK cell line in the presence of a mixture of K^+ channels blockers and by using the whole cell configuration of the patch clamp technique. **a** Control currents (*black-filled circles*, K^+ blockers) were amplified by the application of 10 μM of arachidonic acid (*white-filled circles*, K^+ blockers + AA). After application of 100 nM of spadin or its analogs, remaining currents were measured (*black-filled triangles*, K^+ blockers + AA + spadin or analog). **b** Percentage of inhibition of the TREK-1 current measured at 0 mV obtained by application of 100 nM of spadin and different analogs. **c** Dose–response curves obtained by measuring the percentage of TREK-1 current inhibition at 0 mV with analog 2 (*white-filled circles*), analog 3 (*black-filled circles*), and analog 8 (*black-filled squares*)

Analog stability

For improving the spadin efficacy, in addition to an increased affinity, analogs have to be more stable when injected in vivo. Measured with the FST, the efficacy of spadin decreased from 100 % at t=1 h after the injection to 0 % at t=16 h, with intermediate values of 84 % at t=3 h and 30 % at t=7 h (Fig. 5a). Times of immobility were of 170.3±4.5 s, 102.4±6.2 s (U=0, p<0.001), 113.2±5.0 s (U=0, p<0.001), 150.8±6.5 s (U=19, p<0.05), and 175.3±7.5 s (Fig. 5a). These data indicated that the biological half-life time of spadin is around 6 h.

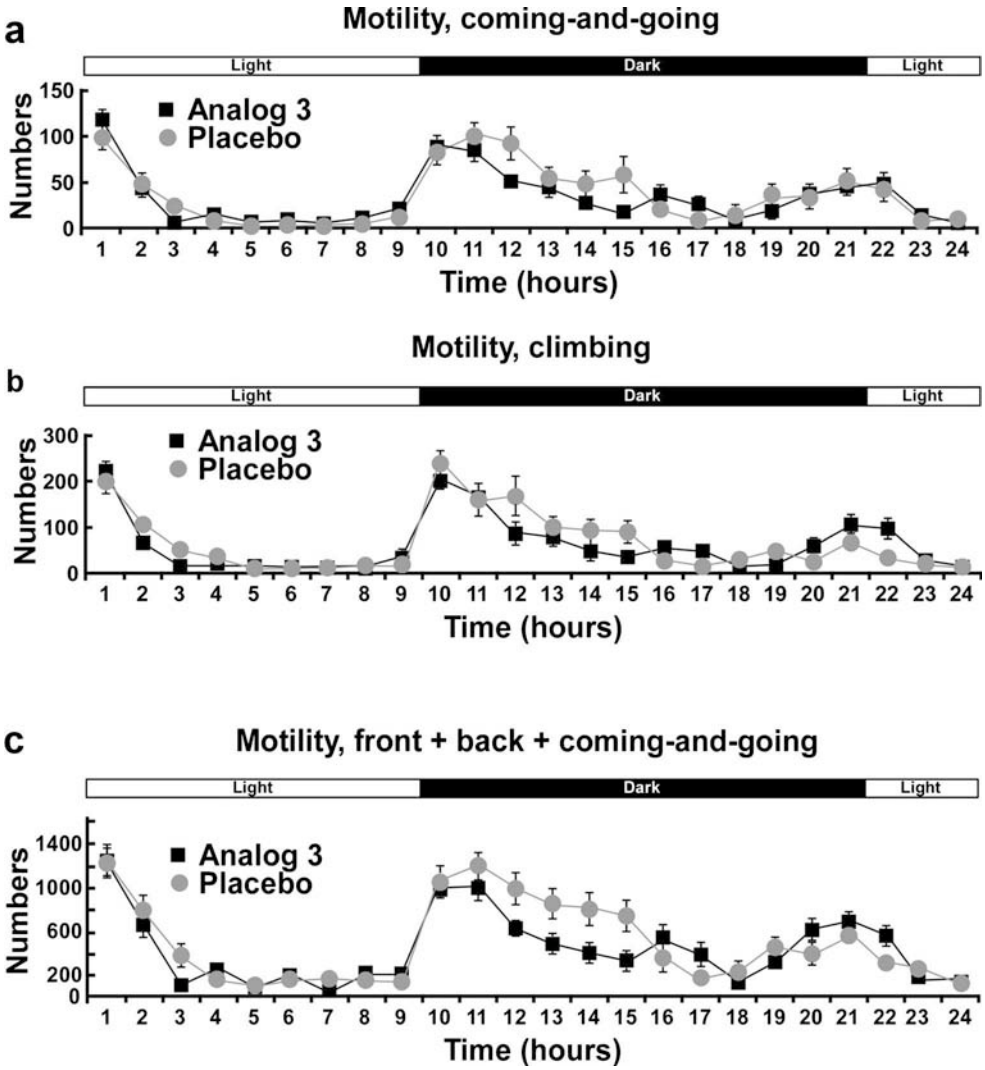

Fig. 3 Spontaneous locomotor activity of analog 3-injected mice. Mice were injected 30 min before to be placed in an infrared photobeam activity monitoring system. Spontaneous locomotor activity was monitored individually for 24 consecutive hours. The number of coming-and-going (**a**), climbing (**b**), and total movements except climbing (**c**) were monitored for each mouse for 10 min section and pooled by 6 to obtain values corresponding to 1 h. Light and dark periods are indicated by the *bar above profiles*

Then, analogs 3 and 8 were tested at different times, 1, 3, 7, 12, 16, 18, 20, and 24 h, after the injection (n=10 naïve mice at each time). Saline-injected animals were only tested at 1 and 24 h (Fig. 5b). It appeared that both analogs remained efficient to reduce the immobility time after 16 h. The immobility times were very similar between 1 and 16 h, 123.4±7.0 and 129.6±12.7 s, and 121.7±5.2 and 129.1±12.0 s for analog 3 and analog 8, respectively (Fig. 5b). The mean value for saline-treated animals was of 162.7±4.7 s (Fig. 5b).

In the aim to determine the ability of analogs to cross the blood–brain-barrier, we used analog 3 as the model. Of analog 3, 10 nmol was intravenously injected, and the amount recovered in the brain was estimated by HPLC analysis (Fig. 6). In the peptide content analyzed from a half brain extract after 30 min of injection, a peak not present in the basal condition (0 min; Fig. 6a) was observed with a retention time of 31.5 min (Fig. 6b). This peak disappeared after 60 min (Fig. 6c). This peak was identified as analog 3 by its retention time identical to standards directly analyzed by HPLC (Fig. 6d) and by mass spectrometry. From different amounts detected by HPLC (Fig. 6d), we determined the amount of analog 3 recovered in the brain (Fig. 6e, arrow) which was estimated to be 100 pmol for a half brain then to be 200 pmol per brain. Therefore, we can estimate to 2 % the yield of analog 3 to cross the blood–brain-barrier. This value corresponds to an increase by a factor 20 of the percentage estimated for spadin (Mazella et al. 2010).

These data clearly indicated that both analogs have better in vivo action duration than spadin itself.

Effects of analogs on neurogenesis

It was previously shown that a 4-day subchronic treatment with spadin increased the hippocampal neurogenesis (Mazella et al. 2010). We investigated the ability of both analogs to induce a neoneurogenesis in the subgranular zone (SGZ) of the hippocampal dentate gyrus, by counting the number of progenitor cells that incorporated the DNA synthesis marker BrdU. In SGZ, a 4-day treatment with spadin or analogs significantly increased the number of BrdU-positive cells by

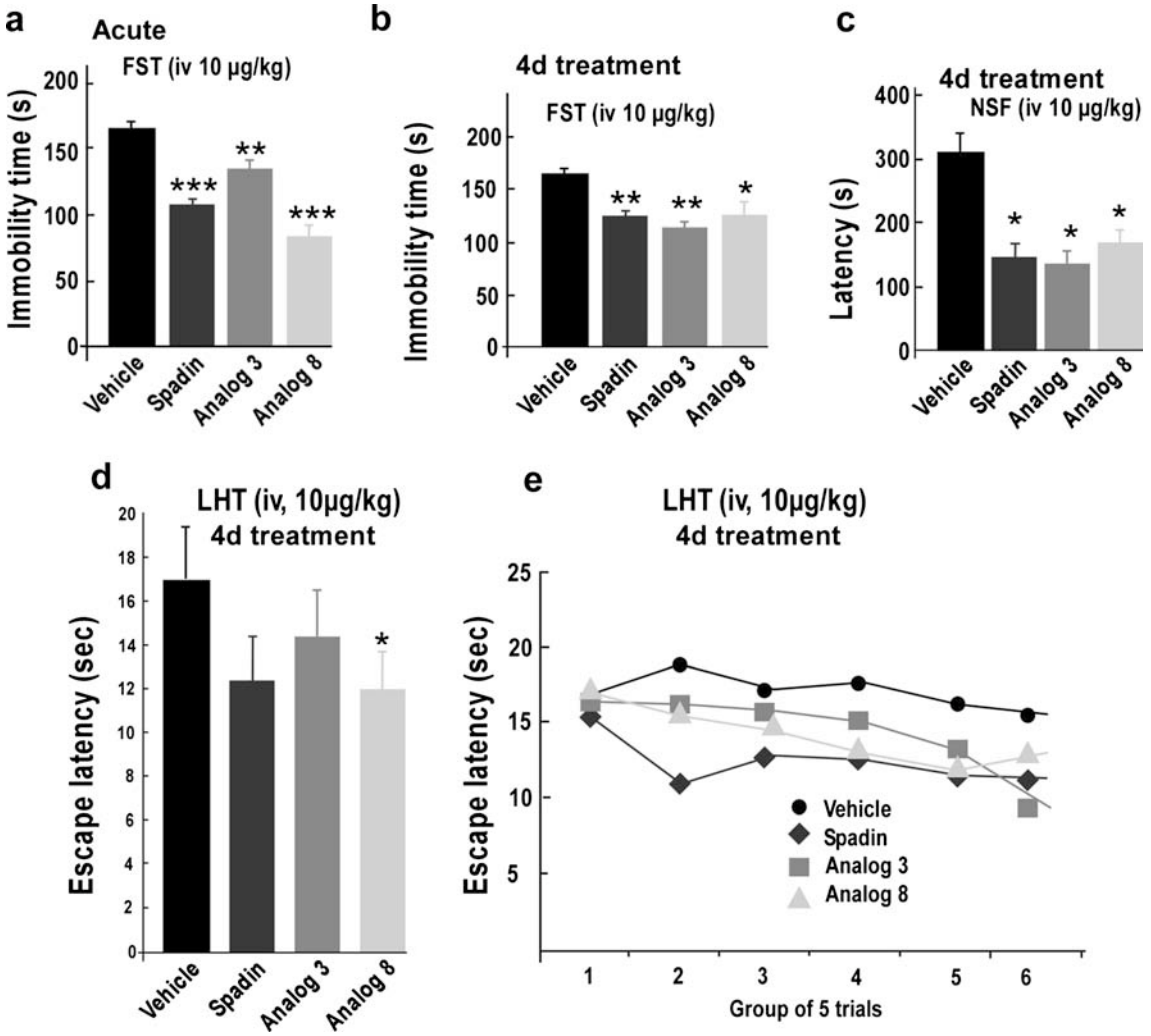

Fig. 4 Behavioral tests with spadin and analogs 3 and 8. **a** FST performed after an acute treatment, immobility times were measured 30 min after the i.v. injection of drugs, 10 µg/kg in a single bolus of 100 µL of NaCl 0.9 %. **b** FST performed after a subchronic treatment (4 days, *4d*); immobility times were measured on the fifth day after a daily i.v. injection of drugs, 10 µg/kg in a single bolus of 100 µL of NaCl 0.9 % for four consecutive days. **c** NSF performed after a subchronic treatment (4 days, *4d*); latencies to feed were measured on the fifth day after a daily i.v. injection of drugs, 10 µg/kg in a single bolus of 100 µL of NaCl 0.9 % for 4 days. **d**, **e** LHT performed after a subchronic treatment (4 days, *4d*); latencies to feed were measured on the fifth day after a daily i.v. injection of drugs, 10 µg/kg in a single bolus of 100 µL of NaCl 0.9 % for 4 days. **d** Mean escape latencies for the entire experiment. **e** The mean escape latencies by blocks of five trials. *$p<0.05$, **$p<0.01$, ***$p<0.001$

at least a factor 2 when compared to saline conditions (Fig. 7a, b).

These data indicated that both analogs are able to induce neurogenesis.

Potential side effects on -TREK-1controlled functions

Because TREK-1 channels are being involved in pain, we analyzed the effects of both analogs 3 and 8 on thermal pain by using the tail immersion test. It clearly appeared that both analogs as well as spadin did not increase the thermal pain sensation (Fig. 8a). Measured tail withdrawal times were of 12.75±0.96, 11.79±0.89, 11.32±1.04, and 13.85±0.72 s for saline, spadin, analog 3, and analog 8, respectively (Fig. 8a).

Because both analogs displayed the same properties and the same efficacy in behavioral tests, we decided to focalize on analog 3. This choice was supported by the fact that analog 3 is the retro-inverso of spadin and consequently shorter than analog 8. Moreover, analog 3 appeared more stable in its in vivo efficacy (see Fig. 5b) than analog 8.

TREK-1 channel deletion is known to induce epilepsy (Heurteaux et al. 2004). We analyzed the effects of analog 3, a potent blocker of TREK-1, on seizures triggered by kaïnate injection (Fig. 8b). Surprisingly, we observed that analog 3 at a dose of 10 µg/kg i.v. injected had an important protective effect against epilepsy seizures triggered by kaïnate injections (25 mg/kg in a bolus of 100 µL). Only two mice among 10 injected with both kaïnate and analog 3 have reached the two less severe stages of the epilepsy seizures, immobility, and

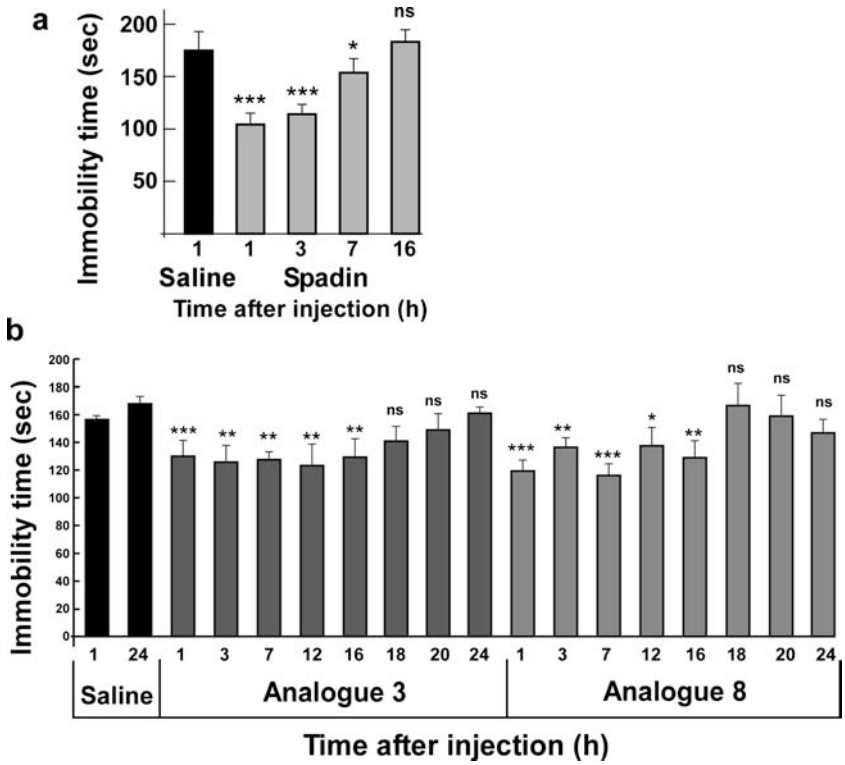

Fig. 5 In vivo stability of spadin and analogs 3 and 8. Using FST, we compared the in vivo action duration of spadin (**a**) with both analogs 3 and 8 (**b**). For each drug at each, times animals were naïve. *$p<0.05$, **$p<0.01$, ***$p<0.001$, *ns* nonspecific

head or neck movements; no other stages of epilepsy were observed for analog 3-treated mice. At least 9 among 10 saline-injected mice have reached the two first stages and five of them died (Fig. 8b). The effect of analog 3 was dose-dependent since a dose of 1 μg/kg showed no protective effect (Fig. 8b).

Potential side effects on cardiac repolarizing currents

It was also important to check that analog 3 as spadin is without effects on the two main repolarizing currents at the cardiac level, the fast component I_{KR} and the slow component I_{KS}. These channels are important because they are responsible for the torsades de pointe which can lead to the death. One of the most important side effects of antidepressant molecules is to induce torsades de pointe. Analog 3 did not modify currents generated either by I_{KR} or I_{KS} channels expressed in HEK cells (Fig. 8c, d).

The current densities measured for I_{KR} at 0 mV at the end of first pulse were 225.14±33.09 pA/pF ($n=5$) and 224.48±35.94 pA/pF ($n=5$) in the absence or the presence of analog 3, respectively (Fig. 8c). At the same potential, tail current densities in the absence or in the presence of analog 3 were 204.59±34.18 pA/pF ($n=5$) and 212.99±38.38 pA/pF ($n=5$), respectively (Fig. 8c). I_{KS} current densities measured at 0 mV were also very close. At the end of pulses, these values were of 17.65±3.84 pA/pF ($n=5$) and 17.58±4.03 pA/pF ($n=5$) in the absence or the presence of analog 3, respectively (Fig. 8d). I_{KS} tail current densities were of 8.33±1.78 pA/pF ($n=5$) and 8.33 ±2.06 pA/pF ($n=5$), in the absence or in the presence of analog 3, respectively (Fig. 8d).

Chronic treatment

To study the effects of a chronic treatment with analog 3, we used the same strategy that we used for spadin, the MedinGel formulation (Moha ou Maati et al. 2011b). Due to fact that a single subcutaneous injection is sufficient to obtain a constant and continuous controlled release of the active molecule for several weeks, this formulation offered the advantage to reduce the stress due to a daily injection.

Formulations were prepared in a way to obtain a release of 10 μg/kg/day of peptide when injected.

The efficacy of analog 3 was measured by FST after 1, 2, and 4 weeks. At each time, tested mice are naïve for the test. Mice treated with the analog 3 formulation showed a significant reduction of immobility times (Fig. 9). After 1 week, the immobility times measured were 134.40±10.45 vs 112.00±9.31 s ($U=21.5$, $p<0.05$) for the placebo-injected and analog 3 formulation-injected mice, respectively. After 2 weeks, the immobility values were 133.80±11.03 vs 99.60±4.92 s ($U=17.5$, $p<0.05$) for the placebo-injected and analog 3 formulation-injected mice, respectively. Interestingly, analog 3 released by the MedinGel formulation was still active after 4 weeks, and the corresponding values are of 137.20±6.93 vs 101.10±14.05 s ($U=20$, $p<0.05$) for the placebo-injected and analog 3 formulation-injected mice, respectively.

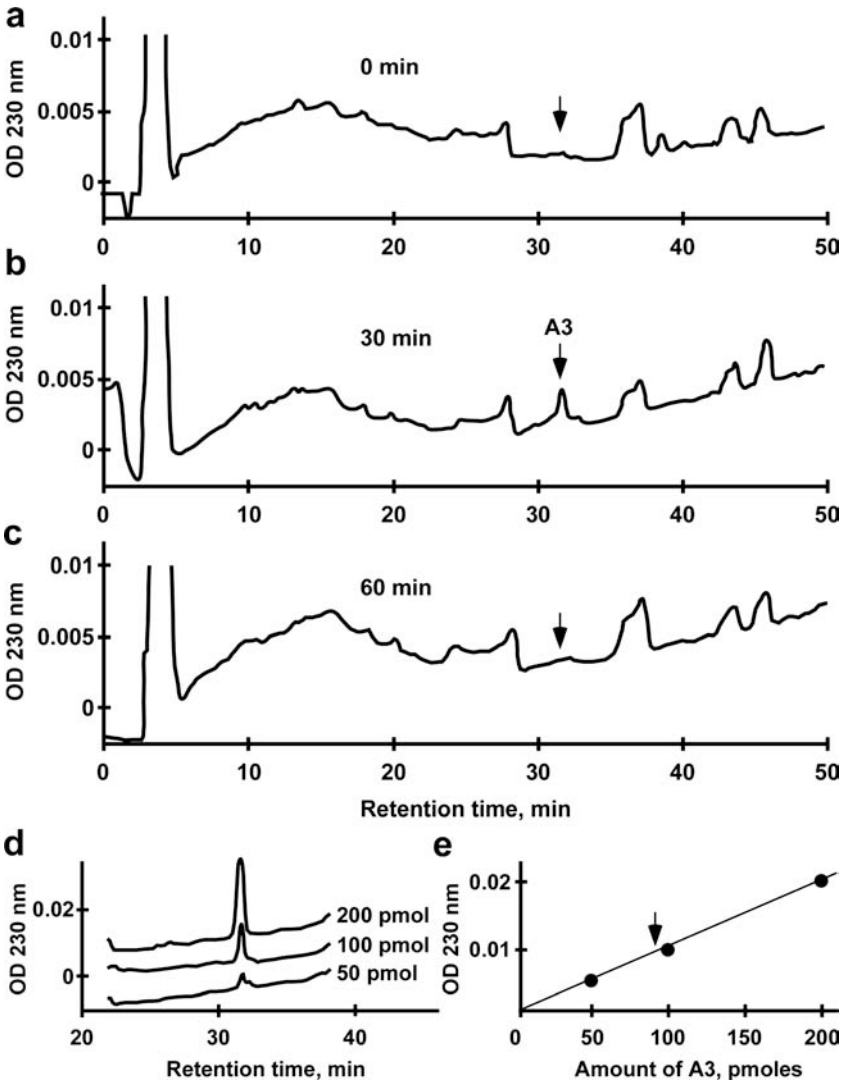

Fig. 6 Analog 3 crosses the blood–brain-barrier. **a**–**c** HPLC profiles of analog 3 recovered in the brain at 0 min (**a**), 30 min (**b**), and 60 min (**c**) after i.v. injection. The brain was subjected to acidic extraction, and the extracted peptide content was analyzed by reverse-phase HPLC. The retention time for analog 3 is indicated by the *arrow* (31.5 min). **d**, **e** 50, 100, and 200 pmol of analog 3 were directly quantified by HPLC (**d**) and the linear representation of the OD obtained as a function of the amount of peptide (**e**) allowed us to determine the amount of analog 3 recovered in the brain extract (*arrow*)

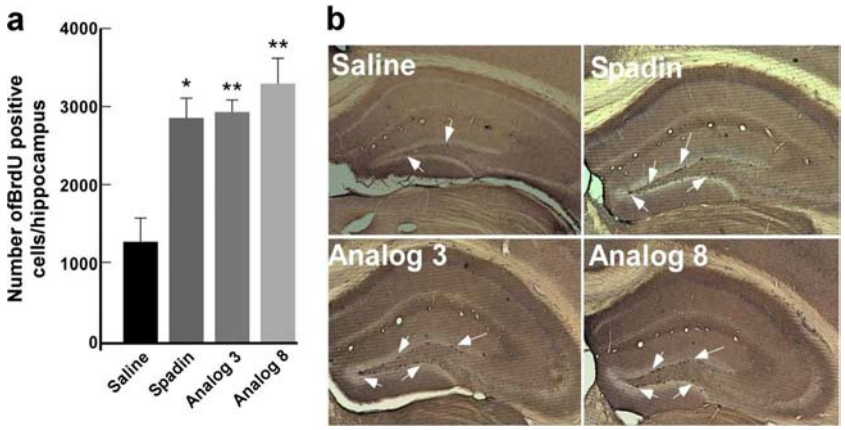

Fig. 7 Neurogenesis. **a** Representative photomicrographs of BrdU-labeled neurons in the dentate gyrus of the mouse hippocampus treated for 4 days either with saline, spadin, analog 3, or analog 8 (i.v., 10 μg/kg for all drugs). *Arrows* showed examples of positive cells. **b** Quantitation of BrdU-positive cells of hippocampus treated with saline, spadin, analog 3, or analog 8 for four consecutive days by an i.v. injection of drugs at 10 μg/kg in a single bolus of 100 μL of NaCl 0.9 %. *$p<0.05$, **$p<0.01$

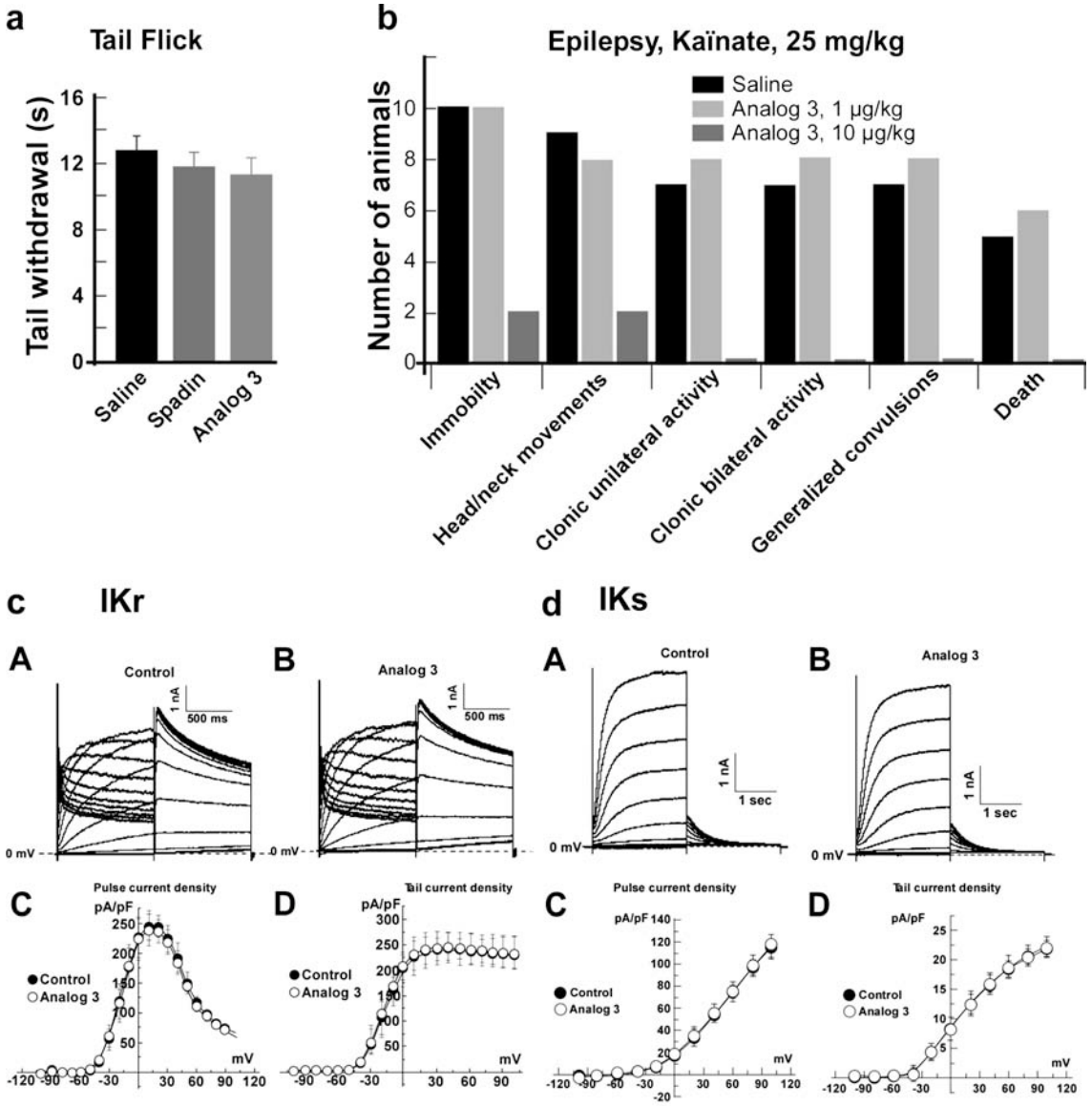

Fig. 8 Side effects. **a** Tail flick test (n=10 per group). For each mouse, the time to withdraw its tail immersed in a water bath at 48 °C was measured twice and averaged. There was no significant difference between saline, spadin, or analog 3-treated mice. **b** Epilepsy. Seizures were triggered by an i.p. injection of kaïnate (25 mg/kg) that was immediately followed an i.v. injection of saline solution or analog 3 at 1 or 10 μg/kg in 100 μL bolus (n=10 per group). The number of animals reaching the different levels of severity was counted. **c**, **d** Analog 3 (10 μM) effects on the cardiac delayed K^+ rectifying currents I_{KR} and I_{KS}. **c** Typical traces of human whole cell hERG current recordings in the absence (control) (**a**) or in the presence of 10 μM analog 3 (**b**). **c**, **d** *I*/*V* curves obtained with the first pulse (**c**, end of pulse) and the second pulse (**d**, tail current) of hERG current (n=5). **d** Typical traces of human whole cell human-I_{KS} current recordings in the absence (control) (**a**) or in the presence of 10 μM analog 3 (**b**). **c**, **d** *I*/*V* curves obtained with the first pulse (**c**, end of pulse) and the second pulse (**d**, tail current) of human-I_{KS} current (n=5)

Discussion

Spadin was recently identified as a new antidepressant in rodent models (Mazella et al. 2010). In this study, we identified two more efficient spadin-derived analogs. The main features of spadin as antidepressant are its rapid onset of action (4 days instead of 21 days) (Mazella et al. 2010) and the absence of side effects (Moha ou Maati et al. 2011b). Nevertheless, in vivo Spadin half-life time measured by the FST was relatively short, around 6 h (Fig. 4). With the aim to decrease the drug intake, we decided to screen spadin analogs showing both an increased affinity for the target TREK-1 channels, which were previously identified as the target for spadin, and an increased bioavailability.

For designing these analogs, we decided to test, among others (Fig. 1), the retro-inverso (RI) peptides. For more than 20 years, it has been shown that these peptides retain their bioactivity (Chorev and Goodman 1995) and often such RI peptides display an increased bioactivity (Chorev and Goodman 1995; Taylor et al. 2000; Taylor et al. 2010). The

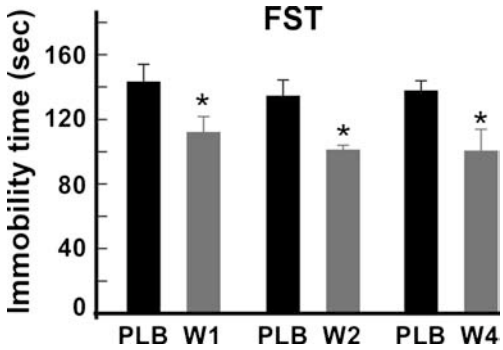

Fig. 9 Effects of long-term treatments with spadin. Spadin–MedinGel formulation and placebo–MedinGel were subcutaneously injected in the neck of mice. Immobility times were measured in FST at 1, 2, or 4 weeks (W1, W2, W4) after injection. For each week, values obtained with formulations were compared with their corresponding placebo values by using the Mann-Whitney test. *PLB*, placebo, *$p<0.05$

fact that RI peptides can cross the BBB was already demonstrated for peptides involved in apoptosis of cerebral granules (Taylor et al. 2000) or for mu-opioid receptor ligands (Dooley et al. 1994).

Electrophysiology and spadin analog screening

Among 11 analogs of spadin, the most efficient TREK-1 channel inhibition was observed with two RI analogs, analogs 3 and 8. It appeared that shorter analogs, analog 4 to 6, displayed a very low inhibition efficacy, less than 30 % when compared to the maximal inhibition. Intriguingly, analog 7 was also a bad inhibitor of TREK-1 channels, while it corresponds to the L-amino acid sequence of the analog 8 which is one of the two most potent TREK-1 channel inhibitors. It only differs by five amino acids (QDRLD) from analog 9 that displayed an inhibitory effect close to that of spadin. The importance of these amino acids in the absence of effect is partly reversed by longer peptides (see analogs 11 and 12). Analog 11 corresponds to the 44 amino acid PE released by the furin in the Golgi vesicle (Munck Petersen et al. 1999). Its reduced blocking effect on TREK-1 channels was already described (Mazella et al. 2010) but, conversely to spadin its RI-analog, analog 12 did not display a better efficacy. In summary, it appeared that better efficacies were found with RI analogs bearing the full spadin sequence such as analogs 3 and 8. Dose–response curves indicated that analog affinities were increased by a factor 5 for analog 3 and a factor 6 for analog 8. These results have allowed us to pursue the investigation with these molecules for pointing out their potential antidepressant properties and their absence of side effects on functions that are controlled by the TREK-1 channel like pain and epilepsy. We also analyzed their action on the cardiac function by measuring their effects on the two main repolarizing potassium channels in the heart.

Spadin analogs, antidepressant effects, and neurogenesis

Both analogs 3 and 8 showed the same antidepressant properties as spadin in several behavioral tests after acute or subchronic treatments. In the FST, after an acute injection or a 4-day treatment, spadin and both analogs behaved similarly. We demonstrated that the decrease in the immobility time was not due to an excitatory effect of analogs since the spontaneous locomotor activity was similar for saline-or analog-injected mice. Analog-injected mice showed an important reduction of the latency to feed in the novelty suppressed feeding test. This test was described to be related with neoneurogenesis in the hippocampus area, a process induced by Alzheimer's disease treatments (Malberg and Schechter 2005; Santarelli et al. 2003). Indeed as spadin did, both analogs increased the number of labelled BrdU neurons in the mouse hippocampus. We have previously shown that 80 % of BrdU-positive neurons were also double cortin positive indicating that the fate of these cells was to become neurons (Mazella et al. 2010). Our data indicated that RI-spadin analogs are not only able to bind on the spadin target the TREK-1 channel but also to trigger antidepressant spadin-like effects.

Spadin analogs and in vivo stability

Interestingly and as expected, these analogs presented an increased in vivo action duration. Measured by the FST, their antidepressant properties were still present 16 h after the injection. This time is about three times longer than this observed for spadin (6 h). In parallel, we showed that analog 3 is able to cross the blood–brain barrier since 30 min after the injection, a peak with a retention time corresponding to analog 3 was recovered in brain extracts. Mass spectroscopy analysis confirmed that this peak was analog 3. This peak is absent at $t=0$, and it has completely disappeared at $t=60$ min. The fact that the antidepressant effect of analog 3 was still measurable 16 h after injection whereas it was no more observable in the brain after 1 h could be accounted by at least two hypotheses. First, the effect is a longlasting effect and the difference between spadin and its analog could be due to the amount that reached the brain (20 times more with analog). Second, after several hours, the level of analog is too weak to be identified by HPLC analysis. A combination of both hypotheses cannot be excluded. Our data confirmed that bioactive retro-inverso peptides presented an increased bioactivity in comparison to the native structure (Chorev and Goodman 1995; Taylor et al. 2000).

Spadin analogs and side effects

Since both analogs have the same binding and antidepressant properties, analog 3 presented the best activity/cost

compromise and was investigated for potential side effects. Treating mice with analog 3 did not increase their thermal pain sensitivity, confirming data obtained with spadin (Moha ou Maati et al. 2011b). Interestingly, on kaïnate-triggered epileptic seizures, analog 3 at a dose of 1 μg/kg had no effect on the severity of seizures. But when administrated at a dose of 10 μg/kg, analog 3 showed a high degree of protection against seizures. At this dose, only two animals reached the two first level of seizure severity while nine saline-injected mice reached these levels. Treating animals with analog 3 amplified the protective effect against seizures which was glimpsed with spadin (Moha ou Maati et al. 2011b). As many drugs can induce cardiac dysfunction, among them ADs (Downes et al. 2005; Heist and Ruskin 2005), we analyzed analog 3 effects on I_{KR} and I_{KS} currents, the two main potassium channels at cardiac level, that are responsible for torsades de pointe and sudden death (Aizawa et al. 2007; Fenichel et al. 2004; Schechter et al. 2005). Analog 3 was without effects on both currents. As in the case of spadin (Moha ou Maati et al. 2011b), these results demonstrated that RI analogs of spadin did not interfere with other TREK-1-controlled pathways and did not modify the cardiac function.

Spadin analogs and chronic treatment

Analog 3 was also used to verify that the antidepressant effect was persistent even after a chronic treatment. This experiment was performed, thanks to a MedinGel formulation that allows following a single subcutaneous injection a continuous controlled release of the peptide during several weeks (Moha ou Maati et al. 2011b). Data showed that the antidepressant effect was the same after 4 weeks and demonstrated that there was no tolerance.

Conclusion

The three fold increase in the bioavailability associated with five- or sixfold increase in the affinity of RI-peptide for the TREK-1 channel indicated that analogs improved by a factor 15 to 18 the efficacy of spadin. Additionally, RI analogs did not induce side effects and their action was stable over the time. Taken together, these properties are very important in the aim to transform spadin or its analogs into a usable drug in human clinic. Indeed, one third of patients remain untreated because they do not correctly take their drugs. Improvements to simplify drug intake will be very helpful for these patients. In this study, we have identified a very potent spadin analog that, associated with a MedinGel formulation, could represent a great step in the spadin drug design concept for treating these untreated patients.

Acknowledgments We thank Anthony Rech for his expert technical assistance in the preparation of injectable formulations. We thank Delphine Debayle for his expert technical assistance in the mass spectroscopy analysis. We thank Layla Djillani for carefully reading the manuscript. This work is supported by the Centre National de la Recherche Scientifique (CNRS) and the Agence Nationale de la Recherche-Emergence (ANR-EMMA-2011-059 and ANR-13-RPIB-0002). J. Veyssiere was supported by a CIFRE fellowship.

Open Access This article is distributed under the terms of the Creative Commons Attribution License which permits any use, distribution, and reproduction in any medium, provided the original author(s) and the source are credited.

References

Aizawa Y, Ueda K, Scornik F, Cordeiro JM, Wu Y, Desai M, Guerchicoff A, Nagata Y, Iesaka Y, Kimura A, Hiraoka M, Antzelevitch C (2007) A novel mutation in KCNQ1 associated with a potent dominant negative effect as the basis for the LQT1 form of the long QT syndrome. J Cardiovasc Electrophysiol 18:972–977

Alloui A, Zimmermann K, Mamet J, Duprat F, Noel J, Chemin J, Guy N, Blondeau N, Voilley N, Rubat-Coudert C, Borsotto M, Romey G, Heurteaux C, Reeh P, Eschalier A, Lazdunski M (2006) TREK-1, a K+ channel involved in polymodal pain perception. EMBO J 25: 2368–2376

Bonny C, Oberson A, Negri S, Sauser C, Schorderet DF (2001) Cell-permeable peptide inhibitors of JNK: novel blockers of beta-cell death. Diabetes 50:77–82

Caldarone BJ, George TP, Zachariou V, Picciotto MR (2000) Gender differences in learned helplessness behavior are influenced by genetic background. Pharmacol Biochem Behav 66:811–817

Checler F, Mazella J, Kitabgi P, Vincent JP (1986) High-affinity receptor sites and rapid proteolytic inactivation of neurotensin in primary cultured neurons. J Neurochem 47:1742–1748

Chorev M, Goodman M (1995) Recent developments in retro peptides and proteins—an ongoing topochemical exploration. Trends Biotechnol 13:438–445

Dooley CT, Chung NN, Wilkes BC, Schiller PW, Bidlack JM, Pasternak GW, Houghten RA (1994) An all D-amino acid opioid peptide with central analgesic activity from a combinatorial library. Science 266: 2019–2022

Downes MA, Whyte IM, Isbister GK (2005) QTc abnormalities in deliberate self-poisoning with moclobemide. Intern Med J 35:388–391

Ducroq J, Moha ou Maati H, Guilbot S, Dilly S, Laemmel E, Pons-Himbert C, Faivre JF, Bois P, Stucker O, Le Grand M (2010) Dexrazoxane protects the heart from acute doxorubicin-induced QT prolongation: a key role for I(Ks). Br J Pharmacol 159:93–101

Fenichel RR, Malik M, Antzelevitch C, Sanguinetti M, Roden DM, Priori SG, Ruskin JN, Lipicky RJ, Cantilena LR (2004) Drug-induced torsades de pointes and implications for drug development. J Cardiovasc Electrophysiol 15:475–495

Greenberg PE, Kessler RC, Birnbaum HG, Leong SA, Lowe SW, Berglund PA, Corey-Lisle PK (2003) The economic burden of depression in the United States: how did it change between 1990 and 2000? J Clin Psychiatry 64:1465–1475

Heist EK, Ruskin JN (2005) Drug-induced proarrhythmia and use of QTc-prolonging agents: clues for clinicians. Heart Rhythm 2:S1–S8

Heurteaux C, Guy N, Laigle C, Blondeau N, Duprat F, Mazzuca M, Lang-Lazdunski L, Widmann C, Zanzouri M, Romey G, Lazdunski M (2004) TREK-1, a K(+) channel involved in neuroprotection and general anesthesia. Embo J 23:2684–2695

Heurteaux C, Laigle C, Blondeau N, Jarretou G, Lazdunski M (2006a) Alpha-linolenic acid and riluzole treatment confer cerebral

protection and improve survival after focal brain ischemia. Neuroscience 137:241–251

Heurteaux C, Lucas G, Guy N, El Yacoubi M, Thümmler S, Peng X, Noble F, Blondeau N, Widmann C, Gobbi G, Costentin J, Debonnel G, Lazdunski M (2006b) Deletion of TREK-1, a background potassium channel, results in a depression-resistant phenotype. Nat Neurosci 9:1134–1141

Lauritzen I, Blondeau N, Heurteaux C, Widmann C, Romey G, Lazdunski M (2000) Polyunsaturated fatty acids are potent neuroprotectors. Embo J 19:1784–1793

Malberg JE, Schechter LE (2005) Increasing hippocampal neurogenesis: a novel mechanism for antidepressant drugs. Curr Pharm Des 11: 145–155

Mazella J, Zsurger N, Navarro V, Chabry J, Kaghad M, Caput D, Ferrara P, Vita N, Gully D, Maffrand JP, Vincent JP (1998) The 100-kDa neurotensin receptor is gp95/sortilin, a non-G-protein-coupled receptor. J Biol Chem 273:26273–26276

Mazella J, Petrault O, Lucas G, Deval E, Beraud-Dufour S, Gandin C, El-Yacoubi M, Widmann C, Guyon A, Chevet E, Taouji S, Conductier G, Corinus A, Coppola T, Gobbi G, Nahon JL, Heurteaux C, Borsotto M (2010) Spadin, a sortilin-derived peptide, targeting rodent TREK-1 channels: a new concept in the antidepressant drug design. PLoS Biol 8:e1000355

Moha ou Maati H, Peyronnet R, Devader C, Veyssiere J, Labbal F, Gandin C, Mazella J, Heurteaux C, Borsotto M (2011a) A human TREK-1/HEK cell line: a highly efficient screening tool for drug development in neurological diseases. PLoS ONE 6:e25602

Moha ou Maati H, Veyssiere J, Labbal F, Coppola T, Gandin C, Widmann C, Mazella J, Heurteaux C, Borsotto M (2011b) Spadin as a new antidepressant: absence of TREK-1-related side effects. Neuropharmacology 62:278–288

Moussavi S, Chatterji S, Verdes E, Tandon A, Patel V, Ustun B (2007) Depression, chronic diseases, and decrements in health: results from the World Health Surveys. Lancet 370:851–858

Munck Petersen C, Nielsen MS, Jacobsen C, Tauris J, Jacobsen L, Gliemann J, Moestrup SK, Madsen P (1999) Propeptide cleavage conditions sortilin/neurotensin receptor-3 for ligand binding. Embo J 18:595–604

Nestler EJ, Barrot M, DiLeone RJ, Eisch AJ, Gold SJ, Monteggia LM (2002) Neurobiology of depression. Neuron 34:13–25

Noel J, Zimmermann K, Busserolles J, Deval E, Alloui A, Diochot S, Guy N, Borsotto M, Reeh P, Eschalier A, Lazdunski M (2009) The mechano-activated K+ channels TRAAK and TREK-1 control both warm and cold perception. EMBO J 28:1308–1318

Porsolt RD, Le Pichon M, Jalfre M (1977) Depression: a new animal model sensitive to antidepressant treatments. Nature 266:730–732

Santarelli L, Saxe M, Gross C, Surget A, Battaglia F, Dulawa S, Weisstaub N, Lee J, Duman R, Arancio O, Belzung C, Hen R (2003) Requirement of hippocampal neurogenesis for the behavioral effects of antidepressants. Science 301:805–809

Schechter LE, Ring RH, Beyer CE, Hughes ZA, Khawaja X, Malberg JE, Rosenzweig-Lipson S (2005) Innovative approaches for the development of antidepressant drugs: current and future strategies. NeuroRx 2:590–611

Sicouri S, Antzelevitch C (2008) Sudden cardiac death secondary to antidepressant and antipsychotic drugs. Expert Opin Drug Saf 7: 181–194

Taylor EM, Otero DA, Banks WA, O'Brien JS (2000) Retro-inverso prosaptide peptides retain bioactivity, are stable In vivo, and are blood–brain barrier permeable. J Pharmacol Exp Ther 295:190–194

Taylor M, Moore S, Mayes J, Parkin E, Beeg M, Canovi M, Gobbi M, Mann DM, Allsop D (2010) Development of a proteolytically stable retro-inverso peptide inhibitor of beta-amyloid oligomerization as a potential novel treatment for Alzheimer's disease. Biochemistry 49: 3261–3272

Tsirka SE, Gualandris A, Amaral DG, Strickland S (1995) Excitotoxin-induced neuronal degeneration and seizure are mediated by tissue plasminogen activator. Nature 377:340–344

Van Regenmortel MH, Muller S (1998) D-peptides as immunogens and diagnostic reagents. Curr Opin Biotechnol 9:377–382

Weeden T, Stefano J, Duan S, Edling A, Hou L, Chuang WL, Perricone MA, Pan C, Dzuris JL (2011) A retro-inverso alpha-melanocyte stimulating hormone analog with MC1R-binding selectivity. J Pept Sci 17:47–55

frontiers in Pharmacology

ORIGINAL RESEARCH
published: 12 September 2017
doi: 10.3389/fphar.2017.00643

Shortened Spadin Analogs Display Better TREK-1 Inhibition, *In Vivo* Stability and Antidepressant Activity

*Alaeddine Djillani†, Mariel Pietri†, Sébastien Moreno, Catherine Heurteaux, Jean Mazella and Marc Borsotto **

Centre National de la Recherche Scientifique, Institut de Pharmacologie Moléculaire et Cellulaire, UMR7275, Université Côte d'Azur, Valbonne, France

Depression is a devastating mental disorder that affects 20% of the population worldwide. Despite their proven efficacy, antidepressants present a delayed onset of action and serious adverse effects. Seven years ago, we described spadin (PE 12-28) as a promising endogenous peptide with antidepressant activity. Spadin specifically blocks the TREK-1 channel. Previously, we showed *in vivo* that, spadin activity disappeared beyond 7 h after administration. In order to improve *in vivo* spadin stability and bioavailability, we screened spadin analogs and derivatives. From the study of spadin blood degradation products, we designed a 7 amino-acid peptide, PE 22-28. *In vitro* studies on hTREK-1/HEK cells by using patch-clamp technique, showed that PE 22-28 displayed a better specificity and affinity for TREK-1 channel compared to spadin, IC_{50} of 0.12 nM vs. 40–60 nM for spadin. In the same conditions, we also pointed out that different modifications of its N or C-terminal ends maintained or abolished TREK-1 channel activity without affecting PE 22-28 affinity. *In vivo*, the antidepressant properties of PE 22-28 and its derivatives were demonstrated in behavioral models of depression, such as the forced swimming test. Mice treated with spadin-analogs showed a significant reduction of the immobility time. Moreover, in the novelty suppressed feeding test after a 4-day sub-chronic treatment PE 22-28 reduced significantly the latency to eat the food pellet. PE 22-28 and its analogs were able to induce neurogenesis after only a 4-day treatment with a prominent effect of the G/A-PE 22-28. On mouse cortical neurons, PE 22-28 and its derivatives enhanced synaptogenesis measured by the increase of PSD-95 expression level. Finally, the action duration of PE 22-28 and its analogs was largely improved in comparison with that of spadin, up to 23 h instead of 7 h. Taken together, our results demonstrated that PE 22-28 and its derivatives represent other promising molecules that could be an alternative to spadin in the treatment of depression.

Keywords: spadin-analogs, TREK-1 channel, PE 22-28, neurogenesis, synaptogenesis, antidepressant

OPEN ACCESS

Edited by:
Maurizio Taglialatela, University of Naples Federico II, Italy

Reviewed by:
Giulia Maria Camerino, Università degli Studi di Bari Aldo Moro, Italy
Sergei Noskov, University of Calgary, Canada

***Correspondence:**
Marc Borsotto
borsotto@ipmc.cnrs.fr

†These authors have contributed equally to this work.

Specialty section:
This article was submitted to Pharmacology of Ion Channels and Channelopathies, a section of the journal Frontiers in Pharmacology

Received: *16 June 2017*
Accepted: *30 August 2017*
Published: *12 September 2017*

Citation:
Djillani A, Pietri M, Moreno S, Heurteaux C, Mazella J and Borsotto M (2017) Shortened Spadin Analogs Display Better TREK-1 Inhibition, In Vivo Stability and Antidepressant Activity. Front. Pharmacol. 8:643. doi: 10.3389/fphar.2017.00643

INTRODUCTION

Depression is one of the most common mood disorders that represents a heavy economic burden in industrialized countries (Smith, 2014). Severe depression affects 2–5% of US citizens and up to 20% of the population suffer from mild depression (Nestler et al., 2002; Maletic et al., 2007; Krishnan and Nestler, 2008; Kessler et al., 2012). Depression is a complex syndrome with a variety of causes

mostly genetic and environmental (Nestler et al., 2002). One of the main hypotheses proposed to explain the physiopathology of depression is the monoamine hypothesis where depletion of three monoamines serotonin (5-HT), norepinephrine (NA) or dopamine (DA) is thought to cause depression (Hillhouse and Porter, 2015). Later, several antidepressant (AD) drugs were developed in the aim to restore the physiological synaptic levels of the three neurotransmitters (Hillhouse and Porter, 2015). Several types of AD drugs were and are still used in the treatment of depression. Initially, depression was mainly treated by tricyclics family and at lesser extent by monoamine oxidase inhibitors (MAOIs) and serotonin-norepinephrine re-uptake inhibitors (SNRIs). However, these classes of ADs exhibit numerous and serious side effects (Hirschfeld, 2012). To reduce the frequency and occurrence of these side effects, these drugs were replaced by a generation of ADs more specific and with lesser adverse effects. This includes serotonin-selective re-uptake inhibitors (SSRIs) and norepinephrine selective re-uptake inhibitors (NSRIs) that are widely used nowadays and recommended as first-line treatment for depression (Nestler et al., 2002; Cleare et al., 2015). SSRIs and NSRIs are thought to increase monoamine synaptic concentrations by inhibiting the re-uptake of 5-HT or NA by blocking their specific transporters, SERT and NAT, respectively (Kohler et al., 2016). These AD drugs are more tolerated but their efficacy on depressive patients is not really improved. On the other hand, the actual ADs like fluoxetine are only efficient after 3–4 weeks of treatment, a latency period that still remains unexplained (Nestler et al., 2002). Thus, it is necessary to discover and characterize new targets for new AD drugs. Recently, different fast-onset AD drugs have been described like ketamine, scopolamine or GLYX-13 (Ramaker and Dulawa, 2017). Nevertheless, these molecules, particularly ketamine produces a number of adverse effects (Katalinic et al., 2013). Multimodal drugs, such as vortioxetine or vilazodone are a new class of ADs latterly approved by the US Food and Drug Administration for the treatment of major depressive disorders (Wang et al., 2015; Sowa-Kucma et al., 2017). Nevertheless, these drugs have not represented a clear improvement of antidepressant efficacy, but vortioxetine showed beneficial effects in depression-related cognitive impairment whereas vilazodone appeared to induce minor sexual dysfunctions (Deardorff and Grossberg, 2014; Li et al., 2015; Thase et al., 2016). Despite this therapeutic arsenal, more than 30% of depressive patients never remit even after several classical treatments (Rush et al., 2006). An alternate for drug therapy in resistant patients is the electroconvulsive therapy (ECT). ECT is efficient in 50% of pharmacotherapy-resistant patients (Heijnen et al., 2010) but ECT also induces some adverse effects mainly in the cognitive processes (Semkovska and McLoughlin, 2010). Thus, the discovery of new AD drugs is challenging. Ten years ago, we have identified the selective two-pore domain potassium channel TREK-1 (TWIK-related potassium channel-1) as a potential target for depression treatment (Heurteaux et al., 2006; Borsotto et al., 2015). TREK-1 channels are ubiquitous potassium channels that play pivotal role in stabilizing membrane potential and thus prevent cellular excitability (Honore, 2007). TREK-1 channels are very particular K_{2P} channels since they are involved in many physiological and physiopathological processes, such as pain, epilepsy, stroke, and depression (Lauritzen et al., 2000; Alloui et al., 2006; Heurteaux et al., 2006). TREK-1 became also an attractive target in cardiovascular research because it plays an important role in atrial fibrillation, pulmonary arterial hypertension and ventricular arrhythmia (Wiedmann et al., 2016; Decher et al., 2017). In the field of depression, we showed in five different models of depression that deletion of *kcnk2* gene, which encodes for TREK-1 channels results in a depression-resistant phenotype associated with an enhanced serotonergic neurotransmission and an increased neurogenesis in the hippocampus (Heurteaux et al., 2006). These observations led us to search for potent TREK-1 blockers. Then, we identified spadin which derives from a larger peptide called propeptide (PE) (Mazella et al., 2010). PE is a 44 amino-acid that results from the post-translational maturation in the Golgi apparatus of sortilin, also known as the neurotensin receptor-3 (Mazella, 2001). Spadin is a fast-acting AD which does not produce any side effects on functions that are controlled by the TREK-1 channel (Moha Ou Maati et al., 2012). It is able to counteract depression in only 4 days when classical ADs require 3–4 weeks to be efficient (Mazella et al., 2010). Moreover, spadin blocks TREK-1 with higher affinity, $IC_{50} \sim 40$–60 nM vs. $IC_{50} \sim 6\,\mu M$ for the most used SSRI fluoxetine (Mazella et al., 2010; Moha ou Maati et al., 2011). However, in mice, the AD activity of spadin measured by FST disappears beyond 7 h after an acute ip administration (Veyssiere et al., 2015). In order to improve the spadin stability *in vivo*, we decided to search for analogs or derivatives of spadin. In a previous study we have identified two analogs, analogs 3 and 8, that were synthesized by using the retro-inverso technology (Veyssiere et al., 2015). Although the gain in term of affinity and action duration was about 20, it is not sufficient to make these analogs competitive in regard of their synthesis cost in comparison to spadin. Then, we decided to search for shortened analogs. We first studied whether or not spadin is degraded in the blood circulation. We identified two shortened peptides. By comparing their ability to inhibit TREK-1 channel expressed in the hTREK-1/HEK cell line (Moha ou Maati et al., 2011), we identified the shortest efficient sequence that only contained 7 amino-acid called PE 22-28. This peptide was used as a core sequence for preparing analogs by chemical modifications of its N- or C-terminus ends and also by substitution of amino-acids. As PE 22-28, some modified peptide-analogs displayed a better potency in blocking TREK-1 channel and more importantly, they have retained their AD properties when injected in acute or sub-chronic treatments.

Abbreviations: AD, antidepressant; FST, Forced Swim Test; NSF, Novelty-suppressed Feeding; LHT, Learned Helplessness Test; ip, intraperitoneal; PSD-95, Post-Synaptic Density protein 95.

MATERIALS AND METHODS

In Vitro Analysis

Cell Lines

The human TREK-1/HEK cell line (Moha ou Maati et al., 2011) and the native HEK293 cell line were maintained in Dulbecco's

Modified Eagle's Medium (DMEM) supplemented with 10% (v/v) heat-inactivated fetal bovine serum, 1% (v/v) penicillin-streptomycin, 1% Glutamax. For the hTREK-1/HEK cells, 0.5 mg/ml G418 were added to the medium.

Cells were incubated in a humidified atmosphere containing 5% CO_2. For electrophysiological measurements, cells were plated at a density of 20,000 cells per 35 mm dish.

In order to study the effects of shortened spadin analogs on hTREK-2, hTASK-1, hTRAAK and hTRESK, the native HEK293 cells were transfected with DNAs corresponding to the channels using JetPEI (Polyplus-transfection, France) following the provider's instructions.

Electrophysiological Measurements

Cells from the hTREK-1/HEK cell line were seeded at a density of 20,000 cells/35 mm dish. Electrophysiological recordings were performed 24–48 h after plating using the whole-cell configuration of patch-clamp technique. TREK-1 currents (I_{TREK-1}) were recorded using RK400 patch-clamp amplifier (Axon Instrument, USA). They were low-pass filtered at 3 kHz and digitized at 10 kHz using a 12-bit analog-to-digital converter digidata (1322 series, Axon Instrument, USA). I_{TREK-1}amplitudes were expressed as current densities [current amplitude (pA)/membrane capacitance (pF)]. The results were expressed as mean ± SEM (standard error of the mean).

Pipettes were pulled from borosilicate glass capillaries using a dual-stage micropipette puller (PC-10, Narishige); they had a resistance of 1.5–3 MΩ. Cells were continuously perfused using an external bath solution containing in mM: 150 NaCl, 5 KCl, 3 $MgCl_2$, 1 $CaCl_2$, and 10 HEPES. The bath solution was initially adjusted to pH 7.4 with NaOH. The intra-pipette solution contained in mM: 155 KCl, 3 $MgCl_2$, 5 EGTA, and 10 HEPES adjusted to pH 7.2 with KOH. In order to measure I_{TREK-1}, a cocktail of potassium channel blockers was added to the bath solution. This cocktail contained: 3 mM 4-AP (4-aminopyridine), 10 mM TEA (tetraethylammonium), 10 μM Glibenclamide, 100 nM Apamin, and 50 nM Charybdotoxin. Data acquisition was carried out using a computer (Dell Pentium) with pClamp software (Axon Instrument, USA). Whole-cell currents were generated by running a pulse or ramp protocol every 5 s from −100 to +60 mV with a holding potential maintained at −80 mV. To evaluate the inhibitory effect on TREK-1 channels of shortened spadin analogs compared with spadin, cells were first activated by 10 μM arachidonic acid (AA). Dose-response curves were realized to compare spadin-analog effects with spadin using Origin 8.6 (Northampton, MA, USA).

Patch-clamp recording data were analyzed using Clampfit (Molecular Devices, USA). $I = f(V)$ curves were obtained from −100 to +60 mV ramp. Data were presented as mean ± SEM.

In Vivo Analysis

Animals

Naïve male C57Bl/6J mice from 7 to 9 weeks old were used in all experiments (Janvier laboratory, Saint Berthevin, France). Mice were housed (10 animals per cage) under a 12-h light/12-h dark cycle (light on at 8:00 am) in a ventilated room at a temperature of 22 ± 1°C. Animals had free access to water and food (A03; SAFE, Augy, France). All experiments were conducted according to policies on the care and use of laboratory animals of the Society for Neuroscience, and also with respect to national laws on animal use. The local Ethics Committee (CIEPAL, N° 736-02) approved the experiments.

Chemicals

Spadin, PE 22-28 and PE 22-28 analogs were purchased from GeneCust Europe, Luxembourg. G418, Arachidonic acid (AA), 4-AP (4-aminopyridine), TEA (tetraethylammonium), Apamin and Charybdotoxin were purchased from Sigma-Aldrich, France, Glibenclamide was purchased from ICN Biomedicals (USA).

In Vitro Half-Life Time of Spadin in Serum

The half-life time of spadin was measured in serum by incubating 10 nmoles of the peptide with 200 μl of mouse serum in the absence or in the presence of the metalloprotease inhibitor 1–10 phenanthroline (1 mM) for various times (2, 5, 15, 30, and 60 min) at room temperature. Incubations were stopped by direct acidification (5 μl of 2.5 M HCl), loaded in C-18 sepack cartridges, lyophilized, resuspended in 20% acetonitrile before loading onto HPLC for analysis of PE degradation/stability. Elutions of HPLC products were carried out by means of a 50-min linear gradient of acetonitrile from 20 to 70% at a flow rate of 1 ml/min. The amount of the intact PE for each incubation time was expressed as the percent of the initial amount of spadin.

Behavioral Tests

Porsolt Forced Swim Test (FST)

Mice were individually placed for 6 min in a non-escapable cylinder (30 cm height and 15 cm diameter) half-filled with water at 22 ± 1°C. The immobility time was manually measured only during the last 4 min. A mouse was considered immobile when it remained immobile with only slight movements in order to keep its head above water (Porsolt et al., 1977).

Novelty Suppressed Feeding Test (NSF)

Mice were deprived from food for 24 h before the test. A food pellet was placed on a white platform in the center of a highly illuminated area (45 × 45 × 20 cm). The floor was covered with wooden bedding. Mice were placed in the corner of the arena, during a period of 10 min, the latency to start eating the pellet was measured (Santarelli et al., 2003).

Learned Helplessness Test (LHT)

The learned helplessness test consists in a 4-day training session and a single day test.

During the training session mice were exposed to 360 inescapable 2 s foot shocks, with an inter-trial interval of 8 s. A non-shocked group was exposed to the apparatus for the same duration but no shock was delivered.

The test consisted in 30 trials separated by a 30 s interval. One trial was defined as a 5 s period before shock onset and was terminated when the mouse moved to the second compartment or at the end of the shock onset. The latency to escape for each mouse during every trial was recorded (Caldarone et al., 2000).

BrdU Labeling

Twenty hours after the injections of 5-Bromo-2′-deoxyuridine (BrdU) (12 mg per animals administered in three bolus of 100 μL of a solution of 40 mg/mL of BrdU diluted in 0.9% NaCl), mice were anesthetized with isoflurane and transcardially perfused first with NaCl 0.9% and, second with 4% paraformaldehyde. Brains were cut in 40 μm sections, by using a vibratome (Leica), throughout the entire hippocampus. Eight slices, from bregma 3.3 to bregma 5.3, were taken to process the BrdU immunohistochemistry as previously described (Heurteaux et al., 2006). For each BrdU labeling, slices were first incubated with a mouse monoclonal anti-BrdU antibody (1/7,000, Becton Dinckinson). For chromogenic immunodetection, sections were incubated during 2 h in specific biotin-conjugated secondary antibodies (1/400; Vector Laboratories) followed by a peroxidase-avidin complex solution, to amplify the reaction. The peroxidase activity of immune complex was visualized with DAB staining using the VectaStain ABC kit according to the manufacturer's protocol (Vector Laboratories).

Synaptogenesis

Mouse cortical neurons were treated with 0.1 μM of the indicated spadin analog for different times and homogenized in the Laemmli buffer and analyzed onto 10% SDS PAGE gels. Separated proteins were then transferred from gels onto nitrocellulose membranes (VWR, Fontenay-sous-Bois, France) and blocked with either 5% skim milk or 5% BSA as indicated in PBS for 30 min at room temperature. Membranes were incubated with antibodies directed against PSD-95, overnight at 4°C. Tubulin or β-actin contents were determined after stripping using a 1/1,000 dilution anti-tubulin or anti-β-actin antibodies (Sigma-Aldrich, Saint-Quentin Fallavier). After four washes in 0.1% Tween/PBS, secondary anti-mouse or anti-rabbit horseradish peroxidase-conjugated antibodies (1/10000, Amersham Biosciences, Orsay, France) were incubated for 1 h at room temperature. Proteins were detected with the ECL plus detection reagents (Amersham Biosciences, Orsay, France) using a LAS-3000 imaging system (Fujifilm, Düsseldorf, Germany).

Relative intensities of the labeled bands were analyzed by densitometric scanning using ImageJ software (Wayne Rasband, Bethesda, USA). PSD-95 expression was normalized using total tubulin or β-actin labeling.

Statistical Analysis

Data are presented as mean ± SEM of at least 3 independent experiments. In GraphPad Prism (GraphPad software, La Jolla, USA), statistical comparisons were performed using Student's *t*-test or ANOVA one-way. A result is considered as statistically significant when $p < 0.05$.

RESULTS

Spadin Degradation in the Serum

From the analysis of spadin degradation after 30 min of incubation with serum at 37°C, we observed the disappearance of almost all spadin and the appearance of two other peaks, peak 1 and peak 2 (**Figure 1A**). Mass spectroscopy analyses indicated that peak 1 and peak 2 corresponded to sequences PE 14-25 and PE 12-27, respectively (**Figure 1C**). These peaks appeared rapidly and reached a maximal value at 15 min for peak 1 followed by a further degradation (**Figure 1B**). By contrast, peak 2 reached its maximal appearance at 30 min which was maintained up to 60 min (**Figure 1B**).

Identification of the PE 22-28 Sequence as the Most Efficient TREK-1 Blocker with Higher Affinity Compared to Spadin

Spadin shortened analogs were individually screened on the hTREK-1/HEK cell line (Moha ou Maati et al., 2011) using the patch-clamp technique (**Figure 1C**). Shortened PE peptides showed differences in their capacity to inhibit TREK-1 activity in comparison with spadin (PE 12-28) and PE 1-44 sequences. In all experiments (**Figure 2**), TREK-1 channels were prior activated with 10 μM AA (Patel et al., 1998). When the maximal amplitude was reached, we measured the ability of each peptide at 100 nM to inhibit the TREK-1 channel activity induced by AA and we compared them with spadin (**Figure 2** and **Table 1**). We first tested the two peptides identified above (PE 14-25 and PE 12-27) (**Figures 2B,C,P**). No significant effect on TREK-1 channels was observed with the PE 14-25 analog (**Figures 2C,P**). The current density measured at 0 mV and compared with AA activity alone (100%) was 114.7 ± 10.6% ($n = 8$, $p = 0.09$). Interestingly, we found that PE 12-27 was able to strongly inhibit TREK-1 activity (28.4 ± 9.9%, $n = 22$, $p = 0.03$; **Figures 2B,P**).

Then, we designed three other shortened peptides, PE 22-25, PE 22-27 and PE 22-28 (**Table 1**). Neither PE 22-27 (**Figures 2D,P**, **Table 1**) nor PE 22-25 (**Figures 2E,P**, **Table 1**) had significant effect in inhibiting $I_{TREK\text{-}1}$ (27.5 ± 20%, $n = 10$, $p = 0.23$) and (36.02 ± 17.5%, $n = 14$, $p = 0.06$), respectively. Only, the PE 22-28 (**Figures 2F,P**, **Table 1**) was able to efficiently block TREK-1 activity (55.46 ± 4.6%, $n = 13$, $p < 0.0001$).

Spadin-Analog Design

After the screening of these analogs with the hTREK-1/HEK cells, PE 22-28 was identified as the most efficient TREK-1 blocker and was retained for further studies. With the aim to increase again the stability and the efficacy of the peptide we used PE 22-28 as core peptide for the design of several analogs. Peptides that were able to block TREK-1 activity were described in the **Figures 2G–P**) and in **Table 1**. They include biotinylated PE 22-28, PI-PE 22-28, corresponding to the PE 20-28 sequence, biotinylated-PI-PE 22-28, G/A-PE 22-28 corresponding to the PE 22-28 sequence where the Glycine at position 22 was replaced by an Alanine residue, biotinylated-G/A-PE 22-28, dansyl-PE 22-28 where a dansyl chemical group was added at the N-terminus of the peptide, O-methyl-PE 22-28 and O-ethyl-PE 22-28 where a O-methyl or a O-ethyl chemical group was added to the C-terminus of the peptides, respectively.

We tested other analogs but they were unable to inhibit TREK-1 current (**Table 1**). Corresponding current-voltage curves are depicted in the Supplementary Figure 1.

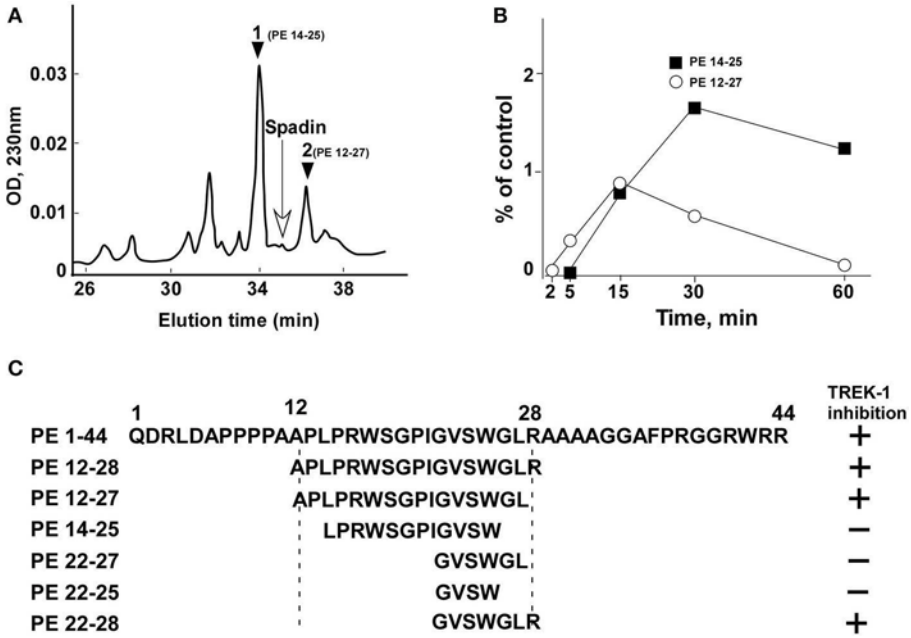

FIGURE 1 | HPLC profiles of spadin degradation products in serum. **(A)** A typical HPLC profile obtained after 30 min incubation of spadin with mouse serum at 37°C. The position of spadin peak is indicated by an arrow. **(B)** Kinetics of appearance of peaks 1 (PE 14-28) and 2 (PE 12-27). **(C)** Sequences of shortened peptides and their capacity to inhibit TREK-1 activity compared with PE and spadin (PE 12-28) sequences.

All screened analogs able to inhibit TREK-1 channel also displayed AD properties measured with the Forced Swim Test (FST) (**Figure 3A**, **Table 1**).

Analyses of electrophysiological and behavioral data allowed us to focus further studies on PE 22-28, G/A-PE 22-28 and biotinylated-G/A-PE 22-28. These three peptides are hereafter called spadin-analogs (bolded in **Table 1**). They shared common AD properties, a high percentage of TREK-1 current inhibition and, they had an affinity for TREK-1 that was largely increased in comparison to spadin (**Figure 3B**). The IC_{50} measured were 40, 0.12, 0.10, and 1.2 nM for PE 12-28 (Spadin), PE 22-28, G/A-PE 22-28 and biotinylated-G/A-PE 22-28, respectively.

Spadin-Analogs Specifically Block TREK-1 Channel Activity

PE 22-28 was chosen as representative peptide among spadin-analogs and was tested on other K_{2P} channels like hTREK-2, hTRAAK, hTRESK, and also hTASK-1 (Lesage and Lazdunski, 2000; Kim et al., 2001; Talley et al., 2001; Lauritzen et al., 2003; Lafreniere et al., 2010). Native HEK cells were transfected by plasmids coding for these channels. TREK-2 and TRAAK were activated by 10 μM AA. Then 100 nM of PE 22-28 combined to AA were applied when current amplitude reached the maximum. PE 22-28 was inefficient in producing any change in the amplitude of the current (**Figures 4A,B**). Similarly, PE 22-28 was unable to modify currents generated by hTRESK and hTASK-1, two important K_{2P} channels in the brain (**Figures 4C,D**). Spadin-analogs represented by PE 22-28 did not inhibit these K_{2P} channels indicating that they are as specific as spadin for blocking TREK-1 channels.

More importantly, spadin-analogs tested at higher concentration (10 μM) did not modify the I_{Kr} current generated by hERG channels (**Figures 4E–G**). I_{Kr} current is the most important repolarizing current in the heart (Sanguinetti and Jurkiewicz, 1990; Cheng and Kodama, 2004). Dysfunction of these channels could cause death by Torsades de Pointes that are one of the most important side effects observed with AD drugs (Cheng and Kodama, 2004).

Spadin-Analogs Display Antidepressant Properties in Depression Tests and in Mouse Model of Depression

After an acute ip administration of 3.0–4.0 μg/kg spadin-analogs, the immobility time of mice was decreased significantly, 91.80 ± 6.1 s ($n = 10$, $p < 0.0001$), 110.2 ± 6.6 s ($n = 10$, $p < 0.0001$), and 140.7 ± 7.1 s ($n = 10$, $p = 0.02$) for PE 22-28, G/A-PE 22-28 and biotinylated-G/A-PE 22-28, respectively, values that have to be compared with that of the saline solution (161.7 ± 6.49 s) (**Figure 3A**).

As spadin, spadin-analogs were efficient after sub-chronic treatments. Whether administered by ip injections (3.0 μg/kg) or gavage (1 mg/kg) (**Figure 5A**), they remained active in the FST. Then, we subjected mice to the Learned Helplessness Test, a validated and efficient test for identifying AD molecules. A 4-day sub-chronic treatment with spadin-analogs (3.0 μg/kg, ip) significantly reduced the escape latencies (**Figure 5B**). In the chemically induced model of depression using long term

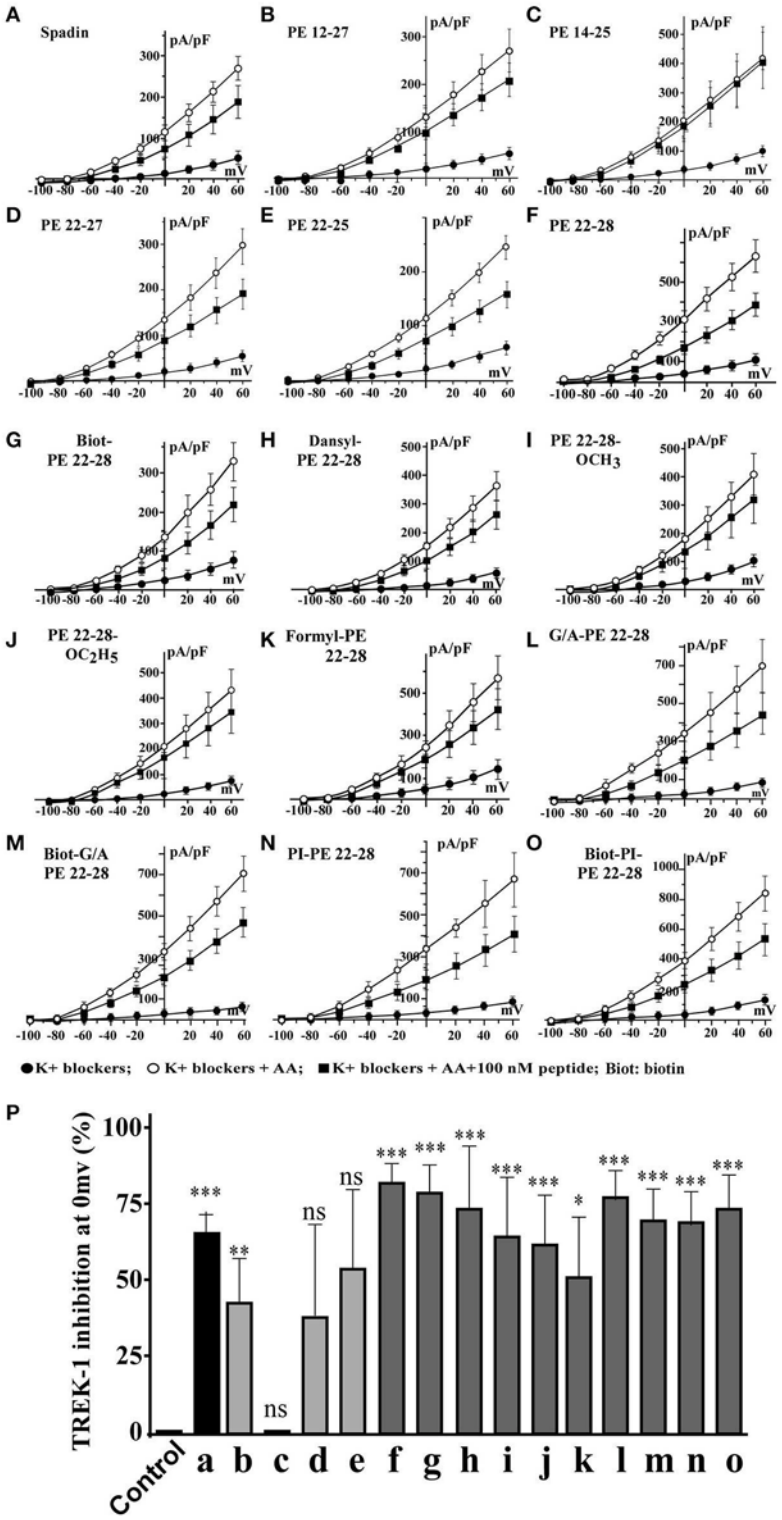

FIGURE 2 | I = f(V) curves and % of TREK-1 inhibition. **(A–F)**, current density curves obtained with spadin and shortened peptides described in **Figure 1C**. **(G–O)**, current density curves obtained with PE 22-28 analogs. **(P)** Inhibition percentages of TREK-1 current measured at 0 mV for corresponding peptides described from "**A**" to "**O**". Control value was obtained by using a solution of 0.9% NaCl. ns, not significant. $^{*}p < 0.05$, $^{**}p < 0.01$, $^{***}p < 0.001$.

TABLE 1 | Spadin analogs and their ability to inhibit TREK-1 channel activity and reduce immobility times in FST.

Figure 2 code	Peptide names	Modifications	% of TREK-1 inhibition	*n*	*P*	FST immobility times (s)	*p*
a	PE 12-28 (Spadin)	Not modified	44.37 ± 8.817	7	0.0024	88.3 ± 7.0	0.0001
b	PE 12-27	Not modified	28.39 ± 9.916	22	0.0093	100.2 ± 5.0	0.0001
c	PE 14-25	Not modified	−14.73 ± 10.6	8	0.2074	112.2 ± 7.1	0.0080
d	PE 22-27	Not modified	25.7 ± 20.01	10	0.2311	168.2 ± 4.2	ns
e	PE 22-25	Not modified	36.02 ± 17.47	14	0.0599	100.2 ± 5.0	0.0001
f	**PE 22-28**	**Not modified**	**55.46 ± 4.555**	**13**	**0.0001**	**91.8 ± 6.1**	**0.0001**
g	Biotinylated-PE 22-28	Addition N-terminus	53.03 ± 6.416	12	0.0001	112.1 ± 4.3	0.0001
h	Dansyl-PE 22-28	Addition N-terminus	48.78 ± 14.52	10	0.0084	104.6 ± 11.8	0.0010
i	PE 22-28-O-Methyl	Addition C-terminus	42.98 ± 13.47	12	0.0086	137.1 ± 8.1	0.0200
j	PE 22-28-O-Ethyl	Addition C-terminus	41.39 ± 11.52	10	0.0058	113.2 ± 8.5	0.0001
k	Formyl-PE 22-28	Addition N-terminus	32.45 ± 12.22	10	0.0262	ND	
l	**G/A-PE 22-28**	**Substitution-N- terminus**	**50.61 ± 7.935**	**10**	**0.0001**	**110.2 ± 3.6**	**0.0001**
m	**Biotinylated G/A-PE 22-28**	**Addition + substitution N-terminus**	**46.11 ± 7.743**	**11**	**0.0001**	**140.7 ± 7.1**	**0.0200**
n	PI-PE 22-28	Addition N-terminus	46.19 ± 7.565	7	0.0009	119.7 ± 11.8	0.0070
o	Biotinylated-PI-PE 22-28	Addition N-terminus	49.11 ± 7.454	10	0.0001	124.1 ± 11.7	0.0080
	Palmitoyl-PE 22-28	Addition N-terminus	26.69 ± 16.45	12	0.133	ND	
	FITC-PE 22-28	Addition N-terminus	22.1 ± 12.63	9	0.1183	ND	
	Acetyl-PE 22-28	Addition N-terminus	20.49 ± 8.777	15	0.035	ND	
	Myristoyl-PE 22-28	Addition N-terminus	18.04 ± 17.77	13	0.3302	ND	
	Long Chain biotinylated-PE 22-28	Addition N-terminus	15.86 ± 11.21	12	0.1847	ND	
	5'FAM-PE 22-28	Addition N-terminus	6.633 ± 7.065	11	0.3699	ND	
	F-Moc-PE 22-28	Addition N-terminus	5.826 ± 10.91	11	0.6051	ND	
	Stearic acid-PE 22-28	Addition N-terminus	5.412 ± 5.496	32	0.3399	ND	

n, numbers of cells. In FST experiments, n, 10 mice for each peptide.
ns, not significant, ND, Not determined, p-values are from Student's t-test.
Bolded values correspond to the spadin-analogs retained for further studies.

(7 weeks) corticosterone treatment (Zhao et al., 2008), PE 22-28 displayed the same AD properties as spadin after acute or sub-chronic treatments (3.0 μg/kg) (**Figures 5C–E**). In the FST, PE 22-28 (3.0 μg/kg, ip) was slightly more efficient in decreasing immobility time (98.1 ± 8.78 s, $n = 10$, $p < 0.0001$) than spadin (100 μg/kg; 117.4 ± 6.85 s, $n = 10$, $p < 0.0001$) in this model of depression in comparison with control (164.9 ± 6.03 s) (**Figure 5C**). Moreover, 4-day sub-chronic administrations of spadin-analogs were significantly efficient in decreasing the immobility time (89.60 ± 7.7 s, $n = 10$, $p < 0.0001$) compared to spadin (107.5 ± 6.5 s, $n = 10$, $p < 0.0001$) or saline (158.3 ± 7.15 s, $n = 10$; **Figure 5D**). These data confirmed the AD action of spadin-analogs on control or corticosterone induced depressive mice.

In the NSF, 4-day sub-chronic treatments with PE 22-28 (3 μg/kg) or spadin (100 μg/kg) significantly reduced the latency to eat the food pellet (129.2 ± 15.28 s, $n = 10$, $p < 0.05$) and (153.2 ± 5.41 s, $n = 10$, $p < 0.05$) in spadin and PE 22-28 groups, respectively in comparison with control (226.1 ± 34.97 s, $n = 10$) in the corticosterone induced model of depression (**Figure 5E**). The NSF test predicts not only depression but also neurogenesis (Duman et al., 2001; Santarelli et al., 2003). We hypothesized that spadin-analogs could increase neurogenesis in the cortex and the hippocampus.

Spadin-Analogs Increase Neurogenesis *in Vivo* in the Hippocampus after 4-Day Treatment

Several studies demonstrated that a chronic AD treatment up-regulates neurogenesis in the hippocampus (Duman et al., 2001; Santarelli et al., 2003). We have previously shown that spadin increased neurogenesis and CREB activation in the hippocampus only after a 4-day treatment (Mazella et al., 2010). We wondered whether spadin-analogs produced the same effects. Mice were ip treated (3.0–4.0 μg/kg/day) for 4 days with spadin-analogs and, on the 5th day, were sacrificed. the 4-day treatment with spadin-analogs significantly increased BrdU positive cells (1736 ± 126 ($n = 5$, $p < 0.0001$), 2110 ± 132, ($n = 5$, $p < 0.0001$), 1809 ± 267 ($n = 5$, $p < 0.0001$), for PE 22-28, G/A-PE 22-28, and biotinylated-G/A-PE 22-28, respectively) in comparison with saline injected mice (899 ± 109, $n = 5$) (**Figure 6A**). These data confirmed that similarly to spadin, spadin-analogs have kept their ability to induce *in vivo* hippocampal neurogenesis.

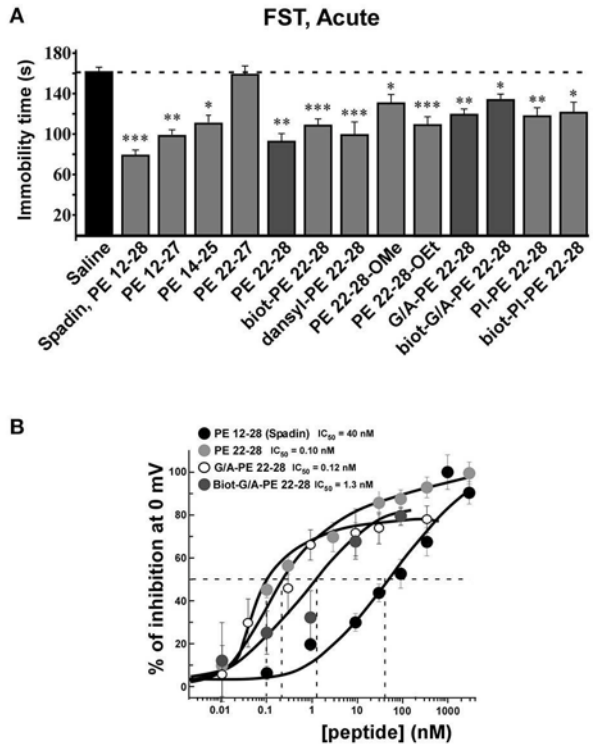

FIGURE 3 | FST and dose-response curves of TREK-1 current inhibition by spadin-analogs. **(A)** Peptides able to inhibit TREK-1 channel activity were tested in the FST. Immobility times were measured 30 min after ip injection and compared with the immobility time obtained with saline injected mice. Spadin was injected at 100 μg/kg and spadin-analogs were injected at 3.2–4.0 μg/kg. $^{*}p < 0.05$, $^{**}p < 0.01$, $^{***}p < 0.001$. **(B)** Dose-response curves of TREK-1 current inhibition at 0 mV obtained with spadin-analogs compared with spadin. IC_{50} were 0.1, 0.12, 1.2, and 40.0 nM for PE 22-28, G/A-PE 22-28, biotinylated-G/A-PE 22-28 and spadin, respectively.

Spadin-Analogs Increase Synaptogenesis *in Vitro* in Cortical Neurons

Incubation of cortical neurons with 0.1 μM of spadin-analogs enhanced synaptogenesis as illustrated by the increase in the expression of PSD-95 36 h after incubation (**Figures 6B–D**). Except a slight decrease during the first 5 h, spadin-analog treatments continuously increased the expression of PSD-95 up to 36 h (**Figure 6E**). These data showed that spadin-analogs not only increased neurogenesis but also synaptogenesis, indicating that the fate of a majority of newborn cells is to generate mature neurons.

Action Duration of Spadin-Analogs

Naïve mice (10 per time groups) were injected once to obtain a dose of 3.2 μg/kg or 32 μg/kg of G/A-PE 22-28 or a dose of 4.0 μg/kg or 40 μg/kg of biotinylated-G/A-PE 22-28. These doses were injected in a bolus of 100 μL of 0.9% NaCl. At times 1, 3, 5, 7, 12, 16, 20, and 24 h after injection, mice were submitted to FST (**Figure 7A**). Immobility times were compared to those obtained with mice injected with the saline solution (0.9% NaCl). FST for saline injected mice were only performed at times 1 and 24 h, immobility times were very similar, 171.2 ± 8.2 s and 175.5 ± 6.8 s, respectively (**Figure 7A**). To calculate the half-effect time, the immobility time measured at 1 h of saline injected mice was subtracted from the immobility time measured at 1 h for spadin-analogs, the difference value was considered as 100%. Other immobility times were normalized to the 100% value (**Figure 7B**). Calculated half-effect time values were 14, 17, 21, and 23 h for G/A-PE 22-28 (3.2 μg/kg), biotinylated-G/A-PE 22-28 (4.0 μg/kg), G/A-PE 22-28 (32 μg/kg) and biotinylated-G/A-PE 22-28 (40 μg/kg), respectively (**Figure 7B**). These values were higher than the one previously obtained with spadin (6 h) (Veyssiere et al., 2015).

DISCUSSION

Spadin-Analogs Are More Potent TREK-1 Blockers than Spadin

Depression is the most devastating and common mood disorder (Wong and Licinio, 2001). Treatments available nowadays target several proteins and undergo different mechanisms of action (Schechter et al., 2005). However, classical ADs are not fully specific and generally lead to side effects with different degree of severity. In order to avoid these adverse effects and improve the selectivity of the AD drugs, our strategy has consisted in focusing on improvement of the affinity, bioavailability and efficacy of the endogenous peptide that we have previously identified and called spadin (Mazella et al., 2010). Spadin was designed from a larger peptide called PE, a 44 aa peptide released in the blood flow following the translational maturation of the sortilin or neurotensin receptor 3 (Munck Petersen et al., 1999; Mazella, 2001). First, we identified degradation products of PE in the blood. From the peptides we identified we have designed a short 7 aa peptide, called PE-22-28. It displayed a better affinity for the TREK-1 potassium channel, a target that we have previously identified in the depression mechanism (Heurteaux et al., 2006). PE 22-28 was used for the design of 16 analogs. Because increasing the drug crossing through the blood brain barrier is a crucial goal for a therapeutic drug acting on brain targets and, because it was shown that biotinylation can increase peptide brain uptake, we synthesized some biotinylated derivatives (Scherrmann, 2002; Wu et al., 2002). By testing the different PE 22-28 derived peptides for their ability to inhibit TREK-1 channels expressed in the hTREK-1/HEK cell line (Moha ou Maati et al., 2011), we only retained those that inhibited more than 35% of TREK-1 activity in order to measure their AD properties by FST. Then, by comparing both abilities, we only retained 3 peptides (that we called spadin-analogs) PE 22-28, G/A-PE 22-28 and biotinylated-G/A-PE 22-28 for further studies.

Here, we showed that spadin-analogs displayed higher potencies in blocking TREK-1 channels when compared with spadin. Their IC_{50} were increased by more than 300 fold, 0.10 nM, and 0.12 nM for PE 22-28 and G/A-PE 22-28, respectively, these values have to be compared with spadin affinity, 40–60 nM (Mazella et al., 2010; Moha Ou Maati et al., 2012).

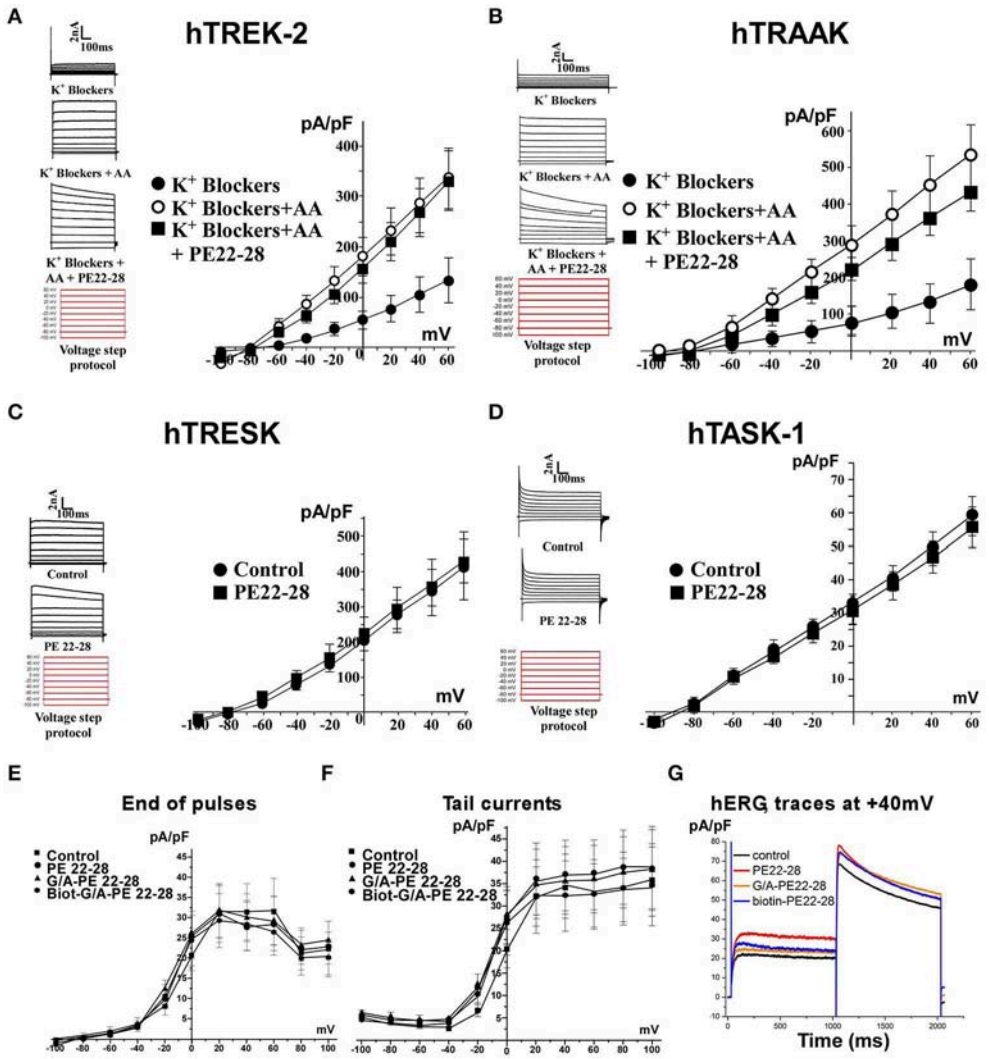

FIGURE 4 | Spadin-analog specificity. **(A–D)** PE 22-28 was used as the representative peptide for testing the specificity of spadin-analogs vs. other K_{2P} channels, TREK-2 **(A)**, TRAAK **(B)**, TRESK **(C)**, and TASK-1 **(D)**. **(E–G)** Spadin-analogs were without effect on hERG channel activity. Current densities at the end of pulses **(E)**, current densities of tail currents **(F)**, and typical traces obtained at +40 mV with spadin-analogs **(G)**.

Spadin-Analogs Are Specific for the TREK-1 Channel

Additionally, spadin-analogs have kept their specificity for TREK-1 channels (Moha Ou Maati et al., 2012). They were unable to inhibit TREK-2 and TRAAK channels, the two other members of the TREK channel sub-family (Kim et al., 2001; Honore, 2007). The specificity of spadin and its analogs for TREK-1 channel could be accounted by the sequence differences between the three channels: TREK-1 and TREK-2 share 63% of identity and only 45% between TREK-1 and TRAAK (Noel et al., 2011). They were also unable to inhibit TRESK (Lafreniere et al., 2010; Wood, 2010) and TASK-1 (Lauritzen et al., 2003) channels, two K_{2P} channels that are important in the brain and, as TREK-1 they are both modulated by volatile anaesthetics (Patel and Honore, 2001). Here again, sequence differences could account for the absence of effects, homologies between TREK-1 and both channels are around 50% (Noel et al., 2011). More noteworthy, spadin-analogs were devoid of effects on hERG channels that are responsible for the cardiac I_{Kr} current, one of the main potassium repolarizing current in the cardiac ventricle (Sanguinetti and Jurkiewicz, 1990; Cheng and Kodama, 2004).

Spadin and its analogs block TREK-1 channels more efficiently when they are activated by arachidonic acid indicating the need of an open-state conformation of the channel. The weak direct inhibition of TREK-1 in basal condition could be due to the necessity for spadin to access the selectivity filter in a closed channel.

The monoamine hypothesis of depression was expanded to other recent hypotheses mainly the neurotrophic and neurogenesis hypothesis that suggest that a decrease in neurotrophic factors, such as the brain-derived neurotrophic factor (BDNF) or in adult hippocampal neurogenesis are

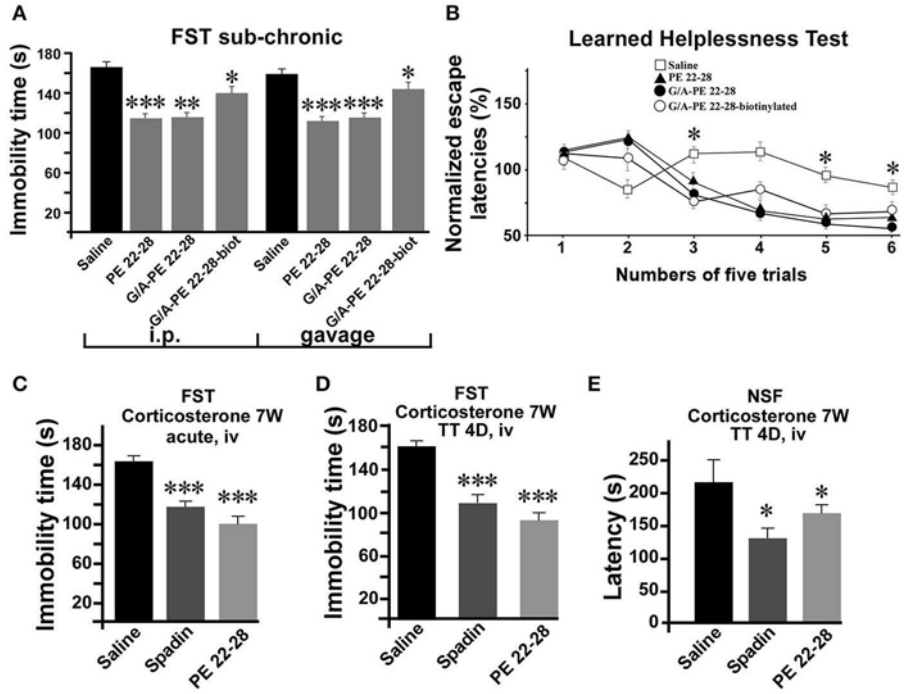

FIGURE 5 | Behavior of spadin-analogs in mouse model of depression. **(A)** FST performed after a sub-chronic (4 days) treatment (3.0–4.0 μg/kg) with each spadin-analog or the 0.9% NaCl saline solution. Treatments were administered either by ip injection (100 μg/kg) or by gavage (1.0 mg/kg). **(B)** The Learned Helplessness test performed with each spadin-analog (3.0–4.0 μg/kg). 30 trials were divided in 6 pools of five trials. $^{*}p < 0.05$. **(C,D)** Corticosterone-induced model of depression. PE 22-28 was used as the representative peptide for spadin-analogs for comparing the effects of spadin-analogs with those of spadin in this chemically-induced mouse model. FST performed after acute (30 min after injection, **(C)** or sub-chronic (4 days treatment, **D**) ip injections of spadin (100 μg/kg) or PE 22-28 (3.0 μg/kg). Sub-chronic treatments administered at the same doses were also used before the NSF **(E)**. $^{*}p < 0.05$, $^{**}p < 0.01$, $^{***}p < 0.001$.

in one way or another associated with depression (Yohn et al., 2017). Classical ADs take several weeks to produce antidepressant activity, a mechanism that is thought to be mediated through neurogenesis (Santarelli et al., 2003; Malberg and Schechter, 2005). Interestingly, spadin and analogs display their antidepressant response within 4-day treatment, this short time correlates with the same period required for hippocampal neurogenesis to develop (Devader et al., 2015). The rapid increase in the BDNF expression in the hippocampus after *in vivo* administration of spadin points out the fact that spadin and derivative peptides induce a fast expression of BDNF to be distinguished from the slow BDNF expression observed with the conventional ADs. Two phases, fast and slow, are also observed with ketamine (Kavalali and Monteggia, 2015). Nevertheless, cellular pathway of neurogenesis activation are different. Ketamine uses the mTOR pathway (Kavalali and Monteggia, 2015) whereas spadin does not interfere with mTOR signaling (Devader et al., 2015).

Spadin-Analogs Are Potent Antidepressants

Spadin-analogs have also kept the AD properties of spadin. We showed that spadin-analogs behaved as an AD drug in the FST but also in the learned helplessness test. Both tests are commonly and widely used by pharmaceutical industries for characterizing new AD drugs. Importantly, we showed that spadin-analogs were also efficient after gavage, indicating that these molecules could be administered *per os*. Interestingly, in a chemically (corticosterone)-induced model of depression spadin-analogs were as efficient as spadin for decreasing depression-like behavior generated by the corticosterone treatment. As expected for spadin derivatives, spadin-analogs were efficient after only 4 days of treatment. This unique property is crucial because it considerably reduces the onset time to observe the efficiency of the AD treatment. That is particularly interesting because the majority of suicides occurs during the first weeks following an AD treatment (Moller, 2003).

Spadin-Analogs Are More Stable than Spadin *in Vivo*

Another remarkable property of spadin-analogs is their prolonged action duration. Despite a relatively short *in vitro* serum half-life time, the *in vivo* antidepressant efficacy measured by FST lasted for almost 24 h. G/A-PE 22-28 or biotinylated-G/A-PE 22-28 injected at doses as low as 32.0 or 40.0 μg/kg, respectively had a half-time of effect of 23 and 21 h after injection. These values represent a huge improvement in comparison with spadin. In the same conditions, the half-time effect of spadin at a dose of 100 μg/kg was only of 6 h (Veyssiere et al., 2015).

Chronic treatments with ADs are known to induce neurogenesis in the hippocampus (Duman et al., 2001; Malberg and Schechter, 2005). However, neurogenesis up-regulation

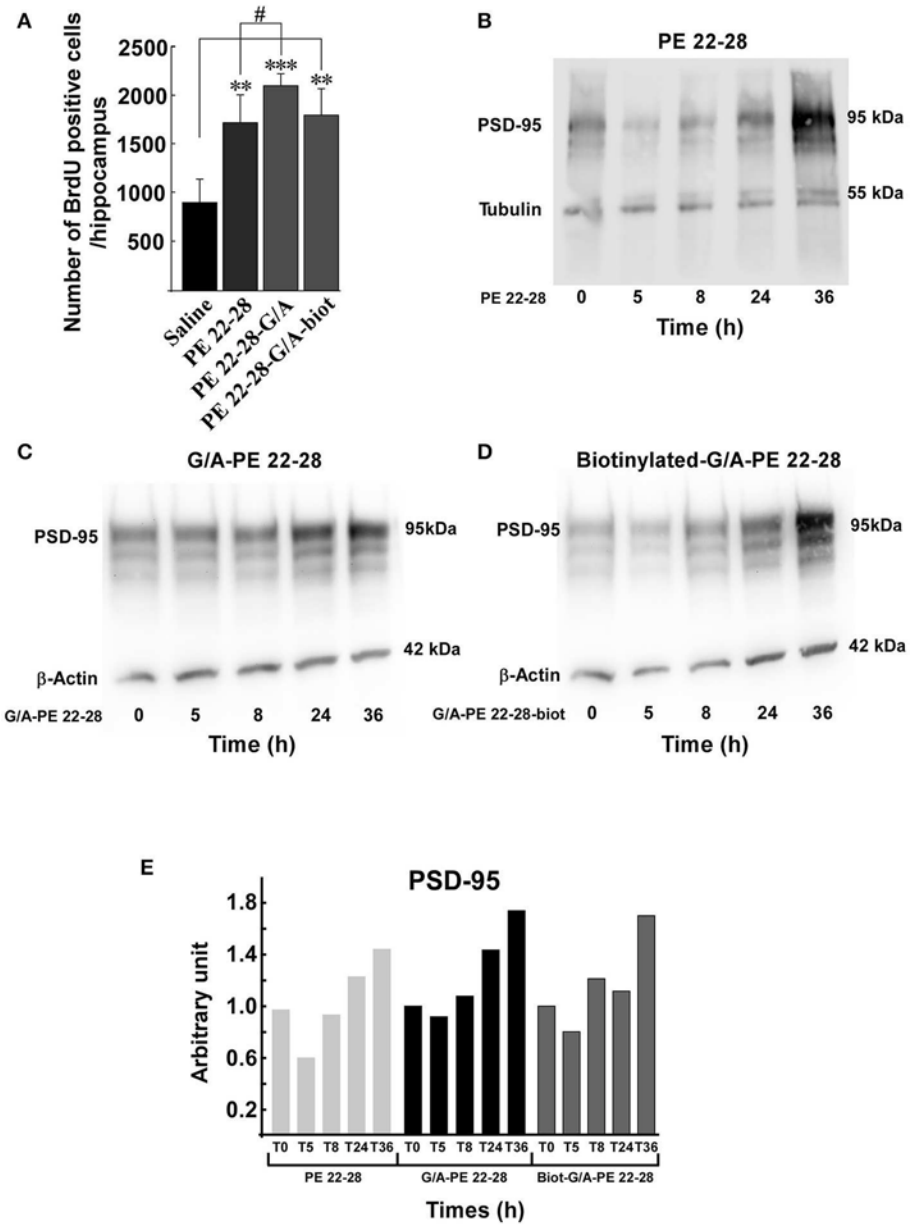

FIGURE 6 | Neurogenesis and synaptogenesis. **(A)** Neurogenesis was assessed by measuring the number of BrdU positive cells per hippocampus after sub-chronic treatments (3.0–4.0 μg/kg, 4 days) with spadin-analogs. The cell number was given for the entirety of hippocampus. $^{**}p < 0.01$, $^{***}p < 0.001$, $^{\#}p < 0.05$. **(B–D)** Synaptogenesis was assessed by measuring the increase in the level of PSD-95 in mouse cortical neuron. Mouse cortical neurons were treated with 0.1 μM of the indicated spadin-analog PE 22-28 **(B)**, G/A-PE 22-28 **(C)** and biotinylated-G/A-PE 22-28 **(D)**. At the indicated times neurons were homogenized in Laemmli buffer and submitted to Western blot analysis. **(E)** Histogram illustration of the PSD-95. For each spadin-analog, the PSD-95 amount at 36 h was about twice than that measured at 5 h.

currently occurs after 2–4 weeks of administration. This is consistent with the fact that classical ADs are efficient only after the same period. Previously, we have shown that spadin was able to increase BrdU incorporation and CREB activation after only 4 days of treatment (Mazella et al., 2010). *In vivo* administration of spadin induces neurogenesis over different time scale through two phases, a rapid increase in the expression of BDNF and a slow spine maturation (Devader et al., 2015). Since targets and specificity for these targets are the same between spadin and its derivatives, we could speculate that spadin analogs could behave identically to spadin. Here, we demonstrated that spadin-analogs were also able to induce neurogenesis in the dentate gyrus. Interestingly, spadin-analog treatments also increased the PSD-95 expression, a biomarker of synaptogenesis. These observations indicated that number of newborn neurons were functional and should participate to

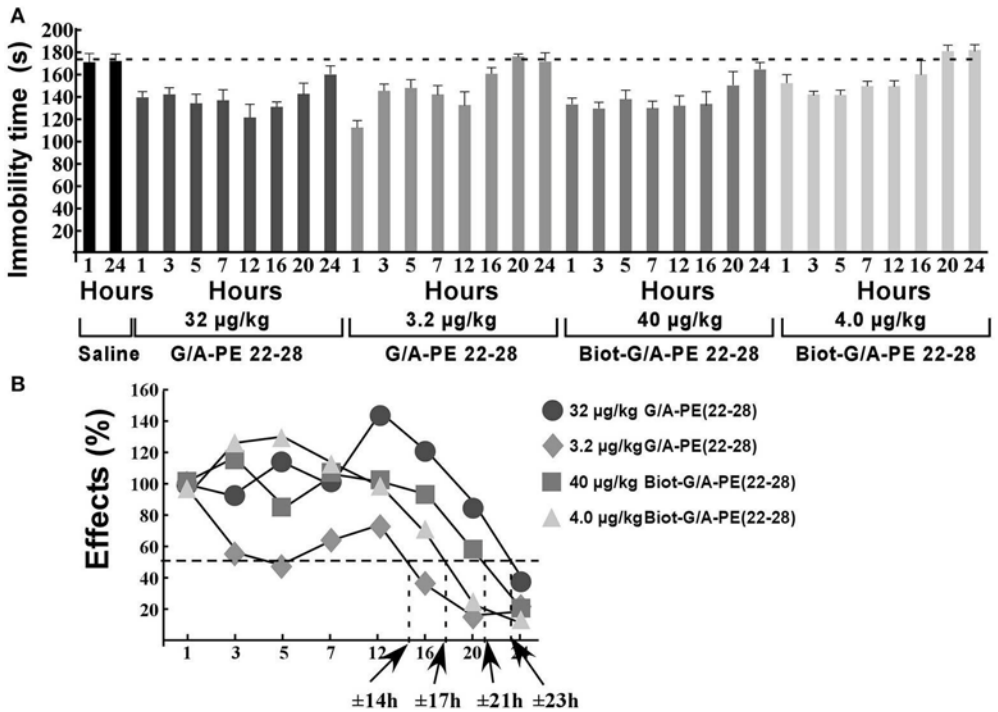

FIGURE 7 | Action duration of G/A-PE 22-28 and biotinylated-G/A-PE 22-28 measured by FST. **(A)** At each time-point, 10 naïve mice were tested for immobility in the FST. Saline injected mice were tested only at two times, 1 and 24 h. For each spadin-analog, at time 1 h the difference between saline and spadin-analog treated mice was considered as 100%, Time-point immobility times were normalized to this 100% value. **(B)** Half-time effects were approximately of 14, 21, 17, and 23 h for 3.2 μg/kg of G/A-PE 22-28, 32 μg/kg of G/A-PE 22-28, 4.0 μg/kg of biotinylated-G/A-PE 22-28 and 40 μg/kg of biotinylated-G/A-PE 22-28, respectively.

the brain network. This property is crucial for the AD action of spadin-analogs.

CONCLUSION

Our final goal is to make spadin-analogs drugs usable in clinics. All our data converge toward this goal. Spadin-analogs are specific for the TREK-1 channel, a target in the depression pathway, and efficient as AD. They induce neurogenesis after only 4 days of treatment. We have demonstrated that spadin and its retro-inverso analogs have no deleterious effects on pain, ischemia or at the cardiac levels (Moha Ou Maati et al., 2012). Since spadin analogs share the same targets (TREK-1 and NTR-3) and, have no effect on the other K_{2P} channels, more importantly they do not modify hERG channel activity then, we could expect that spadin analogs would be devoid of side effects. The absence of adverse effects differentiates spadin-analogs from other antidepressant drugs, such as SSRIs, SNRIs, tricyclics (Ferguson, 2001), or ketamine (Katalinic et al., 2013). Additionally to the shared properties with spadin, spadin-analogs display a largely increased affinity for TREK-1 and, also a largely increased action duration. Another important point concerns the shortening of the peptide that will induce a lower cost for the drug manufacturing and *in fine* a decrease of economic burden to treat depressive patients. All these reasons encourage us to think that in the really near future spadin-analogs will constitute a promising alternative to spadin and become efficient AD drugs usable in clinic.

AUTHOR CONTRIBUTIONS

AD, performed electrophysiological experiments. MP, performed behavioral experiments. SM, performed biochemical experiments. CH, JM, and MB, conceived and designed the experiments. CH, JM, and MB, contributed reagents/materials/analysis tools and wrote the paper.

FUNDING

This work was supported by the Centre National de la Recherche Scientifique and the Agence Nationale de la Recherche (ANR-13-SAMA-0001 and 0002 and ANR-13-RPIB-0001 and 0002). We also thank the French Government for the "Investments for the Future" LabEx ICST # ANR-11 LabEx 0015 and the Fondation de l'Avenir N° AP-RMA-2015-021. MP was supported by a CIFRE fellowship.

SUPPLEMENTARY MATERIAL

The Supplementary Material for this article can be found online at: http://journal.frontiersin.org/article/10.3389/fphar.2017.00643/full#supplementary-material

REFERENCES

Alloui, A., Zimmermann, K., Mamet, J., Duprat, F., Noel, J., Chemin, J., et al. (2006). TREK-1, a K^+ channel involved in polymodal pain perception. *EMBO J.* 25, 2368–2376. doi: 10.1038/sj.emboj.7601116

Borsotto, M., Veyssiere, J., Moha Ou Maati, H., Devader, C., Mazella, J., and Heurteaux, C. (2015). Targeting two-pore domain K^+ channels TREK-1 and TASK-3 for the treatment of depression: a new therapeutic concept. *Br. J. Pharmacol.* 172, 771–784. doi: 10.1111/bph.12953

Caldarone, B. J., George, T. P., Zachariou, V., and Picciotto, M. R. (2000). Gender differences in learned helplessness behavior are influenced by genetic background. *Pharmacol. Biochem. Behav.* 66, 811–817. doi: 10.1016/S0091-3057(00)00271-9

Cheng, J. H., and Kodama, I. (2004). Two components of delayed rectifier K^+ current in heart: molecular basis, functional diversity, and contribution to repolarization. *Acta Pharmacol. Sin.* 25, 137–145.

Cleare, A., Pariante, C. M., Young, A. H., Anderson, I. M., Christmas, D., Cowen, P. J., et al. (2015). Evidence-based guidelines for treating depressive disorders with antidepressants: a revision of the 2008 British Association for Psychopharmacology guidelines. *J. Psychopharmacol.* 29, 459–525. doi: 10.1177/0269881115581093

Deardorff, W. J., and Grossberg, G. T., (2014). A review of the clinical efficacy, safety and tolerability of the antidepressants vilazodone, levomilnacipran and vortioxetine. *Expert Opin. Pharmacother.* 15, 2525–2542. doi: 10.1517/14656566.2014.960842

Decher, N., Kiper, A. K., and Rinne, S. (2017). Stretch-activated potassium currents in the heart: focus on TREK-1 and arrhythmias. *Prog. Biophys. Mol. Biol.* doi: 10.1016/j.pbiomolbio.2017.05.005. [Epub ahead of print].

Devader, C., Khayachi, A., Veyssiere, J., Moha Ou Maati, H., Roulot, M., Moreno, S., et al. (2015). *In vitro* and *in vivo* regulation of synaptogenesis by the novel antidepressant spadin. *Br. J. Pharmacol.* 172, 2604–2617. doi: 10.1111/bph.13083

Duman, R. S., Nakagawa, S., and Malberg, J. (2001). Regulation of adult neurogenesis by antidepressant treatment. *Neuropsychopharmacology* 25, 836–844. doi: 10.1016/S0893-133X(01)00358-X

Ferguson, J. M. (2001). SSRI Antidepressant medications: adverse effects and tolerability. *Prim. Care Companion J. Clin. Psychiatry* 3, 22–27. doi: 10.4088/PCC.v03n0105

Heijnen, W. T., Birkenhager, T. K., Wierdsma, A. I., and van den Broek, W. W. (2010). Antidepressant pharmacotherapy failure and response to subsequent electroconvulsive therapy: a meta-analysis. *J. Clin. Psychopharmacol.* 30, 616–619. doi: 10.1097/JCP.0b013e3181ee0f5f

Heurteaux, C., Lucas, G., Guy, N., El Yacoubi, M., Thümmler, S., Peng, X., et al. (2006). Deletion of TREK-1, a background potassium channel, results in a depression-resistant phenotype. *Nature Neurosci.* 9, 1134–1141. doi: 10.1038/nn1749

Hillhouse, T. M., and Porter, J. H. (2015). A brief history of the development of antidepressant drugs: from monoamines to glutamate. *Exp. Clin. Psychopharmacol.* 23, 1–21. doi: 10.1037/a0038550

Hirschfeld, R. M. (2012). The epidemiology of depression and the evolution of treatment. *J. Clin. Psychiatry* 73(Suppl. 1), 5–9. doi: 10.4088/JCP.11096su1c.01

Honore, E. (2007). The neuronal background K_{2P} channels: focus on TREK1. *Nat. Rev. Neurosci.* 8, 251–261. doi: 10.1038/nrn2117

Katalinic, N., Lai, R., Somogyi, A., Mitchell, P. B., Glue, P., and Loo, C. K. (2013). Ketamine as a new treatment for depression: a review of its efficacy and adverse effects. *Aust. N. Z. J. Psychiatry* 47, 710–727. doi: 10.1177/0004867413486842

Kavalali, E. T., and Monteggia, L. M. (2015). How does ketamine elicit a rapid antidepressant response? *Curr. Opin. Pharmacol.* 20, 35–39. doi: 10.1016/j.coph.2014.11.005

Kessler, R. C., Petukhova, M., Sampson, N. A., Zaslavsky, A. M., and Wittchen, H. U. (2012). Twelve-month and lifetime prevalence and lifetime morbid risk of anxiety and mood disorders in the United States. *Int. J. Methods Psychiatr. Res.* 21, 169–184. doi: 10.1002/mpr.1359

Kim, Y., Gnatenco, C., Bang, H., and Kim, D. (2001). Localization of TREK-2 K^+ channel domains that regulate channel kinetics and sensitivity to pressure, fatty acids and pHi. *Pflugers Arch.* 442, 952–960. doi: 10.1007/s004240100626

Kohler, S., Cierpinsky, K., Kronenberg, G., and Adli, M. (2016). The serotonergic system in the neurobiology of depression: relevance for novel antidepressants. *J. Psychopharmacol.* 30, 13–22. doi: 10.1177/0269881115609072

Krishnan, V., and Nestler, E. J. (2008). The molecular neurobiology of depression. *Nature* 455, 894–902. doi: 10.1038/nature07455

Lafreniere, R. G., Cader, M. Z., Poulin, J. F., Andres-Enguix, I., Simoneau, M., Gupta, N., et al. (2010). A dominant-negative mutation in the TRESK potassium channel is linked to familial migraine with aura. *Nat. Med.* 16, 1157–1160. doi: 10.1038/nm.2216

Lauritzen, I., Blondeau, N., Heurteaux, C., Widmann, C., Romey, G., and Lazdunski, M. (2000). Polyunsaturated fatty acids are potent neuroprotectors. *EMBO J.* 19, 1784–1793. doi: 10.1093/emboj/19.8.1784

Lauritzen, I., Zanzouri, M., Honore, E., Duprat, F., Ehrengruber, M. U., Lazdunski, M., et al. (2003). K^+-dependent cerebellar granule neuron apoptosis. Role of task leak K^+ channels. *J. Biol. Chem.* 278, 32068–32076. doi: 10.1074/jbc.M302631200

Lesage, F., and Lazdunski, M. (2000). Molecular and functional properties of two pore domain potassium channels. *Am. J. Physiol.* 279, 793–801.

Li, Y., Abdourahman, A., Tamm, J. A., Pehrson, A. L., Sanchez, C., and Gulinello, M. (2015). Reversal of age-associated cognitive deficits is accompanied by increased plasticity-related gene expression after chronic antidepressant administration in middle-aged mice. *Pharmacol. Biochem. Behav.* 135, 70–82. doi: 10.1016/j.pbb.2015.05.013

Malberg, J. E., and Schechter, L. E. (2005). Increasing hippocampal neurogenesis: a novel mechanism for antidepressant drugs. *Curr. Pharm. Des.* 11, 145–155. doi: 10.2174/1381612053382223

Maletic, V., Robinson, M., Oakes, T., Iyengar, S., Ball, S. G., and Russell, J. (2007). Neurobiology of depression: an integrated view of key findings. *Int. J. Clin. Pract.* 61, 2030–2040. doi: 10.1111/j.1742-1241.2007.01602.x

Mazella, J. (2001). Sortilin/neurotensin receptor-3: a new tool to investigate neurotensin signaling and cellular trafficking? *Cell. Signal.* 13, 1–6. doi: 10.1016/S0898-6568(00)00130-3

Mazella, J., Petrault, O., Lucas, G., Deval, E., Beraud-Dufour, S., Gandin, C., et al. (2010). Spadin, a sortilin-derived peptide, targeting rodent TREK-1 channels: a new concept in the antidepressant drug design. *PLoS Biol.* 8:e1000355. doi: 10.1371/journal.pbio.1000355

Moha ou Maati, H., Peyronnet, R., Devader, C., Veyssiere, J., Labbal, F., Gandin, C., et al. (2011). A human TREK-1/HEK cell line: a highly efficient screening tool for drug development in neurological diseases. *PLoS ONE* 6:e25602. doi: 10.1371/journal.pone.0025602

Moha Ou Maati, H., Veyssiere, J., Labbal, F., Coppola, T., Gandin, C., Widmann, C., et al. (2012). Spadin as a new antidepressant: absence of TREK-1-related side effects. *Neuropharmacology* 62, 278–288. doi: 10.1016/j.neuropharm.2011.07.019

Moller, H. J. (2003). Suicide, suicidality and suicide prevention in affective disorders. *Acta Psychiatr. Scand. Suppl.* 418, 73–80. doi: 10.1034/j.1600-0447.108.s418.15.x

Munck Petersen, C., Nielsen, M. S., Jacobsen, C., Tauris, J., Jacobsen, L., Gliemann, J., et al. (1999). Propeptide cleavage conditions sortilin/neurotensin receptor-3 for ligand binding. *EMBO J.* 18, 595–604. doi: 10.1093/emboj/18.3.595

Nestler, E. J., Barrot, M., DiLeone, R. J., Eisch, A. J., Gold, S. J., and Monteggia, L. M. (2002). Neurobiology of depression. *Neuron* 34, 13–25. doi: 10.1016/S0896-6273(02)00653-0

Noel, J., Sandoz, G., and Lesage, F. (2011). Molecular regulations governing TREK and TRAAK channel functions. *Channels* 5, 402–409. doi: 10.4161/chan.5.5.16469

Patel, A. J., and Honore, E. (2001). Properties and modulation of mammalian 2P domain K^+ channels. *Trends Neurosci.* 24, 339–346. doi: 10.1016/S0166-2236(00)01810-5

Patel, A. J., Honore, E., Maingret, F., Lesage, F., Fink, M., Duprat, F., et al. (1998). A mammalian two pore domain mechano-gated S-like K^+ channel. *EMBO J.* 17, 4283–4290. doi: 10.1093/emboj/17.15.4283

Porsolt, R. D., Le Pichon, M., and Jalfre, M. (1977). Depression: a new animal model sensitive to antidepressant treatments. *Nature* 266, 730–732. doi: 10.1038/266730a0

Ramaker, M. J., and Dulawa, S. C. (2017). Identifying fast-onset antidepressants using rodent models. *Mol. Psychiatry* 22, 656–665. doi: 10.1038/mp.2017.36

Rush, A. J., Trivedi, M. H., Wisniewski, S. R., Nierenberg, A. A., Stewart, J. W., Warden, D., et al. (2006). Acute and longer-term outcomes in depressed outpatients requiring one or several treatment steps: a STAR*D report. *Am. J. Psychiatry* 163, 1905–1917. doi: 10.1176/ajp.2006.163.11.1905

Sanguinetti, M. C., and Jurkiewicz, N. K. (1990). Two components of cardiac delayed rectifier K^+ current. Differential sensitivity to block by class III antiarrhythmic agents. *J. Gen. Physiol.* 96, 195–215. doi: 10.1085/jgp.96.1.195

Santarelli, L., Saxe, M., Gross, C., Surget, A., Battaglia, F., Dulawa, S., et al. (2003). Requirement of hippocampal neurogenesis for the behavioral effects of antidepressants. *Science.* 301, 805–809. doi: 10.1126/science.1083328

Schechter, L. E., Ring, R. H., Beyer, C. E., Hughes, Z. A., Khawaja, X., Malberg, J. E., et al. (2005). Innovative approaches for the development of antidepressant drugs: current and future strategies. *NeuroRx* 2, 590–611. doi: 10.1602/neurorx.2.4.590

Scherrmann, J. M. (2002). Drug delivery to brain via the blood-brain barrier. *Vascul. Pharmacol.* 38, 349–354. doi: 10.1016/S1537-1891(02)00202-1

Semkovska, M., and McLoughlin, D. M. (2010). Objective cognitive performance associated with electroconvulsive therapy for depression: a systematic review and meta-analysis. *Biol. Psychiatry* 68, 568–577. doi: 10.1016/j.biopsych.2010.06.009

Smith, K. (2014). Mental health: a world of depression. *Nature* 515, 181. doi: 10.1038/515180a

Sowa-Kucma, M., Panczyszyn-Trzewik, P., Misztak, P., Jaeschke, R. R., Sendek, K., Styczen, K., et al. (2017). Vortioxetine: a review of the pharmacology and clinical profile of the novel antidepressant. *Pharmacol. Rep.* 69, 595–601. doi: 10.1016/j.pharep.2017.01.030

Talley, E. M., Solorzano, G., Lei, Q., Kim, D., and Bayliss, D. A. (2001). Cns distribution of members of the two-pore-domain (KCNK) potassium channel family. *J. Neurosci.* 21, 7491–7505.

Thase, M. E., Mahableshwarkar, A. R., Dragheim, M., Loft, H., and Vieta, E. (2016). A meta-analysis of randomized, placebo-controlled trials of vortioxetine for the treatment of major depressive disorder in adults. *Eur. Neuropsychopharmacol.* 26, 979–993. doi: 10.1016/j.euroneuro.2016.03.007

Veyssiere, J., Moha Ou Maati, H., Mazella, J., Gaudriault, G., Moreno, S., Heurteaux, C., et al. (2015). Retroinverso analogs of spadin display increased antidepressant effects. *Psychopharmacology* 232, 561–574. doi: 10.1007/s00213-014-3683-2

Wang, S. M., Han, C., Lee, S. J., Patkar, A. A., Masand, P. S., and Pae, C. U. (2015). Vilazodone for the treatment of major depressive disorder: focusing on its clinical studies and mechanism of action. *Psychiatry Investig.* 12, 155–163. doi: 10.4306/pi.2015.12.2.155

Wiedmann, F., Schmidt, C., Lugenbiel, P., Staudacher, I., Rahm, A. K., Seyler, C., et al. (2016). Therapeutic targeting of two-pore-domain potassium (K_{2P}) channels in the cardiovascular system. *Clin. Sci.* 130, 643–650. doi: 10.1042/CS20150533

Wong, M. L., and Licinio, J. (2001). Research and treatment approaches to depression. *Nat. Rev. Neurosci.* 2, 343–351. doi: 10.1038/35072566

Wood, H. (2010). Migraine: familial migraine with aura is associated with a mutation in the TRESK potassium channel. *Nat. Rev. Neurol.* 6:643. doi: 10.1038/nrneurol.2010.166

Wu, D., Song, B. W., Vinters, H. V., and Pardridge, W. M. (2002). Pharmacokinetics and brain uptake of biotinylated basic fibroblast growth factor conjugated to a blood-brain barrier drug delivery system. *J. Drug Target.* 10, 239–245. doi: 10.1080/10611860290022679

Yohn, C. N., Gergues, M. M., and Samuels, B. A. (2017). The role of 5-HT receptors in depression. *Mol. Brain* 10, 28. doi: 10.1186/s13041-017-0306-y

Zhao, Y., Ma, R., Shen, J., Su, H., Xing, D., and Du, L. (2008). A mouse model of depression induced by repeated corticosterone injections. *Eur. J. Pharmacol.* 581, 113–120. doi: 10.1016/j.ejphar.2007.12.005

Conflict of Interest Statement: The authors declare that the research was conducted in the absence of any commercial or financial relationships that could be construed as a potential conflict of interest.

Copyright © 2017 Djillani, Pietri, Moreno, Heurteaux, Mazella and Borsotto. This is an open-access article distributed under the terms of the Creative Commons Attribution License (CC BY). The use, distribution or reproduction in other forums is permitted, provided the original author(s) or licensor are credited and that the original publication in this journal is cited, in accordance with accepted academic practice. No use, distribution or reproduction is permitted which does not comply with these terms.

REFERENCES

Akil, H., Perraud, A., Mélin, C., Jauberteau, M.-O., and Mathonnet, M. (2011). Fine-tuning roles of endogenous brain-derived neurotrophic factor, TrkB and sortilin in colorectal cancer cell survival. PLoS ONE *6*, e25097.

Allen, A.P., Naughton, M., Dowling, J., Walsh, A., Ismail, F., Shorten, G., Scott, L., McLoughlin, D.M., Cryan, J.F., Dinan, T.G., et al. (2015). Serum BDNF as a peripheral biomarker of treatment-resistant depression and the rapid antidepressant response: A comparison of ketamine and ECT. Journal of Affective Disorders *186*, 306–311.

Alloui, A., Zimmermann, K., Mamet, J., Duprat, F., Noël, J., Chemin, J., Guy, N., Blondeau, N., Voilley, N., Rubat-Coudert, C., et al. (2006). TREK-1, a K+ channel involved in polymodal pain perception. EMBO J. *25*, 2368–2376.

Angelucci, F., Brenè, S., and Mathé, A.A. (2005). BDNF in schizophrenia, depression and corresponding animal models. Mol. Psychiatry *10*, 345–352.

Arango, V., Underwood, M.D., Boldrini, M., Tamir, H., Kassir, S.A., Hsiung, S., Chen, J.J., and Mann, J.J. (2001). Serotonin 1A receptors, serotonin transporter binding and serotonin transporter mRNA expression in the brainstem of depressed suicide victims. Neuropsychopharmacology *25*, 892–903.

Arrighi, I., Lesage, F., Scimeca, J.C., Carle, G.F., and Barhanin, J. (1998). Structure, chromosome localization, and tissue distribution of the mouse twik K+ channel gene. FEBS Lett. *425*, 310–316.

Asberg, M. (1997). Neurotransmitters and suicidal behavior. The evidence from cerebrospinal fluid studies. Ann. N. Y. Acad. Sci. *836*, 158–181.

Baker, G.B., Coutts, R.T., Yeung, J.M., Hampson, D.R., McIntosh, G.J.A., and McIntosh, M.G. (1985). Chronic Administration of Monoamine Oxidase Inhibitors: Basic and Clinical Investigations. In Neuropsychopharmacology of the Trace Amines, (Humana Press), pp. 317–328.

Bath, K.G., and Lee, F.S. (2006). Variant BDNF (Val66Met) impact on brain structure and function. Cogn Affect Behav Neurosci *6*, 79–85.

Battey, F.D., Gåfvels, M.E., FitzGerald, D.J., Argraves, W.S., Chappell, D.A., Strauss, J.F., and Strickland, D.K. (1994). The 39-kDa receptor-associated protein regulates ligand binding by the very low density lipoprotein receptor. J. Biol. Chem. *269*, 23268–23273.

Bekinschtein, P., Cammarota, M., Igaz, L.M., Bevilaqua, L.R.M., Izquierdo, I., and Medina, J.H. (2007). Persistence of long-term memory storage requires a late protein synthesis- and BDNF- dependent phase in the hippocampus. Neuron *53*, 261–277.

Belzeaux, R., Formisano-Tréziny, C., Loundou, A., Boyer, L., Gabert, J., Samuelian, J.-C., Féron, F., Naudin, J., and Ibrahim, E.C. (2010). Clinical variations modulate patterns of gene expression and define blood biomarkers in major depression. Journal of Psychiatric Research *44*, 1205–1213.

Belzeaux, R., Bergon, A., Jeanjean, V., Loriod, B., Formisano-Tréziny, C., Verrier, L., Loundou, A., Baumstarck-Barrau, K., Boyer, L., Gall, V., et al. (2012). Responder and nonresponder patients exhibit different peripheral transcriptional signatures during major depressive episode. Transl Psychiatry *2*, e185.

Béraud-Dufour, S., Coppola, T., Massa, F., and Mazella, J. (2009). Neurotensin receptor-2 and -3 are crucial for the anti-apoptotic effect of neurotensin on pancreatic beta-TC3 cells. Int. J. Biochem. Cell Biol. *41*, 2398–2402.

Béraud-Dufour, S., Abderrahmani, A., Noel, J., Brau, F., Waeber, G., Mazella, J., and Coppola, T. (2010). Neurotensin is a regulator of insulin secretion in pancreatic beta-cells. Int. J. Biochem. Cell Biol. *42*, 1681–1688.

Blaha, C.D., and Phillips, A.G. (1992). Pharmacological evidence for common mechanisms underlying the effects of neurotensin and neuroleptics on in vivo dopamine efflux in the rat nucleus accumbens. Neuroscience *49*, 867–877.

Borroto-Escuela, D.O., Ravani, A., Tarakanov, A.O., Brito, I., Narvaez, M., Romero-Fernandez, W., Corrales, F., Agnati, L.F., Tanganelli, S., Ferraro, L., et al. (2013). Dopamine D2 receptor signaling dynamics of dopamine D2-neurotensin 1 receptor heteromers. Biochem. Biophys. Res. Commun. *435*, 140–146.

Botto, J.M., Guillemare, E., Vincent, J.P., and Mazella, J. (1997). Effects of SR 48692 on neurotensin-induced calcium-activated chloride currents in the Xenopus oocyte expression system: agonist-like activity on the levocabastine-sensitive neurotensin receptor and absence of antagonist effect on the levocabastine insensitive neurotensin receptor. Neurosci. Lett. *223*, 193–196.

Boudin, H., Pélaprat, D., Rostène, W., and Beaudet, A. (1996). Cellular distribution of neurotensin receptors in rat brain: immunohistochemical study using an antipeptide antibody against the cloned high affinity receptor. J. Comp. Neurol. *373*, 76–89.

Boyle, M.P., Brewer, J.A., Funatsu, M., Wozniak, D.F., Tsien, J.Z., Izumi, Y., and Muglia, L.J. (2005). Acquired deficit of forebrain glucocorticoid receptor produces depression-like changes in adrenal axis regulation and behavior. Proc. Natl. Acad. Sci. U.S.A. *102*, 473–478.

Brickley, S.G., Aller, M.I., Sandu, C., Veale, E.L., Alder, F.G., Sambi, H., Mathie, A., and Wisden, W. (2007). TASK-3 two-pore domain potassium channels enable sustained high-frequency firing in cerebellar granule neurons. J. Neurosci. *27*, 9329–9340.

Buckler, K.J., Williams, B.A., and Honore, E. (2000). An oxygen-, acid- and anaesthetic-sensitive TASK-like background potassium channel in rat arterial chemoreceptor cells. J Physiol *525*, 135–142.

Burke, H.M., Davis, M.C., Otte, C., and Mohr, D.C. (2005). Depression and cortisol responses to psychological stress: a meta-analysis. Psychoneuroendocrinology *30*, 846–856.

Buttenschøn, H.N., Demontis, D., Kaas, M., Elfving, B., Mølgaard, S., Gustafsen, C., Kaerlev, L., Petersen, C.M., Børglum, A.D., Mors, O., et al. (2015). Increased serum levels of sortilin are associated with depression and correlated with BDNF and VEGF. Transl Psychiatry *5*, e677.

Canuel, M., Lefrancois, S., Zeng, J., and Morales, C.R. (2008). AP-1 and retromer play opposite roles in the trafficking of sortilin between the Golgi apparatus and the lysosomes. Biochem. Biophys. Res. Commun. *366*, 724–730.

Carlo, A.-S., Gustafsen, C., Mastrobuoni, G., Nielsen, M.S., Burgert, T., Hartl, D., Rohe, M., Nykjaer, A., Herz, J., Heeren, J., et al. (2013). The pro-neurotrophin receptor sortilin is a major neuronal APOE receptor for catabolism of amyloid-β peptide in the brain. J Neurosci *33*, 358–370.

Carraway, R., and Leeman, S.E. (1973). The isolation of a new hypotensive peptide, neurotensin, from bovine hypothalami. J. Biol. Chem. *248*, 6854–6861.

Carroll, B.J., Cassidy, F., Naftolowitz, D., Tatham, N.E., Wilson, W.H., Iranmanesh, A., Liu, P.Y., and Veldhuis, J.D. (2007). Pathophysiology of hypercortisolism in depression. Acta Psychiatr Scand Suppl 90–103.

Ceccatelli, S., Eriksson, M., and Hökfelt, T. (1989). Distribution and coexistence of corticotropin-releasing factor-, neurotensin-, enkephalin-, cholecystokinin-, galanin- and vasoactive intestinal polypeptide/peptide histidine isoleucine-like peptides in the parvocellular part of the paraventricular nucleus. Neuroendocrinology *49*, 309–323.

Chabry, J., Gaudriault, G., Vincent, J.P., and Mazella, J. (1993). Implication of various forms of neurotensin receptors in the mechanism of internalization of neurotensin in cerebral neurons. J. Biol. Chem. *268*, 17138–17144.

Chapman, C.G., Meadows, H.J., Godden, R.J., Campbell, D.A., Duckworth, M., Kelsell, R.E., Murdock, P.R., Randall, A.D., Rennie, G.I., and Gloger, I.S. (2000). Cloning, localisation and functional expression of a novel human, cerebellum specific, two pore domain potassium channel. Brain Res. Mol. Brain Res. *82*, 74–83.

Chavez, R.A., Gray, A.T., Zhao, B.B., Kindler, C.H., Mazurek, M.J., Mehta, Y., Forsayeth, J.R., and Yost, C.S. (1999). TWIK-2, a New Weak Inward Rectifying Member of the Tandem Pore Domain Potassium Channel Family. J. Biol. Chem. *274*, 7887–7892.

Chen, B., Dowlatshahi, D., MacQueen, G.M., Wang, J.F., and Young, L.T. (2001). Increased hippocampal BDNF immunoreactivity in subjects treated with antidepressant medication. Biol. Psychiatry *50*, 260–265.

Chen, C., Wang, L., Rong, X., Wang, W., and Wang, X. (2015). Effects of fluoxetine on protein expression of potassium ion channels in the brain of chronic mild stress rats. Acta Pharm Sin B *5*, 55–61.

Chen, L.W., Yung, K.K.L., Chan, Y.S., Shum, D.K.Y., and Bolam, J.P. (2008). The proNGF-p75NTR-sortilin signalling complex as new target for the therapeutic treatment of Parkinson's disease. CNS Neurol Disord Drug Targets *7*, 512–523.

Chen, Z.-Y., Patel, P.D., Sant, G., Meng, C.-X., Teng, K.K., Hempstead, B.L., and Lee, F.S. (2004). Variant brain-derived neurotrophic factor (BDNF) (Met66) alters the intracellular trafficking and activity-dependent secretion of wild-type BDNF in neurosecretory cells and cortical neurons. J. Neurosci. *24*, 4401–4411.

Chen, Z.-Y., Ieraci, A., Teng, H., Dall, H., Meng, C.-X., Herrera, D.G., Nykjaer, A., Hempstead, B.L., and Lee, F.S. (2005). Sortilin Controls Intracellular Sorting of Brain-Derived Neurotrophic Factor to the Regulated Secretory Pathway. J Neurosci *25*, 6156–6166.

Choi, K.-E., Hall, C.L., Sun, J.-M., Wei, L., Mohamad, O., Dix, T.A., and Yu, S.P. (2012). A novel stroke therapy of pharmacologically induced hypothermia after focal cerebral ischemia in mice. FASEB J. *26*, 2799–2810.

Chou, D., Huang, C.-C., and Hsu, K.-S. (2014). Brain-derived neurotrophic factor in the amygdala mediates susceptibility to fear conditioning. Exp. Neurol. *255*, 19–29.

Clineschmidt, B.V., McGuffin, J.C., and Bunting, P.B. (1979). Neurotensin: antinocisponsive action in rodents. Eur. J. Pharmacol. *54*, 129–139.

Clineschmidt, B.V., Martin, G.E., and Veber, D.F. (1982). Antinocisponsive effects of neurotensin and neurotensin-related peptides. Ann. N. Y. Acad. Sci. *400*, 283–306.

Cohen, A., Ben-Abu, Y., Hen, S., and Zilberberg, N. (2008). A Novel Mechanism for Human K2P2.1 Channel Gating FACILITATION OF C-TYPE GATING BY PROTONATION OF EXTRACELLULAR HISTIDINE RESIDUES. J. Biol. Chem. *283*, 19448–19455.

Congiu, C., Minelli, A., Bonvicini, C., Bortolomasi, M., Sartori, R., Maj, C., Scassellati, C., Maina, G., Trabucchi, L., Segala, M., et al. (2015). The role of the potassium channel gene KCNK2 in major depressive disorder. Psychiatry Res *225*, 489–492.

Cooper, P.E., Fernstrom, M.H., Rorstad, O.P., Leeman, S.E., and Martin, J.B. (1981). The regional distribution of somatostatin, substance P and neurotensin in human brain. Brain Res. *218*, 219–232.

Coppola, T., Béraud-Dufour, S., Antoine, A., Vincent, J.-P., and Mazella, J. (2008). Neurotensin protects pancreatic beta cells from apoptosis. Int. J. Biochem. Cell Biol. *40*, 2296–2302.

Coulson, E.J., Reid, K., Baca, M., Shipham, K.A., Hulett, S.M., Kilpatrick, T.J., and Bartlett, P.F. (2000). Chopper, a new death domain of the p75 neurotrophin receptor that mediates rapid neuronal cell death. J. Biol. Chem. *275*, 30537–30545.

Coutinho, M.F., Prata, M.J., and Alves, S. (2012). Mannose-6-phosphate pathway: A review on its role in lysosomal function and dysfunction. Molecular Genetics and Metabolism *105*, 542–550.

Critchley, H.D. (2004). The human cortex responds to an interoceptive challenge. Proc. Natl. Acad. Sci. U.S.A. *101*, 6333–6334.

Cunha, A.B.M., Frey, B.N., Andreazza, A.C., Goi, J.D., Rosa, A.R., Gonçalves, C.A., Santin, A., and Kapczinski, F. (2006). Serum brain-derived neurotrophic factor is decreased in bipolar disorder during depressive and manic episodes. Neurosci. Lett. *398*, 215–219.

Czirják, G., Tóth, Z.E., and Enyedi, P. (2004). The two-pore domain K+ channel, TRESK, is activated by the cytoplasmic calcium signal through calcineurin. J. Biol. Chem. *279*, 18550–18558.

Dal Farra, C., Sarret, P., Navarro, V., Botto, J.M., Mazella, J., and Vincent, J.P. (2001). Involvement of the neurotensin receptor subtype NTR3 in the growth effect of neurotensin on cancer cell lines. Int. J. Cancer *92*, 503–509.

Deacon, R.M.J. (2006). Digging and marble burying in mice: simple methods for in vivo identification of biological impacts : Article : Nature Protocols. Nat. Protocols *1*, 122–124.

Dechant, G., and Barde, Y.-A. (2002). The neurotrophin receptor p75(NTR): novel functions and implications for diseases of the nervous system. Nat. Neurosci. *5*, 1131–1136.

Delgado, P., and Moreno, F. (1999). Antidepressants and the brain. Int Clin Psychopharmacol *14 Suppl 1*, S9-16.

Devader, C., Khayachi, A., Veyssiere, J., Moha Ou Maati, H., Roulot, M., Moreno, S., Borsotto, M., Martin, S., Heurteaux, C., and Mazella, J. (2015). In vitro and in vivo regulation of synaptogenesis by the novel antidepressant spadin. British Journal of Pharmacology *172*, 2604–2617.

Dolais-Kitabgi, J., Kitabgi, P., Brazeau, P., and Freychet, P. (1979). Effect of neurotensin on insulin, glucagon, and somatostatin release from isolated pancreatic islets. Endocrinology *105*, 256–260.

Drevets, W.C., Videen, T.O., Price, J.L., Preskorn, S.H., Carmichael, S.T., and Raichle, M.E. (1992). A functional anatomical study of unipolar depression. J. Neurosci. *12*, 3628–3641.

Drevets, W.C., Price, J.L., Simpson, J.R., Todd, R.D., Reich, T., Vannier, M., and Raichle, M.E. (1997). Subgenual prefrontal cortex abnormalities in mood disorders. Nature *386*, 824–827.

Drevets, W.C., Price, J.L., Bardgett, M.E., Reich, T., Todd, R.D., and Raichle, M.E. (2002). Glucose metabolism in the amygdala in depression: Relationship to diagnostic subtype and plasma cortisol levels. Pharmacology Biochemistry and Behavior *71*, 431–447.

Dubuc, I., Remande, S., and Costentin, J. (1999). The partial agonist properties of levocabastine in neurotensin-induced analgesia. Eur. J. Pharmacol. *381*, 9–12.

Duprat, F., Lesage, F., Fink, M., Reyes, R., Heurteaux, C., and Lazdunski, M. (1997). TASK, a human background K+ channel to sense external pH variations near physiological pH. EMBO J *16*, 5464–5471.

Duprat, F., Girard, C., Jarretou, G., and Lazdunski, M. (2005). Pancreatic two P domain K+ channels TALK-1 and TALK-2 are activated by nitric oxide and reactive oxygen species. J. Physiol. (Lond.) *562*, 235–244.

Dwivedi, Y., Rao, J.S., Rizavi, H.S., Kotowski, J., Conley, R.R., Roberts, R.C., Tamminga, C.A., and Pandey, G.N. (2003). Abnormal expression and functional characteristics of cyclic adenosine monophosphate response element binding protein in postmortem brain of suicide subjects. Arch. Gen. Psychiatry *60*, 273–282.

Egan, M.F., Kojima, M., Callicott, J.H., Goldberg, T.E., Kolachana, B.S., Bertolino, A., Zaitsev, E., Gold, B., Goldman, D., Dean, M., et al. (2003). The BDNF val66met polymorphism affects activity-dependent secretion of BDNF and human memory and hippocampal function. Cell *112*, 257–269.

Elde, R., Schalling, M., Ceccatelli, S., Nakanishi, S., and Hökfelt, T. (1990). Localization of neuropeptide receptor mRNA in rat brain: initial observations using probes for neurotensin and substance P receptors. Neurosci. Lett. *120*, 134–138.

Elhwuegi, A.S. (2004). Central monoamines and their role in major depression. Prog. Neuropsychopharmacol. Biol. Psychiatry *28*, 435–451.

Etkin, A., Egner, T., Peraza, D.M., Kandel, E.R., and Hirsch, J. (2006). Resolving emotional conflict: a role for the rostral anterior cingulate cortex in modulating activity in the amygdala. Neuron *51*, 871–882.

Evans, S.F., Irmady, K., Ostrow, K., Kim, T., Nykjaer, A., Saftig, P., Blobel, C., and Hempstead, B.L. (2011). Neuronal Brain-derived Neurotrophic Factor Is Synthesized in Excess, with Levels Regulated by Sortilin-mediated Trafficking and Lysosomal Degradation. J. Biol. Chem. *286*, 29556–29567.

Fassio, A., Evans, G., Grisshammer, R., Bolam, J.P., Mimmack, M., and Emson, P.C. (2000). Distribution of the neurotensin receptor NTS1 in the rat CNS studied using an amino-terminal directed antibody. Neuropharmacology *39*, 1430–1442.

Feliciangeli, S., Chatelain, F.C., Bichet, D., and Lesage, F. (2015). The family of K2P channels: salient structural and functional properties. J. Physiol. (Lond.) *593*, 2587–2603.

Fink, M., Duprat, F., Lesage, F., Reyes, R., Romey, G., Heurteaux, C., and Lazdunski, M. (1996). Cloning, functional expression and brain localization of a novel unconventional outward rectifier K+ channel. EMBO J. *15*, 6854–6862.

Fink, M., Lesage, F., Duprat, F., Heurteaux, C., Reyes, R., Fosset, M., and Lazdunski, M. (1998). A neuronal two P domain K+ channel stimulated by arachidonic acid and polyunsaturated fatty acids. The EMBO Journal *17*, 3297–3308.

Fuxe, K., Agnati, L.F., and Borroto-Escuela, D.O. (2014). The impact of receptor-receptor interactions in heteroreceptor complexes on brain plasticity. Expert Rev Neurother *14*, 719–721.

Gardener, M.J., Johnson, I.T., Burnham, M.P., Edwards, G., Heagerty, A.M., and Weston, A.H. (2004). Functional evidence of a role for two-pore domain potassium channels in rat mesenteric and pulmonary arteries. Br. J. Pharmacol. *142*, 192–202.

Gendron, L., Perron, A., Payet, M.D., Gallo-Payet, N., Sarret, P., and Beaudet, A. (2004). Low-affinity neurotensin receptor (NTS2) signaling: internalization-dependent activation of extracellular signal-regulated kinases 1/2. Mol. Pharmacol. *66*, 1421–1430.

Gliemann, J., Nykjaer, A., Petersen, C.M., Jørgensen, K.E., Nielsen, M., Andreasen, P.A., Christensen, E.I., Lookene, A., Olivecrona, G., and Moestrup, S.K. (1994). The multiligand alpha 2-macroglobulin receptor/low density lipoprotein receptor-related protein (alpha 2MR/LRP). Binding and endocytosis of fluid phase and membrane-associated ligands. Ann. N. Y. Acad. Sci. *737*, 20–38.

Gold, P.W., Loriaux, D.L., Roy, A., Kling, M.A., Calabrese, J.R., Kellner, C.H., Nieman, L.K., Post, R.M., Pickar, D., and Gallucci, W. (1986). Responses to corticotropin-releasing hormone in the hypercortisolism of depression and Cushing's disease. Pathophysiologic and diagnostic implications. N. Engl. J. Med. *314*, 1329–1335.

Gönczi, M., Szentandrássy, N., Johnson, I.T., Heagerty, A.M., and Weston, A.H. (2006). Investigation of the role of TASK-2 channels in rat pulmonary arteries; pharmacological and functional studies following RNA interference procedures. Br. J. Pharmacol. *147*, 496–505.

Guha, S., Lunn, J.A., Santiskulvong, C., and Rozengurt, E. (2003). Neurotensin stimulates protein kinase C-dependent mitogenic signaling in human pancreatic carcinoma cell line PANC-1. Cancer Res. *63*, 2379–2387.

Gui, X., Dobner, P.R., and Carraway, R.E. (2001). Endogenous neurotensin facilitates enterohepatic bile acid circulation by enhancing intestinal uptake in rats. American Journal of Physiology - Gastrointestinal and Liver Physiology *281*, G1413–G1422.

Guo, J., Luo, Y.X., Tao, L.X., and Guo, X.H. (2015). Association between 1p13.3 genomic markers and coronary artery disease: a meta-analysis involving patients and controls. Genet Mol Res *14*, 9092–9102.

Haddjeri, N., Blier, P., and de Montigny, C. (1998). Long-term antidepressant treatments result in a tonic activation of forebrain 5-HT1A receptors. J. Neurosci. *18*, 10150–10156.

Hamilton, J.P., Siemer, M., and Gotlib, I.H. (2008). Amygdala volume in Major Depressive Disorder: A meta-analysis of magnetic resonance imaging studies. Mol Psychiatry *13*, 993–1000.

Harris, A.P., Lennen, R.J., Brydges, N.M., Jansen, M.A., Pernet, C.R., Whalley, H.C., Marshall, I., Baker, S., Basso, A.M., Day, M., et al. (2016). The role of brain-derived neurotrophic factor in learned fear processing: an awake rat fMRI study. Genes Brain Behav *15*, 221–230.

Hartness, M.E., Lewis, A., Searle, G.J., O'Kelly, I., Peers, C., and Kemp, P.J. (2001). Combined Antisense and Pharmacological Approaches Implicate hTASK as an Airway O2 Sensing K+Channel. J. Biol. Chem. *276*, 26499–26508.

Heim, C., Newport, D.J., Mletzko, T., Miller, A.H., and Nemeroff, C.B. (2008). The link between childhood trauma and depression: insights from HPA axis studies in humans. Psychoneuroendocrinology *33*, 693–710.

Helmstaedter, V., Taugner, C., Feurle, G.E., and Forssmann, W.G. (1977). Localization of neurotensin-immunoreactive cells in the small intestine of man and various mammals. Histochemistry *53*, 35–41.

Hermans-Borgmeyer, I., Hermey, G., Nykjaer, A., and Chica Schaller (1999). Expression of the 100-kDa neurotensin receptor sortilin during mouse embryonal development. Molecular Brain Research *65*, 216–219.

Hermey, G., Sjøgaard, S.S., Petersen, C.M., Nykjaer, A., and Gliemann, J. (2006). Tumour necrosis factor alpha-converting enzyme mediates ectodomain shedding of Vps10p-domain receptor family members. Biochem. J. *395*, 285–293.

Hervieu, G.J., Cluderay, J.E., Gray, C.W., Green, P.J., Ranson, J.L., Randall, A.D., and Meadows, H.J. (2001). Distribution and expression of TREK-1, a two-pore-domain potassium channel, in the adult rat CNS. Neuroscience *103*, 899–919.

Heurteaux, C., Lucas, G., Guy, N., El Yacoubi, M., Thümmler, S., Peng, X.-D., Noble, F., Blondeau, N., Widmann, C., Borsotto, M., et al. (2006). Deletion of the background potassium channel TREK-1 results in a depression-resistant phenotype. Nat. Neurosci. *9*, 1134–1141.

Huang, G., Buckler-Pena, D., Nauta, T., Singh, M., Asmar, A., Shi, J., Kim, J.Y., and Kandror, K.V. (2013). Insulin responsiveness of glucose transporter 4 in 3T3-L1 cells depends on the presence of sortilin. Mol. Biol. Cell *24*, 3115–3122.

Hwang, J.R., Baek, M.W., Sim, J., Choi, H.-S., Han, J.M., Kim, Y.L., Hwang, J.-I., Kwon, H.B., Beaudet, N., Sarret, P., et al. (2010). Intermolecular cross-talk between NTR1 and NTR2 neurotensin receptor promotes intracellular sequestration and functional inhibition of NTR1 receptors. Biochem. Biophys. Res. Commun. *391*, 1007–1013.

Hyttel, J. (1994). Pharmacological characterization of selective serotonin reuptake inhibitors (SSRIs). International Clinical Psychopharmacology *9*, 19.

Johnson, K.F., and Kornfeld, S. (1992). A His-Leu-Leu sequence near the carboxyl terminus of the cytoplasmic domain of the cation-dependent mannose 6-phosphate receptor is necessary for the lysosomal enzyme sorting function. J. Biol. Chem. *267*, 17110–17115.

Jomphe, C., Lemelin, P.-L., Okano, H., Kobayashi, K., and Trudeau, L.-E. (2006). Bidirectional regulation of dopamine D2 and neurotensin NTS1 receptors in dopamine neurons. Eur. J. Neurosci. *24*, 2789–2800.

Kandror, K.V. (2003). A long search for Glut4 activation. Sci. STKE *2003*, PE5.

Kang, D., and Kim, D. (2006). TREK-2 (K2P10.1) and TRESK (K2P18.1) are major background K+ channels in dorsal root ganglion neurons. American Journal of Physiology - Cell Physiology *291*, C138–C146.

Karege, F., Vaudan, G., Schwald, M., Perroud, N., and La Harpe, R. (2005). Neurotrophin levels in postmortem brains of suicide victims and the effects of antemortem diagnosis and psychotropic drugs. Brain Res. Mol. Brain Res. *136*, 29–37.

Kenchappa, R.S., Zampieri, N., Chao, M.V., Barker, P.A., Teng, H.K., Hempstead, B.L., and Carter, B.D. (2006). Ligand-dependent cleavage of the P75 neurotrophin receptor is necessary for NRIF nuclear translocation and apoptosis in sympathetic neurons. Neuron *50*, 219–232.

Kim, E.R., Leckstrom, A., and Mizuno, T.M. (2008). Impaired anorectic effect of leptin in neurotensin receptor 1-deficient mice. Behavioural Brain Research *194*, 66–71.

Kim, Y., Bang, H., Gnatenco, C., and Kim, D. (2001). Synergistic interaction and the role of C-terminus in the activation of TRAAK K+ channels by pressure, free fatty acids and alkali. Pflugers Arch. *442*, 64–72.

Kimbrell, T.A., Ketter, T.A., George, M.S., Little, J.T., Benson, B.E., Willis, M.W., Herscovitch, P., and Post, R.M. (2002). Regional cerebral glucose utilization in patients with a range of severities of unipolar depression. Biol. Psychiatry *51*, 237–252.

Kjolby, M., Andersen, O.M., Breiderhoff, T., Fjorback, A.W., Pedersen, K.M., Madsen, P., Jansen, P., Heeren, J., Willnow, T.E., and Nykjaer, A. (2010). Sort1, encoded by the cardiovascular risk locus 1p13.3, is a regulator of hepatic lipoprotein export. Cell Metab. *12*, 213–223.

Kjolby, M., Nielsen, M.S., and Petersen, C.M. (2015). Sortilin, encoded by the cardiovascular risk gene SORT1, and its suggested functions in cardiovascular disease. Curr Atheroscler Rep *17*, 496.

Kleczkowska, P., and Lipkowski, A.W. (2013). Neurotensin and neurotensin receptors: characteristic, structure-activity relationship and pain modulation--a review. Eur. J. Pharmacol. *716*, 54–60.

Koenigs, M., Huey, E.D., Calamia, M., Raymont, V., Tranel, D., and Grafman, J. (2008). Distinct regions of prefrontal cortex mediate resistance and vulnerability to depression. J. Neurosci. *28*, 12341–12348.

Kommaddi, R.P., Thomas, R., Ceni, C., Daigneault, K., and Barker, P.A. (2011). Trk-dependent ADAM17 activation facilitates neurotrophin survival signaling. FASEB J. *25*, 2061–2070.

Lauritzen, I., Zanzouri, M., Honoré, E., Duprat, F., Ehrengruber, M.U., Lazdunski, M., and Patel, A.J. (2003). K+-dependent cerebellar granule neuron apoptosis. Role of task leak K+ channels. J. Biol. Chem. *278*, 32068–32076.

LeDoux, J.E. (2000). Emotion circuits in the brain. Annu. Rev. Neurosci. *23*, 155–184.

Lefrancois, S., Zeng, J., Hassan, A.J., Canuel, M., and Morales, C.R. (2003). The lysosomal trafficking of sphingolipid activator proteins (SAPs) is mediated by sortilin. EMBO J. *22*, 6430–6437.

Lépée-Lorgeoux, I., Betancur, C., Rostène, W., and Pélaprat, D. (1999). Differential ontogenetic patterns of levocabastine-sensitive neurotensin NT2 receptors and of NT1 receptors in the rat brain revealed by in situ hybridization. Brain Res. Dev. Brain Res. *113*, 115–131.

Lépine, J.-P., and Briley, M. (2011). The increasing burden of depression. Neuropsychiatr Dis Treat *7*, 3–7.

Lesage, F., Guillemare, E., Fink, M., Duprat, F., Lazdunski, M., Romey, G., and Barhanin, J. (1996). TWIK-1, a ubiquitous human weakly inward rectifying K+ channel with a novel structure. EMBO J. *15*, 1004–1011.

Lesage, F., Lauritzen, I., Duprat, F., Reyes, R., Fink, M., Heurteaux, C., and Lazdunski, M. (1997). The structure, function and distribution of the mouse TWIK-1 K+ channel. FEBS Lett. *402*, 28–32.

Lesage, F., Terrenoire, C., Romey, G., and Lazdunski, M. (2000). Human TREK2, a 2P Domain Mechano-sensitive K+Channel with Multiple Regulations by Polyunsaturated Fatty Acids, Lysophospholipids, and Gs, Gi, and Gq Protein-coupled Receptors. J. Biol. Chem. *275*, 28398–28405.

Leskelä, U., Rytsälä, H., Komulainen, E., Melartin, T., Sokero, P., Lestelä-Mielonen, P., and Isometsä, E. (2006). The influence of adversity and perceived social support on the outcome of major depressive disorder in subjects with different levels of depressive symptoms. Psychol Med *36*, 779–788.

Li, J., Matye, D.J., and Li, T. (2015). Insulin Resistance Induces Posttranslational Hepatic Sortilin 1 Degradation in Mice. J Biol Chem *290*, 11526–11536.

Liang, Y., Boules, M., Li, Z., Williams, K., Miura, T., Oliveros, A., and Richelson, E. (2010). Hyperactivity of the dopaminergic system in NTS1 and NTS2 null mice. Neuropharmacology *58*, 1199–1205.

Lin, B.Z., Pilch, P.F., and Kandror, K.V. (1997). Sortilin is a major protein component of Glut4-containing vesicles. J. Biol. Chem. *272*, 24145–24147.

Lorenzetti, V., Allen, N.B., Fornito, A., and Yücel, M. (2009). Structural brain abnormalities in major depressive disorder: a selective review of recent MRI studies. J Affect Disord *117*, 1–17.

Lou, H., Kim, S.-K., Zaitsev, E., Snell, C.R., Lu, B., and Loh, Y.P. (2005). Sorting and Activity-Dependent Secretion of BDNF Require Interaction of a Specific Motif with the Sorting Receptor Carboxypeptidase E. Neuron *45*, 245–255.

Lu, B., Pang, P.T., and Woo, N.H. (2005). The yin and yang of neurotrophin action. Nat Rev Neurosci *6*, 603–614.

MacQueen, G.M., Yucel, K., Taylor, V.H., Macdonald, K., and Joffe, R. (2008). Posterior hippocampal volumes are associated with remission rates in patients with major depressive disorder. Biol. Psychiatry *64*, 880–883.

Maeno, H., Yamada, K., Santo-Yamada, Y., Aoki, K., Sun, Y.-J., Sato, E., Fukushima, T., Ogura, H., Araki, T., Kamichi, S., et al. (2004). Comparison of mice deficient in the high- or low-affinity neurotensin receptors, Ntsr1 or Ntsr2, reveals a novel function for Ntsr2 in thermal nociception. Brain Res. *998*, 122–129.

Mahar, I., Bambico, F.R., Mechawar, N., and Nobrega, J.N. (2014). Stress, serotonin, and hippocampal neurogenesis in relation to depression and antidepressant effects. Neuroscience & Biobehavioral Reviews *38*, 173–192.

Maingret, F., Patel, A.J., Lesage, F., Lazdunski, M., and Honoré, E. (1999). Mechano- or Acid Stimulation, Two Interactive Modes of Activation of the TREK-1 Potassium Channel. J. Biol. Chem. *274*, 26691–26696.

Maingret, F., Patel, A.J., Lesage, F., Lazdunski, M., and Honoré, E. (2000a). Lysophospholipids Open the Two-pore Domain Mechano-gated K+ Channels TREK-1 and TRAAK. J. Biol. Chem. *275*, 10128–10133.

Maingret, F., Lauritzen, I., Patel, A.J., Heurteaux, C., Reyes, R., Lesage, F., Lazdunski, M., and Honoré, E. (2000b). TREK-1 is a heat-activated background K+ channel. The EMBO Journal *19*, 2483–2491.

Maingret, F., Honoré, E., Lazdunski, M., and Patel, A.J. (2002). Molecular basis of the voltage-dependent gating of TREK-1, a mechano-sensitive K(+) channel. Biochem. Biophys. Res. Commun. *292*, 339–346.

Manji, H.K., Drevets, W.C., and Charney, D.S. (2001). The cellular neurobiology of depression. Nat. Med. *7*, 541–547.

Marcusson, E.G., Horazdovsky, B.F., Cereghino, J.L., Gharakhanian, E., and Emr, S.D. (1994). The sorting receptor for yeast vacuolar carboxypeptidase Y is encoded by the VPS10 gene. Cell *77*, 579–586.

Mari, M., Bujny, M.V., Zeuschner, D., Geerts, W.J.C., Griffith, J., Petersen, C.M., Cullen, P.J., Klumperman, J., and Geuze, H.J. (2008). SNX1 defines an early endosomal recycling exit for sortilin and mannose 6-phosphate receptors. Traffic *9*, 380–393.

Martin, S., Navarro, V., Vincent, J.P., and Mazella, J. (2002). Neurotensin receptor-1 and -3 complex modulates the cellular signaling of neurotensin in the HT29 cell line. Gastroenterology *123*, 1135–1143.

Martin, S., Vincent, J.-P., and Mazella, J. (2003). Involvement of the neurotensin receptor-3 in the neurotensin-induced migration of human microglia. J. Neurosci. *23*, 1198–1205.

Mayberg, H.S., Liotti, M., Brannan, S.K., McGinnis, S., Mahurin, R.K., Jerabek, P.A., Silva, J.A., Tekell, J.L., Martin, C.C., Lancaster, J.L., et al. (1999). Reciprocal limbic-cortical function and negative mood: converging PET findings in depression and normal sadness. Am J Psychiatry *156*, 675–682.

Mayorga, A.J., Dalvi, A., Page, M.E., Zimov-Levinson, S., Hen, R., and Lucki, I. (2001). Antidepressant-like behavioral effects in 5-hydroxytryptamine(1A) and 5-hydroxytryptamine(1B) receptor mutant mice. J. Pharmacol. Exp. Ther. *298*, 1101–1107.

Mazella, J. (2001). Sortilin/neurotensin receptor-3: a new tool to investigate neurotensin signaling and cellular trafficking? Cellular Signalling *13*, 1–6.

Mazella, J., Chabry, J., Kitabgi, P., and Vincent, J.P. (1988). Solubilization and characterization of active neurotensin receptors from mouse brain. J. Biol. Chem. *263*, 144–149.

Mazella, J., Chabry, J., Zsurger, N., and Vincent, J.P. (1989). Purification of the neurotensin receptor from mouse brain by affinity chromatography. J. Biol. Chem. *264*, 5559–5563.

Mazella, J., Botto, J.M., Guillemare, E., Coppola, T., Sarret, P., and Vincent, J.P. (1996). Structure, functional expression, and cerebral localization of the levocabastine-sensitive neurotensin/neuromedin N receptor from mouse brain. J. Neurosci. *16*, 5613–5620.

Mazella, J., Zsürger, N., Navarro, V., Chabry, J., Kaghad, M., Caput, D., Ferrara, P., Vita, N., Gully, D., Maffrand, J.-P., et al. (1998). The 100-kDa Neurotensin Receptor Is gp95/Sortilin, A Non-G-Protein-coupled Receptor. J. Biol. Chem. *273*, 26273–26276.

Mazella, J., Pétrault, O., Lucas, G., Deval, E., Béraud-Dufour, S., Gandin, C., El-Yacoubi, M., Widmann, C., Guyon, A., Chevet, E., et al. (2010). Spadin, a Sortilin-Derived Peptide, Targeting Rodent TREK-1 Channels: A New Concept in the Antidepressant Drug Design. PLoS Biol *8*.

McCormick, P.J., Dumaresq-Doiron, K., Pluviose, A.-S., Pichette, V., Tosato, G., and Lefrancois, S. (2008). Palmitoylation controls recycling in lysosomal sorting and trafficking. Traffic *9*, 1984–1997.

Mechanic, J.A., Sutton, J.E., Berson, A.E., Wu, X., Kwan, J., Schreiber, R., Pang, Z., and Button, D.C. (2009). Involvement of the neurotensin receptor 1 in the behavioral effects of two neurotensin agonists, NT-2 and NT69L: lack of hypothermic, antinociceptive and antipsychotic actions in receptor knockout mice. Eur Neuropsychopharmacol *19*, 466–475.

Merali, Z., Du, L., Hrdina, P., Palkovits, M., Faludi, G., Poulter, M.O., and Anisman, H. (2004). Dysregulation in the suicide brain: mRNA expression of corticotropin-releasing hormone receptors and GABA(A) receptor subunits in frontal cortical brain region. J. Neurosci. *24*, 1478–1485.

Mercuri, N.B., Stratta, F., Calabresi, P., and Bernardi, G. (1993). Neurotensin induces an inward current in rat mesencephalic dopaminergic neurons. Neurosci. Lett. *153*, 192–196.

Molendijk, M.L., Spinhoven, P., Polak, M., Bus, B. a. A., Penninx, B.W.J.H., and Elzinga, B.M. (2014). Serum BDNF concentrations as peripheral manifestations of depression: evidence from a systematic review and meta-analyses on 179 associations (N=9484). Mol. Psychiatry *19*, 791–800.

Monteggia, L.M., Barrot, M., Powell, C.M., Berton, O., Galanis, V., Gemelli, T., Meuth, S., Nagy, A., Greene, R.W., and Nestler, E.J. (2004). Essential role of brain-derived neurotrophic factor in adult hippocampal function. Proc. Natl. Acad. Sci. U.S.A. *101*, 10827–10832.

Morais-Cabral, J.H., Zhou, Y., and MacKinnon, R. (2001). Energetic optimization of ion conduction rate by the K+ selectivity filter. Nature *414*, 37–42.

Morris, B.H., Bylsma, L.M., and Rottenberg, J. (2009). Does emotion predict the course of major depressive disorder? A review of prospective studies. Br J Clin Psychol *48*, 255–273.

Morris, N.J., Ross, S.A., Lane, W.S., Moestrup, S.K., Petersen, C.M., Keller, S.R., and Lienhard, G.E. (1998). Sortilin is the major 110-kDa protein in GLUT4 vesicles from adipocytes. J. Biol. Chem. *273*, 3582–3587.

Mowla, S.J., Pareek, S., Farhadi, H.F., Petrecca, K., Fawcett, J.P., Seidah, N.G., Morris, S.J., Sossin, W.S., and Murphy, R.A. (1999). Differential sorting of nerve growth factor and brain-derived neurotrophic factor in hippocampal neurons. J. Neurosci. *19*, 2069–2080.

Müller, K.M., Tveteraas, I.H., Aasrum, M., Ødegård, J., Dawood, M., Dajani, O., Christoffersen, T., and Sandnes, D.L. (2011). Role of protein kinase C and epidermal growth factor receptor signalling in growth stimulation by neurotensin in colon carcinoma cells. BMC Cancer *11*, 421.

Munck Petersen, C., Nielsen, M.S., Jacobsen, C., Tauris, J., Jacobsen, L., Gliemann, J., Moestrup, S.K., and Madsen, P. (1999). Propeptide cleavage conditions sortilin/neurotensin receptor-3 for ligand binding. EMBO J. *18*, 595–604.

Murbartián, J., Lei, Q., Sando, J.J., and Bayliss, D.A. (2005). Sequential Phosphorylation Mediates Receptor- and Kinase-induced Inhibition of TREK-1 Background Potassium Channels. J. Biol. Chem. *280*, 30175–30184.

Nase, S., Köhler, S., Jennebach, J., Eckert, A., Schweinfurth, N., Gallinat, J., Lang, U.E., and Kühn, S. (2016). Role of Serum Brain Derived Neurotrophic Factor and Central N-Acetylaspartate for Clinical Response under Antidepressive Pharmacotherapy. Neurosignals *24*, 1–14.

Navarro, V., Vincent, J.-P., and Mazella, J. (2002). Shedding of the luminal domain of the neurotensin receptor-3/sortilin in the HT29 cell line. Biochem. Biophys. Res. Commun. *298*, 760–764.

Ni, X., and Morales, C.R. (2006). The lysosomal trafficking of acid sphingomyelinase is mediated by sortilin and mannose 6-phosphate receptor. Traffic *7*, 889–902.

Nicot, A., Rostene, W., and Berod, A. (1994). Neurotensin receptor expression in the rat forebrain and midbrain: a combined analysis by in situ hybridization and receptor autoradiography. J. Comp. Neurol. *341*, 407–419.

Nicot, A., Rowe, W.B., De Kloet, E.R., Betancur, C., Jessop, D.S., Lightman, S.L., Quirion, R., Rostène, W., and Bérod, A. (1997). Endogenous neurotensin regulates hypothalamic-pituitary-adrenal axis activity and peptidergic neurons in the rat hypothalamic paraventricular nucleus. J. Neuroendocrinol. *9*, 263–269.

Nielsen, M.S., Jacobsen, C., Olivecrona, G., Gliemann, J., and Petersen, C.M. (1999). Sortilin/neurotensin receptor-3 binds and mediates degradation of lipoprotein lipase. J. Biol. Chem. *274*, 8832–8836.

Nielsen, M.S., Madsen, P., Christensen, E.I., Nykjær, A., Gliemann, J., Kasper, D., Pohlmann, R., and Petersen, C.M. (2001). The sortilin cytoplasmic tail conveys Golgi–endosome transport and binds the VHS domain of the GGA2 sorting protein. The EMBO Journal *20*, 2180–2190.

Niimi, M., Takahara, J., Sato, M., and Kawanishi, K. (1991). Neurotensin and growth hormone-releasing factor-containing neurons projecting to the median eminence of the rat: a combined retrograde tracing and immunohistochemical study. Neurosci. Lett. *133*, 183–186.

Noël, J., Zimmermann, K., Busserolles, J., Deval, E., Alloui, A., Diochot, S., Guy, N., Borsotto, M., Reeh, P., Eschalier, A., et al. (2009). The mechano-activated K+ channels TRAAK and TREK-1 control both warm and cold perception. EMBO J. *28*, 1308–1318.

Nykjaer, A., Lee, R., Teng, K.K., Jansen, P., Madsen, P., Nielsen, M.S., Jacobsen, C., Kliemannel, M., Schwarz, E., Willnow, T.E., et al. (2004). Sortilin is essential for proNGF-induced neuronal cell death. Nature *427*, 843–848.

Ogawa, K., Ueno, T., Iwasaki, T., Kujiraoka, T., Ishihara, M., Kunimoto, S., Takayama, T., Kanai, T., Hirayama, A., and Hattori, H. (2016). Soluble sortilin is released by activated platelets and its circulating levels are associated with cardiovascular risk factors. Atherosclerosis *249*, 110–115.

Okuma, Y., Fukuda, Y., and Osumi, Y. (1983). Neurotensin potentiates the potassium-induced release of endogenous dopamine from rat striatal slices. Eur. J. Pharmacol. *93*, 27–33.

Palomino, A., Vallejo-Illarramendi, A., González-Pinto, A., Aldama, A., González-Gómez, C., Mosquera, F., González-García, G., and Matute, C. (2006). Decreased levels of plasma BDNF in first-episode schizophrenia and bipolar disorder patients. Schizophr. Res. *86*, 321–322.

Pandya, M., Altinay, M., Malone, D.A., and Anand, A. (2012). Where in the Brain Is Depression? Curr Psychiatry Rep *14*, 634–642.

Pang, P.T., Teng, H.K., Zaitsev, E., Woo, N.T., Sakata, K., Zhen, S., Teng, K.K., Yung, W.-H., Hempstead, B.L., and Lu, B. (2004). Cleavage of proBDNF by tPA/plasmin is essential for long-term hippocampal plasticity. Science *306*, 487–491.

Park, H., and Poo, M. (2012). Neurotrophin regulation of neural circuit development and function. Nature Reviews Neuroscience *14*, nrn3379.

Patel, A.J., Honoré, E., Maingret, F., Lesage, F., Fink, M., Duprat, F., and Lazdunski, M. (1998). A mammalian two pore domain mechano-gated S-like K+ channel. EMBO J. *17*, 4283–4290.

Patel, A.J., Maingret, F., Magnone, V., Fosset, M., Lazdunski, M., and Honoré, E. (2000). TWIK-2, an Inactivating 2P Domain K+ Channel. J. Biol. Chem. *275*, 28722–28730.

Patel, K.M., Strong, A., Tohyama, J., Jin, X., Morales, C.R., Billheimer, J., Millar, J., Kruth, H., and Rader, D.J. (2015). Macrophage sortilin promotes LDL uptake, foam cell formation, and atherosclerosis. Circ. Res. *116*, 789–796.

Paykel, E.S., Myers, J.K., Dienelt, M.N., Klerman, G.L., Lindenthal, J.J., and Pepper, M.P. (1969). Life events and depression. A controlled study. Arch. Gen. Psychiatry *21*, 753–760.

Perrin, J.S., Merz, S., Bennett, D.M., Currie, J., Steele, D.J., Reid, I.C., and Schwarzbauer, C. (2012). Electroconvulsive therapy reduces frontal cortical connectivity in severe depressive disorder. PNAS *109*, 5464–5468.

Perron, A., Sharif, N., Sarret, P., Stroh, T., and Beaudet, A. (2007). NTS2 modulates the intracellular distribution and trafficking of NTS1 via heterodimerization. Biochem. Biophys. Res. Commun. *353*, 582–590.

Petersen, C.M., Nielsen, M.S., Nykjær, A., Jacobsen, L., Tommerup, N., Rasmussen, H.H., Røigaard, H., Gliemann, J., Madsen, P., and Moestrup, S.K. (1997). Molecular Identification of a Novel Candidate Sorting Receptor Purified from Human Brain by Receptor-associated Protein Affinity Chromatography. J. Biol. Chem. *272*, 3599–3605.

Pinnock, R.D. (1985). Neurotensin depolarizes substantia nigra dopamine neurones. Brain Res. *338*, 151–154.

Polak, J.M., Sullivan, S.N., Bloom, S.R., Buchan, A.M., Facer, P., Brown, M.R., and Pearse, A.G. (1977). Specific localisation of neurotensin to the N cell in human intestine by radioimmunoassay and immunocytochemistry. Nature *270*, 183–184.

Popp, E., Schneider, A., Vogel, P., Teschendorf, P., and Böttiger, B.W. (2007). Time course of the hypothermic response to continuously administered neurotensin. Neuropeptides *41*, 349–354.

Quistgaard, E.M., Madsen, P., Grøftehauge, M.K., Nissen, P., Petersen, C.M., and Thirup, S.S. (2009). Ligands bind to Sortilin in the tunnel of a ten-bladed beta-propeller domain. Nat. Struct. Mol. Biol. *16*, 96–98.

Rabinowich, L., Fishman, S., Hubel, E., Thurm, T., Park, W.-J., Pewzner-Jung, Y., Saroha, A., Erez, N., Halpern, Z., Futerman, A.H., et al. (2015). Sortilin deficiency improves the metabolic phenotype and

reduces hepatic steatosis of mice subjected to diet-induced obesity. Journal of Hepatology *62*, 175–181.

Rajan, S., Wischmeyer, E., Karschin, C., Preisig-Müller, R., Grzeschik, K.H., Daut, J., Karschin, A., and Derst, C. (2001). THIK-1 and THIK-2, a novel subfamily of tandem pore domain K+ channels. J. Biol. Chem. *276*, 7302–7311.

Rattiner, L.M., Davis, M., French, C.T., and Ressler, K.J. (2004). Brain-Derived Neurotrophic Factor and Tyrosine Kinase Receptor B Involvement in Amygdala-Dependent Fear Conditioning. J. Neurosci. *24*, 4796–4806.

Raymond, J.R., Mukhin, Y.V., Gelasco, A., Turner, J., Collinsworth, G., Gettys, T.W., Grewal, J.S., and Garnovskaya, M.N. (2001). Multiplicity of mechanisms of serotonin receptor signal transduction. Pharmacol. Ther. *92*, 179–212.

Reagan, L.P., Rosell, D.R., Wood, G.E., Spedding, M., Muñoz, C., Rothstein, J., and McEwen, B.S. (2004). Chronic restraint stress up-regulates GLT-1 mRNA and protein expression in the rat hippocampus: reversal by tianeptine. Proc. Natl. Acad. Sci. U.S.A. *101*, 2179–2184.

Reinecke, M., Weihe, E., Carraway, R.E., Leeman, S.E., and Forssmann, W.G. (1982). Localization of neurotensin immunoreactive nerve fibers in the guinea-pig heart: Evidence derived by immunohistochemistry, radioimmunoassay and chromatography. Neuroscience *7*, 1785–1795.

Remaury, A., Vita, N., Gendreau, S., Jung, M., Arnone, M., Poncelet, M., Culouscou, J.-M., Le Fur, G., Soubrié, P., Caput, D., et al. (2002). Targeted inactivation of the neurotensin type 1 receptor reveals its role in body temperature control and feeding behavior but not in analgesia. Brain Research *953*, 63–72.

Reyes, R., Duprat, F., Lesage, F., Fink, M., Salinas, M., Farman, N., and Lazdunski, M. (1998). Cloning and expression of a novel pH-sensitive two pore domain K+ channel from human kidney. J. Biol. Chem. *273*, 30863–30869.

Richard, F., Barroso, S., Martinez, J., Labbé-Jullié, C., and Kitabgi, P. (2001). Agonism, inverse agonism, and neutral antagonism at the constitutively active human neurotensin receptor 2. Mol. Pharmacol. *60*, 1392–1398.

Roussy, G., Dansereau, M.-A., Doré-Savard, L., Belleville, K., Beaudet, N., Richelson, E., and Sarret, P. (2008). Spinal NTS1 receptors regulate nociceptive signaling in a rat formalin tonic pain model. J. Neurochem. *105*, 1100–1114.

Roussy, G., Dansereau, M.-A., Baudisson, S., Ezzoubaa, F., Belleville, K., Beaudet, N., Martinez, J., Richelson, E., and Sarret, P. (2009). Evidence for a role of NTS2 receptors in the modulation of tonic pain sensitivity. Mol Pain *5*, 38.

Roussy, G., Beaudry, H., Lafrance, M., Belleville, K., Beaudet, N., Wada, K., Gendron, L., and Sarret, P. (2010). Altered Morphine-Induced Analgesia in Neurotensin Type 1 Receptor Null Mice. Neuroscience *170*.

Ruan, C.-S., Yang, C.-R., Li, J.-Y., Luo, H.-Y., Bobrovskaya, L., and Zhou, X.-F. Mice with Sort1 deficiency display normal cognition but elevated anxiety-like behavior. Experimental Neurology.

Sackeim, H.A., Prudic, J., Fuller, R., Keilp, J., Lavori, P.W., and Olfson, M. (2007). The cognitive effects of electroconvulsive therapy in community settings. Neuropsychopharmacology *32*, 244–254.

Sahu, A., Carraway, R.E., and Wang, Y.P. (2001). Evidence that neurotensin mediates the central effect of leptin on food intake in rat. Brain Res. *888*, 343–347.

Sandoz, G., Thümmler, S., Duprat, F., Feliciangeli, S., Vinh, J., Escoubas, P., Guy, N., Lazdunski, M., and Lesage, F. (2006). AKAP150, a switch to convert mechano-, pH- and arachidonic acid-sensitive TREK K+ channels into open leak channels. EMBO J *25*, 5864–5872.

Sandoz, G., Tardy, M.P., Thümmler, S., Feliciangeli, S., Lazdunski, M., and Lesage, F. (2008). Mtap2 Is a Constituent of the Protein Network That Regulates Twik-Related K+ Channel Expression and Trafficking. J. Neurosci. *28*, 8545–8552.

Sano, Y., Inamura, K., Miyake, A., Mochizuki, S., Kitada, C., Yokoi, H., Nozawa, K., Okada, H., Matsushime, H., and Furuichi, K. (2003). A novel two-pore domain K+ channel, TRESK, is localized in the spinal cord. J. Biol. Chem. *278*, 27406–27412.

Sapolsky, R.M., Krey, L.C., and McEwen, B.S. (1984). Glucocorticoid-sensitive hippocampal neurons are involved in terminating the adrenocortical stress response. Proc. Natl. Acad. Sci. U.S.A. *81*, 6174–6177.

Sarret, P., Perron, A., Stroh, T., and Beaudet, A. (2003a). Immunohistochemical distribution of NTS2 neurotensin receptors in the rat central nervous system. J. Comp. Neurol. *461*, 520–538.

Sarret, P., Krzywkowski, P., Segal, L., Nielsen, M.S., Petersen, C.M., Mazella, J., Stroh, T., and Beaudet, A. (2003b). Distribution of NTS3 receptor/sortilin mRNA and protein in the rat central nervous system. J. Comp. Neurol. *461*, 483–505.

Schmidt, V., and Willnow, T.E. (2016). Protein sorting gone wrong--VPS10P domain receptors in cardiovascular and metabolic diseases. Atherosclerosis *245*, 194–199.

Schotte, A., Leysen, J.E., and Laduron, P.M. (1986). Evidence for a displaceable non-specific [3H]neurotensin binding site in rat brain. Naunyn Schmiedebergs Arch Pharmacol *333*, 400–405.

Seaman, M.N.J. (2007). Identification of a novel conserved sorting motif required for retromer-mediated endosome-to-TGN retrieval. J. Cell. Sci. *120*, 2378–2389.

Seidah, N.G., and Chrétien, M. (1997). Eukaryotic protein processing: endoproteolysis of precursor proteins. Curr. Opin. Biotechnol. *8*, 602–607.

Shi, J., and Kandror, K.V. (2005). Sortilin Is Essential and Sufficient for the Formation of Glut4 Storage Vesicles in 3T3-L1 Adipocytes. Developmental Cell *9*, 99–108.

Shirayama, Y., Chen, A.C.-H., Nakagawa, S., Russell, D.S., and Duman, R.S. (2002). Brain-derived neurotrophic factor produces antidepressant effects in behavioral models of depression. J. Neurosci. *22*, 3251–3261.

Smith, K.A., Fairburn, C.G., and Cowen, P.J. (1997). Relapse of depression after rapid depletion of tryptophan. Lancet *349*, 915–919.

Smith, K.E., Boules, M., Williams, K., and Richelson, E. (2012). NTS1 and NTS2 mediate analgesia following neurotensin analog treatment in a mouse model for visceral pain. Behav. Brain Res. *232*, 93–97.

Sobocki, P., Jönsson, B., Angst, J., and Rehnberg, C. (2006). Cost of depression in Europe. J Ment Health Policy Econ *9*, 87–98.

Sparks, C.E., Sparks, R.P., and Sparks, J.D. (2015). The enigmatic role of sortilin in lipoprotein metabolism. Curr. Opin. Lipidol. *26*, 598–600.

Sprengelmeyer, R., Steele, J.D., Mwangi, B., Kumar, P., Christmas, D., Milders, M., and Matthews, K. (2011). The insular cortex and the neuroanatomy of major depression. Journal of Affective Disorders *133*, 120–127.

Strolin Benedetti, M., and Dostert, P. (1987). Overview of the present state of MAO inhibitors. J. Neural Transm. Suppl. *23*, 103–119.

Surguladze, S.A., El-Hage, W., Dalgleish, T., Radua, J., Gohier, B., and Phillips, M.L. (2010). Depression is associated with increased sensitivity to signals of disgust: a functional magnetic resonance imaging study. J Psychiatr Res *44*, 894–902.

Suter, U., Heymach, J.V., and Shooter, E.M. (1991). Two conserved domains in the NGF propeptide are necessary and sufficient for the biosynthesis of correctly processed and biologically active NGF. EMBO J. *10*, 2395–2400.

Talley, E.M., Lei, Q., Sirois, J.E., and Bayliss, D.A. (2000). TASK-1, a two-pore domain K+ channel, is modulated by multiple neurotransmitters in motoneurons. Neuron *25*, 399–410.

Tanganelli, S., O'Connor, W.T., Ferraro, L., Bianchi, C., Beani, L., Ungerstedt, U., and Fuxe, K. (1994). Facilitation of GABA release by neurotensin is associated with a reduction of dopamine release in rat nucleus accumbens. Neuroscience *60*, 649–657.

Tauris, J., Ellgaard, L., Jacobsen, C., Nielsen, M.S., Madsen, P., Thøgersen, H.C., Gliemann, J., Petersen, C.M., and Moestrup, S.K. (1998). The carboxy-terminal domain of the receptor-associated protein binds to the Vps10p domain of sortilin. FEBS Lett. *429*, 27–30.

Teng, H.K., Teng, K.K., Lee, R., Wright, S., Tevar, S., Almeida, R.D., Kermani, P., Torkin, R., Chen, Z.-Y., Lee, F.S., et al. (2005). ProBDNF Induces Neuronal Apoptosis via Activation of a Receptor Complex of p75NTR and Sortilin. J. Neurosci. *25*, 5455–5463.

Thomas, R.P., Hellmich, M.R., Townsend, C.M., and Evers, B.M. (2003). Role of gastrointestinal hormones in the proliferation of normal and neoplastic tissues. Endocr. Rev. *24*, 571–599.

Vincent, J.P., Mazella, J., and Kitabgi, P. (1999). Neurotensin and neurotensin receptors. Trends Pharmacol. Sci. *20*, 302–309.

Vita, N., Oury-Donat, F., Chalon, P., Guillemot, M., Kaghad, M., Bachy, A., Thurneyssen, O., Garcia, S., Poinot-Chazel, C., Casellas, P., et al. (1998). Neurotensin is an antagonist of the human neurotensin NT2 receptor expressed in Chinese hamster ovary cells. Eur. J. Pharmacol. *360*, 265–272.

Vogt, B.A., Finch, D.M., and Olson, C.R. (1992). Functional heterogeneity in cingulate cortex: the anterior executive and posterior evaluative regions. Cereb. Cortex *2*, 435–443.

Walker, N., Lepee-Lorgeoux, I., Fournier, J., Betancur, C., Rostene, W., Ferrara, P., and Caput, D. (1998). Tissue distribution and cellular localization of the levocabastine-sensitive neurotensin receptor mRNA in adult rat brain. Brain Res. Mol. Brain Res. *57*, 193–200.

Wang, H.L., and Wu, T. (1996). G alpha q/11 mediates neurotensin excitation of substantia nigra dopaminergic neurons. Brain Res. Mol. Brain Res. *36*, 29–36.

Wang, A.Z., Li, L., Zhang, B., Shen, G.-Q., and Wang, Q.K. (2011). Association of SNP rs17465637 on chromosome 1q41 and rs599839 on 1p13.3 with myocardial infarction in an American caucasian population. Ann. Hum. Genet. *75*, 475–482.

Warth, R., Barrière, H., Meneton, P., Bloch, M., Thomas, J., Tauc, M., Heitzmann, D., Romeo, E., Verrey, F., Mengual, R., et al. (2004). Proximal renal tubular acidosis in TASK2 K+ channel-deficient mice reveals a mechanism for stabilizing bicarbonate transport. Proc. Natl. Acad. Sci. U.S.A. *101*, 8215–8220.

Westergaard, U.B., Sørensen, E.S., Hermey, G., Nielsen, M.S., Nykjaer, A., Kirkegaard, K., Jacobsen, C., Gliemann, J., Madsen, P., and Petersen, C.M. (2004). Functional organization of the sortilin Vps10p domain. J. Biol. Chem. *279*, 50221–50229.

Willnow, T.E. (1998). Receptor-associated protein (RAP): a specialized chaperone for endocytic receptors. Biol. Chem. *379*, 1025–1031.

Wilson, C.M., Naves, T., Vincent, F., Melloni, B., Bonnaud, F., Lalloué, F., and Jauberteau, M.-O. (2014). Sortilin mediates the release and transfer of exosomes in concert with two tyrosine kinase receptors. J. Cell. Sci. *127*, 3983–3997.

Wu, Z., Martinez-Fong, D., Trédaniel, J., and Forgez, P. (2012). Neurotensin and its high affinity receptor 1 as a potential pharmacological target in cancer therapy. Front Endocrinol (Lausanne) *3*, 184.

Xian Tao Li, null, Dyachenko, V., Zuzarte, M., Putzke, C., Preisig-Müller, R., Isenberg, G., and Daut, J. (2006). The stretch-activated potassium channel TREK-1 in rat cardiac ventricular muscle. Cardiovasc. Res. *69*, 86–97.

Yamada, D., Wada, E., Amano, T., Wada, K., and Sekiguchi, M. (2010). Lack of neurotensin type 1 receptor facilitates contextual fear memory depending on the memory strength. Pharmacol. Biochem. Behav. *96*, 363–369.

Yamada, M., Yamada, M., Lombet, A., Forgez, P., and Rostène, W. (1998). Distinct functional characteristics of levocabastine sensitive rat neurotensin NT2 receptor expressed in Chinese hamster ovary cells. Life Sci. *62*, PL 375-380.

Yamauchi, R., Wada, E., Kamichi, S., Yamada, D., Maeno, H., Delawary, M., Nakazawa, T., Yamamoto, T., and Wada, K. (2007). Neurotensin type 2 receptor is involved in fear memory in mice. J. Neurochem. *102*, 1669–1676.

Zeng, J., Racicott, J., and Morales, C.R. (2009). The inactivation of the sortilin gene leads to a partial disruption of prosaposin trafficking to the lysosomes. Experimental Cell Research *315*, 3112–3124.

Zhou, C., Liu, J., and Chen, X.-D. (2012). General anesthesia mediated by effects on ion channels. World Journal of Critical Care Medicine *1*, 80–93.

Zsürger, N., Mazella, J., and Vincent, J.P. (1994). Solubilization and purification of a high affinity neurotensin receptor from newborn human brain. Brain Res. *639*, 245–252.

RESUME

Le trouble dépressif majeur est une pathologie qui n'atteint pas moins de 20% de la population et qui représente le premier facteur de morbidité et d'incapacité au niveau mondial. La compréhension du trouble dépressif représente un investissement important face au nombre grandissant de personnes touchées chaque année. Maladie d'atteinte psychologique et biologique, incriminant un des organes les plus complexe et élaboré qu'est le cerveau, les causes et conséquences de cette pathologie s'appuient sur de nombreux axes disciplinaires, complexifiant l'émergence d'approches thérapeutiques efficaces pour une réelle guérison.

Récemment, le canal potassique TREK-1 a été identifié comme une cible potentielle dans le traitement de la dépression. La délétion de ce canal ou son blocage par un peptide issu de la maturation du récepteur 3 de la neurotensine (Sortiline), le propeptide (PE) ou son analogue synthétique la Spadine, résulte en un phénotype de résistance à la dépression. La Sortiline est une protéine capable de s'associer à TREK-1 mais également au facteur neurotrophique BDNF, acteur important pour la viabilité neuronale et la régulation de l'état dépressif. La sortiline est donc impliquée dans la régulation de l'adressage intracellulaire de TREK-1 et du BDNF.

Compte tenu de ces informations, l'hypothèse de travail était, d'une part, d'évaluer les conséquences de la délétion du gène codant pour la Sortiline (souris Sort1$^{-/-}$) au niveau de l'adressage de TREK-1 et du BDNF, mais également sur le système neurotensinergique. Les résultats obtenus révèlent au niveau cérébral une diminution de l'expression membranaire de TREK-1 qui résulte en une augmentation du potentiel de membrane des neurones corticaux et une augmentation de l'expression de BDNF dépendant de sa voie constitutive. L'ensemble de ces modifications conduisent les souris Sort1$^{-/-}$ à développer un phénotype de résistance dans les tests comportementaux relatifs à la dépression. Au niveau du système neurotensinergique, ces souris présentent une augmentation de la concentration en neurotensine cérébrale ainsi que de son récepteur de type 2 (NTSR2), ce qui a pour effet de développer chez ces souris une résistance à la perception de la douleur. Dans un second temps, ces travaux se sont intessés à déterminer si le PE, un antidépresseur potentiel, montrait des variations sériques chez les patients dépressifs et pouvait être un indicateur du syndrome dépressif et/ou de sa rémission. Nous avons observé que le niveau sérique du PE est significativement réduit chez les personnes dépressives, niveau restauré après traitement avec des antidépresseurs.

Ce travail met en avant un rôle prépondérant de la Sortiline dans la régulation du développement de troubles dépressifs mais également de la nociception, et permet d'étendre la compréhension des mécanismes sous-jacents de ces pathologies et d'ouvrir des perspectives thérapeutiques intéressantes.